2016

INTRODUCING NOVEL COMBINATORIAL TARGETED THERAPIES IN MULTIPLE TYPES OF CANCER

Mehrad Tavallai
tavallais@vcu.edu

INTRODUCING NOVEL COMBINATORIAL TARGETED THERAPIES IN MULTIPLE

TYPES OF CANCER

A Dissertation submitted in partial fulfillment of the requirements for the degree of Doctor of
Philosophy at Virginia Commonwealth University.

by

MEHRAD TAVALLAI
Masters of Science, Virginia Commonwealth University, 2013
Bachelors of Science, George Mason University, 2011

Director: PAUL DENT, PH.D.
DEPARTMENT OF BIOCHEMISTRY
VCU SCHOOL OF MEDICINE

Virginia Commonwealth University
Richmond, Virginia
April 2016

Acknowledgements

I would like to acknowledge my advisor Dr. Paul Dent for providing me with the opportunity to pursue my Ph.D. degree in his laboratory, and also my committee members, Dr. Sarah Spiegel, Dr. Frank Fang, Dr. Charles Clevenger, Dr. Devanand Sarkar, and the biochemistry program director Dr. Tomasz Kordula, for mentoring me throughout my time as a graduate student.

I would also need to express my gratitude to my former and current lab mates Dr. Hossein Hamed, Dr. Laurence Booth, Dr. Jane Roberts and Dr. Nichola Cruickshanks for kindly teaching me the techniques required for my research, and for selflessly sharing their knowledge and experience with me. Additionally, I would like to thank the other members of Dent lab, especially Tim Webb and Dan Leon, for their help with my research and the lab maintenance.

Finally, I would like to acknowledge my family whose support has always given me the confidence and the encouragement to improve and to fulfill my passion.

Table of Contents

List of Tables and Figures

Abstract

INTRODUCING NOVEL COMBINATORIAL TARGETED THERAPIES IN MULTIPLE

TYPES OF CANCER

BY

MEHRAD TAVALLAI, Ph.D.

A Dissertation submitted in partial fulfillment of the requirements for the degree of Doctor of Philosophy at Virginia Commonwealth University.

Virginia Commonwealth University, 2016

Director: PAUL DENT, PH.D.
DEPARTMENT OF BIOCHEMISTRY
VCU SCHOOL OF MEDICINE

The cancers of liver, colon and breast are amongst the top five most prevalent and most fatal worldwide. Currently, surgical resection, radiotherapy and adjuvant chemotherapy, in some cases combined with certain approved targeted agents, constitute the front line therapies for hepatocellular carcinoma (HCC) and colorectal cancer (CRC). As the Raf/MEK/ERK pathway is frequently deregulated in HCC, sorafenib, a Raf kinase inhibitor, became the first systemic therapy approved for the treatment of patients with HCC. However, sorafenib only produced modest effects with low response rates in the clinic. Similarly, regorafenib, a more potent and more soluble derivative of sorafenib, which was approved for the treatment of metastatic CRC, has had a poor response rate in the clinic. Since phosphodiesterase type 5 has been reported to be overexpressed in HCC and CRC, we hypothesized that sildenafil, a phosphodiesterase type 5 inhibitor, could enhance the toxicities of sorafenib and regorafenib in HCC and CRC cells,

respectively. Our *in vitro* data indicated that the drugs interacted strongly to kill cancer cells via induction of ER stress, autophagy and apoptosis. In accordance with these findings, our *in vivo* data demonstrated a significant reduction in tumor growth.

The second study was conducted based on the growing body of evidence about the significant contribution of EGFR and JAK/STAT signaling to the breast tumorigenesis. Thus, we hypothesized that the concurrent inhibition of JAK/STAT and EGFR signaling pathways would kill breast cancer cells in a synergistic manner. Our preliminary *in vitro* data demonstrated that the inhibition of these two pathways by lapatinib, a dual ERBB1/2 inhibitor, and ruxolitinib, a JAK1/2 inhibitor, synergistically killed breast cancer cells of all types, including the resistant triple negative subtype. Our mechanistic studies showed that the combination of ruxolitinib and lapatinib triggered cytotoxic mitophagy, and autophagy-dependent activation of BAX and BAK leading to the mitochondrial dysfunction.

Collectively, our studies strongly argue that the combination of sorafenib/regorafenib and sildenafil as well as the combination of ruxolitinib and lapatinib can possess significant therapeutic value in the clinic.

CHAPTER 1: Introduction to Cancer Therapy

Cancer

Cancer is a complex compilation of distinct genetic abnormalities, which collectively alter the way normal cells, in a particular part of the body, function, grow and divide.[1] Consistent with Darwinian principles, cancer stems from random mutations within the genes of normal cells in a multistep process that enable these cells to activate or modify certain cellular programs, including proliferation, migration and apoptosis.[1,2] These mutagenic alterations occur in the form of activating (gain-of-function) mutations, amplification and/or overexpression of genes that promote proliferation (oncogenes), as well as inactivating (loss-of-function) mutations, deletion and/or epigenetic silencing of genes that inhibit growth (tumor suppressor genes).[1,3] Many studies have concluded that both intrinsic naturally-occurring errors in DNA replication and extrinsic factors, such as exposure to carcinogens, can affect the rate of mutagenesis although it is not very well clear what portion of total cancer risk stems from each source.[4]

Despite the variable genetic profile of cancer cells, they share common biological characteristics, which have been referred to as the hallmarks of cancer. According to Hanahan and Weinberg[2], these acquired capabilities that distinguish cancer cells from the normal cells include activating proliferative signaling, inhibiting growth suppressors, resisting cell death, gaining replicative immortality, promoting angiogenesis, and activating invasion and metastasis.

In addition to the acquisition of the hallmark traits, which are highlighted as the major driving force behind carcinogenesis, the cancer cells also possess the capability to recruit the surrounding stromal cells to form a histologically diverse microenvironment that enhances growth, progression and metastasis.[1,2] In other words, a tumor is not simply a homogenous aggregate of cancer cells but rather a more complex heterogeneous population of cells, including

cancer cells, cancer stem cells, immune inflammatory cells, endothelial cells and cancer-associated connective tissue.[1,2] The formation of this advanced microenvironment around the cancer cells adds another layer of complexity to understanding the mechanisms of tumorigenesis, and implies that the tumor biology cannot be fully understood without studying the individual cells within it.[2]

Currently, cancer is the second leading cause of death worldwide behind the cardiovascular diseases. In the United States, a quarter of all deaths are caused by cancer, and new statistics suggest that nearly half of men (~45%) and a third of women (~38%) in the United States will be affected by this fast-growing disease during their lifetimes.[5,6] The cancers of lung, colorectum, prostate and breast continue to be among the deadliest, accounting for half of the cancer-related mortalities in American men and women.[6] On the bright side, due to the advent of new therapies, a decrease in tobacco consumption, more effective screening and early detection, cancer death rates dropped 22.9% in men and 15.3% in women between 1990-2008.[6]

A Concise History of Cancer Treatment

A great body of evidence suggests that cancer is not a disease of modern era as paleopathologic findings revealed that cancer existed in prehistoric times, long before human species evolved.[7] The earliest case of cancer in humans was found in Edwin Smith Papyrus dating back to approximately 3000 BC, being described as an incurable grave disease.[7] Similar reports of cancer cases were found in ancient Egyptian manuscripts.[5] The Egyptians utilized cautery, knives, salts and arsenic paste as means of treatment whereas the Sumerians, Chinese, Indians and Persians resorted to herbal remedies.[7] Later the Romans treated aggressive cancers by surgical resection, or amputation in more severe cases, followed by herbal remedies. This

approach remained to be the standard procedure in cancer treatment before the Catholic Church prohibited all surgical operations in 1215.[5,7]

The major breakthrough in cancer therapy came at the turn of the 20th century by an accidental observation of the effect of mustard gas on the depletion of bone marrow and lymph nodes. Supported by further studies, the use of nitrogen mustard as a treatment for lymphoma increased rapidly in the United States. A few years later, it was discovered that folate deficiency could replicate the effects of nitrogen mustard on bone marrow. These findings triggered the use of synthesized anti-folate drugs, most notably methotrexate, as a treatment for leukemia.[8]

In the middle of 1950s, Charles Heidelberger and his colleagues noticed a significant increase in uracil uptake by hepatoma cells relative to normal tissue. Their efforts resulted in the synthesis of 5-fluorouracil (5-FU), which was later utilized against a broad range of solid tumors. Their approach to target a certain biochemical pathway that cancer cells relied upon was the very first example of what we refer to as targeted therapy today.[8,10]

The initial optimism of curing cancer with the use of alkylating agents and antimetabolites soon turned into disappointment as many cases of recurrence and metastasis were reported in the patients. In late 1960s, cancer treatment moved towards combination chemotherapy, and chemotherapeutics were applied in conjugation with surgery and/or radiation.[8,9] In adjuvant therapy, the chemotherapy is administered after surgery to eliminate the remaining cancer cells whereas in neoadjuvant therapy, the chemotherapy is applied before surgery in order to reduce the size of the tumor.[5,9]

Eventually in the late 20th century, through the advancements in genomics, many oncogenes and tumor suppressor genes were identified. The genome sequencing of a variety of cancer cells suggested that many of them possessed abnormalities within genes that coded for

protein kinases. Subsequently, a new class of anti-cancer therapeutics known as kinase inhibitors was soon developed. These small molecules are believed to hold significant promise to treat all sorts of malignancies as they aim at specific targets within the cancer cells and have the capability to exploit oncogene addiction.[8,11,14] The development of imatinib (Gleevec) against the aberrant nonreceptor tyrosine kinase Bcr-Abl in patients diagnosed with chronic myeloid leukemia (CML) is a perfect example of targeted therapy as complete responses were observed in 60-70% of cases.[8,12,14] In addition to kinase inhibitors, monoclonal antibodies such as trastuzumab (Herceptin) and antisense inhibitors have also been developed and studied during the past two decades. Currently, the efficacy of many of these targeted drugs in a variety of cancers is being evaluated in the clinic, both individually and in combination with other targeted or chemotherapy agents.

Targeted Therapy

Chemotherapy has been the cornerstone of cancer therapy for decades; however, its response rate remains low as most cytotoxic chemotherapeutics yielded narrow therapeutic index, caused significant toxicity, and resulted in palliative, unpredictable responses. Furthermore, poor penetrability, low absorption, rapid elimination, development of drug resistance, and the complex heterogeneous nature of the tumor microenvironment contributed to their dysfunctionality.[12,13,23] Therefore, a more target-specific approach based on better understanding of the tumor biology started to take root in the post-genomic era. Since all drugs have targets, the term targeted therapy might be misleading. Therefore, we need to define this category of therapies first before making any comparisons to the conventional chemotherapy.

Targeted therapy refers to treatments, in which a target within the cancer cells, cancer stem cells, or the tumor microenvironment is first identified, before a selective inhibitory drug is

developed against it. The development of Herceptin against Her-2/Neu, an oncogenic receptor tyrosine kinase involved in progression of Her-2 positive breast cancer, is just an example amongst many.[10] Evidently, the major benefit of this type of tailored therapy is that it only interferes with distinct molecular targets that the cancer cells physiologically depend on, thus, providing high specificity, a broader therapeutic index, and less nonspecific toxicities.[12]

Antiangiogenic drugs are another class of targeted therapeutics that has been broadly explored in recent years. It has been well established that tumor blood supply is critical for tumor progression and metastasis.[19,21] One of the key mediators of angiogenesis is known to be vascular endothelial growth factor-A (VEGF-A). Inhibition of angiogenic factors such as VEGF-A have appeared to be an effective approach with near universality application and minimal incidences of acquired resistance.[14,15,19] Bevacizumab is a great representative of this class of drugs, which binds to VEGF with high specificity thus inhibiting angiogenesis. Recent clinical trials have approved the effects of Bevacizumab in combination with 5-fluorouracil in extending survival rate in patients with metastatic colorectal cancer.[15,21] Similarly, kinase inhibitors with anti-VEGF receptor (VEGFR) activity such as sorafenib have produced impressive results in treating renal cell carcinoma.[14,12,20]

Drug Resistance in Cancer

Although the cancer genome profile is genuinely a useful tool that identifies most oncoprotein/tumor suppressor-related mutations, producing Gleevec-like success in most solid tumors through targeted therapy has been proven to be extremely challenging. In fact, over 90% of the targeted compounds in clinical trials fail to gain approval due to their poor efficacy.[10,14] Two major reasons have been proposed to have caused this subpar results.

Firstly, it is extremely difficult to distinguish the mutations that occur early in the life of a tumor from the ones that occur in the later stages. This can severely affect the dependency of a tumor on a certain mutation and the degree by which an inhibitory agent can block tumor growth. For instance, in case of CML, the abnormality in Bcr-Abl tyrosine kinase is generally agreed to be the initiating mutation, to which the significant success of Gleevec is attributed.[14,18] In contrast, there is evidence suggesting that the activating mutation in FMS-like tyrosine kinase 3 receptor (FLT3) in patients with acute myeloid leukemia (AML) occurs later in tumor progression. Therefore, the phase I studies of FLT3 targeted inhibitors have not replicated the impressive response rate of Gleevec.[14,16,17,18]

Secondly, the emergence of different forms of acquired resistance in cancer cells against the cytotoxic chemotherapeutics and the targeted drugs have been largely to blame for their dismal response rate. Here we briefly discuss some of the major mechanisms of resistance acquired in response to both targeted and chemotherapy.

1. Increased expression of drug efflux pumps: among all transporter proteins, the ATP-binding cassette (ABC) transporter family of transmembrane proteins has been most notably linked to multi drug resistance (MDR). This protein family consists of 49 members, grouped into seven subfamilies (designated A to G) that are involved in transportation of a broad range of substrates, including amino acids, ions, lipids, sugars and drugs across the membrane.[23-26] Multi-drug resistance protein 1 (MDR1, also known as ABCB1), MDR-associated protein 1 (MRP1, also known as ABCC1) and breast cancer resistance protein (BCRP, also referred to as ABCG2) are the 3 members of this family that are overexpressed in many cancers. These transporters can efflux a wide range of chemotherapeutics such as taxanes, topoisomerase inhibitors and antimetabolites.[23,24,26] Statistical studies have established a correlation between increased

expression of ABC transporters and a poor response to chemotherapy.[27] For instance, the low response rate to anthracyclines in pancreatic cancer has been suggested to be in part due to the MDR phenotype.[28,29] In spite of the initial optimism, the combination of the inhibitors of these transporters with the standard of care chemotherapy generated disappointing results. For instance, the combination of valspodar, a specific ABCB1 inhibitor, in combination with paclitaxel and carboplatin in patients with stage IV ovarian or primary peritoneal cancer did not yield any benefit as compared to chemotherapy alone.[24,30] These findings argued that the contribution of MDR phenotype to drug resistance might not be as significant as previously presumed.[23,24]

2. Drug inactivation: another obstacle in cancer therapy is diverse cellular mechanisms of drug inactivation or insufficient drug activation. Resistance to the platinum drugs such as cisplatin by glutathione is a good example of such inactivation mechanisms.[31] Epigenetic silencing can also contribute to the activity of certain drugs.[23] For instance, o^6-methylguanine-DNA methyltransferase (MGMT) is a repair enzyme whose function counteracts the formation of DNA double strand breaks induced by temozolomide (TMZ) in patients suffering from glioblastoma multiforme (GBM). The clinical studies have indicated that the methylated status of MGMT promoter in GBM patients who received concurrent radiotherapy and TMZ treatment was associated with a significant increase in survival time as this group of patients lived on average 6.4 months longer than the patients who possessed normal MGMT expression level.[32,33]

3. Secondary mutations in drug targets: drug resistance can also stem from the secondary somatic alterations within the oncogenic targets. The first case of this resistance mechanism was identified in CML patients treated with Gleevec, and similar genetic alterations have been observed in other cancers ever since.[22,23] In general, these mutations either promote an

active enzymatic conformation or the target or prevent drug binding.[22] One of The best examples of such target alterations is the gatekeeper mutations within the catalytic domain of epidermal growth factor receptor (EGFR) in patients with non-small cell lung cancer (NSCLC), which increases the affinity of EGFR for ATP, thus lowering the efficacy of EGFR inhibitors. These alterations have been directly linked to the dramatic response rates of erlotinib and gefitinib in patients with NSCLC.[22,23,34]

4. DNA damage repair: Most chemotherapeutics cause DNA damage either directly as seen by platinum drugs or indirectly as observed by the function of topoisomerase inhibitors. Therefore, the capacity of DNA damage repair in cancer cells, as explained by the aforementioned example of MGMT in TMZ therapy, plays a critical role in the response rate of chemotherapy.[23,33] Thus, targeting the components of the DNA repair machinery has emerged as a new strategy to enhance the toxicity of chemotherapeutics. The development of poly (ADP-ribose) polymerase 1 (PARP1) inhibitors exemplifies this targeted approach. PARP1 is a ubiquitous single-strand-break DNA repair enzyme, and its inhibition results in accumulation of single-strand breaks followed by double-strand breaks.[23,35] A phase I trial of olaparib, a potent PARP1 inhibitor, in patients with breast and ovarian cancer, including carriers of mutated BRCA1 and BRCA2 genes, generated positive results.[36] There are also ongoing clinical trials evaluating the effect of olaparib in combination with chemotherapy in all solid tumors.[35]

5. Deregulation of apoptotic components: as previously mentioned, resistance to cell death is one of the hallmarks of cancer, thus it is evident that deregulation of apoptosis is one of the mechanisms of drug resistance utilized by cancer cells. This deregulation can occur in both pro-apoptotic and anti-apoptotic components of the programmed cell death. Previous studies have reported that overexpression of anti-apoptotic proteins caused resistance to

chemotherapeutics in leukemic cells.[23,37] Studies from our laboratory also suggested that lapatinib-resistant HCT116 cells had higher expression of anti-apoptotic proteins Bcl-xL and Mcl-1 and reduced expression of pro-apoptotic protein BAX compared to the wild type cells, and that inhibition of Mcl-1 restores lapatinib toxicity to a great extent.[38]

6. Activation of pro-survival signaling pathways: the activation of survival pathways in response to chemotherapy is another way for cancer cells to resist cell death. Plenty of studies have proposed the activation of EGFR as a resistance mechanism to chemotherapy.[23] Similar studies indicated that EGFR inhibitors could enhance the effects of paclitaxel and 5-FU in renal and colorectal cancer, respectively.[39,40] Furthermore, some clinical trials have supported the beneficial addition of EGFR inhibitors to irinotecan-based therapy, leading to approval of these targeted agents by the Food and Drug Administration (FDA) for treatment of certain subtypes of colorectal cancer.[23,41]

7. Activation of bypass mechanisms: activation of compensatory parallel signaling pathways has emerged as a major concern rendering cells resistant to targeted therapy. In this mechanism of resistance, also referred to as oncogenic bypass, activation of an alternative kinase through an adaptive feedback loop or a secondary mutation triggers signaling through parallel pro-survival pathways, which ultimately counteracts the effect of the targeted agent.[22,23] A good example of this type of resistance is the activation of ERBB3 and its downstream PI3K/AKT pathway in response to EGFR inhibitors such as cetuximab.[42,43] Similar mechanism has been reported in patients with NSCLC that responded poorly to gefitinib, as an amplification of MET proto-oncogene led to the activation of ERBB3 compensatory signaling.[44]

Advantages of Combinatorial Targeted Therapy

Investigating the various mechanisms of drug resistance undoubtedly provides a plethora of information that can be directed towards the development of more effective future therapies. For example, the increased affinity of the mutant EGFR^{T790M} for ATP in patients with NSCLC has led to the production of new restructured irreversible inhibitors that bind to EGFR catalytic cleft more readily than erlotinib and gefitinib. This new generation of EGFR inhibitors have shown improved efficacy in murine models.[22,45] However, most types of acquired resistance are mediated by the activation of the alternative compensatory pathways rather than alteration of the drug target itself. Therefore, resorting to a rational combinatorial approach seems imperative. There are two distinct types of drug combinations:

1. Combinations of targeted drugs with chemotherapy: many studies have recently indicated that the specific targeted agents can enhance the effect of chemotherapy in a variety of tumor types through interference with the DNA repair enzymes or inhibition of pro-survival pathways. The FDA-approved combination of lapatinib with capecitabine in women with advanced breast cancer resistant to trastuzumab, or the combination of cetuximab with irinotecan in patients with metastatic colorectal carcinoma are two examples of how the targeted inhibition of an activated survival pathway leads to a more responsive chemotherapy.[11,41,46] Concurrent inhibition of DNA repair enzymes (e.g. PARP1) or checkpoint kinases (e.g. CHK1) with chemotherapy has also significantly improved the standard of care in a variety of cancers.[35,47]

2. Combinations of target-specific drugs: a major setback to single-agent targeted therapy is the potential for crosstalk between pro-survival pathways. This may result in the cell activating an alternative survival pathway in the event of blockade of a specific pathway; thus, leading to drug resistance. Therefore, there is growing evidence that the use of targeted therapeutics in combination provides a more rational strategy to increase the efficacy of

treatment. The combinatorial targets might lie within the same oncogenic pathway (referred to as vertical) or located within two distinct pathways (described as horizontal).[11] For instance, recent clinical trials revealed that EGFR inhibitors, used as single agents, are of little therapeutic benefit in patients with GBM, which commonly possess deregulated EGFR signaling pathway.[48] One of the mechanisms of resistance to EGFR inhibition in GBM cells has been shown to be the upregulation of platelet-derived growth factor receptor β (PDGFRβ).[49] A recent study from our laboratory indicated that the addition of sorafenib, a multi-kinase inhibitor with anti-PDGFRβ activity, significantly enhances lapatinib toxicity in GBM cells.[50] Another relevant example is the crosstalk between estrogen receptors (ER) and EGFR family members, which has been shown to modulate resistant to hormone therapy.[51,52] These findings led to accelerated approval of lapatinib in combination with letrozole, an aromatase inhibitor, for the treatment of postmenopausal women with ER-positive metastatic breast cancer.[53]

The purpose of this study is to introduce novel targeted drug combinations in multiple types of cancer using the same rationale. But prior to presenting the results, we need to introduce some of the important signaling pathways involved in survival and cell death, which are affected by the proposed drug combinations in this manuscript.

Mitogen-Activated Protein Kinase Pathway (MAPK)

MAPK pathways are evolutionary conserved signaling cascades involved in fundamental intracellular processes such as growth, proliferation, migration and apoptosis. MAPK pathways consist of a three-tier kinase module in which a downstream MAPK is activated upon phosphorylation by MAPK kinase (MAPKK), which in turn is activated when phosphorylated by its upstream MAPK kinase kinase (MAPKKK). There are four major well characterized mammalian MAPK kinase pathways that activate four distinct terminal serine/threonine kinases,

ERK1/2, c-Jun amino-terminal kinase (JNK), p38 kinase and ERK5 (Figure 1).[54-56] ERK1/2 is normally activated by growth factors whereas JNK, p38 and ERK 5 usually become activated in response to cytokines or environmental stress such as osmotic shock and ionizing radiation. Recently, two more mammalian MAPK pathways have been discovered that lead to activation of ERK3/4 and ERK 7/8 while the rest of the components of these pathways are currently unknown.[54-56] Among all, the ERK1/2 MAPK signaling pathway, commonly deregulated in many cancers, has drawn a great deal of attention due to its pivotal role in vital cell functions including growth, differentiation, survival, migration and angiogenesis, and has grown as a major target for cancer drug discovery.[54-57] Deregulation of this pathway occurs at several different levels as the mutational activation of Raf, Ras and their upstream receptors such as EGFR has been reported in a variety of human cancers.[54,55]

p38 is strongly responsive to pro-inflammatory cytokines and environmental stress, and gets activated by two main MAPKKs, MKK3 and MKK6. Two main substrates of p38 are MAP kinase-activated protein kinase 2 (MK2) and MK3. Activated MK2 and MK3 interact with various targets, including heat shock protein (HSP) 27, CREB, and ATF.[58,59]

The JNK kinase family (also known as stress-activated protein kinases (SAPK)) includes three proteins JNK1, JNK2 and JNK3, which get activated by MKK4 and MKK7 in response to cytokines, growth factors and stress. Upon activation, JNKs interact with numerous substrates, most prominently the transcription factor activator protein-1 (AP-1), which is formed by dimerization of the Fos and Jun proteins.[60,61]

JNKs and p38 MAPKs regulate many pathways involved in inflammation, proliferation, differentiation, survival and cell death. They can act both as tumor suppressors and oncoproteins depending on cell type, duration of activation and the nature of stimulus.[60,62]
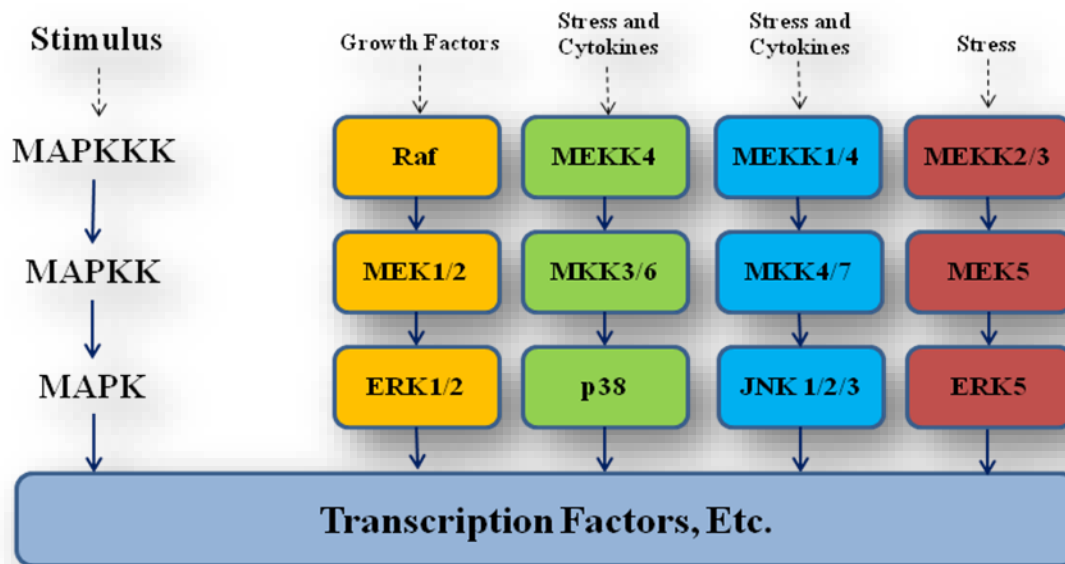
Figure 1. Four major mammalian MAPK pathways. MAPK pathways are comprised of three-tier kinase module in which a MAPKKK phosphorylates the downstream MAPKK, which in turn phosphorylates its downstream serine/threonine MAPK. Among the MAPKs activated by these four pathways, only ERK1/2 responds to growth factors. ERK5, JNK and p38 are mainly activated due to environmental stress such as osmotic shock and ionizing radiation.

Ras/Raf/MAPK Pathway

When growth factors bind to their receptors, they induce dimerization and auto-phosphorylation of tyrosine residues on the catalytic domains of these receptors. These phospho-tyrosines act as docking sites for growth factor receptor-bound protein 2 (GRB2), an adaptor protein, and sons of sevenless (SOS), an exchange factor, which together result in the activation of Ras (Figure 2).[55,57,63]

Ras GTPases (H-, K- and N-Ras) act as molecular switches that mediate activation of many signaling pathways. Inactive guanosine diphosphate (GDP)-bound Ras activity is regulated by guanine nucleotide exchange factors (GEFs), such as SOS, which promote the formation of active guanosine triphosphate (GTP)-bound Ras, whereas GTPase-activating proteins (GAPs), such as neurofibromin 1 (NF1), induce GTP hydrolysis and formation of inactive GDP-bound Ras. Activated GTP-bound Ras then recruits Raf from the cytosol to the cell membrane where a multi step activation process occurs.[54,55,57] Ras regulates survival and proliferation pathways, and is constitutively activated in approximately 30% of all cancers with pancreas (90%), colon (50%) and lung (30%) having the highest rates of aberrant Ras signaling.[55] The most common mutations of Ras are related to GAP insensitivity, which maintains Ras in an active GTP-bound state. As GAP-based targeted therapies failed to impress, the downstream effectors of Ras have grown as more suitable therapeutic targets.[55,57]

Raf serine/threonine kinases are direct downstream effectors of Ras. There are three different forms of Raf (A-, B- and C- Raf) whose structures are similar, but differ considerably in their modes of regulation, tissue distribution, and the ability to activate MAPK/ERK kinase (MEK).[54,63] B-Raf gets activated directly by Ras whereas A- and C-Raf require additional serine- and tyrosine phosphorylation to become fully active.[64] All three isoforms are able to

phosphorylate MEK with B-raf being the strongest activator and A-Raf the weakest.[63] B-Raf mutations are quite prevalent in malignant melanomas (~66%) and many other cancers such as colon and thyroid.[54] The most common B-Raf active mutant form is B-Raf^{V599E}, which constitutively induces ERK signaling.[64]

Activated Raf then phosphorylates MEK1/2 at two serine residues located on the kinase domain, which in turn binds to and phosphorylates ERK1/2. Activated ERK1/2 can translocate to the nucleus and induce genetic responses that regulate processes such as proliferation, differentiation, survival, migration and angiogenesis.[54-57] ERK1/2 can also modulate cell survival through interaction with cytosolic substrates, most notably p90 ribosomal S6 kinase (p90RSK). Activated p90RSK phosphorylates pro-apoptotic protein BAD resulting in its inactivation. It also activates cAMP response element-binding protein (CREB), which translocates to the nucleus and induces transcription of anti-apoptotic genes.[65] Moreover, ERK1/2 can directly mediate phosphorylation and proteasome-dependent degradation of pro-apoptotic protein BIM.[66]
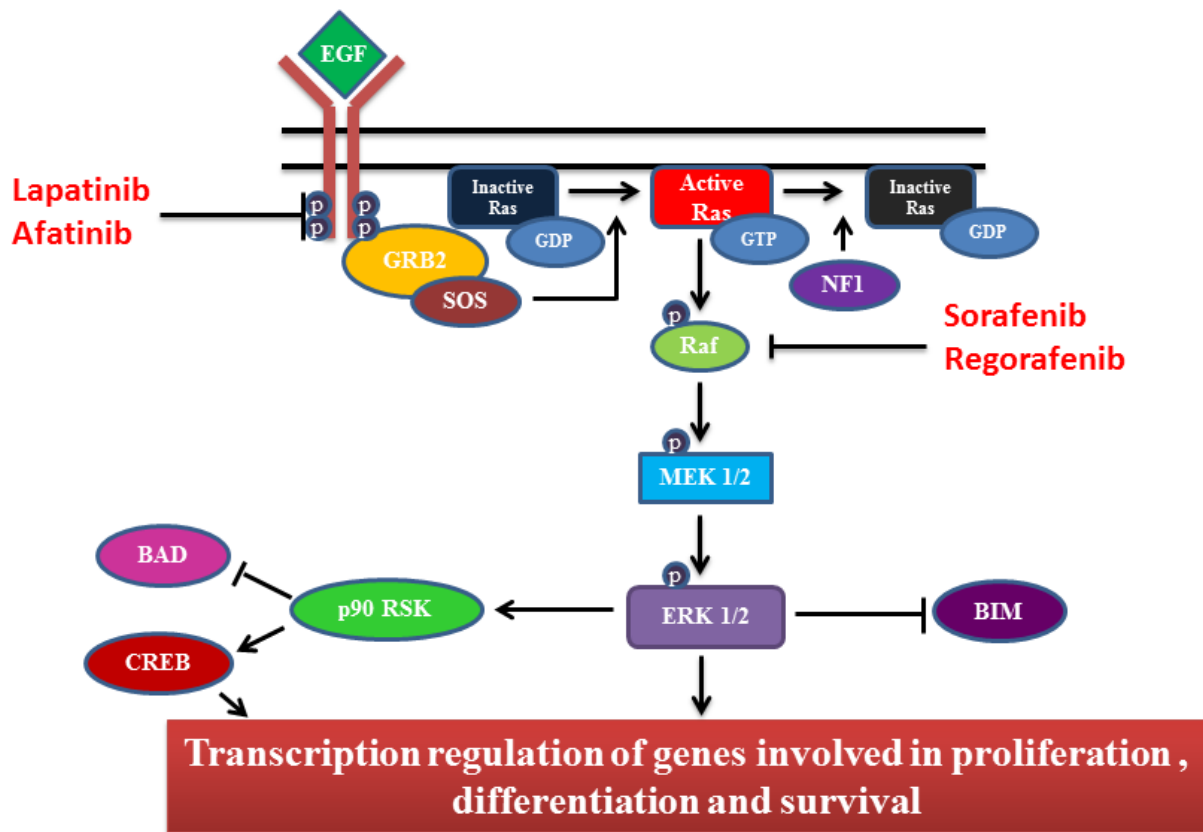
Figure 2. Ras/Raf/MAPK signaling pathway. Upon ligand binding, the tyrosine residues on the kinase domain of EGFRs become transphosphorylated, which act as docking sites for the adaptor protein GRB2. SOS binds to GRB2 and activates Ras by exchanging GDP for GTP. GTP-bound Ras recruits Raf from cytosol to the membrane and activates it, which in turn activates MEK1/2 by phosphorylating two distinct serine residues. Activated MEK1/2 subsequently activates ERK1/2, which translocates to the nucleus and induces multiple cellular responses. ERK1/2 also interacts with cytosolic targets such as p90RSK and BIM leading to activation of survival pathways.

PI3K/AKT Pathway

When growth factors bind to the membrane receptor tyrosine kinases including EGFR, PDGFR, or insulin-like growth factor 1 receptor (IGF1R), they induce receptor phosphorylation and membrane recruitment of PI3K. PI3K is a lipid kinase that is comprised of two separate subunits, a regulatory p85 and a catalytic p110, which heterodimerize upon activation. Activated PI3K phosphorylates the lipid phosphatidylinositol 4,5-biphosphate (PIP2) generating the second messenger phosphatidylinositol 3,4,5-triphosphate (PIP3). PIP3 in turn recruits both phosphatidylinositol-dependent protein kinase 1 (PDK1) and AKT to the membrane, where AKT becomes phosphorylated on threonine 308 (T308) by PDK1 and additionally on serine 473 (S473) by the mechanistic target of rapamycin complex 2 (mTORC2) to become fully active (Figure 3). Activated AKT induces survival, proliferation and growth through phosphorylation of multiple downstream effectors. The PI3K/AKT pathway is negatively regulated by phosphatase and tensin homolog (PTEN), a lipid phosphatase that dephosphorylates PIP3 to PIP2. [67-69]

AKT promotes survival through interaction with multiple substrates. It directly blocks activation of pro-apoptotic proteins BAD and pro-caspase 9. It also phosphorylates mouse double minute chromosome 2 (MDM2). Phosphorylated MDM2 translocates to the nucleus where it induces degradation of p53, an important tumor suppressor, through its E3 ubiquitin ligase activity. In addition, AKT inhibits transcription factor forkhead box 1 (FOXO1), thus blocking FOXO-mediated transcription of apoptotic factors.[67-69]

AKT also induces proliferation through inhibition of glycogen synthase kinase-3β (GSK-3β) resulting in the accumulation of cyclin D1 and progression of cell cycle.[67-69]

Furthermore, AKT promotes protein synthesis and cell growth through activation of mTOR complex 1 (mTORC1). In this process, AKT inhibits tuberous sclerosis complex 2

(TSC2), which with its binding partner TSC1 act as a GAP for the Ras homolog enriched in brain (Rheb) GTPase. Rheb strongly activates mTORC1 when it is in an active GTP-bound state. Activated mTORC1 phosphorylates p70 S6 kinase (p70S6K) and eukaryotic initiation factor 4E (eIF4E)-inhibitory binding protein (4EBP). Activation of p70S6K and eIF4E enhances mRNA translation and increases protein synthesis.[67-69] mTORC1 is also a major regulator of autophagy. Under nutrient starvation, AMP activated protein kinase (AMPK) phosphorylates Unc-51 like autophagy activating kinase 1 (ULK1) on serine residues 317 and 777, leading to initiation of autophagy. Under nutrient sufficiency, mTORC1 phosphorylates ULK1 on serine 757, thus disrupting the interaction between ULK1 and AMPK.[70]

Increasing evidence suggest that many cancers rely on activation of AKT and mTORC1 to drive tumorigenesis, and commonly deregulated status of this pathway has turned it into an attractive target for therapeutic intervention. Activating mutations and gene amplification occur at different levels in this pathway. For instance, loss-of-function mutations and complete loss of PTEN is frequently observed in many cancers, including GBM, colon, breast, lung and prostate.[71] Gene amplification of p110 and AKT as well as activating mutations of p85 occur in many cancers, including ovarian, breast and colon.[72]
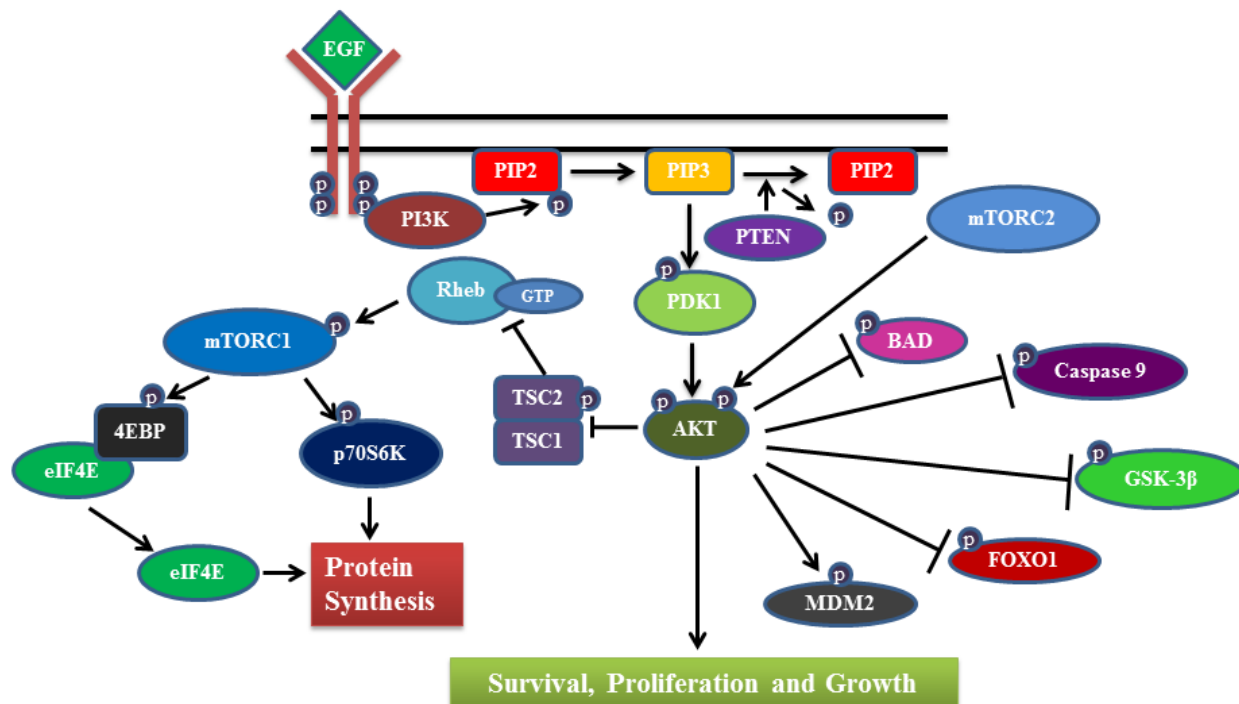
Figure 3. PI3K/AKT signaling pathway. The lipid kinase PI3K binds the kinase domain of the EGFR receptor, and phosphorylates PIP2 to generate PIP3. PIP3 recruits both PDK1 and AKT to the membrane where PDK1 phosphorylates AKT. Activated AKT induces protein synthesis and survival through interaction with various substrates. mTOR, a major AKT target that acts as a nutrient sensor, phosphorylates p70S6K and 4EBP. Released eIF4E and phospho-p70S6K translocate to the nucleus and induce protein synthesis. This pathway is negatively regulated by phosphatase PTEN, which dephosphorylates PIP3 to PIP2.

JAK/STAT Signaling Pathway

The Janus family of kinases (JAKs) includes JAK1, JAK2, JAK3 and tyrosine kinase 2 (TYK2), which are involved in transduction of signals received from a variety of physiological stimuli, including cytokines and growth factors. JAK1 is required in the signaling of pro-inflammatory cytokines such as interleukin (IL)-6, IL-1, and interferon-ɣ (IFN-ɣ). JAK2 is important for hematopoietic growth factors, growth hormone and prolactin signaling. JAK3 plays a role in mediating immune function whereas Tyk2 functions in part with JAK 2 and JAK3 to transduce cytokine signaling. The function of JAK kinases are essential in cytokine signaling since the members of the cytokine receptor superfamily lack intrinsic kinase activity.[73,74]

The signal transducers and activators of transcription (STAT) proteins are a family of transcription factors that function downstream of JAKs. Seven members of the STAT family have been identified so far (STAT1-4, STAT 5a, STAT 5b, and STAT6), which contain a SRC homology 2 (SH2) domain, a DNA binding domain, and a transactivation domain.[75-77]

Upon cytokine binding and receptor dimerization, JAKs are recruited to the cytoplasmic domains of the receptors where they phosphorylate specific tyrosine residues. Subsequently, STATs bind these phosphorylated residues through their SH2 domains, and get tyrosine phosphorylated on their transactivation domains by the JAKs. Once activated, STATs homo- or heterodimerize through reciprocal phosphotyrosine-SH2 domain interactions. The dimmers then translocate to the nucleus where they interact with other transcription modulators to induce gene expression.[73-76] Among the genes regulated by STATs are those coding for pro-survival proteins, such as Bcl-2 family of proteins (e.g. Bcl-xL), those promoting cell proliferation, such as cyclin D1, and those involved in angiogenesis and metastasis, such as VEGF (Figure 4).[78]

JAK/STAT pathway is negatively regulated by two different families of proteins; the suppressors of cytokine signaling (SOCS) proteins, and the protein inhibitors of activated STAT (PIAS). SOCS proteins bind the phosphorylated residues on the cytokine receptors through their SH2 domains. SOCS-1 has become known as a major tumor suppressor that directly binds JAK2 and inhibits JAK/STST signaling.[77,79] The aberrant methylation of SOCS-1 gene has been observed to a great extent in hepatocellular carcinoma, which shows the significance of JAK/STAT signaling in tumor progression.[80] The PIAS family includes PIAS1, PIAS3, PIASx and PIASy. These proteins bind activated STAT dimmers and inhibit their function through multiple different mechanisms.[77,79]

Constitutively activated STATs have been numerously reported in a variety of cancers mainly due to deregulation of their upstream signaling proteins. STATs act as a point of convergence for numerous upstream tyrosine kinases, and hold significant promise for the development of new anti-cancer therapeutics. Many studies have indicated the role of STAT3 and STAT5 in oncogenesis, and their inhibition has been shown to be associated with tumor suppression and cell death. In addition, activated STAT3 and STAT5 signaling has been observed in breast, lung, and head and neck cancer mediated by increased cytokine signaling.[75,77]

Activation of STATs can also be caused by aberrant JAK signaling. A somatic gain-of-function mutation (V617F) in JAK2 is present in 50-60% of patients with primary myelofibrosis and essential thrombocythemia. Amplification of JAK2 has also been implicated in 30-50% of patients with Hodgkin lymphoma and primary B-cell lymphoma. Recently, targeted inhibition of JAK2 generated promising results in patients with myelofibrosis leading to the approval of ruxolitinib (Jakafi) by FDA in 2011.[73,74]
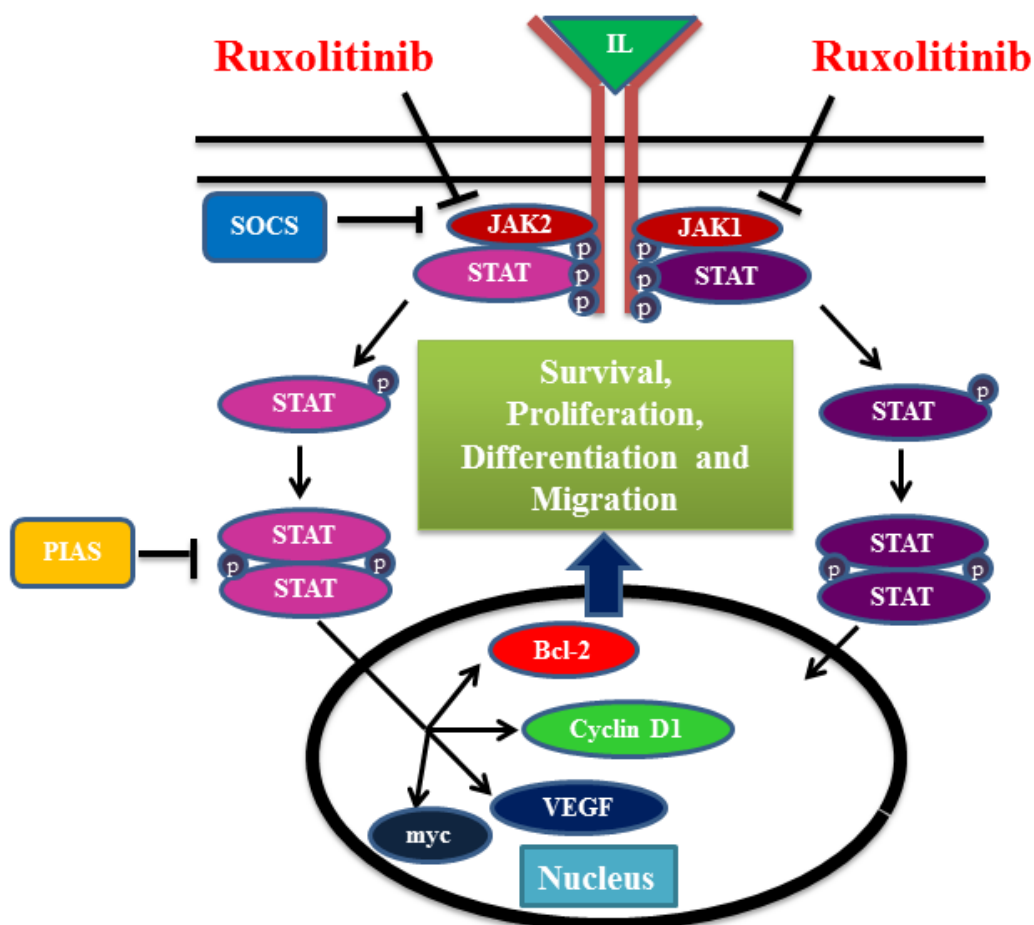
Figure 4. JAK/STAT pathway. Upon cytokine binding and receptor dimerization, JAKs are recruited to the receptor site where they phosphorylate tyrosine residues on the cytosolic domain of the receptor. The phosphotyrosines act as docking sites for STATs to bind, and subsequently get activated through phosphorylation by JAKs. Dimerized STATs translocate to the nucleus and induce expression of genes involved in proliferation, differentiation and survival. This pathway is negatively regulated by SOCS and PIAS family of proteins.

Epidermal Growth Factor Receptor Tyrosine Kinase

The EGFR/ErbB family is a critical component in the autocrine growth regulation of carcinoma, and is comprised of four different receptors; EGFR/ErbB1, ErbB2/HER2, ErbB3/HER3, and ErbB4/HER4. All of these trans-membrane proteins are within the 170-190 kilo Dalton (kDa) size range and are composed of three different domains; the glycosylated extracellular ligand-binding domain, a single hydrophobic trans-membrane domain, and an intracellular catalytic domain.[81,82] The hydrophobic domain anchors the receptor in the membrane and connects the cysteine-rich growth factor binding extracellular domain to the intracellular tyrosine kinase catalytic domain. Unlike ErbB1, 2 and 4 which are catalytically active, ErbB3 does not have an active tyrosine kinase domain, but remains competent for ligand binding and signal transduction. There is no known ligand that binds ErbB2, but ErbB2 remains a favorite dimerization partner for the rest of the members.[81,84]

Ligand binding or receptor over-expression induces homo- or hetero-dimerization of ErbB receptors, which results in trans-phosphorylation of tyrosine residues located on the intracellular catalytic domain. The phospho-tyrosine residues on the cytoplasmic side of the receptor act as docking sites for SH2 domain-containing signaling proteins that are involved in activation of multiple downstream metabolic signaling cascades including PI3K/AKT, Ras/Raf/MAPK and phospholipase C (PLC)/ protein kinase C (PKC).[81,82] EGFR signaling also activates STATs, which lately has been demonstrated to be mediated by Src family of kinases (Figure 5).[83]

Aberrant ErbB signaling has been observed in a variety of cancers, and its activation has been linked to invasion, metastasis, chemoresistance, and poor clinical outcome. Overexpression of EGFR has been reported in many cancers, including 40-80% of NSCLC, 72-82% of colorectal

cancer (CRC), and 50-90% of renal cell carcinoma. Amplification of HER-2 is present in 25-30% of breast cancers. EGFR is also amplified in approximately 40-50% and over-expressed in more than 60% of glioblastomas. Nearly 40% of the GBMs with EGFR amplification possess a constitutively active mutant form of the receptor, EGFRvIII. Therefore, EGFR tyrosine kinases have turned into one of the most sought after targets in cancer therapy.[85,86]

Two classes of EGFR inhibitors have been developed; monoclonal antibodies and tyrosine kinase inhibitors (TKI). Monoclonal antibodies, such as trastuzumab and cetuximab, bind to the extracellular domain of the receptor, and prevent ligand binding whereas TKIs, such as erlotinib and lapatinib, block the ATP binding pocket of the receptors, thus blocking receptor activation.[82,85] In spite of the initial positive results, a variety of mechanisms of acquired resistance have been observed in response to targeted EGFR therapeutics, which have drastically lowered their success rates. The occurrence of secondary mutations, activation of parallel tyrosine kinase signaling pathways, and loss of tumor suppressors, such as PTEN are just a few examples of drug resistance mechanisms frequently counteracting EGFR inhibition-based therapies. Therefore, there is growing evidence that the combination of EGFR inhibitors with chemotherapy or other signal-transduction inhibitors will create a more potent therapy.[82]
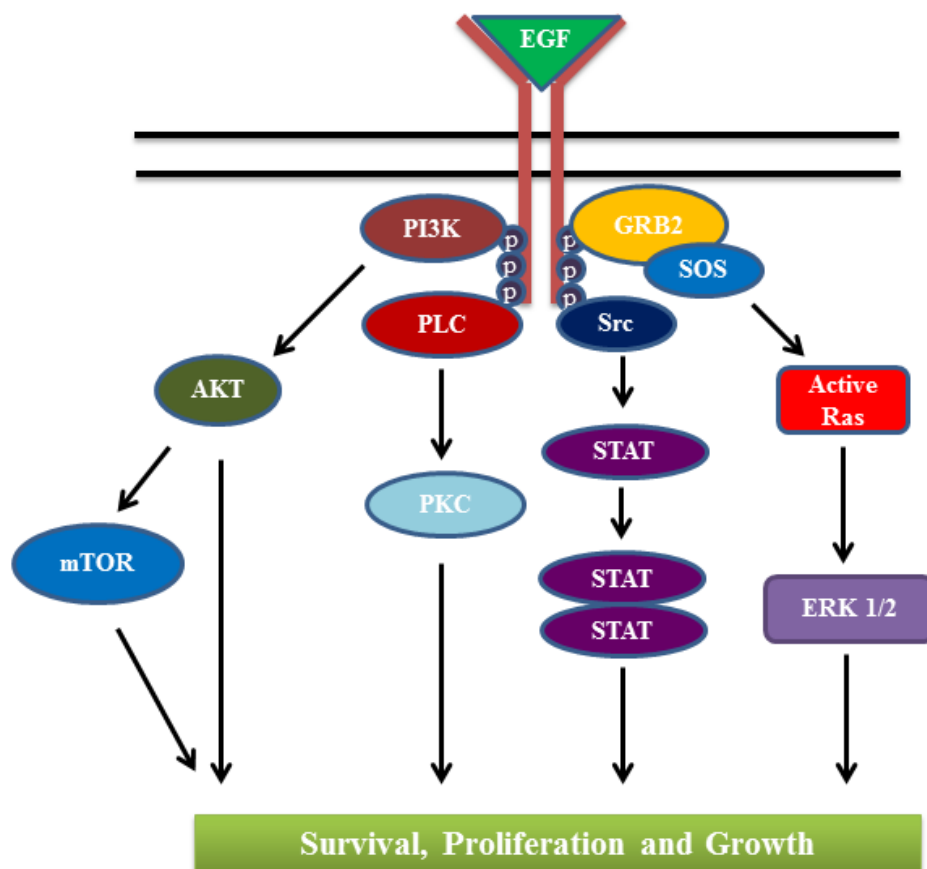
Figure 5. EGFR signaling. Ligand binding induces trans-phosphorylation of tyrosine residues located on the intracellular catalytic domain. The phospho-tyrosine residues on the cytoplasmic side of the receptor act as docking sites for SH2 domain-containing signaling proteins that are involved in activation of multiple downstream metabolic signaling cascades, including PI3K/AKT, Ras/Raf/MAPK and PLC/PKC. STATs also get activated in a Src-mediated fashion.

Nitric Oxide Signaling

Nitric oxide (NO) is a small uncharged highly diffusible gaseous molecule that plays a critical role in regulation of cardiovascular and immune system. NO is generated through the catalytic activity of NO synthases (NOS), which convert L-arginine and molecular oxygen to L-citrulline and NO.[87,88] NOS activity depends on several cofactors, including NADPH and tetrahydrobiopterin (BH4). BH4 plays a critical role in NOS activity. Small ratio of BH4 relative to its oxidized form, dihydrobiopterin (BH2), causes NOS uncoupling, leading to production of reactive oxygen species (ROS) and reactive nitrogen species (RNS) rather than NO. Uncoupling of NOS results in a decrease in vascular NO level, which commonly occurs during aging, inflammatory diseases, cardiovascular diseases and cancer.[87,89] There are three isoforms of NOS: the inducible NOS (iNOS) that functions in inflammatory response, the endothelial NOS (eNOS) that generates NO as a paracrine signal in the vascular system, and the neuronal NOS (nNOS) that produces NO that acts as a neurotransmitter in the nervous system.[87,88]

Shear stress generated by streaming blood is sensed by the endothelial cells through activation of PI3K/AKT pathway. AKT phosphorylates eNOS, leading to its catalytic activation and generation of NO.[90] Soluble guanylate cyclase (sGC) is the primary target of NO, which converts GTP to cyclic GMP (cGMP) upon activation. cGMP-dependent protein kinase G (PKG) is a major recipient of cGMP , which phosphorylates numerous targets, resulting in diverse physiological responses including vasodilatation and angiogenesis.[87,88] Phosphodiesterases (PDE) are a family of enzymes that hydrolyze cAMP and cGMP to their inactive forms 5'-AMP and 5'-GMP, respectively (Figure 6). PDE5 inhibitors, such as sildenafil (Viagra), increase NO signaling by preventing the cGMP breakdown, and are currently approved for the treatment of erectile dysfunction and pulmonary arterial hypertension.[87,88]
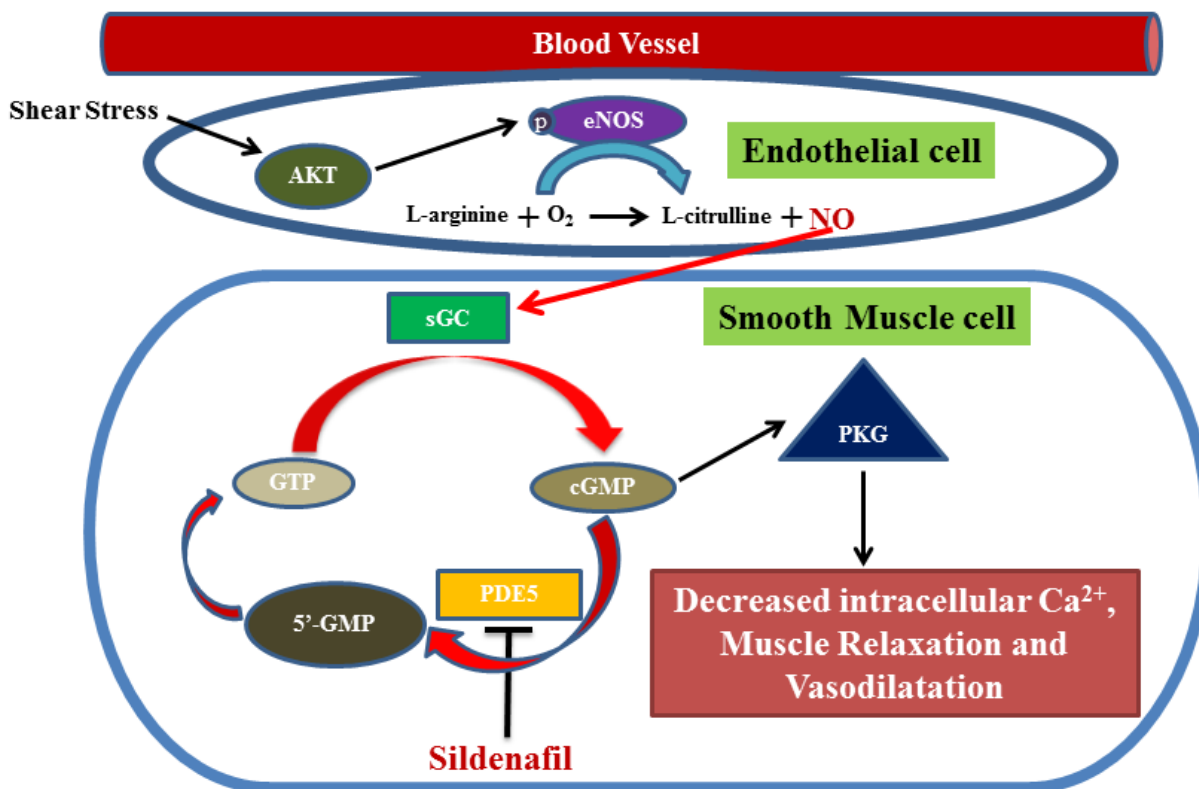
Figure 6. NO signaling in the vascular system. The endothelial cells sense the shear stress from the streaming blood, leading to the activation of PI3K/AKT pathway. Activated AKT phosphorylates eNOS and induces NO generation into the adjacent connective tissue. The Soluble GC in the smooth muscle cells is the major target of NO. Activated sGC converts GTP to cGMP, which acts as an important secondary messenger. PKG is a major recipient of cGMP that phosphorylates numerous targets, resulting in diverse physiological responses including vasodilatation. This cycle is negatively regulated by PDEs that break down the cGMP to its inactive 5'-GMP form.

Apoptosis: Intrinsic and Extrinsic Pathways

Apoptosis, also referred to as programmed cell death type I (PCDI), is an energy-dependent multi-step biochemical process that plays a crucial role in tissue homeostasis in multicellular organisms, and its deregulation contributes to many diseases, including cancer, autoimmunity and AIDS. Morphologically, apoptosis is characterized by membrane blebbing, cell shrinkage, nucleus fragmentation, chromatin condensation and DNA degradation.[91-93] There are two distinct apoptotic pathways: the extrinsic or death receptor pathway and the intrinsic or mitochondrial pathway. However, new evidence suggested that these two pathways are connected and the components of one pathway can influence the other.[91] Both extrinsic and intrinsic pathways converge on the activation of specific intracellular poteases, the caspase family. Caspases are intracellular cysteine proteases that cleave proteins next to aspartate residues. Caspases, typically categorized into initiators and executioners, are synthesized as inactive zymogens and become activated upon cleavage by their upstream modulators.[91,94] Caspase 3 is the most important of the executioner caspases, and is activated by any of the initiator caspase 8, 9 and 10 in both extrinsic and intrinsic pathways. Executioner caspases (caspase 3, 6 and 7) cleave various substrates including cytoskeletal and nuclear proteins, and also activate other proteases and endonucleases involved in protein degradation and DNA fragmentation.[91,94]

Unlike the extrinsic pathway that is mediated by death receptors, the intrinsic pathway is strictly controlled by the B-cell lymphoma-2 (Bcl-2) family of proteins.[91,94] The Bcl-2 family consists of three different classes: the anti-apoptotic group I, the pro-apoptotic group II and group III proteins that bind and regulate the activity of anti-apoptotic group II proteins. Group I family members such as Bcl-2, Bcl-x long (Bcl-xL) and myeloid cell leukaemia-1 (Mcl-1)

directly bind and inhibit pro-apoptotic group II family members including Bcl-2-associated X protein (BAX) and Bcl-2 homologous antagonist/killer (BAK). Whereas, the group III family members, commonly referred to as Bcl-2 homology (BH) 3-only proteins, including p53 unregulated modulator of apoptosis (PUMA), NADPH oxidase activator (NOXA), BH3 interacting domain death agonist (BID) and Bcl-2 interacting mediator of cell death (BIM) either directly or indirectly interact with pro-apoptotic group II family members and induce their insertion in the mitochondrial membrane.[91,94] The indirect activation of BAX and BAK by BH3-only proteins seems to be more validated since recent studies concluded that BAK can only induce cell death if it is displaced from prosurvival proteins Mcl-1 and Bcl-xL through BAD and NOXA.[95] Further studies demonstrated a role for the tumor suppressor p53 in synthesis of PUMA and NOXA, linking DNA damage to apoptotic cell death.[96,97]

The intrinsic pathway is activated by various stimuli such as viral infection, DNA damage and absence of certain growth factors, hormones and cytokines. After exposure to these stimuli, BAX and BAK homo-oligomerizae in the outer membrane of mitochondria leading to mitochondrial membrane permeabilization, formation of pores, and release of cytochrome-c and other pro-apoptotic proteins, such as caspase-activated deoxyribonuclease (CAD), apoptosis-inducing factor (AIF) and endonuclease G, from the inter-membrane space into the cytosol.[91,94] In the cytosol, cytochrome-c binds apoptotic protease-activating factor-1 (Apaf-1), which in turn binds pro-caspase 9 to form a complex known as the apoptosome. Binding to Apaf-1 induces conformational change and activation of caspase 9, which proteolytically activates executioner caspase 3.[91,94] Besides its proteolytic activity in the cytosol, cleaved caspase 3 can also activate caspase 6, another executioner caspase, and CAD by cleaving its inhibitor (ICAD). CAD

alongside AIF and endonuclease G, which unlike CAD function in a caspase-independent manner, translocate to the nucleus where they lead to DNA fragmentation.[91,93,94]

The extrinsic signaling pathway is activated when death receptors bind their natural ligands from the tumor necrosis factor (TNF) family. These death receptors, which belong to the TNF receptor family, consist of a cysteine-rich extracellular domain for ligand binding and a cytoplasmic domain of 80 amino acids called the death domain (DD) involved in signal transduction.[91-93] The best-characterized member of this family is Fas receptor, also known as cluster of differentiation 95 (CD95). The Fas receptor is a 45-kDa trans-membrane protein that binds to its ligand (FasL) through its cysteine-rich extracellular domain. Ligand binding induces conformational changes in the receptor structure that allows Fas to recruit an adaptor protein called Fas-associated death domain (FADD). FADD contains another important motif, the death-effector domain (DED) that binds initiator caspases 8 and 10 through complementary DED domains. This death-inducing signaling complex (DISC) leads to auto-proteolytic cleavage and activation of caspases 8 and 10, which subsequently activate executioner caspases 3 and 7 to induce apoptotic response (Figure 7).[91-93] The extrinsic pathway may also result in the release of cytochrome-c and the induction of the intrinsic pathway through activation of BID that serves as a substrate for caspase 8. Upon activation at the DISC, truncated BID (tBID) translocates to the mitochondria and induces the release of apoptotic proteins from the intermembrane space into the cytosol.[91,98] The extrinsic apoptotic pathway is regulated at early stage by FLICE-inhibitory proteins (FLIP), which bind to the DISC and inhibit activation of caspase 8.[92,93]
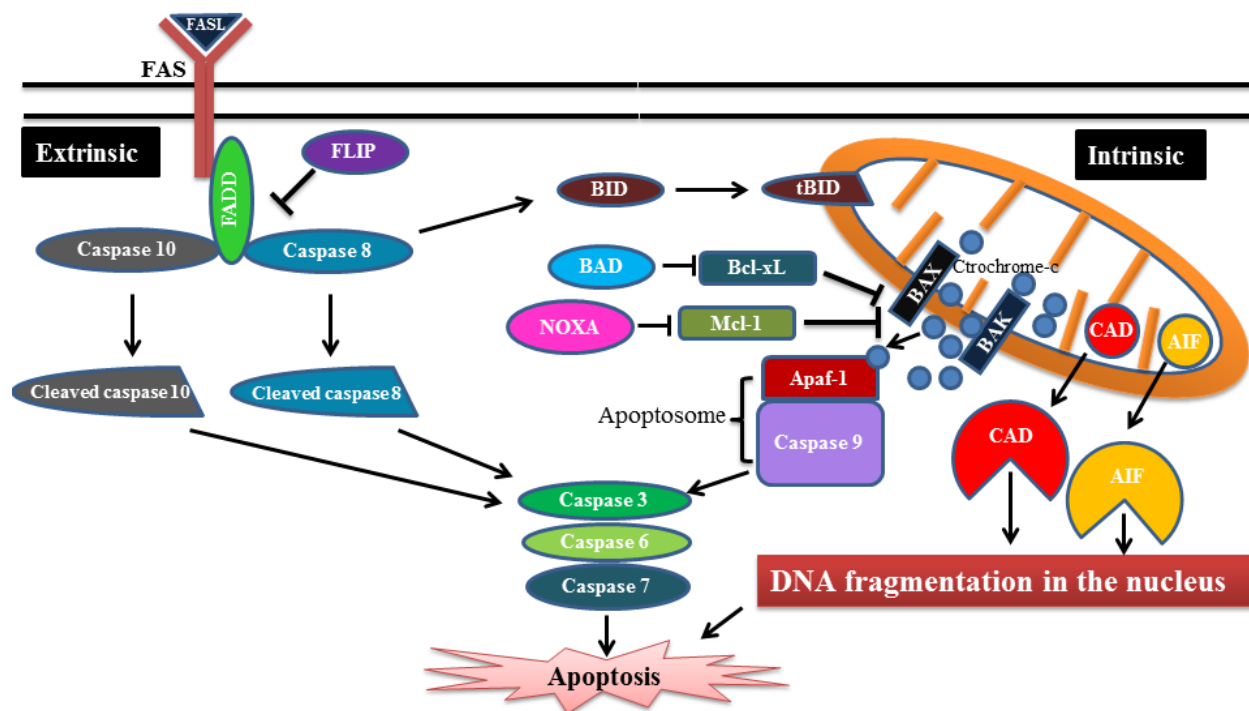
Figure 7. Intrinsic and extrinsic apoptotic pathways. The intrinsic pathway is controlled by Bcl-2 family of proteins that induce release of cytochrome c from the intermembrane space of mitochondria into the cytosol. Cytochrome c causes Apaf-1 to bind and activate initiator caspase 9. Cleaved caspase 9 then activates executioner caspase 3. On the other hand, the extrinsic pathway is initiated by binding of TNFs to the TNFRs. The TNFRs then recruit adaptor protein that can bind and activate initiator caspases 8 and 10. These initiator caspases in turn activate caspases 3 and 7. Caspase 8 can also activate BID, which can translocate to the mitochondria and induce release of cytochrome c.

Deregulation of Apoptosis in Cancer

Deregulation of apoptosis plays a critical role in the development of cancer and drug resistance.[2,99] Apoptosis is highly regulated through the interplay between the proapoptotic and antiapoptotic Bcl-2 family of proteins. Numerous studies have pointed at the oncogenic capability of proapoptotic Bcl-2 family members.[95] A study by Amundson *et al*[100] demonstrated a strong correlation between the expression level of Bcl-xL and resistance to chemotherapy. Alternatively, based upon the loss-of-function mutagenic studies, it has been rightfully argued that antiapoptotic proteins act as tumor suppressors.[95] In support of this claim, studies indicated that the *BIM* gene underwent biallelic deletion and promoter hypermethylation in majority of mantle cell and Burkitt lymphomas, respectively.[101,102] The tumor suppressor activity of antiapoptotic proteins is further supported by the increasing evidence that BH3-only proteins get activated in response to anticancer drugs.[95] For example, it has been suggested that Gleevec induces apoptosis through activation of BIM and BAD.[103] Another study by Tan *et al*[104] showed that paclitaxel induced BIM-dependent apoptosis, which was abrogated by activation of Ras and subsequent degradation of BIM in proteasomes. They also argued the potentials benefit of the proteasome inhibitor Velcade and paclitaxel combination in the treatment of epithelial tumors.

p53 is another regulator of apoptosis that induces cell death in response to DNA breaks, hypoxia and proliferative signals.[2,99] *TP53* is the most commonly mutated gene in cancer cells, and studies have established a strong correlation between the wild type p53 status and the response to anticancer agents.[105] p-53-mediated apoptosis is primarily linked to an increase in the transcription of PUMA and NOXA, two BH3-only proteins that interact with antiapoptotic Bcl-2 family members.[95-97] Collectively, these findings articulate the significance of Bcl-2 family of proteins in regulating apoptosis in cancer, which can be exploited as targets in future therapies.

Autophagy

Autophagy is an evolutionary conserved degradative mechanism that is required for maintaining cellular homeostasis by recycling and turnover of cytoplasmic components. Autophagy is associated with various physiological and pathological processes including development, aging, cancer, neurodegenerative disorders and infectious diseases.[106-108] Cancer therapeutics also have the ability to induce autophagy predominantly through interruption of EGFR pathway, activation of MAPK signaling pathways and induction of ER stress.[107]

Autophagy occurs in three different modes: macroautophagy, microautophagy and chaperone-mediated autophagy. Macroautophagy (hereafter referred to as autophagy) is the main lysosomal rout for recycling long-lived macromolecules and also organelles, such as mitochondria and peroxisomes, when damaged or in excess. It is characterized by formation of double-membrane vesicles named autophagosomes around targeted cellular components, which directly fuse with lysosomes for enzymatic degradation. Microautophagy involves direct engulfment of cytoplasmic components into the lysosome through invagination of the lysosomal membrane, whereas chaperone-mediated autophagy is the selective degradation of cytoplasmic proteins, which contain a specific motif that can be recognized by lysosomal receptors.[106-108]

Out of 31 autophagy-related genes (ATG) discovered by yeast genetic studies, 18 genes are involved in autophagosome formation. Since autophagy is an evolutionary conserved process, most of these genes have mammalian homologs with similar functionality.[108,109]

Mammalian ATG9 is a trans-membrane protein essential for autophagosome formation that has localizes to the trans-Golgi Network (TGN). Upon starvation, BAX-interacting factor-1 (Bif-1) co-localizes with ATG9 and induces fragmentation of Golgi. The ATG9-containing fragments are dispersed in the cytosol and are utilized for autophagosome formation.[108] This

process requires activation of classIII PI3K (PI3KC3) complex, which consists of PI3KC3, p150, Beclin-1, ultraviolet radiation resistance-associated gene (UVRAG) and ATG14L that acts upstream of ATG9 trafficking. PI3KC3 forms a complex with p150 adaptor that tethers the enzyme to the cytoplasmic membrane. PI3KC3 then binds Beclin-1 that serves as a binding partner for UVRAG and ATG14L. Bif-1 binds the complex by interacting with UVRAG. Activation of PI3KC3 complex II is regulated by mTOR signaling and is crucial for ATG9 trafficking and initiation of autophagosome formation.[108-110] AMPK and mTORC1 are major regulators of autophagy. Under nutrient starvation, AMPK phosphorylates ULK1 on serine residues 317 and 777, leading to initiation of autophagy. Under nutrient sufficiency, mTORC1 phosphorylates ULK1 on serine 757, thus disrupting the interaction between ULK1 and AMPK.[70] Activated ULK1 is recruited by ATG14L to directly phosphorylate Beclin-1 and induce activation of PI3KC3. Activated PI3KC3 phosphorylates phosphatidylinositol (PI) to produce phosphatidylinositol 3-phosphate (PI3P) that serves as an anchor for PI3P-binding proteins such as ATG18 to bind to form phagophores.[110] Recent studies have shown that there are two different PI3KC3 complexes: complex I contains PI3KC3, p150, Beclin-1 and ATG14L whereas in complex II ATG14L is replaced by UVRAG. Complex I is involved in Formation of phagophores while complex II contributes to autophagosome maturation.[109,110] The crescent-shaped phagophores, also known as isolation membranes, are extended to form double-membrane autophagosomes in a process that involves two ubiquitin-like (UBL) conjugation systems. These UBL systems function in a manner that resembles the ubiquitylation process involved in protein degradation, which is composed of a ubiquitin-activating enzyme (E1), a ubiquitin-conjugating enzyme (E2) and a ubiquitin-protein ligase enzyme (E3).[106,111] In the first UBL system, ATG12 is activated by E1-like enzyme ATG7, forming an ATG12-ATG7 thioester

intermediate before being transferred to ATG10, an E2-like enzyme. In the last step ATG12 covalently binds ATG5, and ATG12-ATG5 conjugate non-covalently interacts with ATG16L to form the final complex. This complex dissociates from the membrane when autophaosome formation process is complete. The second UBL system involves modification and incorporation of microtubule-associated Protein 1 Light Chain 3 (LC3) into the autophagosome membrane. The C-terminal region of LC3 is first cleaved by ATG4 to form LC3-I. E1-like enzyme, ATG7, activates LC3-I, which is then transferred to ATG3, an E2 like enzyme. In the final step, LC3-I is covalently bound to phosphatidylethanolamine (PE) to form the lipid-protein conjugate LC3-II (Figure 8). LC3-II is tightly associated with autophagosomes, and can be used as an autophagic marker in mammalian cells. Upon formation, autophagosomes are fused with lysosomes to complete protein degradation.[106,111]

In addition to bulk degradation of cytoplasmic macromolecules and excessive organelles as a result of nutrient deprivation, autophagy can also take part in degradation of mis-folded proteins. This process is mediated by the adaptor molecule p62 (sequestosome 1), which possesses specific domains to bind both the ubiquitin moiety on the poly-ubiquitinated misfolded proteins and the LC3 on the autophagosome membranes. Lysosomal degradation of autophagosomes results in a decrease in p62 levels, which makes p62 a suitable marker for tracking autophagy in mammalian cells.[112]
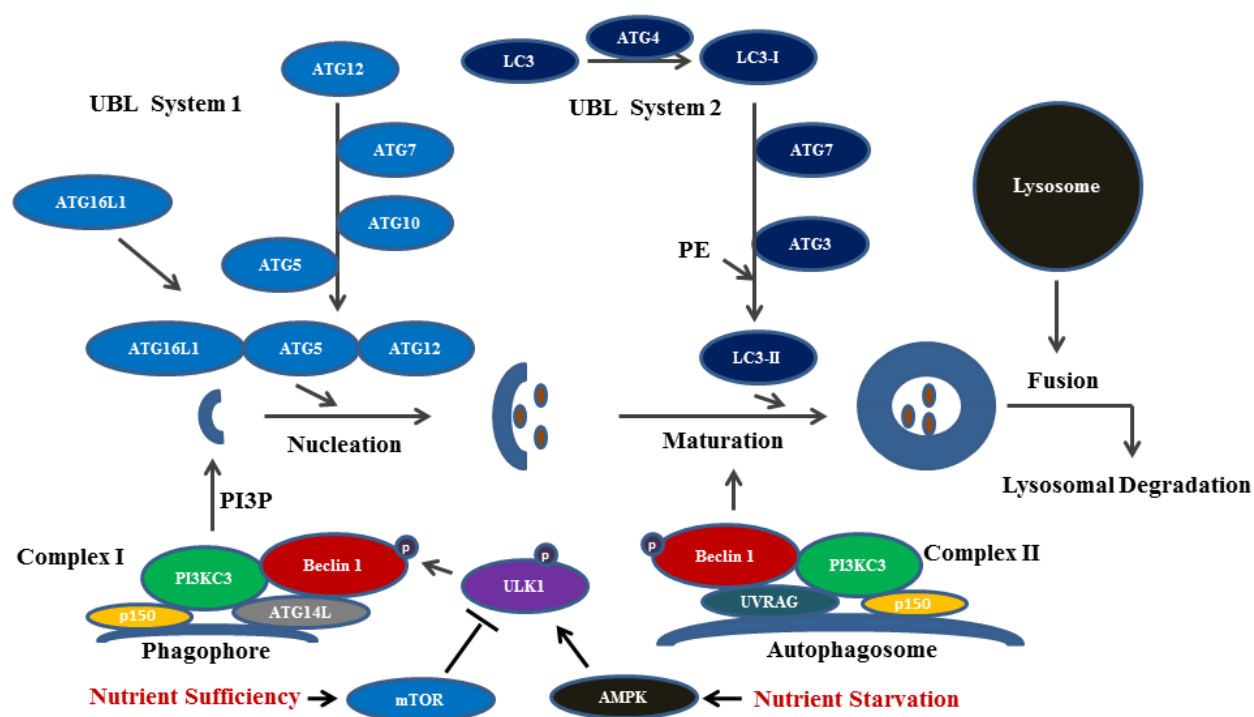
Figure 8. Autophagosome formation in mammalian cells. AMPK gets activated in response to amino acid starvation, and phosphorylates ULK1. Activated ULK1 subsequently binds ATG14L to phosphorylate Beclin-1. Phosphorylation of Beclin 1 activates PI3KC3 in complex I leading to production of PIP3 that in turn induces nucleation. Autophagosome formation requires two UBL conjugation systems. UBL system 1 produces ATG5-ATG12-ATG16L1 conjugates that attach the isolation membranes and facilitate membrane nucleation. UBL system 2 modifies LC3 and incorporates the final product, LC3-II, into the autophagosome membrane. The final step in this process is fusion of the lysosomes with the autophagosomes that leads to complete degradation of autophagosome contents.

The Role of Autophagy in Cancer

The role of autophagy in cancer resembles a double-edged sword; acting as a cytoprotective as well as a cytotoxic mechanism.[2,113] Radiotherapy and many anticancer drugs induce autophagy that seemingly impairs cell death.[113] However, quite contrary to its protective nature, there is increasing evidence that autophagy acts as a tumor suppressor.[113,114] Monoallelic loss of *beclin1* gene has been shown to promote tumorigenesis associated with chromosomal instability and gene amplification, suggesting Beclin1 as a tumor suppressor.[115] Another study demonstrated that breast cancer cell lines frequently possessed allelic deletion of *beclin1* gene.[116] Moreover, exogenous expression of Beclin1 in MCF7 cells, which lack the endogenous Beclin1 expression, inhibited tumorigenesis.[114] Beclin1, a necessary regulator of autophagy, is a novel BH3-only protein, which provides a crosstalk point between autophagy and apoptosis. Antiapoptotic proteins Bcl-2 and Bcl-xL can bind to Beclin1 and inhibit autophagy whereas other proapoptotic BH3-only proteins such as BID, BAD and PUMA can displace Beclin1, and induce apoptosis and/or autophagy.[2,117]

Autophagy and apoptosis can also crosstalk through of mTOR. Activation of the pro-survival AKT/mTOR pathway blocks apoptosis as well as autophagy through inactivation of ULK1. A role of activated PI3K/AKT/mTOR signaling, which is a common characteristic of many cancer cells, in the negative regulation of autophagy provides more evidence for the role of autophagy in tumor suppression.[2,114]

Perhaps, the formation of autophagic vesicles in the drug-treated cancer cells could initially be a cytoprotective mechanism to degrade the damaged organelles. However, after a certain degree of damage, autophagy might induce activation of cell death. Nevertheless, whether cells are ultimately destroyed by cytotoxic autophagy requires more investigation.[114]

Endoplasmic Reticulum Stress

Proteins targeted for secretory pathway are folded in the lumen of endoplasmic reticulum (ER) by chaperones before being transported to Golgi apparatus for final modification and secretion. Interruption in this process results in accumulation of unfolded proteins in the lumen of ER, referred to as ER stress, and induction of the unfolded protein response (UPR). The UPR is a series of actions that collectively reduce the rate of protein synthesis and activate transcription factors that enhance function of the ER.[118-120] There are three transmembrane proteins in the membrane of ER that sense the accumulation of misfolded proteins and trigger the UPR: PKR-like eukaryotic initiation factor 2α kinase (PERK), inositol requiring enzyme 1 (IRE1) and activating transcription factor-6 (ATF6). This sensory mechanism is mediated by the chaperone protein glucose-regulated protein of 78 kDa (GRP78), also known as binding immunoglobulin protein (BiP), present in the lumen of the ER. Under normal conditions, GRP78 is bound to the luminal domains of PERK, IRE1 and ATF6 inhibiting their function. Upon ER stress occurrence, GRP78 is released to bind to the unfolded protein leading to the activation of the three stress sensors. Upon activation, ATF6 is proteolytically cleaved and directly translocated into the nucleus to induce the expression of the genes required for the UPR. However, activation of PERK and IRE1 is associated with dimerization and subsequent autophosphorylation of specific residues on their cytoplasmic kinase domains.[118-120] Activated IRE1, induces formation of the transcription activator spliced X-box binding protein (XBP-1) through splicing of the XBP-1 messenger RNA whereas PERK phosphorylates the α subunit of eukaryotic initiation factor 2 (eIF2α) (Figure 9). Normally, GTP-bound eIF2 binds to methionyl-transfer RNA and enhances recognition of start codon and is released from ribosomal machinery when GTP is hydrolyzed. Phosphorylation of the α subunit of eIF2 inhibits the exchange of GDP

for GTP; thus, reducing protein synthesis. Furthermore, activated PERK translationally controls the expression of activating transcription factor 4 (ATF4) that induces the expression of variable UPR-related genes involved in amino acid metabolism, regulation of oxidative stress and apoptosis.[119]

To prevent aggregation of misfolded proteins in the lumen of ER during ER stress, XBP1 and ATF6 increase expression of proteins that facilitate ER-associated degradation (ERAD). ERAD is accomplished by retrotranslocation of misfolded proteins into the cytosol followed by ubiquitination and proteasomal degradation. ER stress can also induce autophagy as an alternate route for protein degradation.[118] The exact mechanism of ER stress-induced autophagy and its probable cytoprotective function is not very well elucidated yet, but as previously stated, this process is highly regulated by p62, which has the proper domains to bind the ubiquitin moiety of the misfolded proteins as well as the LC3 on the autophagosomes.[112]

Severe ER stress can also induce apoptosis, through a process mediated by the interplay between Bcl-2 proteins and the UPR components. C/EBP homologous protein (CHOP) is a transcription factor that is induced by all three arms of the UPR that can regulate the expression of Bcl-2 proteins.[120] There is also evidence that CHOP can directly interact and activate certain BH3-only proteins such as BIM, thereby directly promoting apoptosis.[121] Moreover, It has been suggested that ER stress-induced apoptosis occurs through cleavage of caspase 4, a member of caspase 1 subfamily that localizes to the ER membrane.[121]
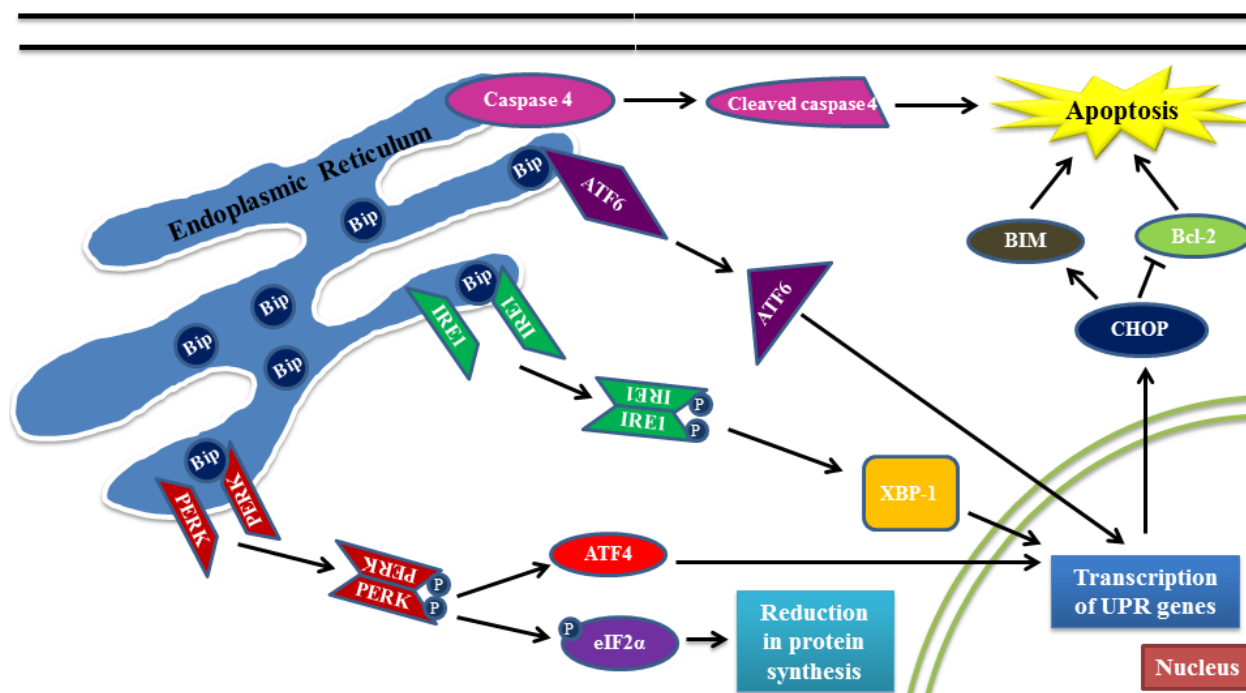
Figure 9. The mechanism of unfolded protein response. Upon accumulation of unfolded proteins in the lumen of the ER, the chaperone GRP78 (BiP) is released from the luminal domains of PERK, ATF6 and IRE1. These activated transmembrane proteins then trigger cascades of events that collectively result in expression of UPR-related genes. Severe ER stress can also induce apoptosis through CHOP-mediated changes in the expression of Bcl-2 proteins, direct activation of BH3-only proteins by CHOP, or cleavage of ER membrane-bound caspase 4.

ER Stress in Cancer

The high proliferative and metabolic rates in cancer cells lead to a tumor microenvironment characterized by glucose limitation, acidosis, and hypoxia. These conditions can result in accumulation of misfolded proteins and induction of UPR.[123,124] In fact, an increased expression of GRP78 and GRP94 have been observed in many different cancers, including cancers of breast, colon and liver. Both of these chaperones have been shown to play a role in resisting cell death.[124,125] In the same cancers, elevated level of GRP78 has also been linked to high pathologic grade, greater risk of recurrence, and poor survival.[123] Moreover, GRP78 has been shown to confer resistance to chemotherapeutics in multiple tumor type, and its knockdown has been demonstrated to sensitize the glioma cells to TMZ.[123] Furthermore, In support of the role of GRP78 in cancer, studies have indicated that heterozygous GRP78 mice had impaired tumor progression, reduced tumor sized and a longer latency period.[123,125] In addition, other studies have suggested the involvement of ER stress in the induction of angiogenesis and metastasis through upregulation of VEGF-A.[123,124] This claim is further supported by studies in xenograft models where knockdown of GRP78 was associated with less invasion and metastasis.[123] Surprisingly, GRP78 has also been detected on the surface of highly metastatic prostate cancer cells, further supporting its probable function in tumor progression and metastasis. The surface GRP78 provides a suitable, more accessible target that can be potentially utilized in combination therapies.[123] Recent studies from our laboratory have indicated that targeting GRP78 is of therapeutic utility for cancer and also for the treatment of bacterial and viral infections.[126] Collectively, these findings suggest that GRP78 can serve as a potential therapeutic target in cancer as well as a novel biomarker to enhance patient treatment in the future.[123]

CHAPTER 2: Materials and Methods

Materials

All drugs were purchased from Selleckchem (Houston, TX). Cell lines were obtained from ATCC (Bethesda, MD) and were not further validated beyond the validation statements of the provider. All media for cell culture (DMEM, RPMI, MEM Alpha, F-12 and Opti-MEM), trypsin-EDTA, penicillin-streptomycin and 1X Phosphate-buffered saline solution (PBS) were all purchased from GIBCOBRL (Invitrogen-GIBCOBRL Life Technologies, Grand Island, NY). Fetal bovine serum (FBS) was purchased from HyClone Laboratories, Inc (Thermo Scientific Hyclone, South Logan, UT). Bovine serum albumin (BSA), sodium dodecyl sulfate (SDS) and glycine were purchased from Fisher Scientific (Fair Lawn, NJ). Trypan blue solution, formaldehyde, 6-Diamidino-2-Phenylidole (DAPI), dimethyl sulfoxide (DMSO), rat serum, RIPA buffer, bovine insulin, hydrocortisone, crystal violet stain and McCoy's 5A Medium Modified were all obtained from Sigma-Aldrich (St. Louis, MO). Chaps cell extract buffer (10X) was obtained from Cell Signaling Technology (Danvers, MA). Anti-Bak, NT polyclonal and anti-Bax (active monomer, mAb, 6A7) antibodies were purchased from EMD Millipore (Temecula, CA) and Enzo Life Sciences (Farmingdale, NY), respectively. All other primary phospho-/total-antibodies were purchased from Cell Signaling Technology (Danvers, MA), Santa Cruz Biotechnology (Santa Cruz, CA) and Abcam (Cambridge, MA). Secondary antibodies (IRDye 680LT Goat anti-Mouse and IRDye 800CW Goat anti-Rabbit) and Odyssey infrared imaging system blocking buffer were obtained from LI-COR Biosciences (Lincoln, NE). Alexa Fluor 680 goat anti-mouse IgG, Alexa Fluor 594 goat anti-rabbit IgG, ethidium homodimer-1 and calcein-AM were obtained from Life Technologies (Carlsbad, CA). Validated siRNAs were purchased from QIAGEN (Valencia, CA). Recombinant adenoviruses to express

constitutively activated c-FLIP-s and Bcl-xL and dominant negative caspase 9 were purchased from Vector Biolabs, (Philadelphia, PA). Dr. S. Spiegel (VCU) kindly supplied the plasmid to express green fluorescent protein-tagged (GFP) human LC3 for vesicle formation assay. All other plasmids were obtained from Addgene (Cambridge, MA). The JNK Inhibitor VII, TAT-TI-JIP was purchased from Calbiochem (EMD Chemicals, Inc. San Diego, CA). All western blotting equipments were purchased from BIO-RAD (Hercules, CA).

Methods

Cell Culture

HUH7, HEPG2, HEP3B and HT29 cells were cultured in DMEM supplemented with 5% (vol/vol) FBS. HT1080 cells cultured in MEM supplemented with 10% (vol/vol) FBS. HCC38, BT474, MCF7 and BT549 cells were cultured in RPMI supplemented with 10% (vol/vol) FBS. HCT116, MES-SA, Saos-2 and SKES-1 were cultured in McCoy's 5a Medium Modified supplemented with 10% (vol/vol) FBS. SUM149PT cells were cultured in Ham's F-12 medium supplemented with 5% (vol/vol) FBS, 0.5% (vol/vol) bovine insulin and 0.1% (vol/vol) hydrocortisone. All media used in cell culture were also supplemented with 100 μg/ml (1% vol/vol) penicillin/streptomycin. Cells were incubated in a humidified atmosphere of 5% CO_2 at 37 °C. For cell viability assays and immunoblotting/immunofluorescence, cells were plated at a density of 2×10^4 (per well of a 12-well plate) or 5×10^3 (per well of a 96-well plate) for 24-30 hours prior to any treatment.

Drug Treatment

Plated cells were treated with desired drugs, which were taken from a 10mM stock solution and diluted in DMSO to reach the desired concentration. The maximal concentration of vehicle (DMSO) in media was 0.02% (v/v).

Assessment of Cell Viability

For trypan blue exclusion assays in 12-well plates, the media from each well was transferred into a 15ml tube. Attached cells were harvested by trypsinization with trypsin/EDTA for 5 minutes at 37°C and then transferred into the corresponding tube. After centrifugation at 1,200 rpm for 5 minutes the supernatant was removed and the pellet was re-suspended and mixed with the vital stain trypan blue. Insertion of trypan blue stain into the cell cytoplasm was used as an indicator of cell death. A total of 500 cells from randomly selected fields per experimental point were counted using a hemocytometer and a light microscope. The percentage of dead cells was expressed as a percentage of the total number of cells counted.

For live/dead imaging assays in 96-well plates, 100 µL aliquots of 1X PBS containing 1:2000 dilutions of red fluorescent ethidium homodimer-1 (to detect cells with disrupted cell membranes) and green fluorescent calcein-AM (to indicate intracellular esterase activity) was added to each well and plates were spun at 800 rpm for 3 minutes to sediment detached dead cells onto the plate. Cells were then visualized using a Hermes Wiscan instrument (IDEA Bio-Medical, Rehovot, Israel) under 10X magnification. The number of viable (green) and dead (red) cells were counted manually from several images taken from each well. All viability assays were performed in triplicates.

Western Blot Analysis

Cells were plated in 60 x 15mm dishes for 24 hours prior to treatment. They were treated with the desired concentration of drugs and were incubated for 3, 6, 12 or 24 hours. After incubation, cells were lysed and scraped using whole-cell lysis buffer (0.5 M Tris-HCl, pH 6.8, 2% (w/v) SDS, 10% (v/v) glycerol, 1% (v/v) β-mercaptoethanol, 0.02% (w/v) bromophenol blue). Collected samples were boiled for 10 minutes and then loaded onto 8-14% sodium

dodecyl sulfate–polyacrylamide gel (SDS-PAGE). Proteins were electrophoretically separated and transferred onto 0.45 μm PVDF membrane. The membrane was blocked in Odyssey blocking buffer. The membrane was then exposed to desired primary antibodies overnight. After removal of the primary antibody, the membrane was then incubated with the corresponding goat anti-mouse or rabbit secondary antibody for 2 hours at room temperature. After being washed three times with TBST, the immunoblots were visualized using an Odyssey Infrared Imager (LI-COR Biosciences, Lincoln, NE).

Infection with Adenovirus

Cells were plated in 12-well. 24 hours later the media was removed and replaced by 1ml of plain medium (lacking FBS and penicillin-streptomycin). Recombinant adenoviruses to express constitutively activate c-FLIP-s, Bcl-xL and dominant negative caspase 9 or empty vector virus were added at a multiplicity of infection (MOI) of 50. In case of infection in 96-well plates, the plain medium containing the adenoviruses was prepared in 1.5 mL-eppendorf tubes and then distributed in 100 μL portions into the corresponding wells. The plates were incubated for 6 hours and then the plain media was replaced by serum-containing medium (supplemented by FBS and penicillin-steptomycin). The cells were then incubated for 24 hours to ensure adequate expression of transduced gene products prior to drug exposures.

Plasmid and siRNA Transfection

For transfection, 0.5 μg of each plasmid was diluted into 50 μl of Opti-MEM medium with no added serum or antibiotic and was incubated in solution for 5 minutes at room temperature. Concurrently, 1 μl of Lipofectamine 2000 reagent (Invitrogen, Carlsbad, CA) was diluted into 50 μl of the same medium and was given the same incubation time. After 5 minutes, the two solutions were mixed together and incubated at room temperature for 20 minutes. The

total mix was added to each well containing 400 µl of the same serum/antibiotic free medium. Cells were incubated for 4 hours before equal volume (500 µl) of the appropriate medium containing twice the volume of required FBS was added to each well. Cells were then incubated for 24 hours before being exposed to desired drugs.

Transfection with validated siRNAs was performed in a similar fashion to plasmids with all specified siRNAs used at 10nM concentration of the annealed siRNA or the negative control (a "scrambled" sequence with no homology to any known genes in human or mouse cell lines).

Protein Analysis by Immunofluorescence Imaging

Cells plated in 96 well plates were treated with desired drugs for certain amount of time and were then washed with 1X PBS and fixed in 4% paraformaldehyde for 15 minutes. Fixated cells were then blocked with 0.5% triton-X-100 PBS solution supplemented with 10% rat serum for 1-2 hours followed by an overnight exposure to 1:500 solution of desired primary antibodies. Cells were then washed with PBS and incubated with a 1:2000 dilution of appropriate secondary Alexa Fluor anti-mouse or anti-rabbit for 2-4 hours. Fluorescent signals were detected using a Hermes Wiscan instrument (IDEA Bio-Medical, Rehovot, Israel).

LC3-GFP Vesicle Formation Assay

Cells were plated in 4-well glass slides and were transfected with the LC3-GFP plasmid. 24 hours after transfection, cells were treated with the indicated drugs and were visualized on a ZeissAxiovert 200 micoscope (Carl Zeiss, Wake Forest, NC) 6 and 12 hours after the treatment. The number of vesicles in 40 cells representing each group was counted, and the average vesicles formed in each group was calculated. Colocalization of LC3 to the lysosomal and the mitochondrial membranes was assessed using LysoTracker Red DND-99 (Life Technologies, #L7528) and MitoTracker Red CMXRos (Life Technologies, #M7512), respectively. 24 hours

after drug exposure, the medium was removed and the cells were incubated with plain medium (no serum added) containing 25nM of either LysoTracker or MitoTracker probe for 30 minutes before being subjected to fluorescent microscopy as previously described.

Tumor Cell Isolation

Tumor dissociation was performed using a GentleMACS Dissociator purchased from Miltenyi Biotec (San Diego, CA) and was carried out according to the manufacturer's recommended protocol. In short, extracted tumors were cut into small pieces of 2-4 mm and were put in a compatible GentleMACS tube with the recommended enzyme mixture. The samples were mixed and homogenized by GentleMACS Dissociator and were incubated for 30 minutes at 37ºC under continuous rotation. After a short centrifugation at 1500 rpm, cells were re-suspended and applied to a strainer 30-70 μm (based on cell size). Cells were then grown in appropriate cell medium.

In Vitro **and** *Ex Vivo* **Colony Formation Assay**

250-1000 cells/well were seeded in a 6-well plate. A day later, cells were treated with appropriate drugs for 24 hours before the drug-containing medium was aspirated and replaced by fresh medium. The cells were then cultured for up to two weeks until colonies were observed in the control group. The medium was then removed and cells were washed with 1X PBS. The cells were then fixed in 100% methanol for 10 minutes. After methanol removal, 0.1% (vol/vol) crystal violet stain was added to each well for at least 1 hour. Wells were the washed and number of colonies was counted manually.

For *ex vivo* colony formation assay, the tumors were harvested from the nude mice at the time of sacrifice and were isolated (as previously described) to obtain a single cell suspension.

Cells were then plated 100-10000/well of a 6-well plate. Colonies were permitted to form for 7-10 days and were fixed, stained and counted.

Analysis of ROS and RNS Levels

Cells were plated into a 96-well plate at a density of 10,000 cells/well. 24 hours later, cells were incubated with 2',7'-Dichlorofluorescin diacetate (Sigma, #122M4000V) at a concentration of 10 µM, or 3-Amino-4-(N-methylamino)-2', 7'-difluorofluorescein diacetate (DAF-FM DA) at a concentration of 4 µM for 30 minutes. The DCF-containing medium was then removed and cells were washed with 1X PBS before 100 µL of fresh medium containing desired drugs was added to the wells. DCFDA/ DAF-FM DA fluorescence signals were detected 2 and 6 hours after drug exposure using a VICTOR 3 plate reader (PerkinElmer, Waltham, MA).

Lipid Analysis by Mass Spectrometry

Equal number of cells (6×10^6 per well of a 6-well plate) were treated with indicated drugs for 6 hours and lipids were extracted. Bioactive lipid levels were quantified at VCU Lipidomics/Metabolomics Core Facility by liquid chromatography-electrospray ionization-tandem mass spectrometry (LC-ESI-MS/MS) with a Shimadzu LC-20AD binary pump HPLC system (Shimadzu, Kyoto, Japan) and a 4000 QTRAP (Applied Biosystems, Carlsbad, CA) operating in a triple quadruple mode as previously described by Hait et al., 2009.[127]

Immunoprecipitation

1X Chaps cell extract buffer was prepared according to the manufacturer's protocol from a 10X stock purchased from Cell Signaling Technology (#9852). 24 hours after treatment with indicated drugs, cells were lysed in 1X Chaps buffer and scraped off into a 1.5 mL tube. Cells were frozen at -80ºC and thawed at room temperature twice, and were spun down at 14,000 rpm for 10 minutes. The supernatant was kept and pelleted cell debris was discarded. Concurrently,

polystyrene beads (15 µm) (Nalgene, #114218900) were incubated with desired primary antibody overnight. Beads were then washed with 1X PBS and were centrifuged at 5000 rpm for 2 minutes (this step was repeated at least two times). Cell lysates were then added to the antibody-coated beads and were incubated overnight at 4ºC on a suitable shaker. Immunoprecipitated complexes were collected by centrifugation at 5,000 rpm for 2 minutes, and the supernatant was discarded. The pellet from the previous step was washed with 1X Chaps buffer at least 3 times to remove any non-specific proteins or unbound antibody. Finally, SDS sample buffer (as previously described in western blot analysis) was added to the pellets and samples were heated at 100ºC for 5 minutes. Samples were then cooled on ice and were subjected to western blot analysis.

Immunohistochemistry

In order to deparaffinize the sectioned tissues, Slides were heated in a Hybaid hybridization oven (Thermo Scientific) at 60 ºC for 30 minutes and were then washed with xylene substitute (Thermo Scientific, #9990505) three times (10 minutes each). Then, the slides were washed for 5 minutes with 100% ethanol (Decon Labs, Inc., #2401), 95% ethanol and 70% ethanol, respectively. In the next step, antigen retrieval was carried out using 10mM sodium citrate (Sigma, #71497) buffer (pH 6.0). The samples were placed in the buffer, boiled for 15 minutes and were allowed to cool down in room temperature for 1.5-2 hours. Samples were washed three times with 1X PBS and a hydrophobic line was drawn around each specimen using an immunopen (Calbiochem, #402176). The samples were incubated for 1 hour with a blocking buffer containing 1% BSA (Fisher Scientific, #138191) and 1% goat serum (Life Technologies, #16210064) dissolved in TBST. After the blocking buffer was removed, the primary antibodies

(1:200) followed by the fluorescent secondary antibodies (1:5000) were added and the slides were viewed using the Hermes Wiscan instrument (IDEA Bio-Medical, Rehovot, Israel).

Tissue Microarray and Immunostaining

Human HCC tissue microarrays were purchased from Imgenex Corporation (San Diego, CA). Two tissue microarrays were used: one containing 40 primary HCC, 10 metastatic HCC and 9 normal adjacent liver samples (Imgenex, IMH-360), the other containing 46 primary HCC and 13 metastatic HCC (Imgenex, IMH-318). Antigen retrieval was performed by the Department of Pathology, VCU (with thanks to Dr. George Alemara). Immunostaining was performed using anti-PDE5 antibody (1:50) or using a mixture of anti PDGFRα and anti-PDGFRβ (1:50 for each) as described in the previous page under immunohistochemistry. After immunostaining slides were stained in Harris hematoxylin solution for 8 minutes and were then rinsed in running tap water. In the next step, differentiation was performed in 1% acid alcohol for 30 seconds and slides were washed again in running tap water. Bluing was done in 0.2% ammonia water for 30 seconds to 1 minute and samples were rinsed again in tap water. Samples were then counterstained with eosin-phloxine for 1 minute. Samples were then dehydrated through 2 five-minute washes with 95% ethanol. Finally, slides were mounted with xylene-based mounting medium and were examined by a confocal microscope.

Tissue Sectioning and H&E Staining

All harvested tissues and organs from animals were preserved in Formalin solution 10% (Sigma, #SLBH1382V) for 24 hours and were sent out to the Biological Macromolecule Core Facility at VCU for paraffin sectioning and H&E staining. Basic histology was performed at the VCU Massey Cancer Center Macromolecule Core Facility, sponsored, in part, with funding from NCI Cancer Core Grant P30 CA16059.

Animal Studies

Athymic female NCr-nu/nu mice (National Cancer Institute) weighing 20-25 grams were used for the human tumor xenograft studies. Mice were maintained in a pathogen-free vivarium approved by the American Association for Accreditation of Laboratory Animal Care and in accordance with current regulations and standards of the US Department of Agriculture, the US Department of Health and Human Services, and the National Institute of Health. For each experiment, ~40 mice (~10 per treatment group) were inoculated each with 5×10^6 cells in 100 µL (total) of Matrigel (BD, #354234) and 1X PBS (1:1 ratio), subcutaneously either into the right rear flank (HUH7, HT29 and HT1080) or into the right fourth mammary fat pad (BT474). Seven days after tumor implantation, mice were treated with either vehicle (1:1 ratio of Cremophor EL (Sigma, #037K0213) and sterile water) or indicated drugs (dissolved in the same solution as the vehicle) for 3-7 days (different for each experiment) by oral gavage. Animals were monitored daily and the size (length and width) of each tumor was measured twice a week. The tumor volumes were calculated using the formula $(L \times W^2)/2$. When the volume of the tumors reached >1500 mm^3, animals were humanely sacrificed and the tumor, blood and specific organs were collected for further studies. Animal survival was plotted on a Kaplan-Meier graph and longitudinal statistical assays were performed.

Multiplex Assay for Cytokine Expression

The Bio-Plex Multiplex Reader with associated software and all the related kits and reagents were obtained from BIO-RAD (Hercules, CA). The collected blood plasma and tumors from the animal experiments were assayed according to the manufacturer's protocol and with BIO-RAD technical assistance. The following Bio-Plex assay plates were used for the assessment of human cytokines: Bio-Plex Pro Human Cytokine Group 14-Plex (Y500023JM2),

Human CYTO STD GRPII 23-Plex (171D60001), Human CYTO HGF set (171B6008M), Human CYTO SDF-1a set (171B6019M), Pro Human Cancer 2 18-Plex (171AC600M) and BP Pro TGF-B 3-Plex (171W4001M).

Multiplex Assay for Signal Transduction Protein Phosphorylation and Expression

The following Bio-Plex assay plates were used to examine tumor cell signal transduction proteins: Bio-Plex Pro Phosphoprotein magnetic 8-Plex (LQ000041XUYDC4), Bio-Plex Pro Phosphoprotein magnetic 15-Plex (LQ000064Q3MJ1). Tumor lysates were assayed according to the instructions provided by the manufacturer.

Data Analysis

The effects of various treatments were analyzed using one-way analysis of variance and a two-tailed Student's *t*-test. Median dose effect isobologram analysis to determine synergism of drug interaction was carried out according to the methods of Chou and Talalay[151] using the CalcuSyn program for Windows (Biosoft). Based on this method, a combination index value of < 1.00 indicates synergistic effect, a value of 1.00 indicates additivity, and a value of greater > 1.00 equates antagonism of action between the drugs. Statistical examination of *in vivo* animal survival data utilized log rank statistical analyses between the different treatment groups. Results with a *P* value of <0.05 were considered statistically significant. Experiments shown are the means of multiple individual points from multiple experiments (±SEM).

CHAPTER 3: Sildenafil Enhances the Toxic Effects of Sorafenib and Regorafenib in Hepatoma and Colon Cancer Cells

Hepatocellular Carcinoma

Hepatocellular carcinoma (HCC) is the fifth most prevalent cancer in the world, with nearly half a million new cases per year.[128-130] Major risk factors for this highly fatal cancer include, hepatitis C, hepatitis B, heavy alcohol consumption, hemochromatosis, and cirrhosis.[128,129] Approximately 80% of the new HCC cases are diagnosed in Africa and Asia, mainly due to the hepatitis B virus infection. However, the incidence of HCC has been rising rapidly in the western world because of the high prevalence of hepatitis C virus infection.[130] HCC is associated with poor prognosis, and the disease is generally diagnosed late in its progression. Therefore, only ~30% of the patients are eligible for curative therapies, including tumor resection and liver transplantation.[128] Current curative and palliative treatments available to the patients vary depending on the stage of the disease.[128] They include:

1. Surgical resection: the optimal candidates for surgery are non-cirrhotic patients with solitary non-metastatic lesions. The risk of recurrence 5 years after surgical resection is more than 70%. There are no adjuvant or neoadjuvant therapies available to reduce the recurrence rate.

2. Orthotopic liver transplantation: transplantation just like surgery is among the best treatments available for the patients diagnosed at early stage of their disease. However, due to a shortage of organ donors, nearly 40% of the patients drop out because of tumor progression.[128]

3. Radiofrequency ablation (RFA): this method involves application of radiofrequency thermal energy locally to the lesions, and induction of necrosis in the tissue surrounding the electrode. This treatment is considered safe and effective for the patients ineligible for surgery.[128]

4. Transarterial chemoembolization (TACE): since the majority of blood supply for the hepatic tumors is received through the hepatic artery, injection of chemotherapeutic lipiodol emulsion into the hepatic artery presents a feasible approach. The common chemotherapeutics used in HCC treatment are adriamycin and cisplatin. However, this method has failed to provide any survival advantage.[128]

5. Targeted therapy: due to the frequent deregulation of Raf/MEK/ERK pathway and highly vascularized nature of HCC tumors, sorafenib became the first approved form of systemic therapy in the treatment of HCC. However, sorafenib produced only a modest effect in a phase II trial, where 33% of the patients showed stable disease for a period of 16 weeks.[128] Therefore, there is a substantial need to improve the clinical outcome of the systemic therapy in HCC.

Sorafenib

The bi-aryl urea sorafenib (BAY 43-9006, Nexavar) is an oral multi-kinase inhibitor, which inhibits a wide range of targets, including Raf-1, B-Raf (wild type and mutant V600E), VEGFR 1/2/3, PDGFRβ, FLT3, RET, and c-Kit with half maximal inhibitory concentration (IC_{50}) values in low nanomolar ranges.[130-134] The development cycle of sorafenib (Figure 10) took approximately 11 years and it was first approved by Food FDA in December 2005 for the treatment of advanced renal cell carcinoma (RCC).[132] Sorafenib was later approved as the first systemic therapy in advanced HCC as monotherapy with this targeted agent was proven to prolong overall survival and delay the progression time.[131] Crystallographic studies of sorafenib interaction with the kinase domain of B-Raf revealed that the drug bound to the ATP-binding pocket, thus blocking substrate binding and phosphorylation.[132] The steady-state plasma concentrations for Sorafenib in patients who received 800 milligram daily dose of the drug (400 mg bid) were reached in 7 days, and its toxicity was well tolerated, with adverse effects limited

to fatigue, diarrhea and hand or foot skin reactions.[131] Sorafenib has an estimated half-life of 25-48 hours, and is primarily metabolized in the liver via cytochrome P450 (CYP) 3A4.[131] *In vivo* and *in vitro* studies have indicated the ability of sorafenib to interrupt tumor growth and tumor microvasculature through anti-proliferative, anti-angiogenic, and pro-apoptotic effects.[134]
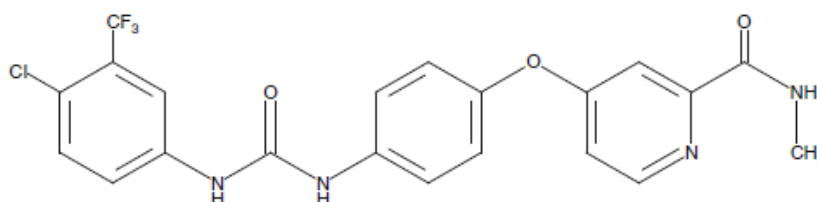

Figure 10. Chemical structure of sorafenib.[131]

Colorectal Cancer

Colorectal cancer (CRC) is the fourth most prevalent cancer in men and the third most common cancer in women worldwide.[135] It is also the third most fatal cancer, claiming the lives of almost a half a million people annually.[136] Surgical resection followed by 5-FU-based chemotherapy remains the standard of care for CRC patients.[135-137] The current recommended adjuvant treatments include: folinic acid + 5-FU + oxaliplatin (FOLFOX) or folinic acid + 5-FU + irinotecan (FOLFIRI) in combination with an anti-EGFR targeted agent such as bevacizumab, cetuximab, or panitumumab. The use of anti-EGFR antibodies is not recommended in patients with K-Ras mutations.[135] Regorafenib is another targeted agent that initially got approved for the treatment of metastatic CRC, but its approval was later expanded to include all the gastrointestinal stromal tumors (GISTs).[138] Lately, the sequential administration of regorafenib with standard chemotherapy has been shown to have a promising effect with a manageable level of toxicity.[139] A phase II clinical study is currently investigating the potency of the combination

of regorafenib and FOLFIRI in patients with K-Ras- or B-Raf-mutant CRC after a FOLFOX regimen.[139]

Regorafenib

Regorafenib (BAY 73-4506, Stivarga) is an oral diphenylurea multi-kinase inhibitor that is structurally similar to sorafenib. The addition of a fluorine atom in the central phenyl ring makes it pharmacologically more potent than sorafenib (Figure 11).[139] Just like sorafenib, regorafenib have been shown to have an inhibitory effect on a broad range of kinases, including Raf-1, B-raf (wild type and mutant V600E), VEGFR 1/2/3, PDGFRβ, FLT3, RET, c-Kit, p38, tyrosine kinase with immunoglobulin and epidermal growth factor homology domain-2 (TIE-2), an fibroblast growth factor receptor 1 (FGFR1).[138-140] One of the major reasons of failure behind antiangiogenic therapies is the infiltration of tumor-associated macrophages in the tumor microenvironment. These TIE-2-expressing macrophages (TEMs) have been found in a variety of tumors and are known to enhance angiogenesis and tumor progression. Therefore, regorafenib, a TIE-2 and VEGFR inhibitor, is a more potent inhibitor of angiogenesis than sorafenib.[140] Regorafenib is metabolized primarily in the liver by CYP3A4, and its half-life has been determined to be 20-30 hours.[138] The recommended daily dose for regorafenib is 160 mg with toxic side effects limited to skin rash, fatigue, hypertension, mucositis and diarrhea.[138,139]
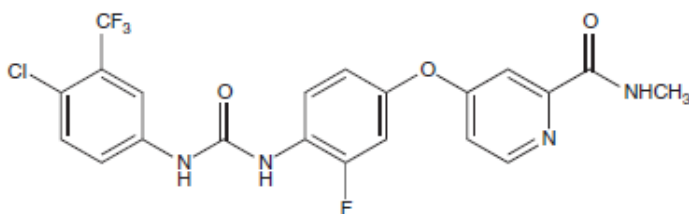

Figure 11. Chemical structure of regorafenib.[139]

Sildenafi Citrate

Manufactured by Pfizer, Sildenafil citrate (Viagra) was approved by FDA in March 1998 as the first orally active drug for the treatment of erectile dysfunction.[141] Sildenafil is a potent selective inhibitor of cGMP-specific PDE5, and has also been clinically approved for the treatment of pulmonary hypertension.[142] Sildenafil is rapidly absorbed and reaches maximum plasma concentration (C_{max}) within 1 hour after dosing. Sildenafil has a terminal half-life of ~4 hours, and is metabolized by hepatic enzymes CYP3A4 (major) and CYP2C9 (minor).[142] The adverse effects of sildenafil are limited to headache, flushing and dyspepsia.[142]
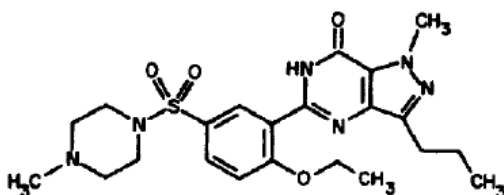
Figure 12. Chemical structure of sildenafil.[141]

Fingolimod

Developed by Novartis, fingolimod (FTY720, Gilenya) is a sphingosine 1-phosphate (S1P) receptor agonist that was approved by FDA as the first oral agent for the treatment of relapsing forms of multiple sclerosis (MS).[143,144] Upon entering the blood circulation, fingolimod is phosphorylated by sphingosine kinase 2 and converted to the S1P analogous form, *S*-fingolimod-phosphate. This active phosphorylated form of the drug is an agonist for the S1P receptors.[143,144] Further studies indicated that fingolimod acts as a functional antagonist leading to S1P receptor internalization and degradation.[143,144] Fingolimod causes retention of lymphocytes in lymph nodes, thereby reducing the peripheral lymphocytes. It also crosses the

blood brain barrier where it further reduces the severity of neuropathological outcomes of MS.[143,144] Fingolimod is very slowly absorbed and reaches C_{max} in 12-24 hours. It has an approximate half-life of 9-10 days, and is predominantly metabolized by CYP4F.[144] The major side effects of fingolimod are bradycardia and slowing of the atrioventricular conduction accompanied by fatigue and dizziness.[144]
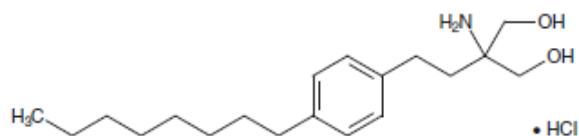

Figure 13. Chemical structure of fingolimod hydrochloride.[143]

The drug Combination Rationale

Prior studies from our laboratory demonstrated that PDE5 inhibitors enhanced the toxicities of multiple chemotherapies.[145,146] In these studies PDE5 inhibitors, in a NOS-dependent fashion, were shown to enhance chemotherapy effect through activation of CD95 receptors, the generation of ROS, and mitochondrial dysfunction. Das *et al*[147] have reported similar results, further establishing a link between the activation of CD95 death receptor pathway and sildenafil-mediated lethality. Additionally, other studies have indicated that sildenafil reversed the ABCB1- and ABCG2-mediated MDR phenotype, leading to an increase in intracellular concentration of chemothetrapeutics.[148] Inhibition of major efflux pumps could also be another contributing factor to the sildenafil-mediated enhanced chemotherapy. Furthermore, several studies have reported increased PDE5 expression in multiple cancers, including metastatic breast cancer, colon adenocarcinoma, bladder squamous carcinoma, and lung cancer, implying a potential role in the cancer progression.[147] Collectively, these discoveries suggested that PDE5 inhibitors could be repurposed as targeted anti-cancer therapeutics. Therefore, we

hypothesized that PDE5 inhibitors would enhance the effect of sorafenib, which is currently approved for the treatment of HCC in the clinic. Since regorafenib is a more potent analogue of sorafenib approved for the treatment of colon cancer, we later expanded our studies to evaluate its interaction with sildenafil to kill colon cancer cells *in vivo*.

Later in our investigations, we also observed an increase in ceramides and S1P levels in response to regorafenib. S1P has previously been linked to the induction of colitis-associated cancer (CAC), and treatment with FTY720 has been shown to block CAC progression.[149,150] Therefore, we hypothesized that the addition of FTY720 would enhance the lethality of regorafenib individually or in combination with sildenafil in killing colon cancer cells.

Hypothesis

Inhibition of PDE5 enhances the toxicities of sorafenib and regorafenib through activation of CD95 death receptor signaling, and NOS-dependent generation of ROS and RNS.

Cell Line	Major Characteristics
HEP3B	Mutant p53, CD95, Wild Type RAS
HEPG2	Wild Type p53, CD95, Mutant N-RAS
HUH7	Mutant p53, CD95 null, Wild Type RAS
HT29	Mutant p53, CD95, Wild Type K-RAS
HCT116	Wild Type p53, CD95, Mutant K-RAS

**Table 1. Hepatic and colon cancer cell lines used in this study.**

Results

Sildenafil and sorafenib/regorafenib interact to kill hepatoma cells

Initial studies examined the dose-response of death receptor CD95 expressing HEP3B cells to increasing concentrations of sorafenib (also referred to as SOR in the figures) individually and in combination with sildenafil (also referred to as SIL in the figures). Sildenafil enhanced sorafenib toxicity in HEP3B cells in a dose dependent fashion (Figure 14A). Sildenafil (2 µM) also interacted with sorafenib (2 µM) to kill other hepatoma cells, regardless of whether the cells expressed CD95, i.e., HUH7 cells are CD95 null (Figure 14B).

Regorafenib is a derivative of sorafenib with greater solubility and potency *in vitro* and *in vivo* than the parent compound. The dose-response of death receptor CD95 null HUH7 cells to increasing concentrations of regorafenib (also referred to as REGO/REG in the figures) individually and in combination with sildenafil was examined. Similarly to sorafenib, sildenafil enhanced regorafenib toxicity in a dose dependent fashion (Figure 15A). Sildenafil (2 µM) also interacted with regorafenib (0.5 µM) to kill colon cancer cells (Figure 15B).

As previously stated, PDE5, the target of sildenafil, has been shown to be overexpressed in multiple cancer types.[147] In addition, in prior studies, we had demonstrated that PDGFRα/β play an important role in the biology of sorafenib in terms of its toxic combination with other therapeutics.[152] Knockdown of PDE5 expression enhanced regorafenib toxicity in HUH7 cells (Figure 16), and, similarly, knockdown of PDGFRα/β recapitulated the combinatorial effect of sorafenib when combined with sildenafil. (Figure 17).

A
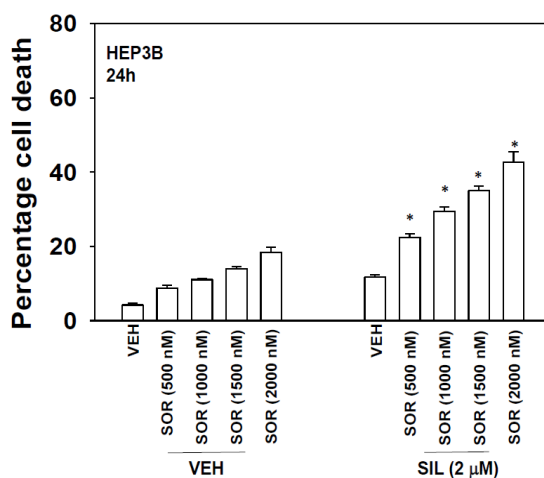
B

Figure 14. Sorafenib and sildenafil interact to kill hepatoma cells. (A) HEP3B cells were treated with vehicle (DMSO), increasing concentration of sorafenib (0.5-2 μM), and/or Sildenafil (2 μM). Cells were isolated 24 hours after drug exposure and viability was determined via trypan blue exclusion assay. (B) Hepatoma cells were treated with indicated drugs for 24 hours. Cells were then isolated and subjected to trypan blue exclusion assay (n = 3, ± SEM). *$P < 0.05$ greater than vehicle control.
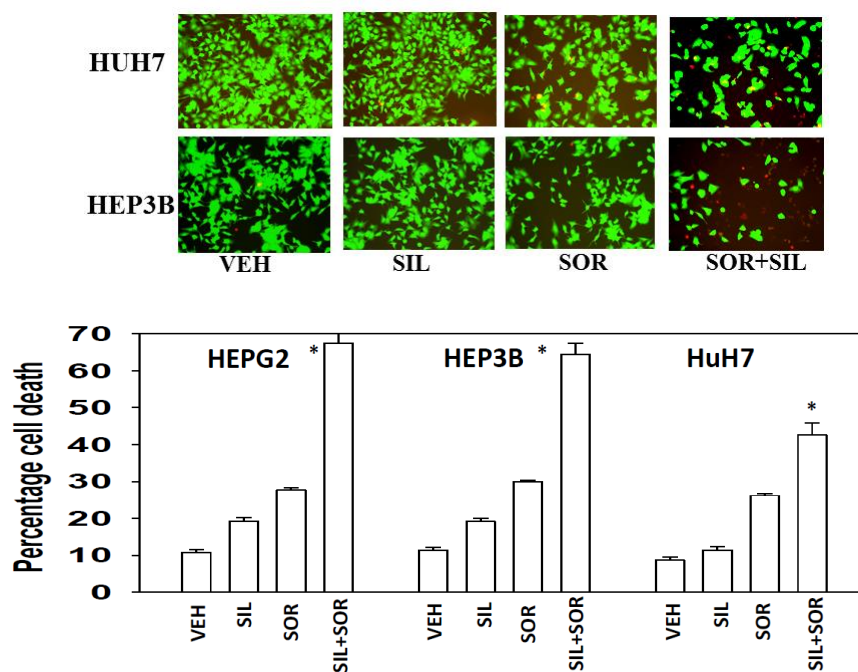
A

B
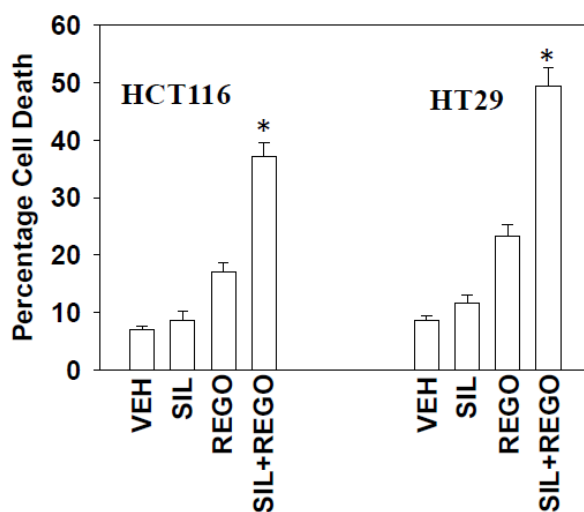
Figure 15. Regorafenib and sildenafil interact to kill hepatoma and colon cancer cells. (A) HUH7 cells were treated with vehicle (DMSO), increasing concentration of regorafenib (300-1500 nM), and/or Sildenafil (2 μM). Cells were isolated 24 hours after drug exposure and viability was determined via trypan blue exclusion assay. (B) Colon cancer cells were treated with indicated drugs for 24 hours. Cells were then isolated and subjected to trypan blue exclusion assay (n = 3, ± SEM). *$P < 0.05$ greater than vehicle control.
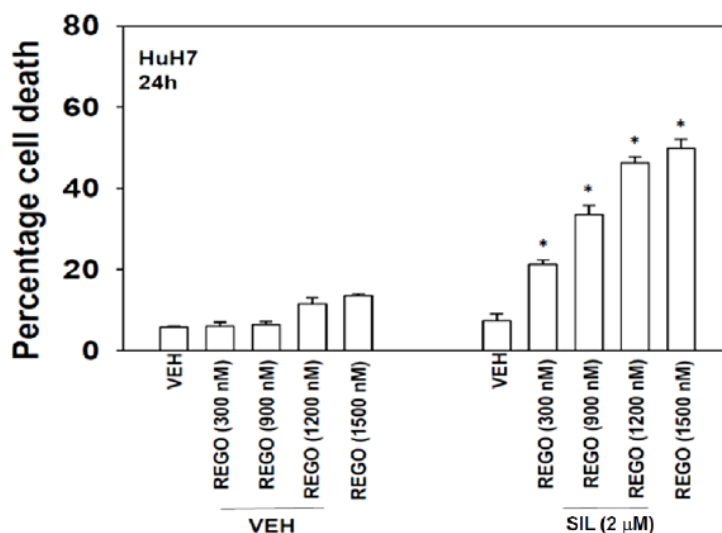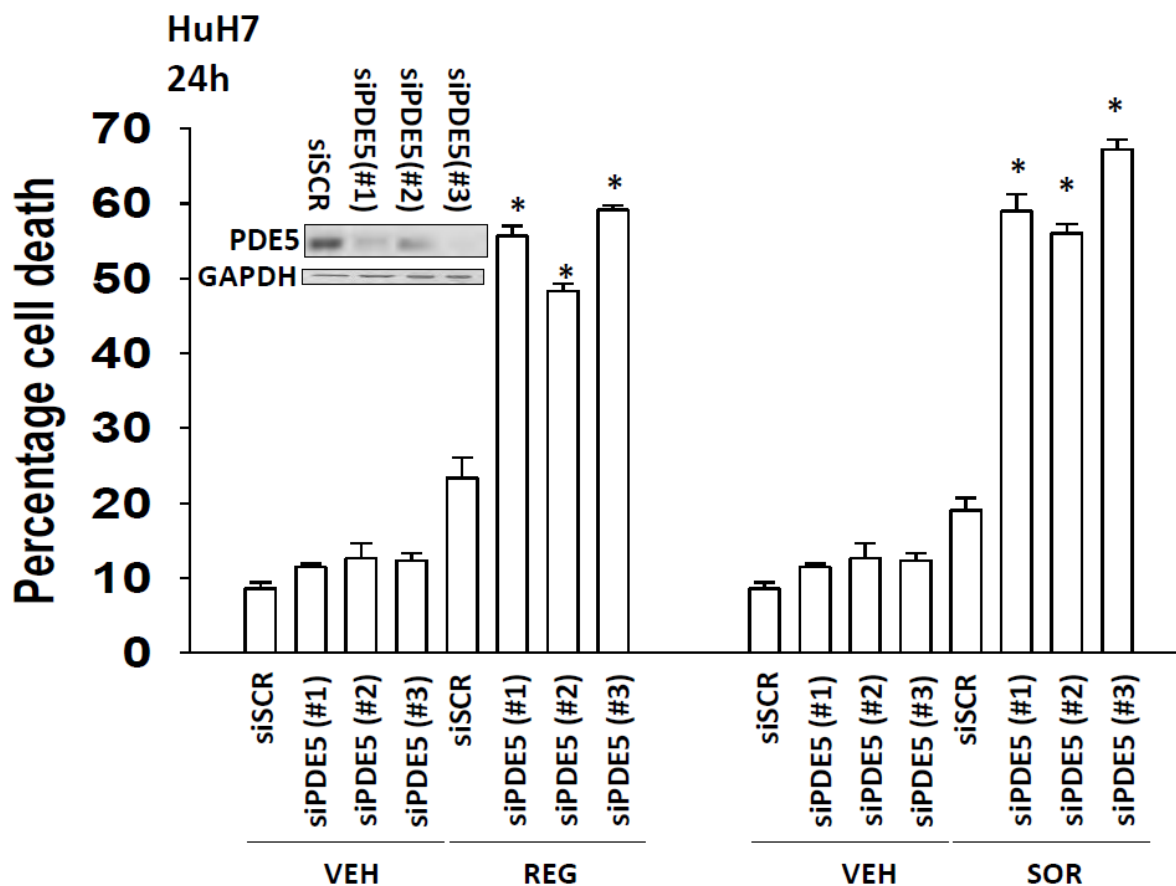
Figure 16. Knockdown of PDE5 enhances regorafenib toxicity. HUH7 cells were transfected with a control scrambled siRNA (siSCR) or three different siRNAs to knockdown expression of PDE5. 36 hours after transfection, cells were treated with vehicle (DMSO), or regorafenib (0.5 μM), or sorafenib (2 μM). 24 hours after drug exposure, cells were isolated and viability determined by trypan blue exclusion assay (n = 3, ± SEM). *$P<0.05$ greater than corresponding value in siSCR cells.

Figure 17. Knockdown of PDGFRα/β enhances sildenafil toxicity. HEP3B cells were transfected with a control scrambled siRNA (siSCR) or two different siRNAs to knockdown expression of PDGFRα and PDGFRβ. 36 hours after transfection, cells were treated with vehicle (DMSO), or sildenafil (1-2 μM). 24 hours after drug exposure, cells were isolated and viability determined by trypan blue exclusion assay (n = 3, ± SEM). *P<0.05 greater than corresponding value in siSCR cells.
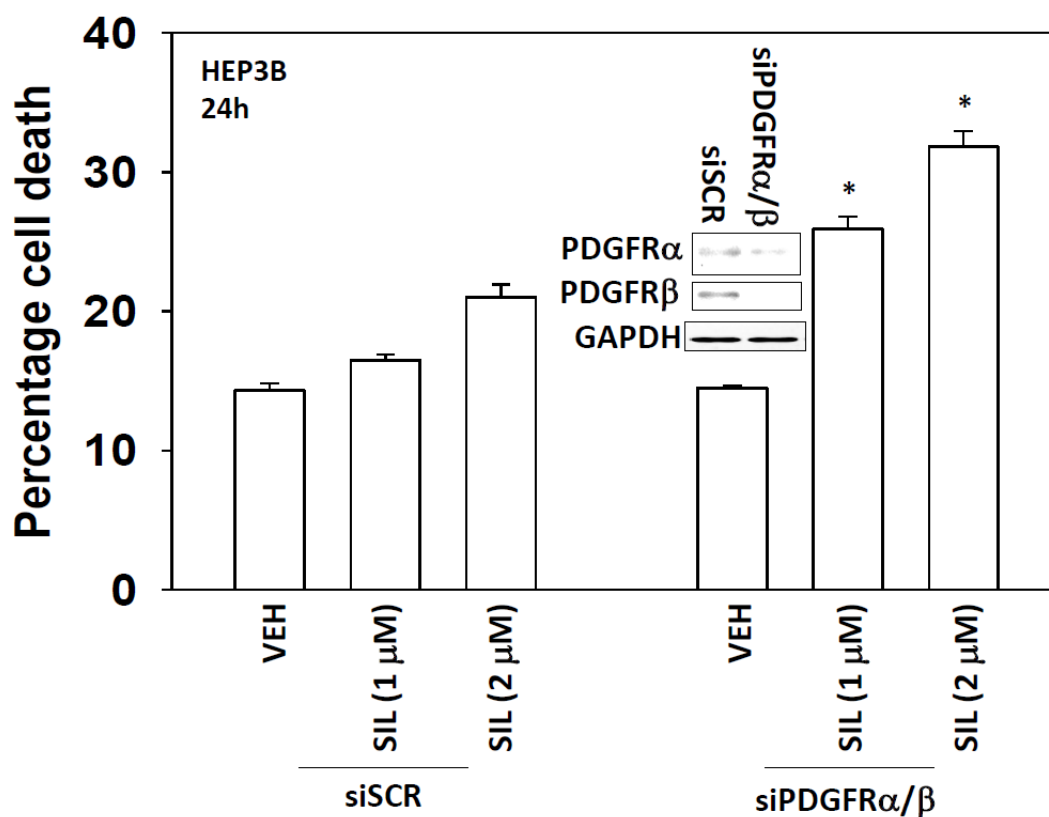
The drug combination activates JNK1/2 and inhibits AKT, mTOR and ERK1/2

Treatment of HUH7 cells with the combination of regorafenib (0.5 µM) and sildenafil (2 µM) reduced the phosphorylation of p38, ERK1/2, AKT (T308) and mTOR (S2448), and enhanced phosphorylation of JNK1/2 (Figure 18A). The drug combination also reduced the phosphorylation of MEK1 (S218/S222). No obvious change was noted in MEK1 (S298) phosphorylation (Figure 18B).

Next, we determined if the aforementioned alterations in the phosphorylation of key signaling proteins affected the drug combination toxicity. Expression of activated forms of MEK1 (caMEK1) or AKT (caAKT) partially suppressed the drug combination lethality whereas activated form of mTOR (camTOR) or inhibition of JNK1/2 abolished the drug combination toxicity in HEPG2 cells (Figure 19) and HUH7 cells (Figure 20).
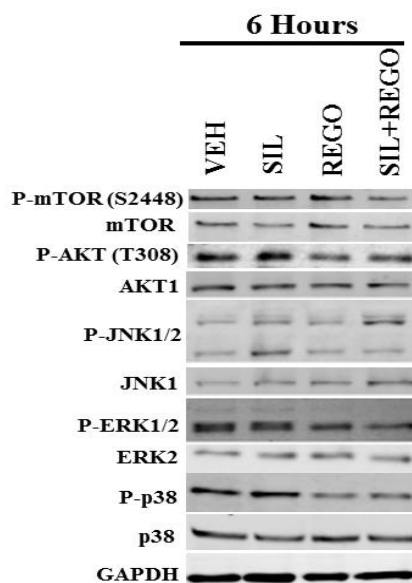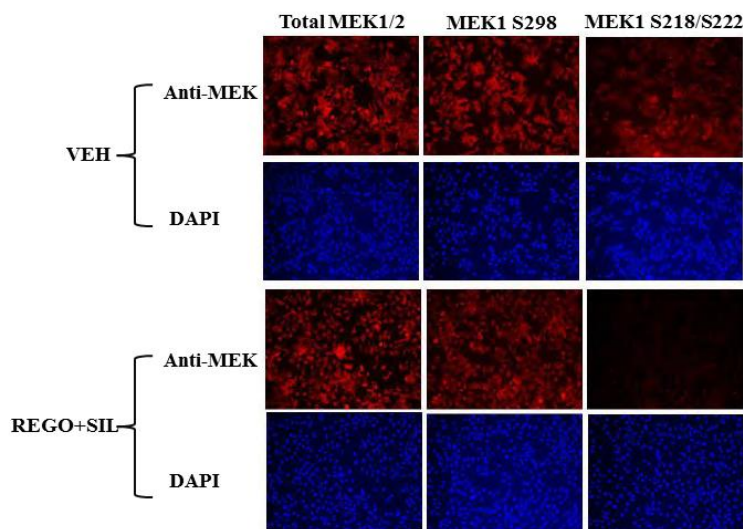
Figure 18. The REGO+SIL combination alters major signaling pathways. (A) HUH7 cells were treated with vehicle (DMSO), regorafenib (0.5 μM), sildenafil (2 μM), or the drug combination for 6 hours. Cells were lysed and expression of indicated proteins was determined by western blot. (B) HUH7 and HT29 cells plated in 96-well plates were treated with indicated drugs (REGO 0.5 μM + SIL 2μM). 6 hours after drug exposure, cells were fixed and probed with the indicated antibodies. Images were acquired using a Hermes Wiscan system.
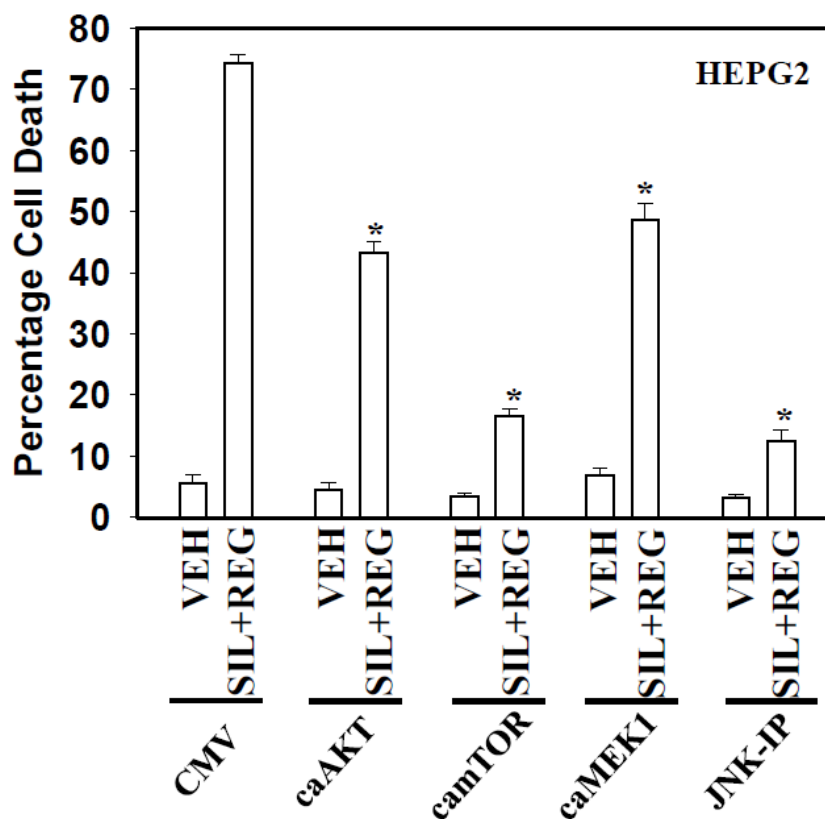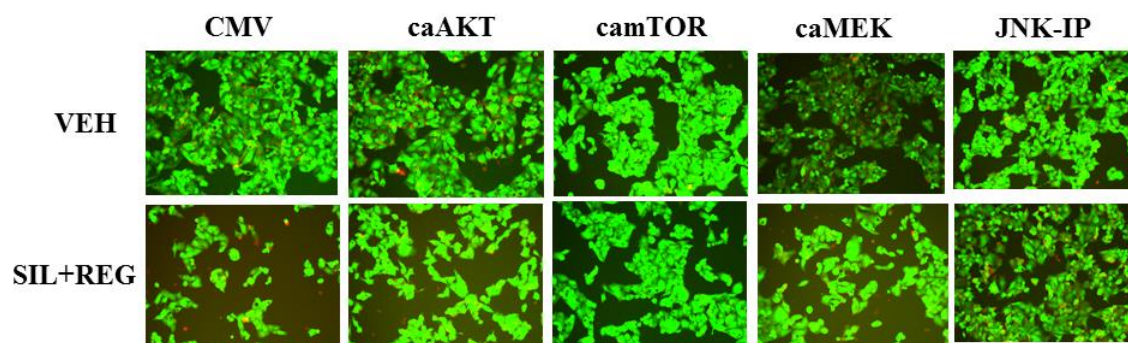
Figure 19. Inhibition of JNK1/2 and activation of AKT, mTOR, and MEK1suppresses the REGO+SIL combination lethality in HEPG2 cells. HEPG2 cells were transfected with plasmids to express either empty vector (CMV), activated MEK1 (caMEK1), activated AKT (caAKT), or activated mTOR (ca mTOR). 24 hours after transfection, cells were treated with vehicle (DMSO) or regorafenib (0.5 μM) + sildenafil (2 μM) combination. Cell viability was assessed 24 hours after drug exposure using a Hermes Wiscan instrument (n = 3, ± SEM). *$P<$ 0.05 lower than corresponding value in CMV cells. For JNK1/2 inhibition, plated cells were treated with the JNK inhibitory peptide (JNK-IP) for 30 minutes before the drugs were added accordingly. The viability was determined in a similar way using a Hermes Wiscan instrument.

Figure 20. Inhibition of JNK1/2 and activation of AKT, mTOR, and MEK1suppresses the REGO+SIL combination lethality in HUH7 cells. HUH7 cells were transfected with plasmids to express either empty vector (CMV), activated MEK1 (caMEK1), activated AKT (caAKT), or activated mTOR (ca mTOR). 24 hours after transfection, cells were treated with vehicle (DMSO) or regorafenib (0.5 µM) + sildenafil (2 µM) combination. Cell viability was assessed 24 hours after drug exposure using a Hermes Wiscan instrument (n = 3, ± SEM). *$P < 0.05$ lower than corresponding value in CMV cells. For JNK1/2 inhibition, plated cells were treated with the JNK inhibitory peptide (JNK-IP) for 30 minutes before the drugs were added accordingly. The viability was determined in a similar way using a Hermes Wiscan instrument.

The drug combination induces ER stress

A major biological effect of sorafenib is the induction of ER stress/UPR, with reduced expression of proteins that have short hal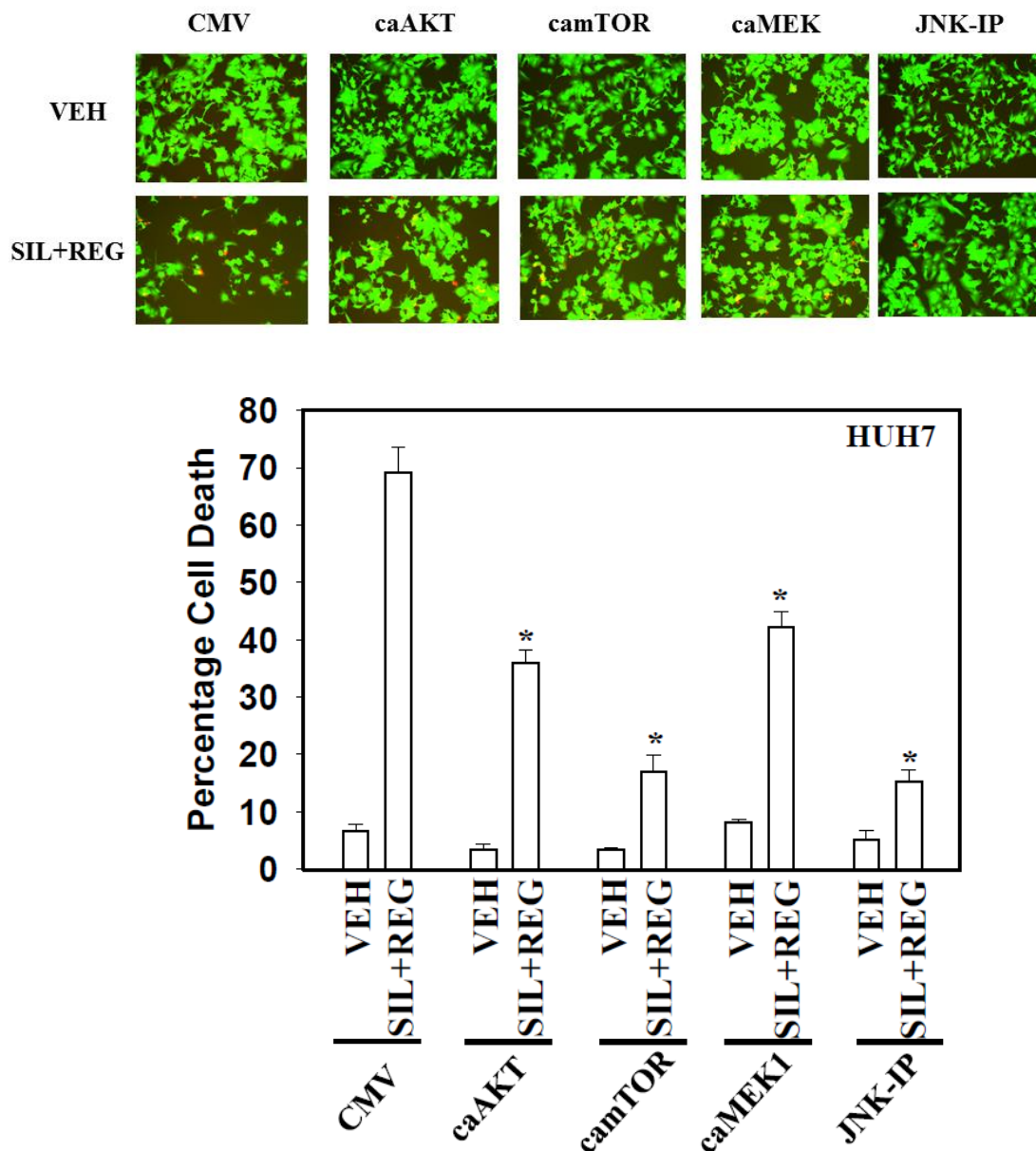f-lives such as Mcl-1 and Bcl-xL.[153,154] In this study, treatment of HUH7 cells with the combination of regorafenib (0.5 µM) and sildenafil (2 µM) increased the phosphorylation of PERK and eIF2α (Figure 21). Inhibition of PERK, ATF4 and CHOP in HUH7 cells protected them from the drug combination toxicity (Figure 22).

The drug combination reduced the levels of Mcl-1 and GRP78. Worthy   Of note, the drug combination also reduced the expression of ABCB1 and ABCG2 transporters (Figure 21). To investigate these observations further *in vivo*, athymic mice were given vehicle diluent (cremophor/ethanol), or sildenafil (5 mg/kg) and sorafenib (25 mg/kg) combination, or sildenafil (5 mg/kg) and regorafenib (15 mg/kg) combination by oral gavage once a day. After 5 days of treatment, mice were sacrificed, their brains and livers obtained and fixed. The tissues were sectioned and subjected to immunohistochemistry and viewed at 10X magnification. In accordance with the *in vitro* observations, the drug combination strongly down-regulated GRP78, ABCB1 and ABCG2 in the liver and the brain tissues collected from the athymic mice. The drug combination also weakly modulated other chaperones, including GRP94, HSP90 and HSP70 (Figure 23).
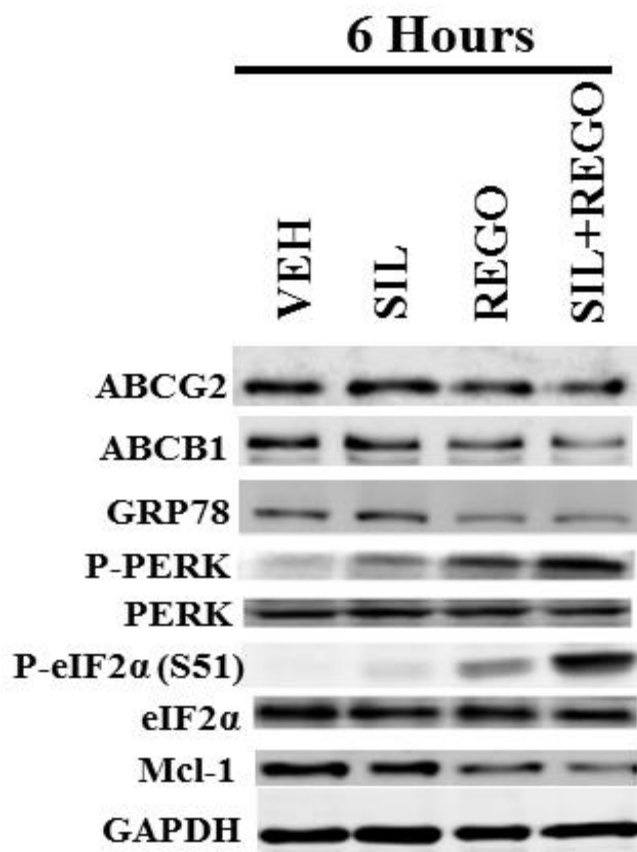
Figure 21. The REGO+SIL combination induces unfolded protein response. HUH7 cells were treated with vehicle (DMSO), regorafenib (0.5 μM), sildenafil (2 μM), or the drug combination for 6 hours. Cells were lysed and the expression of indicated proteins was determined by western blot.
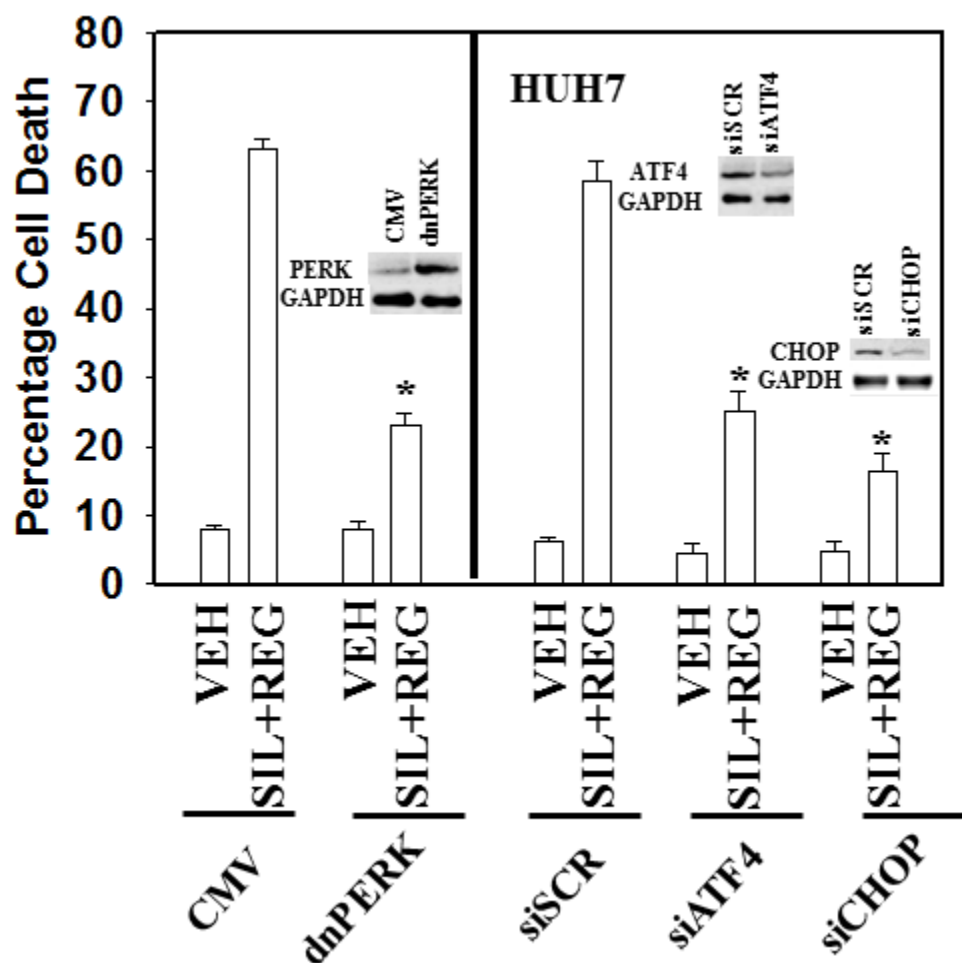
Figure 22. Inhibition of the UPR components reduced the REGO+SIL combination lethality. HUH7 cells were transfected with a control scrambled siRNA (siSCR) or two different siRNAs to knockdown expression of ATF4 and CHOP, or cells were transfected with plasmids to express either empty vector (CMV) or dominant negative PERK (dnPERK). 36 hours after transfection, cells were treated with vehicle (DMSO), or regorafenib (0.5 µM) and sildenafil (2 µM) combination. 24 hours after drug exposure, cells were isolated and viability determined by trypan blue exclusion assay (n = 3, ± SEM). *P< 0.05 lower than corresponding value in siSCR/CMV cells.
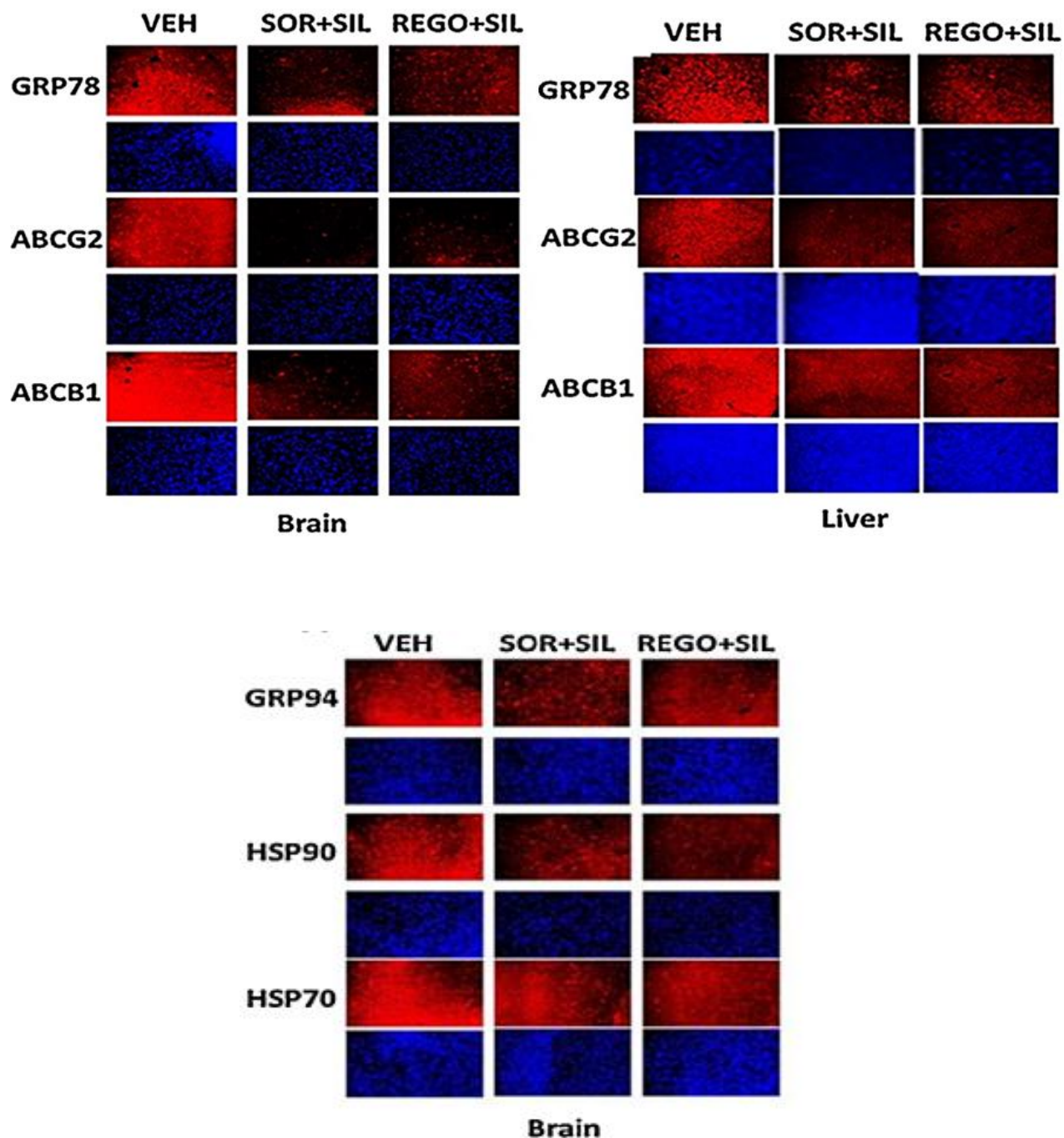
Figure 23. The REGO/SOR+SIL combination reduced expression of chaperones as well as ABCB1 and ABCG2 transporters *in vivo*. athymic mice were given vehicle diluent (cremophor/ethanol), or sildenafil (5 mg/kg) and sorafenib (25 mg/kg) combination, or sildenafil (5 mg/kg) and regorafenib (15 mg/kg) combination by oral gavage once a day. After 5 days of treatment, mice were sacrificed, their brains and livers obtained and fixed. The tissues were sectioned and subjected to immunohistochemistry and viewed at 10X magnification.

The drug combination induces the generation of ROS and RNS

Prior studies from our laboratory demonstrated that PDE5 inhibitors enhanced the toxicities of multiple chemotherapies.[145,146] In these studies PDE5 inhibitors, in a NOS-dependent fashion, were shown to enhance chemotherapy effect through activation of CD95 receptors. PDE5 inhibitors are also known to enhance the levels of reactive oxygen and reactive nitrogen species in treated cells.[155,156] Treatment of tumor cells with sildenafil and sorafenib combination rapidly increased the levels of ROS and RNS (Figure 24A). Inhibition of nitric oxide synthase enzymes using L-NG-Nitroarginine Methyl Ester (L-NAME) reduced the drug combination-mediated lethality, as did quenching of ROS production by incubating cells with N-acetyl cysteine (NAC) (Figure 24B). Knockdown of iNOS or eNOS expression suppressed killing by the drug combination (Figure 25). Of note, knockdown of iNOS abolished the drug combination interaction but did not alter sorafenib toxicity as a single agent, whereas knockdown of eNOS significantly reduced sorafenib toxicity.

As the drug combination increased ROS and RNS levels, and L-NAME and NAC protected the cells against the combination-mediated lethality, we determined whether ROS regulated CD95 activation. Incubation of cells with NOS inhibitor, L-NAME, suppressed drug-induced CD95 activation (Figure 26).

A
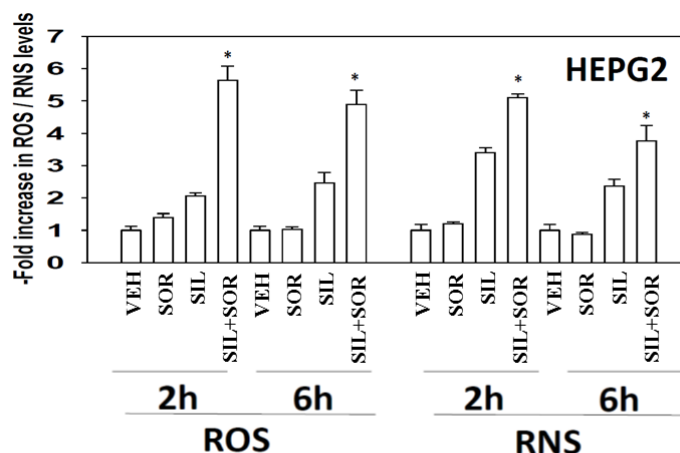
B
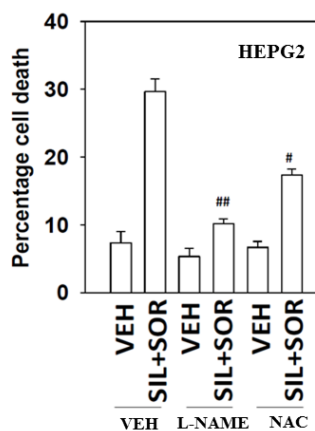
Figure 24. SOR+SIL combination increases the generation of ROS and RNS. (A) HEPG2 cells were incubated for 30 minutes with either DCFDA, which is sensitive to oxidation by hydroxyl radicals and peroxynitrite directly, and hydrogen peroxide, or DAF-FM DA, which is sensitive to oxidation by NO. Cells were then treated with vehicle (DMSO), regorafenib (1 µM), sildenafil (2 µM), or the drugs in combination. DCFDA/ DAF-FM DA fluorescence signals were detected 2 and 6 hours after drug exposure using a VICTOR 3 plate reader. (B) HEPG2 cells were pre-treated with vehicle, L-NAME (1 µM), or NAC (10 mM). Cells were then treated with vehicle or sorafenib (2 µM) and sildenafil (2 µM) in combination. 24 hours after drug exposure, cells were isolated and viability determined by trypan blue exclusion assay (n = 3, ± SEM). #*P* < 0.05 lower than corresponding value in VEH cells. ##*P* < 0.05 less than corresponding value in NAC cells.
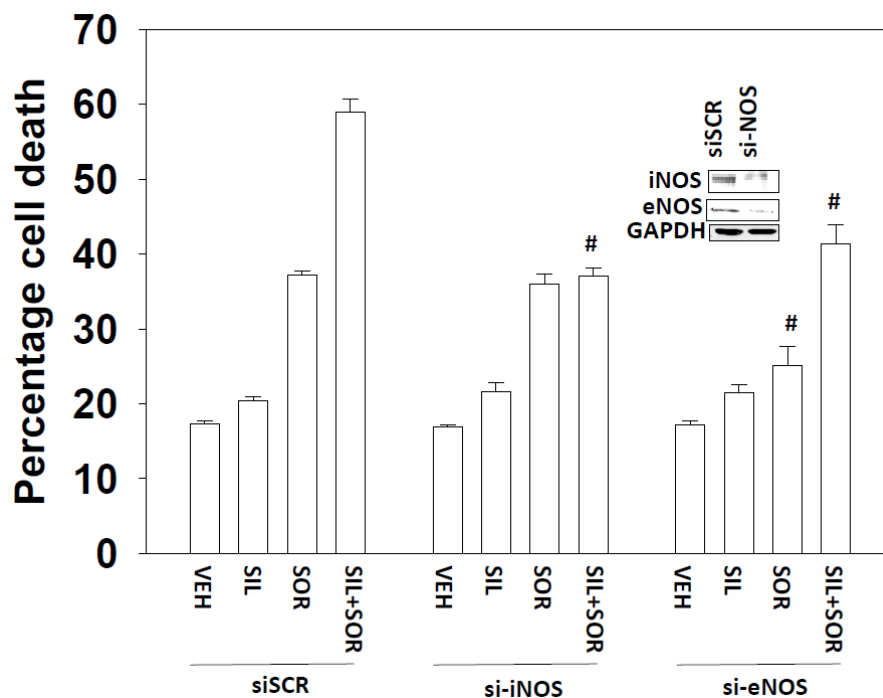
Figure 25. Inhibition of iNOS and eNOS suppresses SOR+SIL combination toxicity. HEPG2 cells were transfected with a control scrambled siRNA (siSCR) or two different siRNAs to knockdown expression of iNOS and eNOS. 36 hours after transfection, cells were treated with vehicle (DMSO), or sildenafil (2 µM) and sorafenib (2 µM) in combination. 24 hours after drug exposure, cells were isolated and viability determined by trypan blue exclusion assay (n = 3, ± SEM). #$P<0.05$ less than corresponding value in siSCR cells.
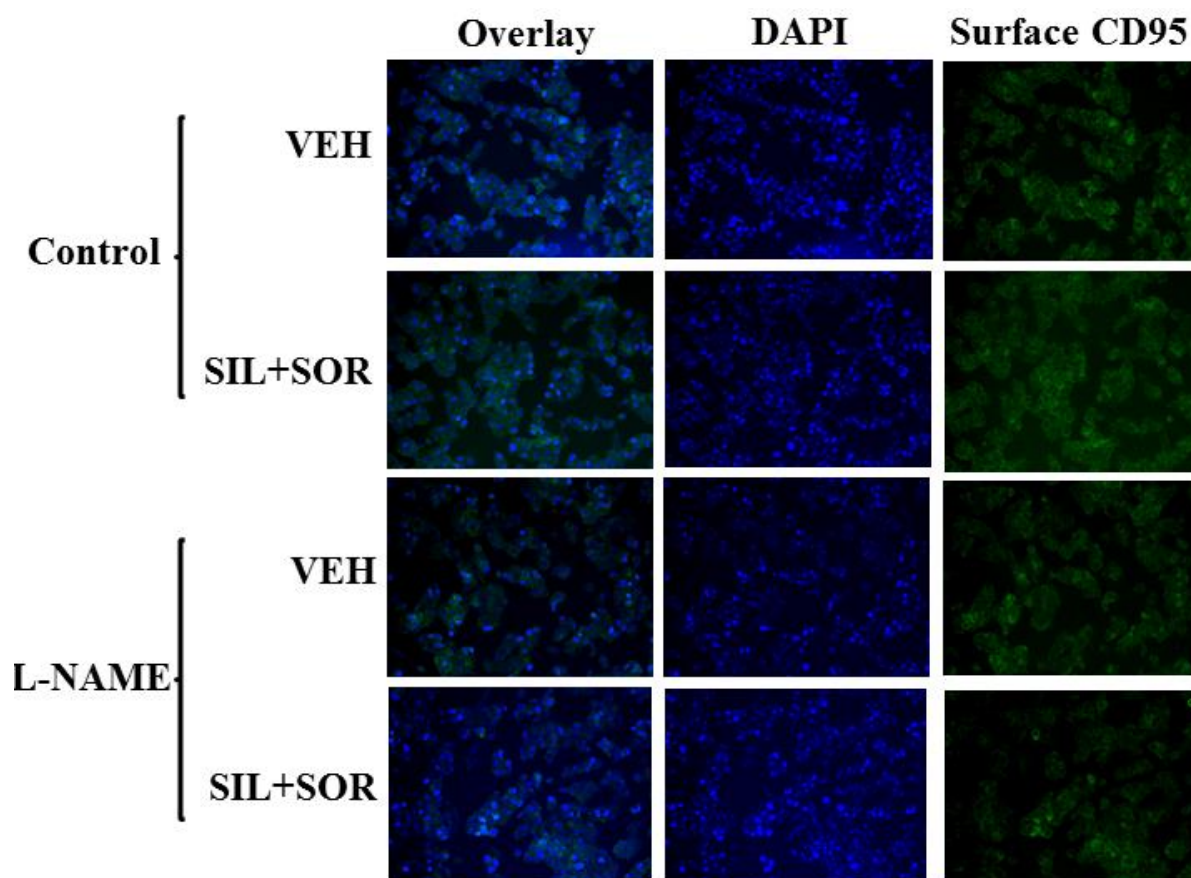
Figure 26. Inhibition of NOS reduces the level of surface CD95 receptors. HEPG2 cells plated in a 96-well plate were treated with vehicle or L-NAME (1 µM), then treated with vehicle (DMSO), or sildenafil (2 µM) and sorafenib (2 µM) in combination. 6 hours after drug exposure, cells were fixed and probed for CD95 expression. Images were acquired using a Hermes Wiscan system.

The drug combination induces autophagy

In prior studies, we have shown that sorafenib as a single agent can modestly promote increased numbers of autophagosomes.[50,152] As previously stated, lysosomal degradation of autophagosomes results in a decrease in p62 levels, which makes p62 a suitable marker for tracking autophagy in the mammalian cells.[112] The level of p62 was reduced 6 hours after HUH7 cells were treated with the combination of regorafenib (0.5 µM) and sildenafil (2 µM) (Figure 27) Treatment of cells with the combination of sorafenib and sildenafil increased the numbers of autophagosomes and autolysosomes in a greater than additive fashion (Figure 28A). The increase in the numbers of autophagosomes was suppressed when cells were pre-treated with L-NAME and NAC, establishing a link between the ROS generation and the induction of autophagy (Figure 28B). The knockdown of autophagy components ATG5 and Beclin1 reduced the drug combination lethality in HEP3B and HUH7 cells (Figure 29).
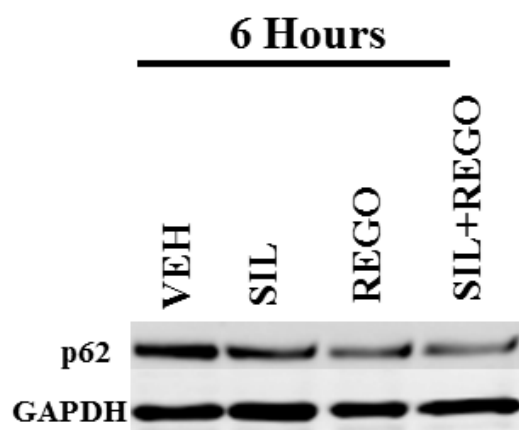
Figure 27. The REGO+SIL combination reduces p62 level. HUH7 cells were treated with vehicle (DMSO), regorafenib (0.5 µM), sildenafil (2 µM), or the drug combination for 6 hours. Cells were lysed and the expression of p62 was determined by western blot.

A
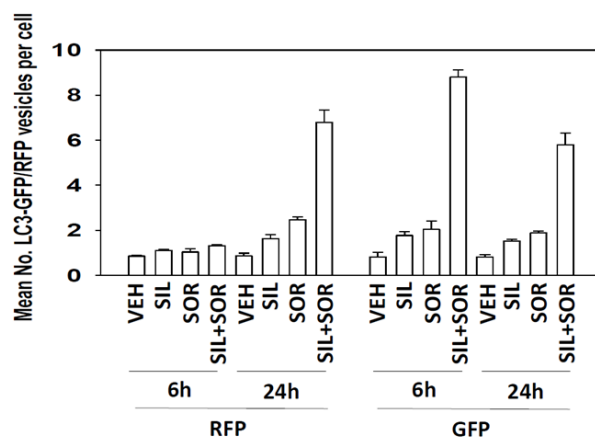
B
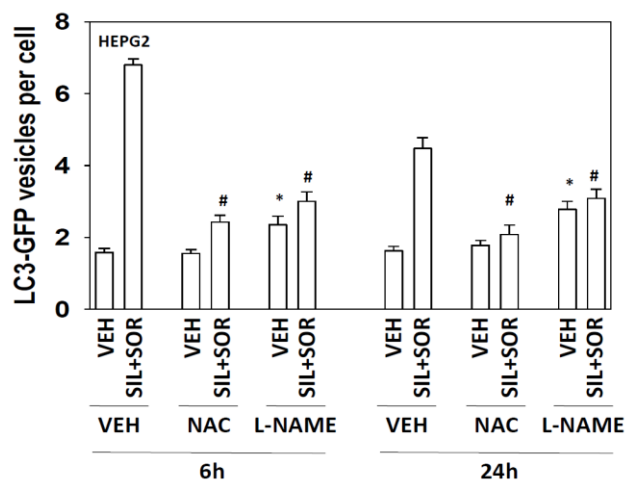
Figure 28. The SOR+SIL combination induces formation of autophagosomes and autolysosomes. (A) HEPG2 cells were transfected with a plasmid to express LC3-GFP-RFP. 24 hours after transfection, cells were treated with vehicle (DMSO), sorafenib (2 μM), sildenafil (2 μM), or the combination of both drugs. The number of GFP vesicles (early autophagosomes) and RFP vesicles (late autolysosomes) were determined 6 and 24 hours after drug exposure. (B) LC3-GFP-RFP transfected cells were pre-treated with L-NAME (1 μM) and NAC (10 mM), and then exposed to the combination of sorafenib (2 μM) and sildenafil (2 μM). The number of GFP and RFP vesicles were determined 6 and 24 hours after drug treatment (n = 3, ± SEM). *$P < 0.05$ lower than corresponding value in control group.
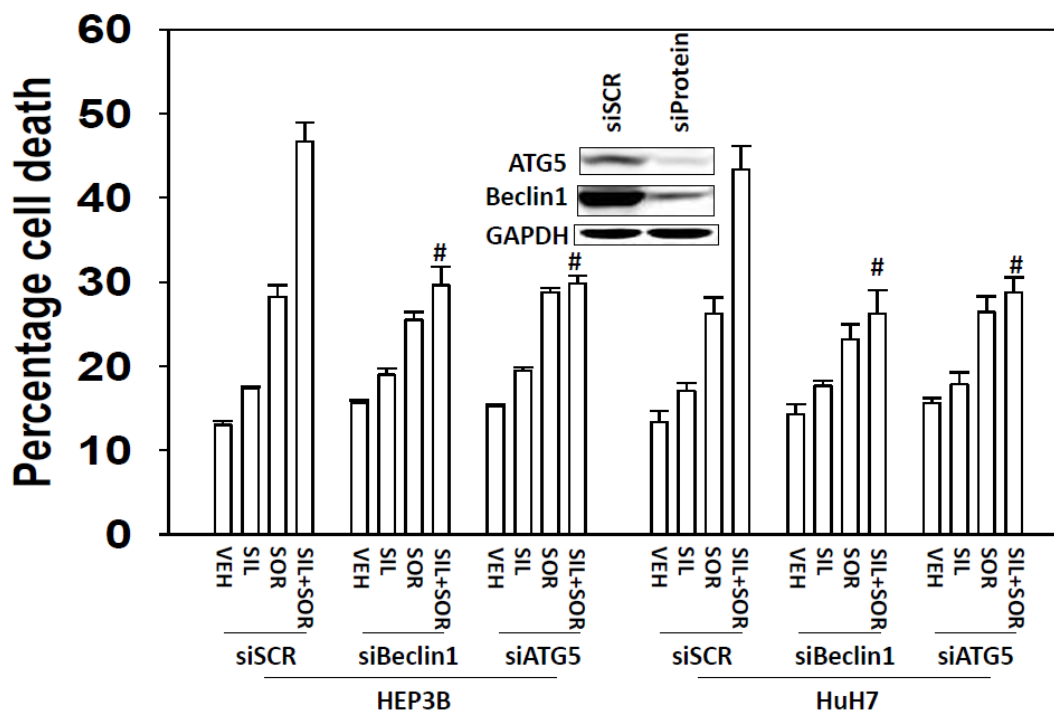
Figure 29. Inhibition of autophagy reduced the SOR+SIL combination toxicity. HUH7 and HEP3B cells were transfected with a control scrambled siRNA (siSCR) or two different siRNAs to knockdown expression of ATG5 and Beclin1. 36 hours after transfection, cells were treated with vehicle (DMSO), sorafenib (2 μM), sildenafil (2 μM), or the combination of both drugs. 24 hours after drug exposure, cells were isolated and viability determined by trypan blue exclusion assay (n = 3, ± SEM). *$P< 0.05$ lower than corresponding value in siSCR cells.

The drug combination activates extrinsic and intrinsic apoptosis pathways

In our previous studies, we have described how sorafenib can interact with agents that generate ROS to facilitate activation of the death receptor CD95.[152] In these studies HUH7 cells, which lack endogenous CD95 expression, were particularly resistant to the tested sorafenib drug combinations. However, in this study, we have found that sorafenib and sildenafil interact to kill both CD95 null HUH7 cells and hepatoma cells that express CD95 (HEP3B and HEPG2), though the drug combination killing appears to be more efficient in HEP3B and HEPG2 cells (Figure 14B). Thus, we next determined whether inhibition of the extrinsic and/or intrinsic apoptosis pathways could suppress drug combination-mediated toxicity. Expression of Bcl-xL and dominant negative caspase 9 that suppress activation of the intrinsic apoptosis pathway protected both HEPG2 and HUH 7 cells (Figure 30). Expression of the caspase 8 inhibitor c-FLIP-s protected HEPG2 cells, suggesting that the activation of extrinsic apoptosis pathway played a role in cell killing. Expression of c-FLIP-s did not alter the cell death response in HUH7 cells (Figure 30). We further explored signaling by the extrinsic pathway in by looking at caspase 8 and FADD levels associated with CD95. Both caspase 8 and FADD rapidly increased in response to the drug combination (Figure 31A). In addition, Inhibition of FADD and CD95 reduced the cell death in HEP3B cells (Figure 31B). Finally, expression of wild type CD95 in HUH7 cells enhanced cell killing by sorafenib and the combination of sorafenib and sildenafil whereas expression of a mutant CD95, lacking the specific tyrosine residues required for activation, did not alter cell death (Figure 32).
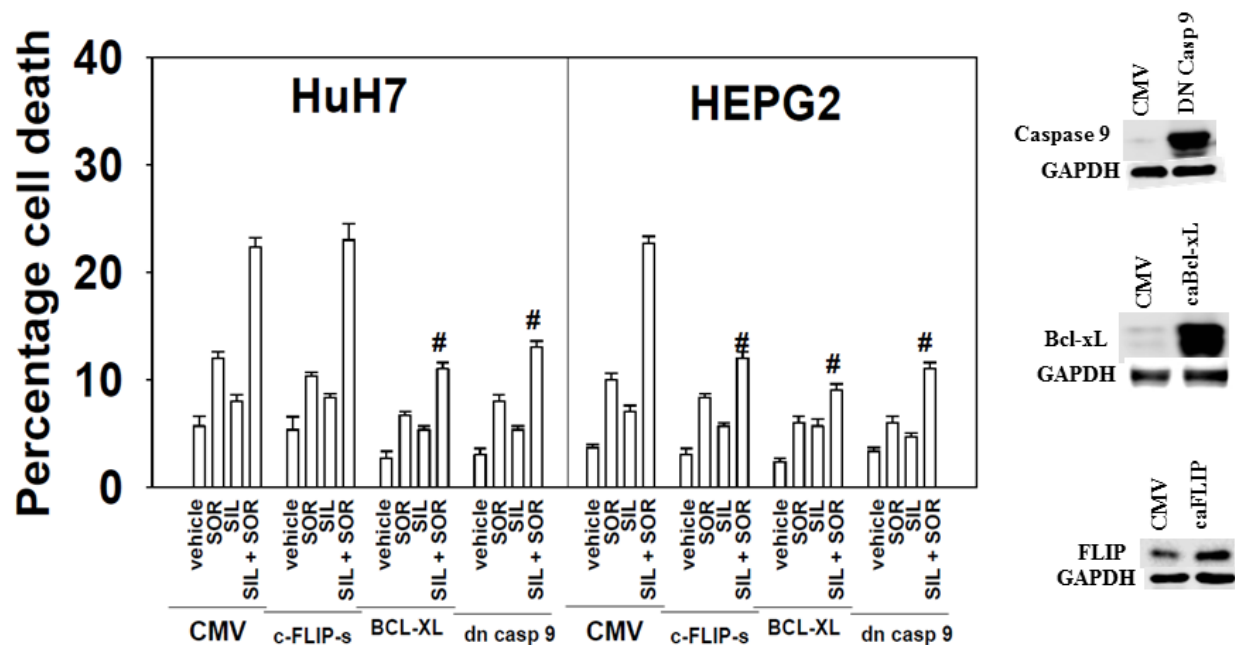
Figure 30. The SOR+SIL combination activates extrinsic and intrinsic apoptosis pathways. HUH7 and HEPG2 cells were infected with recombinant adenoviruses to express empty vector (CMV), dominant negative caspase 9 (dn casp 9), Bcl-xL, or c-FLIP-s. 24 hours after infection cells were treated with vehicle (DMSO), sorafenib (2 μM), sildenafil (2 μM), or the combination of both drugs. 24 hours after drug exposure, cells were isolated and viability determined by trypan blue exclusion assay (n = 3, ± SEM). #*P*< 0.05 lower than corresponding value in CMV cells.

A
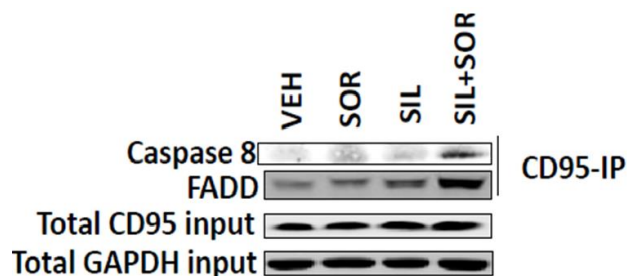
B
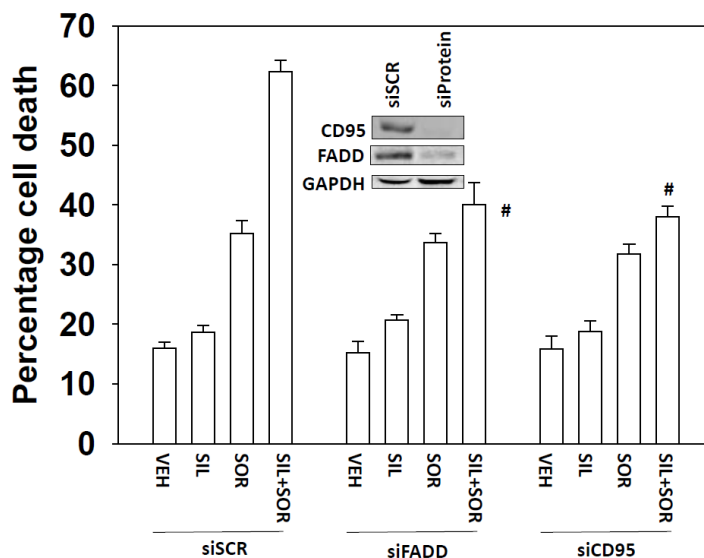
Figure 31. The SOR+SIL combination activates CD95 death receptors. (A) HEPG2 cells were treated with vehicle (DMSO), sorafenib (2 μM), sildenafil (2 μM), or the combination of both drugs. 6 hours after treatment, cells were lysed and prepared for immuoprecipitation (IP) of CD95. After IP, immunoblotting was performed to determine the levels of caspase 8 and FADD in the immunoprecipitate. Total levels of CD95 and GAPDH in the lysates are also presented. (B) HEP3B cells were transfected with a control scrambled siRNA (siSCR) or two different siRNAs to knockdown expression of FADD and CD95. 36 hours after transfection, cells were treated with vehicle (DMSO), sorafenib (2 μM), sildenafil (2 μM), or the combination of both drugs. 24 hours after drug exposure, cells were isolated and viability determined by trypan blue exclusion assay (n = 3, ± SEM). #$P < 0.05$ lower than corresponding value in siSCR cells.
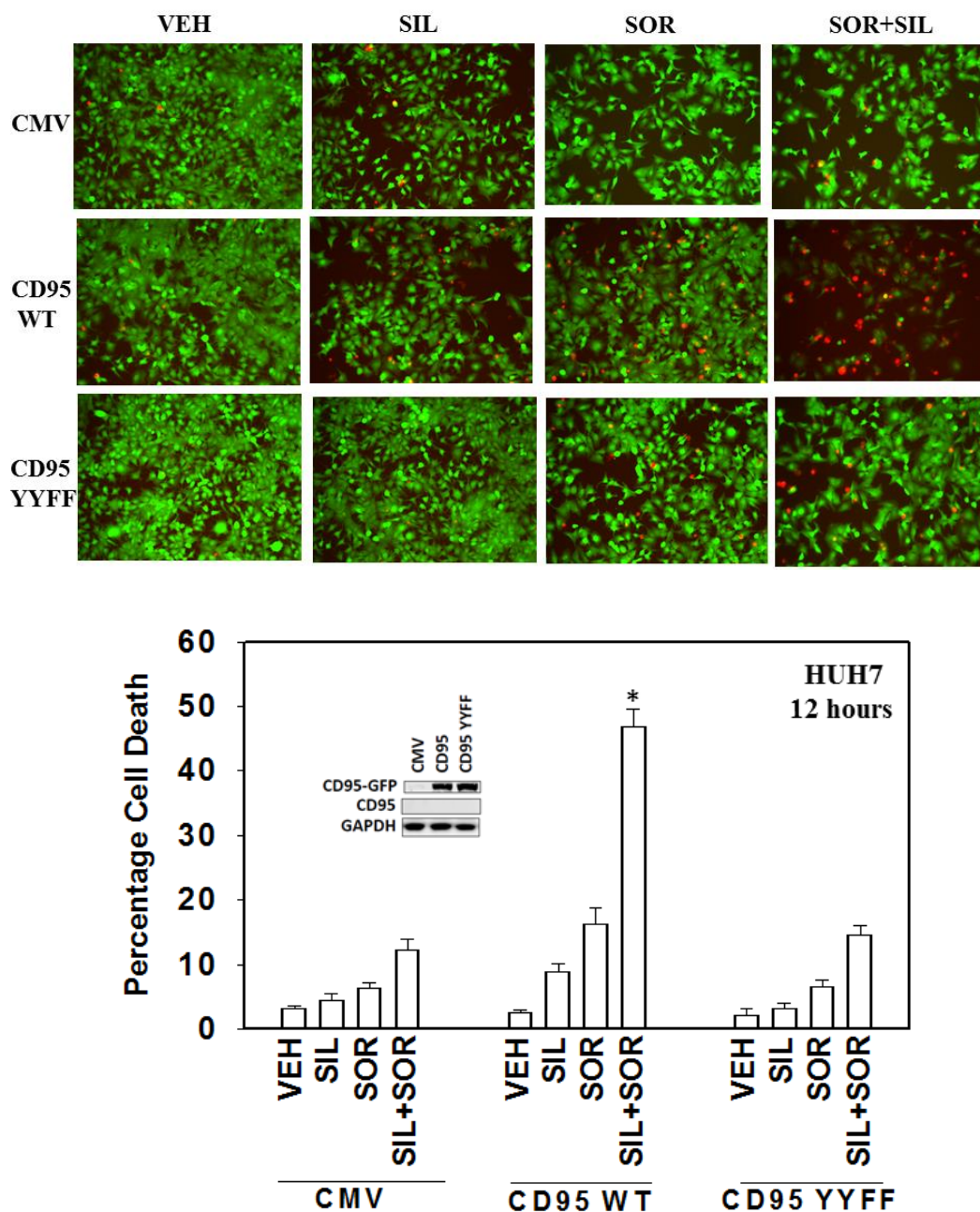
Figure 32. CD95 expression enhances SOR+SIL combination toxicity in HUH 7 cells. HUH7 cells were transfected with plasmids to express either empty vector (CMV), a plasmid to express CD95-GFP, or a plasmid to express CD95-GFP-Y232F Y291F. 24 hours after transfection, cells were treated with vehicle (DMSO), sorafenib (2 μM), sildenafil (2 μM), or the combination of both drugs. 12 hours after drug treatment, cell viability was assessed using a Hermes Wiscan instrument (n = 3, ± SEM). *$P < 0.05$ greater than corresponding value in CMV cells.

The drug combination increases the ceramide levels

Prior reports from our group have shown that sorafenib can increase the levels of ceramides in hepatoma cells.[152] In accordance with our previous findings, regorafenib and sildenafil treatment increased the levels of multiple ceramide and dihydro-ceramides in HUH7 cells (Figure 33). Regorafenib also increased the levels of sphingosine-1 phosphate (Figure 34). The approved multiple sclerosis drug FTY720 (fingolimod, Gilenya) inhibits the production of S1P as an active site inhibitor of sphingosine kinase 1 and 2.[143,144] Treatment of cells with low clinically relevant concentration s of FTY720 suppressed the ability of regorafenib to increase S1P (Figure 34).

We next determined if FTY720 can enhance the toxicity of the combination of regorafenib and sildenafil. Our data indicated that the addition of FTY720 to the drug combination significantly increased percentage cell death in HUH7 and HT29 cells (Figure 35).
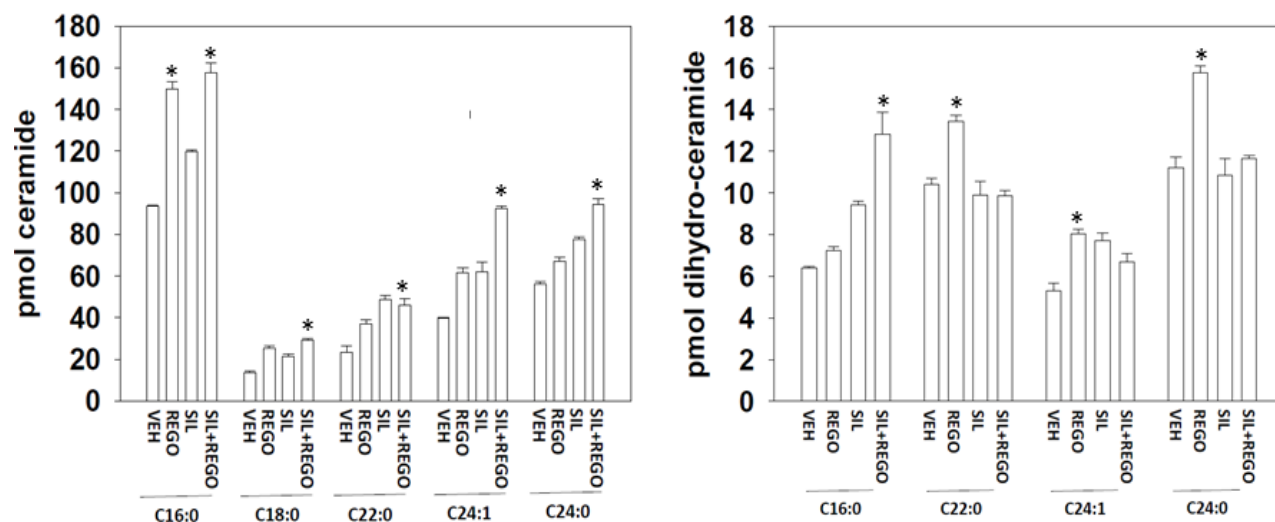
Figure 33. The REGO+SIL combination increases ceramide levels. HUH7 cells were treated with vehicle (DMSO), regorafenib (0.5 μM), sildenafil (2 μM), or the drug combination for 6 hours. Cells were then isolated and bioactive lipids were extracted. Multiple bioactive lipids were analyzed using GC/MS techniques (n=2 in triplicate ±SEM). *$P< 0.05$ greater than corresponding value in VEH cells.
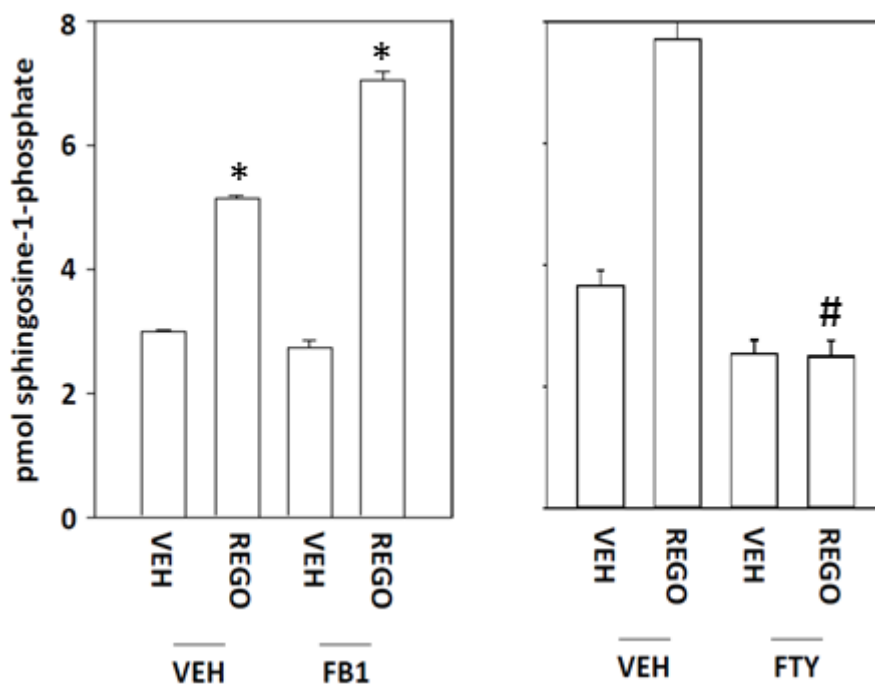
Figure 34. Regorafenib increases S1P levels. HUH7 cells were treated with vehicle (DMSO) or regorafenib (0.5 µM), and/or Fumonisin B1 (25 µM) or FTY720 (50 nM). 6 hours after treatment, cells were isolated and bioactive lipids were extracted. S1P levels were analyzed using GC/MS techniques (n=2 in triplicate ±SEM). *P< 0.05 greater than corresponding value in VEH cells. #P< 0.05 lower than corresponding value in regorafenib-treated VEH cells.
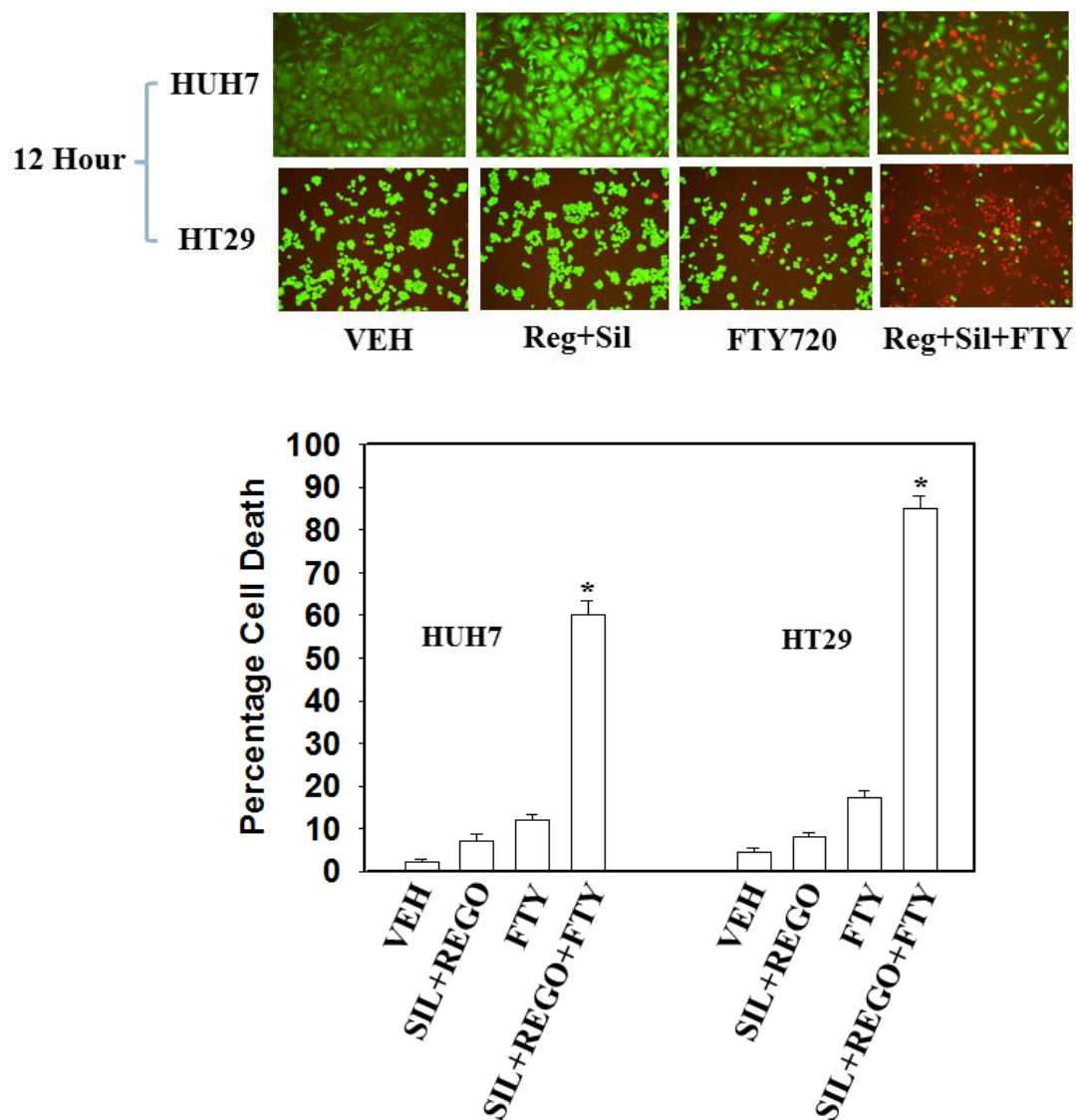
Figure 35. FTY720 enhances REGO+SIL combination-mediated toxicity. HUH7 and HT29 cells were treated with vehicle (DMSO), regorafenib (0.5 μM) and sildenafil (2 μM) combination, FTY720 (50 nM), or the combination of all three drugs. 12 hours after drug treatment, cell viability was assessed using a Hermes Wiscan instrument (n = 3, ± SEM). *$P <$ 0.05 greater than corresponding value in SIL+REGO cells.

Sildenafil interacts with sorafenib/regorafenib to kill tumor cells *in vivo*

We next determined whether sorafenib/regorafenib interacted with sildenafil *in vivo* to kill tumor cells. Initial studies examined the *ex vivo* plating efficiency of tumor cells treated *in vivo* with regorafenib and sildenafil. Treatment of cells with sildenafil (5 mg/kg) and regorafenib (25 mg/kg) *in vivo* caused a reduction in *ex vivo* plating efficiency of isolated tumor cells following drug exposure; thus the long-term colony forming ability of the drug-treated cells was reduced beyond that achieved due to the proximal anti-tumor effects of the individual drugs (Figure 36A). We then performed additional studies using preformed HUH7 tumors (~150 mm^3). In our prior studies, HUH7 cells had a significantly greater tumorigenic potential than either HEPG2 or HEP3B cells to grow in an athymic mouse. Due to the lack of CD95 expression in these cells, the relative effect of the drug combination might be less efficient even though data from previous figure (Figure 36A) argues than interaction between the two drugs occurs *in vivo*. Transient treatment of animals with sildenafil (5 mg/kg) did not alter tumor growth whereas treatment with sorafenib (25 mg/kg) caused a non-significant trend towards reduced growth. Combined treatment of mice with both drugs for 3 days caused a significant reduction in HUH7 tumor growth (Figure 36B).

Based on the data from FTY720 interaction with the drug combination (Figure 37), we then determined if FTY720 interacted with regorafenib and the combination of regorafenib and sildenafil to kill HT29 cells *in vivo* (Figure 37). FTY720 (0.05 mg/kg) as a single agent, had a modest effect on reducing tumor growth but did cause a modest significant increase in overall survival (Figure 37 and 38). Surprisingly, we found that a transient 7-day treatment of HT29 tumors with regorafenib and FTY720 or with regorafenib (25 mg/kg) and sildenafil (5 mg/kg) and FTY720 caused tumors exposed to FTY720 to re-grow at a much faster rate after cessation

of drug treatment than either regorafenib treatment alone or treatment with regorafenib and sildenafil (Figure 37). The growth of tumors treated with the combination of regorafenib and sildenafil was profoundly reduced both during and for many weeks following the cessation of treatment, which was reflected in a significant increase in animal survival (Figure 38).

Morphological examination of the tumors *in situ* in the mouse flank (pictures were chosen with tumors in each condition at the same approximate volume) demonstrated that the tumors treated with FTY720 exhibited a more vascularized appearance on their surface (Figure 39). H&E staining of sectioned tissues of multiple organs collected from the vehicle group and the group that received the combination of regorafenib and sildenafil indicated that the drug combination did not damage the normal tissues (Figure 40).

In addition to previous *in vivo* studies, we also collected portions of the tumors from each group at the time of sacrifice. The tumors were digested and single cells were plated to determine the *ex vivo* plating efficiency of cells. Treatment of tumors with FTY720 individually, that had a marginal effect on tumor growth and animal survival, significantly reduced *ex vivo* plating efficiency (Figure 41). Regorafenib as a single agent did not alter *ex vivo* colony formation that correlated with our tumor growth and survival findings and with the clinical data where regorafenib has only a ~1% response rate. The reduced plating efficiency of tumors treated with regorafenib and sildenafil correlated with suppressed tumor growth and increased animal survival.

A
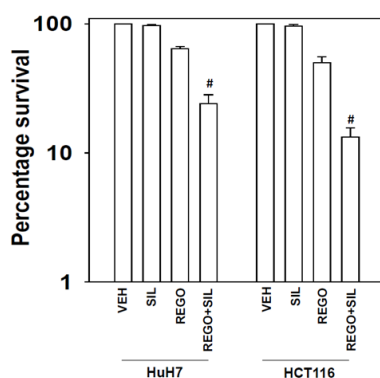
B
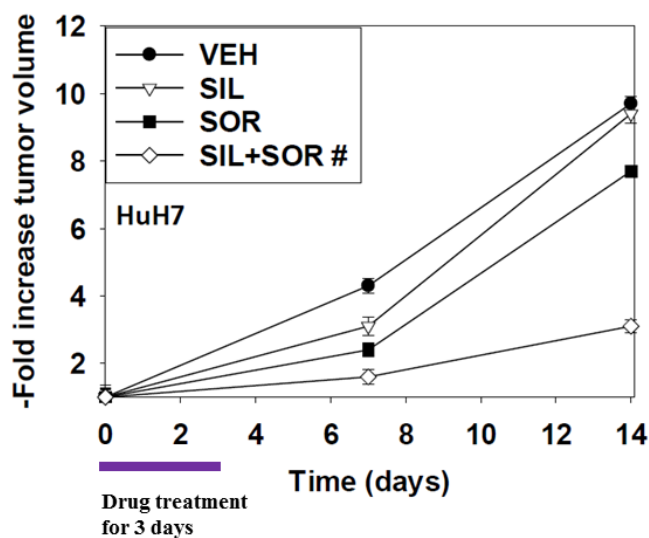
Figure 36. The drug combination suppresses tumor growth *in vivo*. (A) HUH7 and HCT116 tumors were formed in the flank of athymic mice (~150 mm^3). Animals were treated with vehicle (cremophor/ethanol), sildenafil (5 mg/kg), regorafenib (25 mg/kg), or the combination. Tumors were isolated, digested and single cells were plated. Colonies were permitted to form in 7-10 days. Colonies were then fixed, stained and counted. Survival value in the vehicle group was defined as 100% (n=6 ±SEM). #*P*< 0.05 lower than corresponding value in regorafenib-treated cells. (B) HUH7 tumors were formed in the flank of athymic mice (~150 mm^3). Animals were treated with vehicle (cremophor/ethanol), sildenafil (5 mg/kg), sorafenib (25 mg/kg), or the combination for 3 days. Tumor volumes were measure 7 and 14 days after the start of the treatment. (n=2 studies, 8 animals per group ± SEM). #*P*< 0.05 less than sorafenib-treated cells.
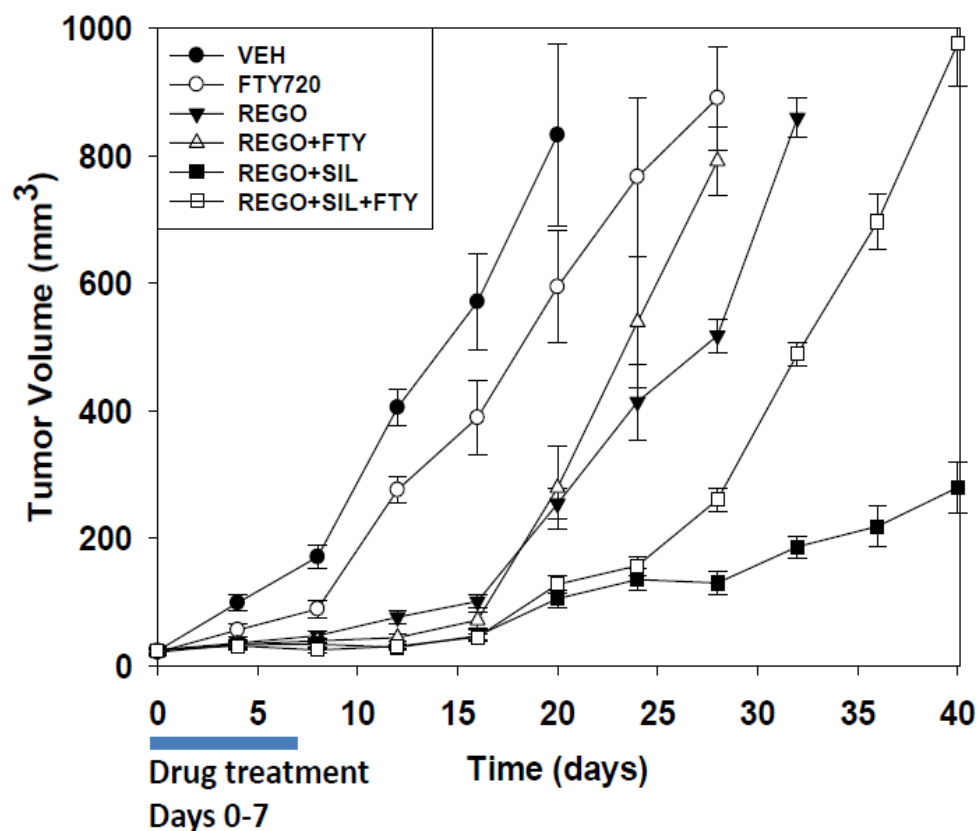
Figure 37. Regorafenib interacts with sildenafil to kill HT29 cells *in vivo*. HT29 tumors were formed in the flank of athymic mice (~30 mm^3). Animals were treated with vehicle (cremophor/ethanol), sildenafil (5 mg/kg) and regorafenib (25 mg/kg), FTY720 (0.05 mg/kg) or the combination of all drugs for 7 days. Tumor volumes were measured every 4 days after the end of the drug treatment (n = 2 studies, 8 animals per group ± SEM).
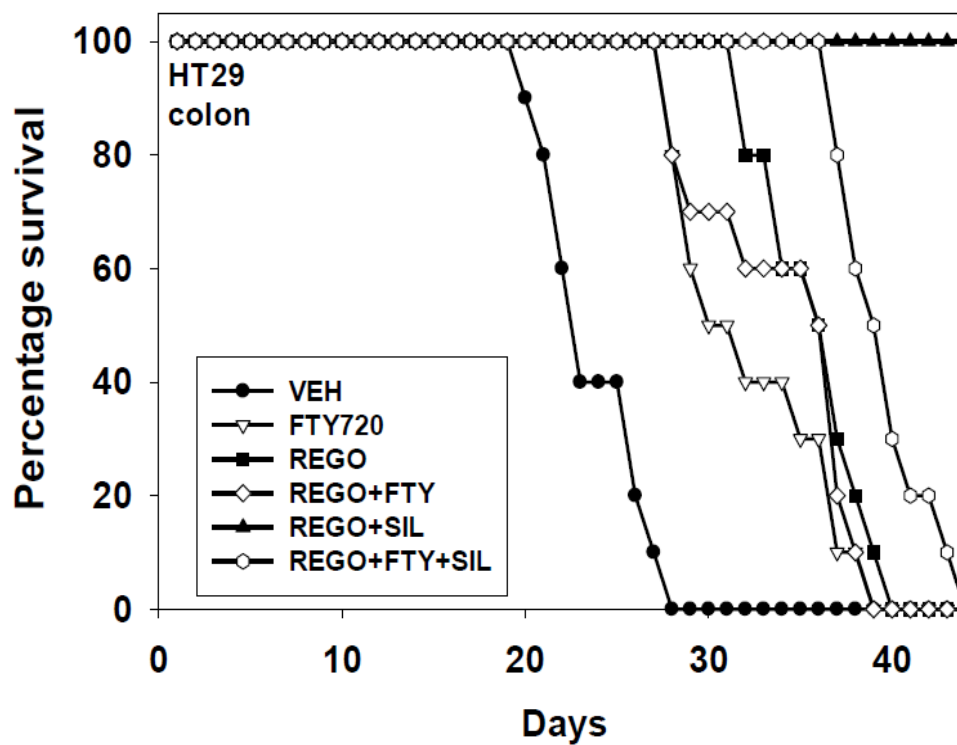
Figure 38. Combination of regorafenib and sildenafil significantly increased the survival time. Kaplan Meier survival plot of animals treated in previous study (Figure 39); animals were humanely sacrificed when tumor volumes exceeded 1500 mm^3.
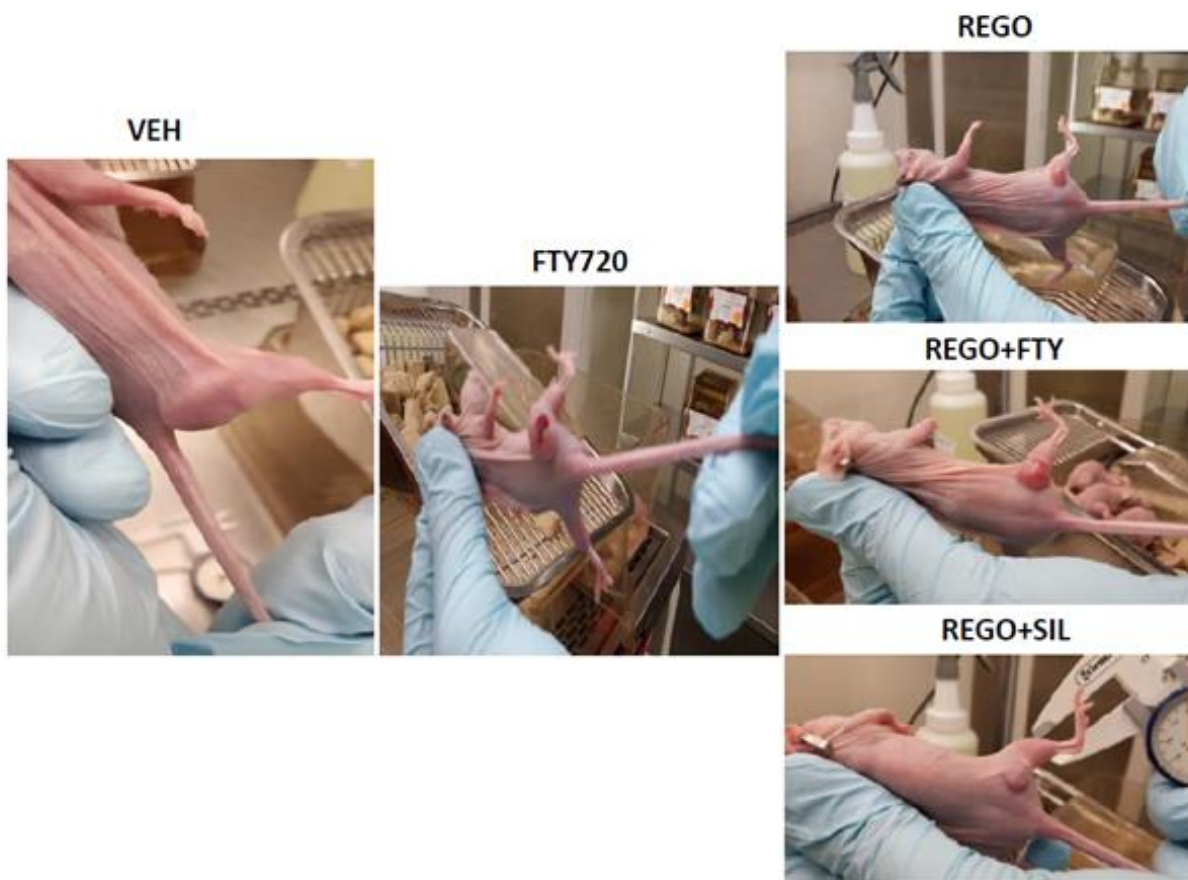
Figure 39. HT29 tumors pictured between days 15-30. Representative images of tumors from each group were taken between days 15 and 30 when tumors were of approximately the same volume. Tumors from the FTY720-treated groups have a more vascularized appearance.
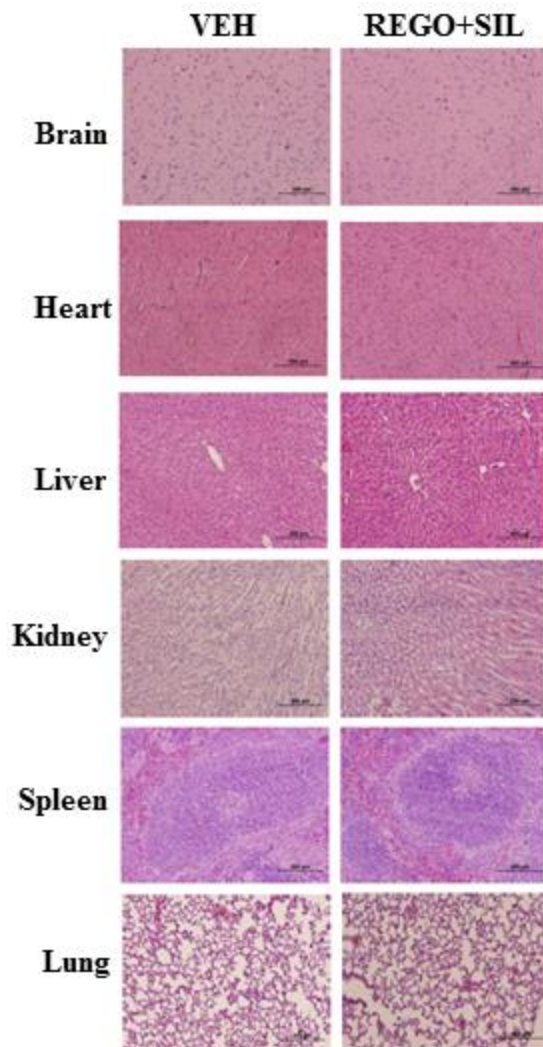
Figure 40. The REGO+SIL combination did not damage the normal tissue. Vital organs were collected from the mice that received the vehicle (cremophor/ethanol) or the combination of regorafenib and sildenafil for 7 days. Tissues were sectioned and H&E stained, and were examined under 10X magnification.
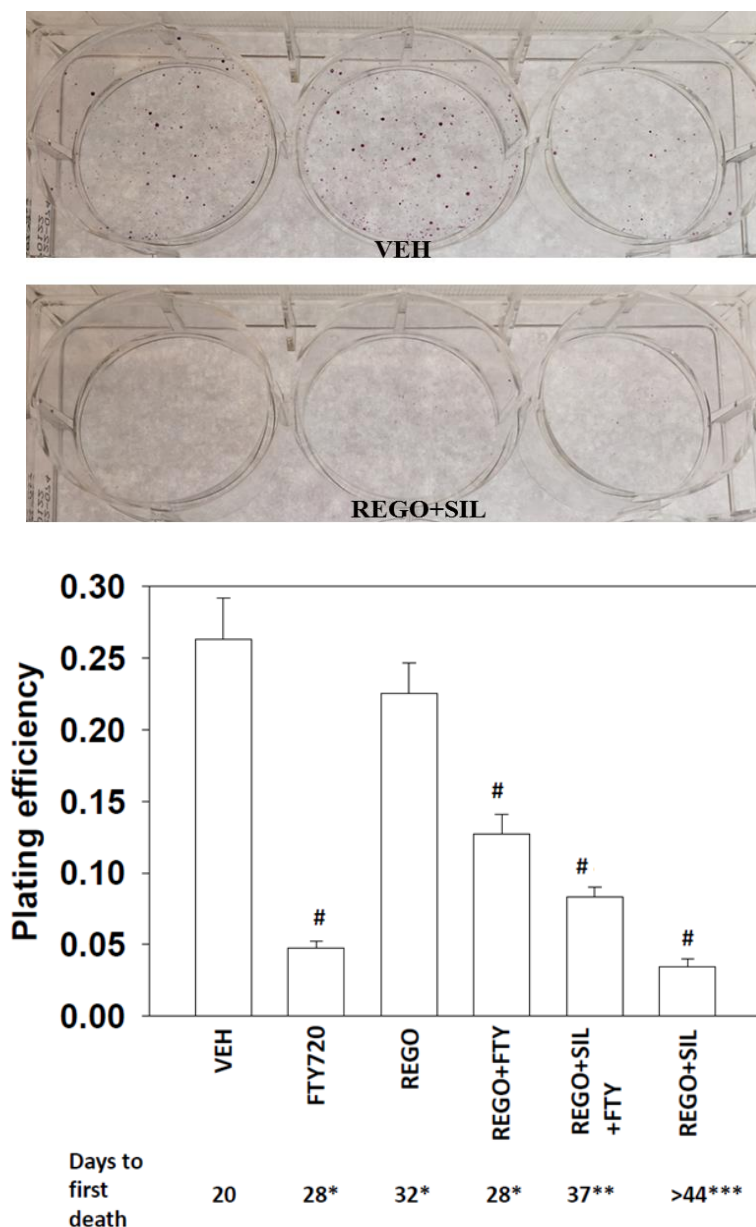
Figure 41. The REGO+SIL combination significantly reduced the *ex vivo* plating efficiency. HT29 tumor cells, at the time of sacrifice, were isolated and gently digested to obtain a single cell suspension of tumor cells. Cells were plated as single cells 100-10,000 per well of a 6-well plate. Colonies were permitted to form in 7-10 days. Colonies were then fixed, stained and counted, and plating efficiency was determined (n=8 ± SEM). #*P*< 0.05 lower than corresponding value in VEH and REGO-treated cells.

The drug combination alters the cytokine expression levels in mouse plasma

Based on our *in vivo* findings, we determined the expression levels of human cytokines in mouse plasma and activity of signal transduction proteins within the established tumor itself. Regorafenib and sildenafil exposure for 7 days decreased the plasma levels of bFGF and GM-CSF but significantly increased PDGFbb (Figure 42A). Treatment of tumors with FTY720 for 7 days increased plasma levels of FAS-L (Figure 42B). For a number of cytokines, including endoglin, IL-6, VEGF-A/C/D, endopoietin 2, and EGF the plasma level declined in vehicle control treated tumors over 7 days of growth, which was associated with a mean of approximately seven fold increase in tumor volume (Figure 42B-F). In this respect, treatment of tumors with FTY720 or with regorafenib and FTY720 combination prevented the decline in plasma cytokine levels that were observed in mice with vehicle control treated tumors at day 7 (Figure 42B-G). For tumors exposed to regorafenib and sildenafil, the expression of pro-growth, pro-angiogenic, and pro-invasion cytokines was either unchanged compared to the vehicle control or was significantly reduced (Figure 42C-G).

Additionally, treatment of tumors with regorafenib and FTY720 combination increased the expression of pro-growth/pro-angiogenic/pro-invasion cytokine endoglin, which enhances TGFβ signaling (Figure 42G). as treatment of tumors with FTY720 caused an increase in endoglin expression, which would enhance TGFβ receptor family as well as integrin signaling, we determined whether the toxicity of regorafenib and FTY720 combination was enhanced *in vitro* using TGFβ inhibitor LY2157299 (Galunisertib). Our data indicated that the inhibition of TGFβ receptor 1 signaling in a dose-dependent fashion significantly enhanced the toxicity of regorafenib+FTY720 combination (Figure 43).

A
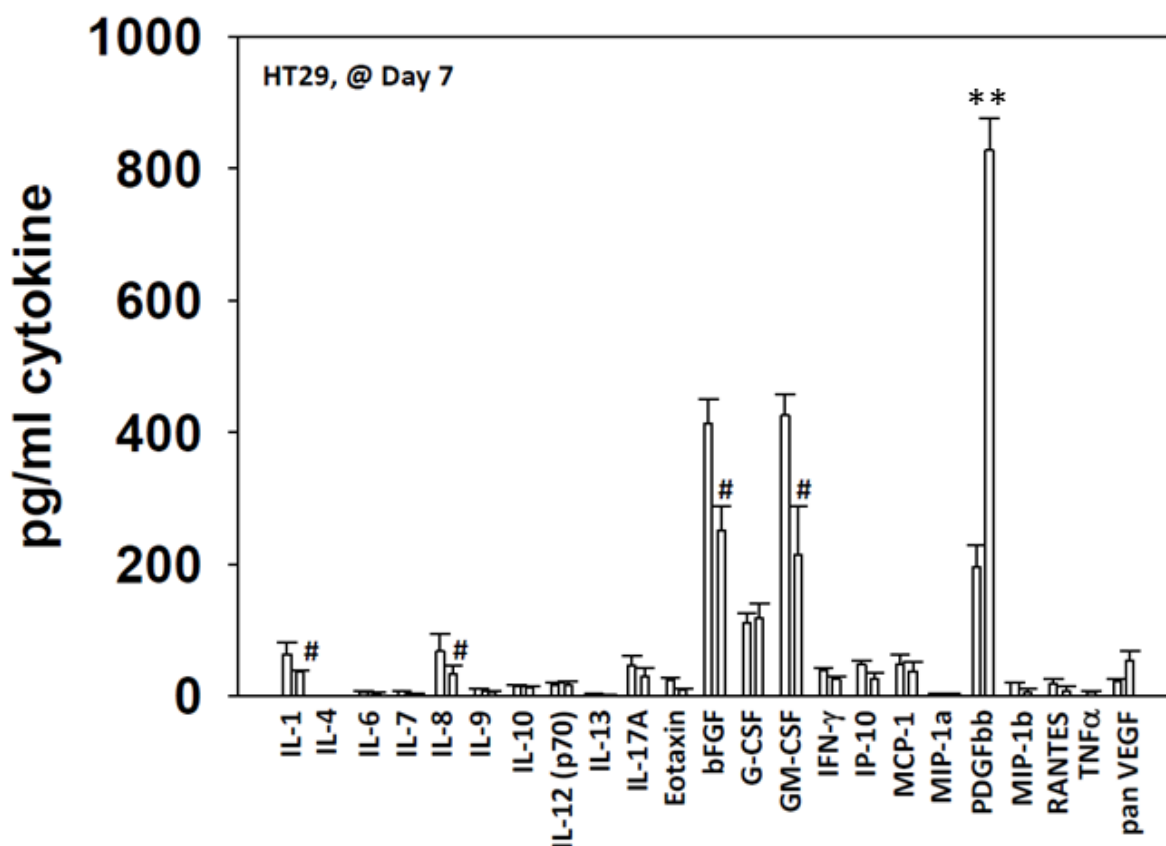
Figure 42. The drug combination alters the cytokine expression levels in mouse plasma. (A-G) HT29 tumors (~30 mm^3) were formed in the flanks of athymic mice. Aliquots (~75 µL) of mouse blood were obtained in a heparin/EDTA coated Eppendorf tube. Animals were then treated with vehicle diluent (cremophor/ethanol), sildenafil (5 mg/kg) and regorafenib (25 mg/kg), FTY720 (0.05 mg/kg) or the combination of all drugs for 7 days. Data in part A are vehicle control and the combination of regorafenib and sildenafil tumor data. After 7 days aliquots of mouse blood were obtained again. Clarified mouse plasma free of blood cells was then subjected to multiplex assays in a BIO-RAD MAGPIX system to determine the expression of the indicated cytokines before and following treatment (n=2 studies, 8 animals per group ± SEM). *$P< 0.05$ greater than day 0 pre-treatment value. **$P< 0.05$ greater than day 7 vehicle control value. #$P< 0.05$ less than day 0 pre-treatment value. ##$P< 0.05$ less than day 7 vehicle control value. лP< 0.05 less than day 7 regorafenib treatment value.

42B

Bars, left to right:

Day 0 pre-treatment
Day 7 vehicle
Day 7 FTY720

42C

Bars, left to right:

Day 0 pre-treatment
Day 7 vehicle
Day 7 FTY720
Day 7 REGO
Day 7 FTY+REGO
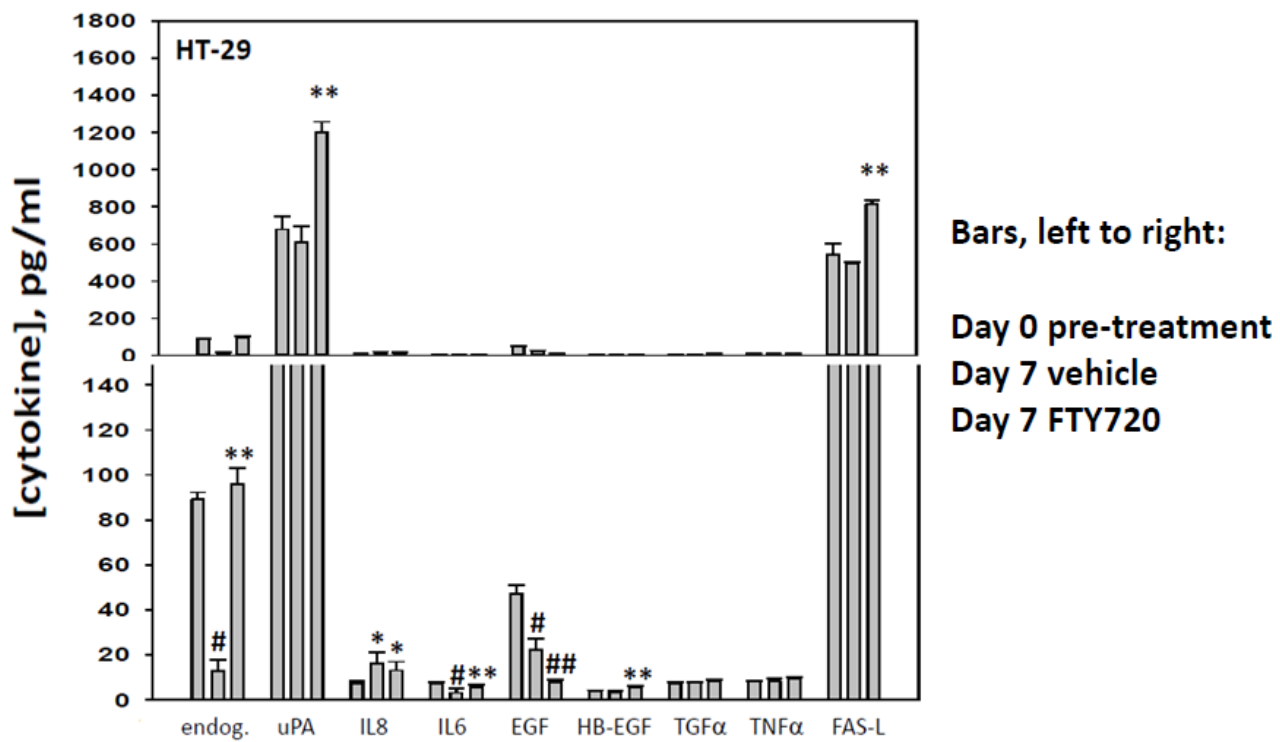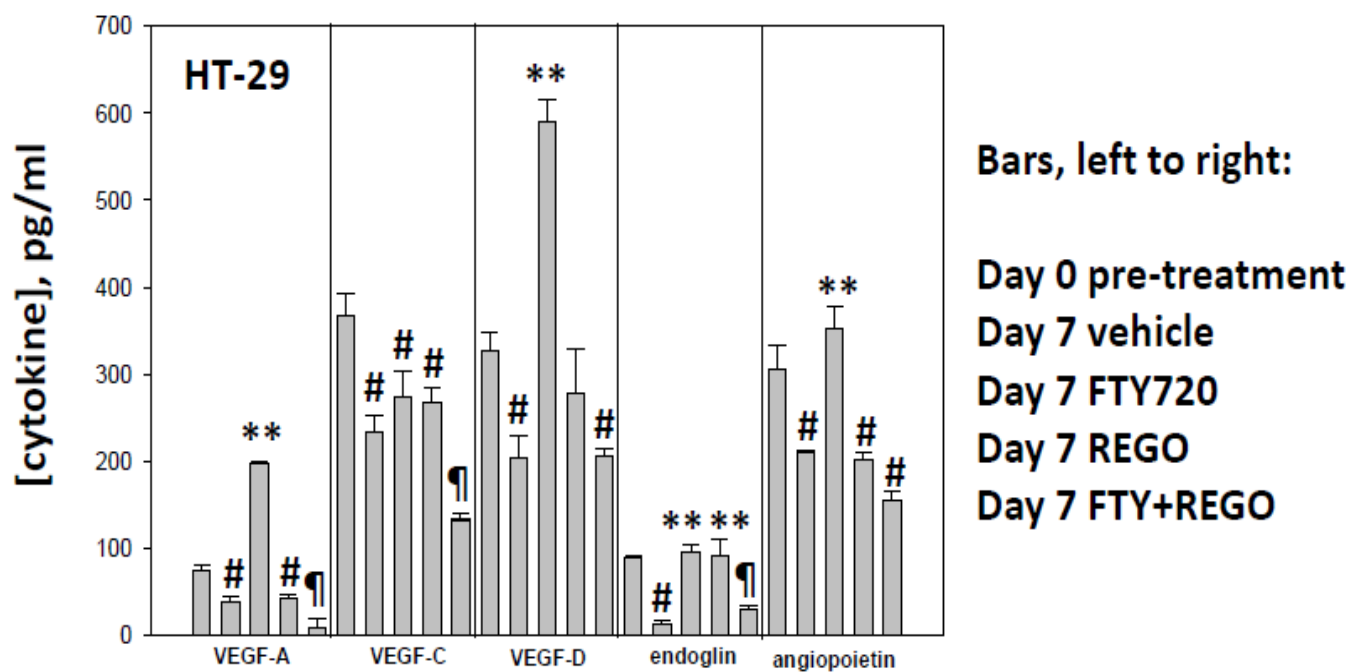
42D
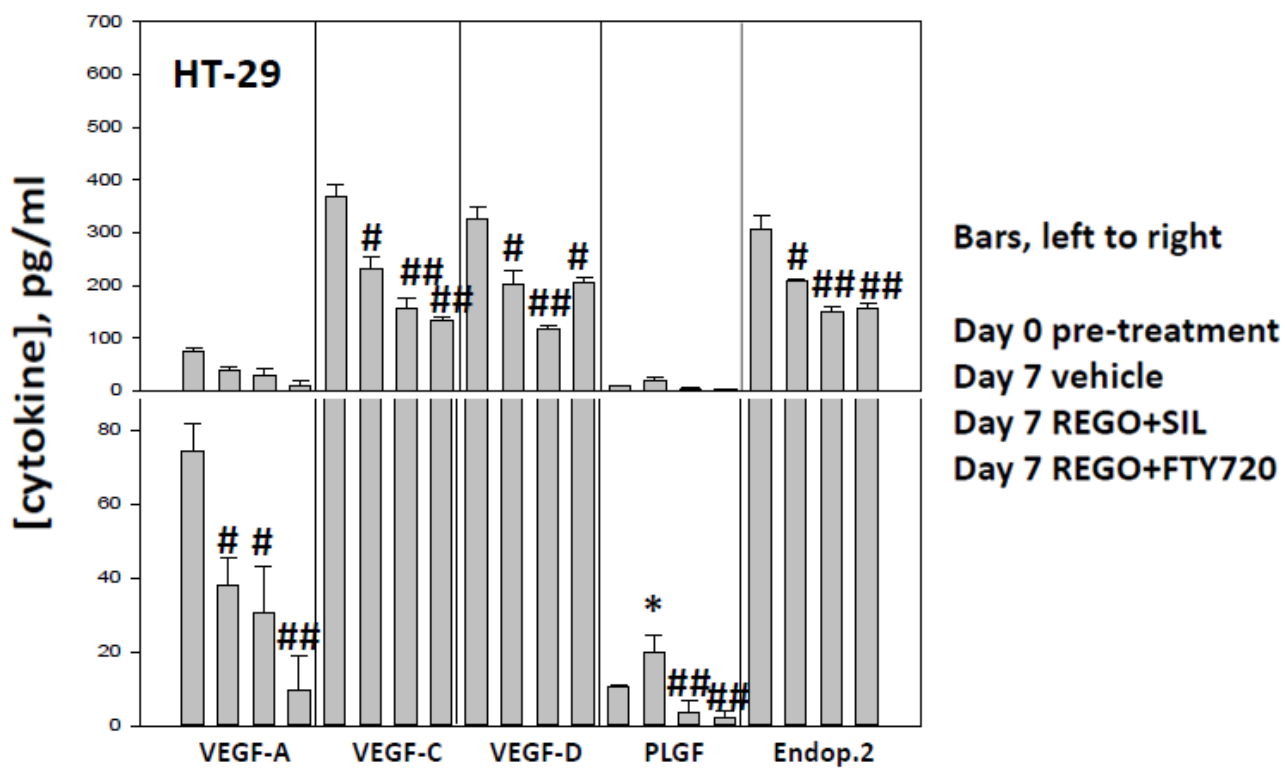
42E
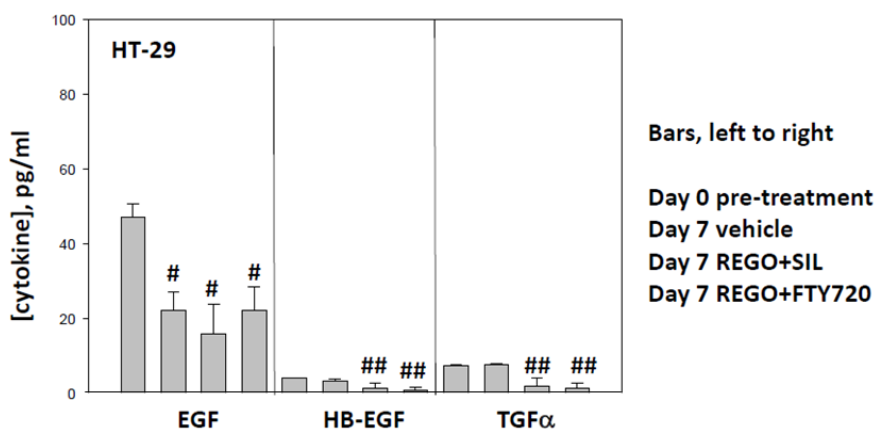
42F
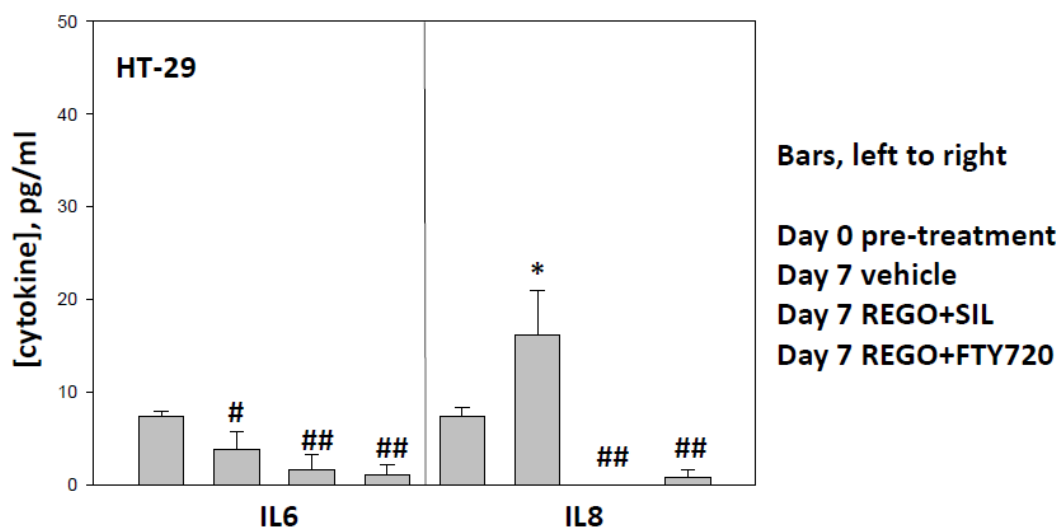
42G
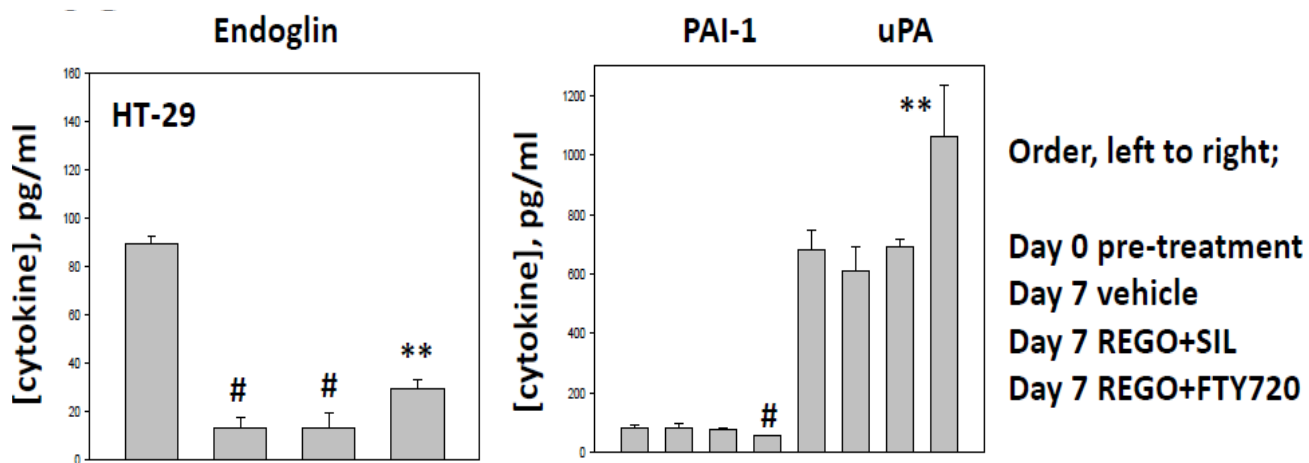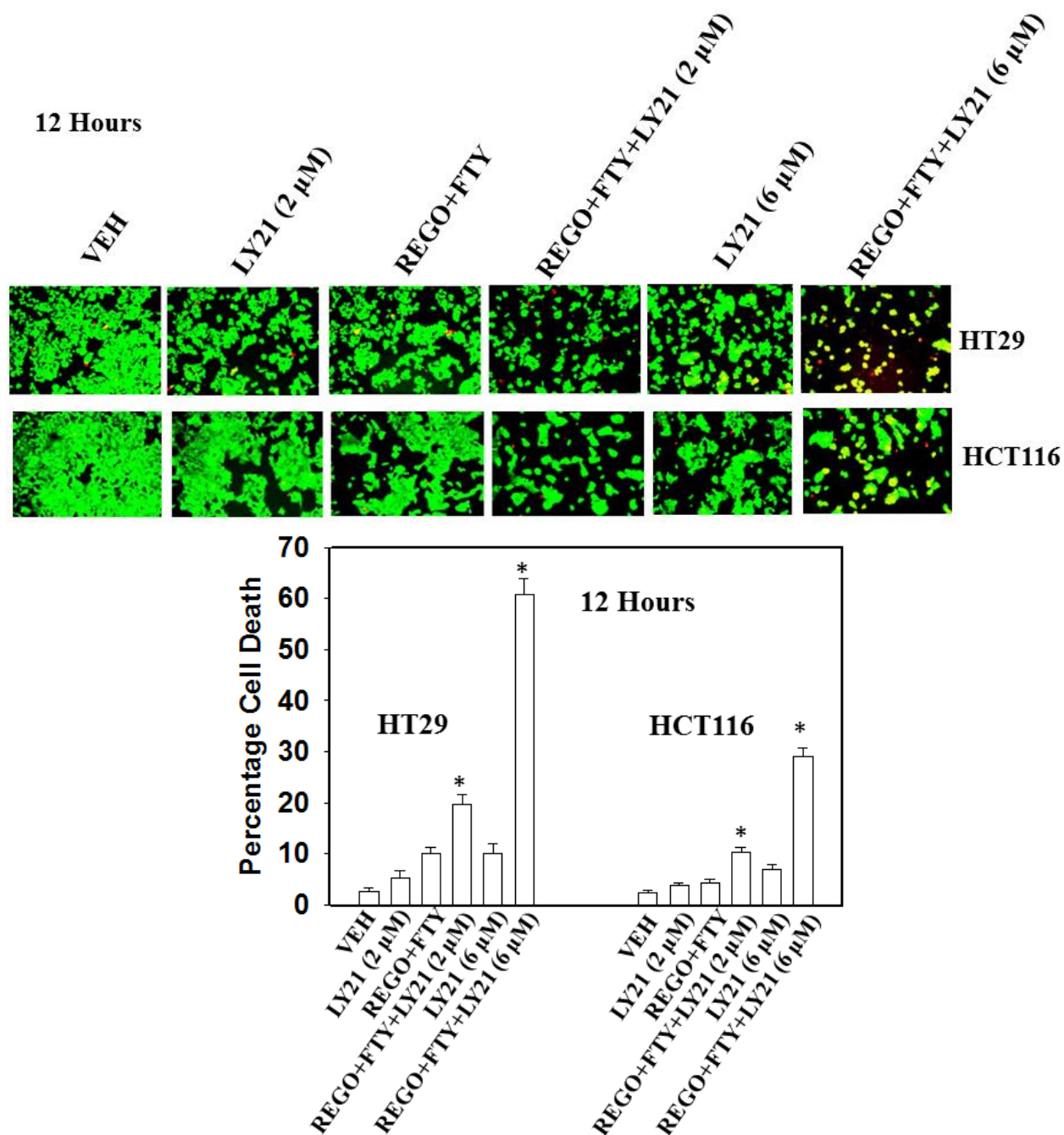
Figure 43. Inhibition of TGFβ signaling enhances the toxicity of regorafenib and FTY720 combination. HT29 and HCT116 cells were treated with vehicle (DMSO), regorafenib (0.5 µM) and FTY720 (50 nM) combination, LY2157299 (2, 6 µM), or the combination of all drugs as indicated. 12 hours after drug treatment, cell viability was assessed using a Hermes Wiscan instrument (n = 3, ± SEM). *$P < 0.05$ greater than corresponding value in REGO+FTY cells.

The drug combination alters multiple signaling pathways

We also collected tumor and blood materials at the time of humane sacrifice of the mice from our HT29 experiment. Most notably the expression of growth factors bFGF and PDGFbb were elevated and the expression of GM-CSF reduced (Figure 44A). This was associated with increased AKT activity and reduced p70S6K phosphorylation (Figure 44B). Changes in receptor phosphorylation or transcription factor phosphorylation were not significant (Figure 44C and D). Based on our data showing that drug-treated tumors had stable high EGFR phosphorylation, expressed more FGF and had higher AKT activity, we determined the impact of the inhibitors of EGFR (lapatinib), FGFR (BGJ398), and AKT (MK2206) on the toxicity of regorafenib and sildenafil combination. Inhibition of either AKT or EGFR enhanced the lethality of regorafenib and sildenafil combination (Figure 45).

We then determined the activities of multiple signal transduction pathways/proteins in tumors collected 7 days after the start of the treatment. Treatment of HUH7 and HT29 tumors with the combination of regorafenib and sildenafil reduced plasma levels of FGF and GM-CSF and increased the levels of PDGFbb (Figure 42A and 46A). Regorafenib and sildenafil treatment also reduced the expression of multiple tumor growth factors in the blood of mice carrying HUH7 tumors (Figure 46B). In both HUH7 and HT29 tumors, the drug combination caused activation of AKT though total p70S6K phosphorylation was reduced in both tumor types (Figure 48C). These findings were associated with reduced PDGFRβ phosphorylation and decreased NFκB activity (Figure 46D and E). Based on the biomarkers for activated compensatory survival pathways, the candidates for third drug combinations include AKT inhibitors, FGFR inhibitors, and EGFR inhibitors. The impact of such inhibitors on the toxicity of regorafenib and sildenafil were validated *in vitro* (Figure 45).
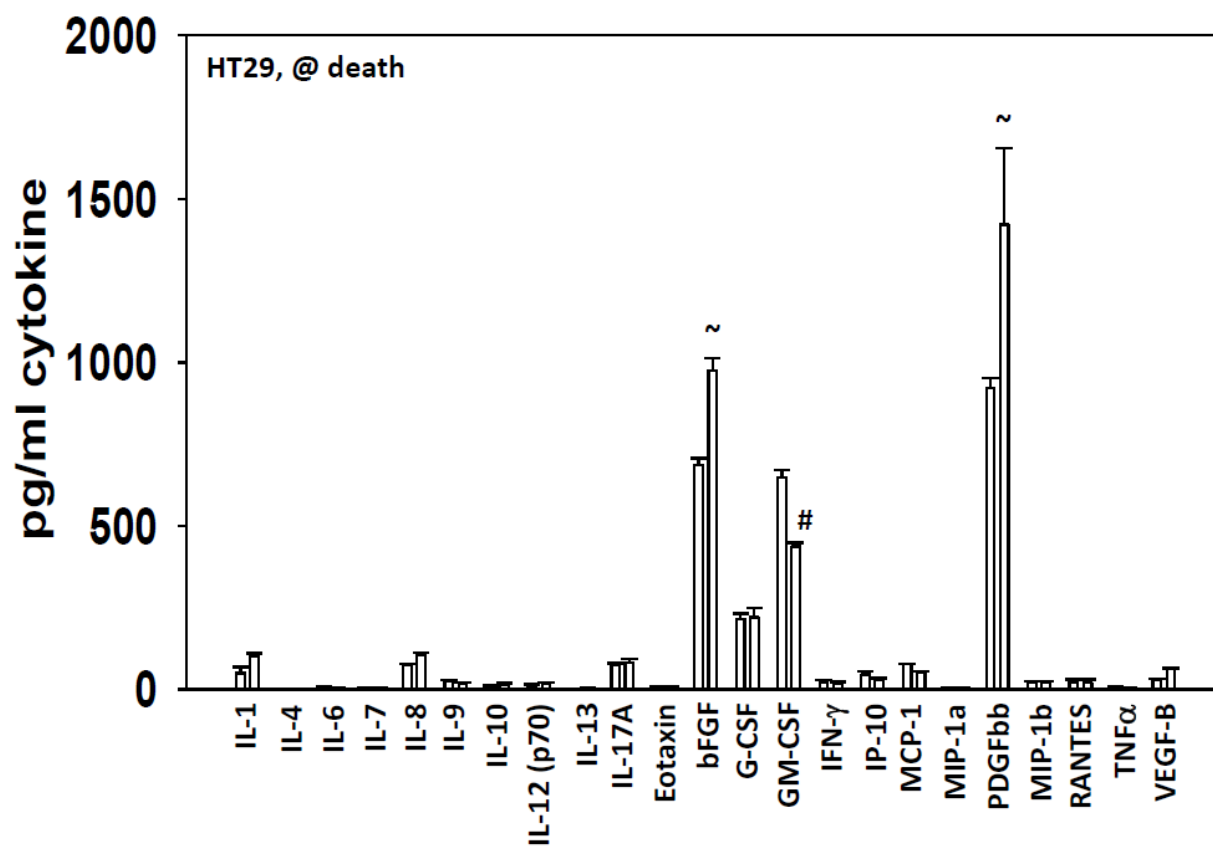
Figure 44. The drug combination alters multiple signaling pathways in tumor cells. (A-D) HT29 tumors isolated from the vehicle control or the combination of regorafenib and sildenafil-treated mice collected at the time of sacrifice were subjected to multiplex assays in a BIO-RAD MAGPIX instrument to determine the expression of cytokines in plasma and the phosphorylation of the indicated signal transduction proteins (n=8 ± SEM). ~$P< 0.05$ greater than vehicle control value. #$P< 0.05$ less than corresponding vehicle control value.

44B

HT29, @ death
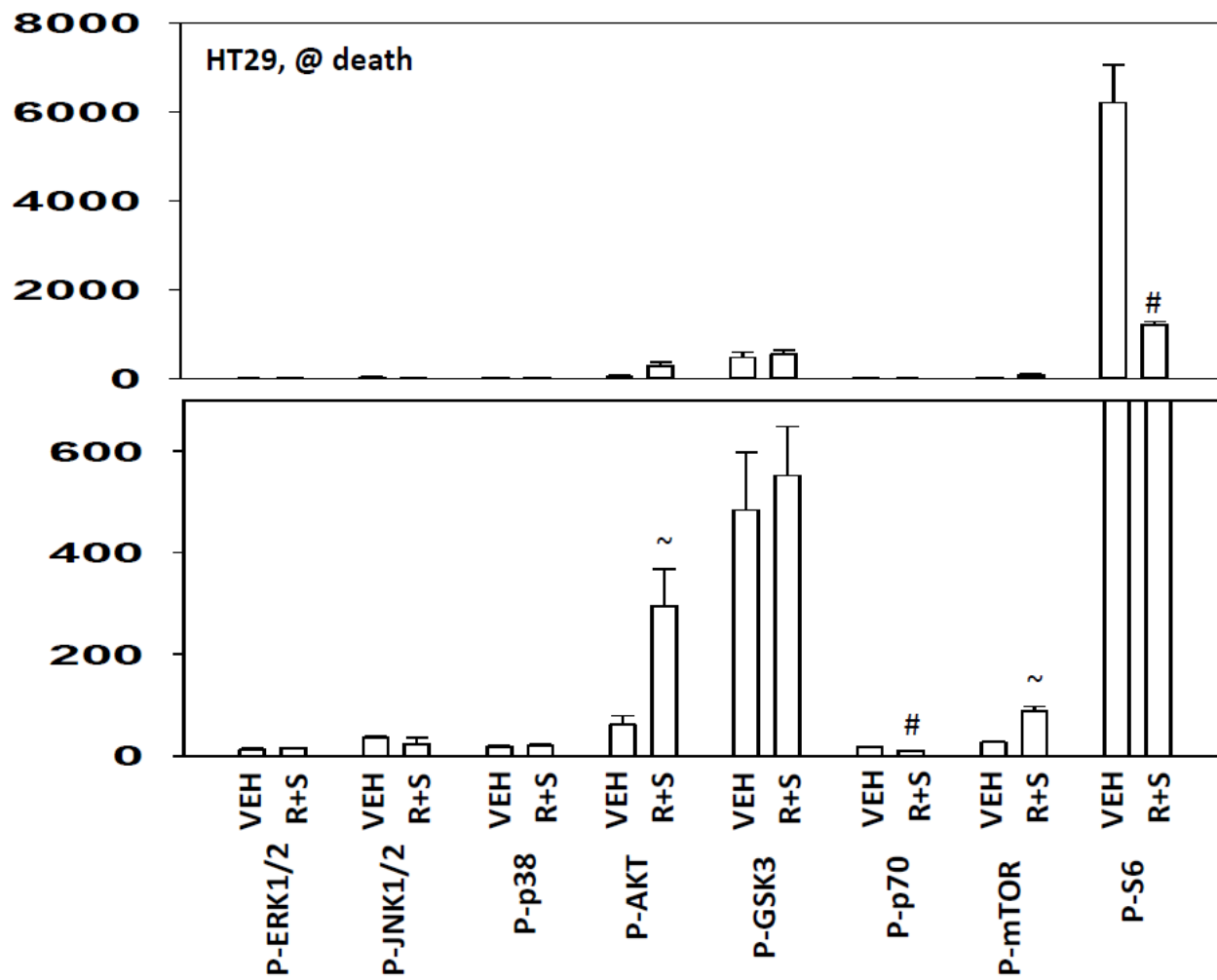
44C
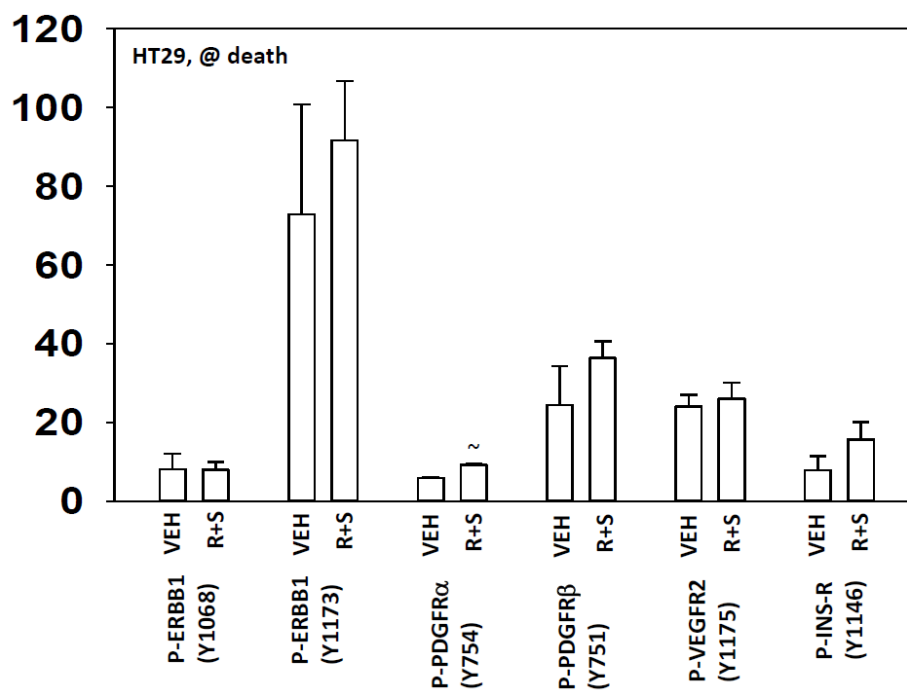
44D
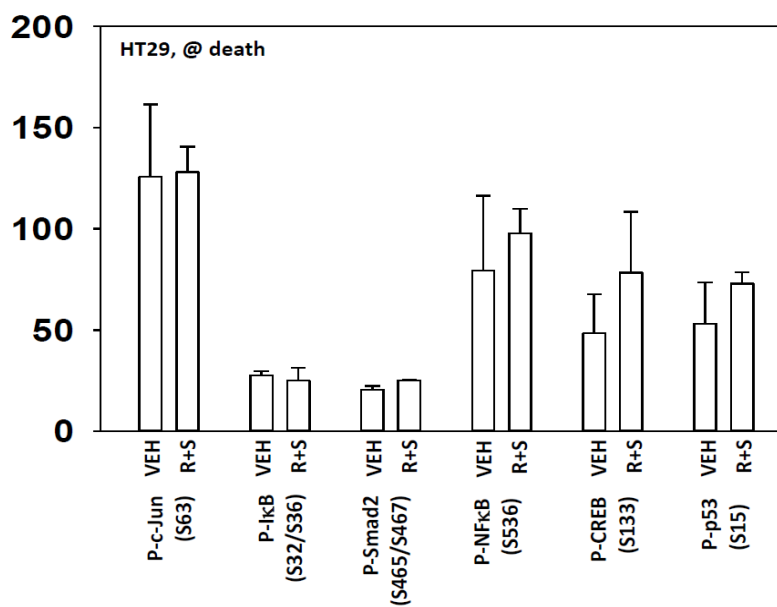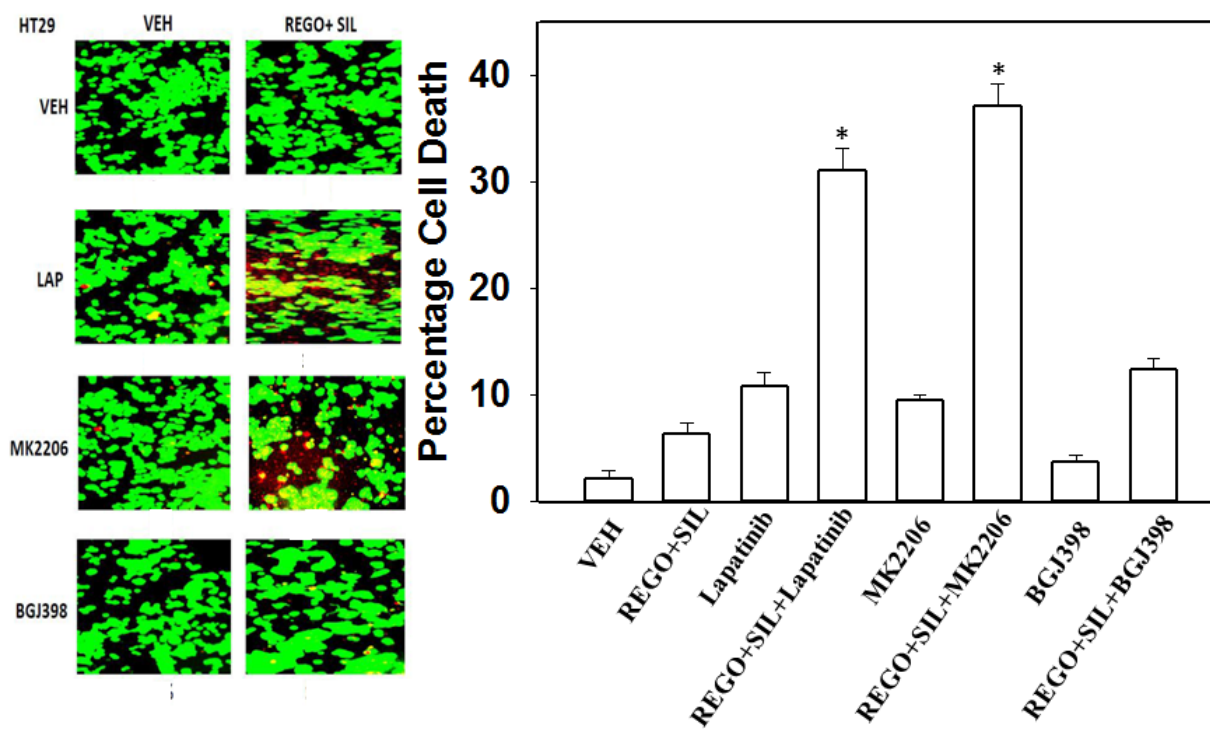
Figure 45. AKT, FGFR and EGFR inhibitors enhance the REGO+SIL combination lethality. HT29 cells were treated with vehicle (DMSO), regorafenib (0.5 μM) and sildenafil (2 μM) combination, lapatinib (1 μM), MK2206 (1 μM), BGJ398 (1 μM), or the combinations as indicated in the figure. 12 hours after drug treatment, cell viability was assessed using a Hermes Wiscan instrument (n = 3, ± SEM). *$P< 0.05$ greater than corresponding value in REGO+SIL group.
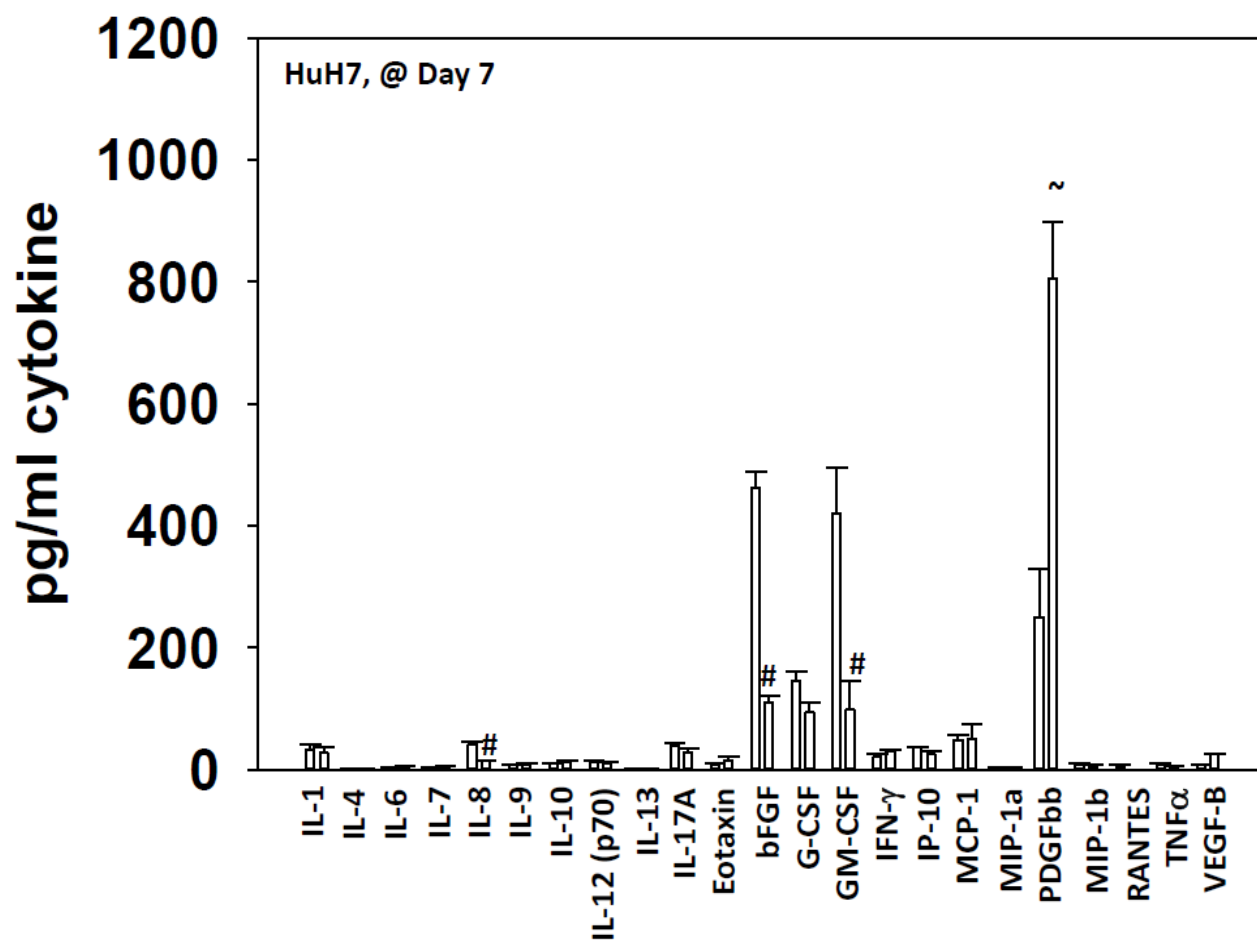
Figure 46. Multiplex analysis of tumors collected at the time of sacrifice. (A-E) HT29 and HUH7 tumors isolated from the vehicle control or the combination of regorafenib and sildenafil-treated mice collected at the time of sacrifice were subjected to multiplex assays in a BIO-RAD MAGPIX instrument to determine the expression of cytokines in plasma and the phosphorylation of the indicated signal transduction proteins (n=8 ± SEM). ~$P< 0.05$ greater than vehicle control value. #$P< 0.05$ less than corresponding vehicle control value.

46B

46C

46D

46E

HuH7 @ 7 days   HT29 @ 7 days
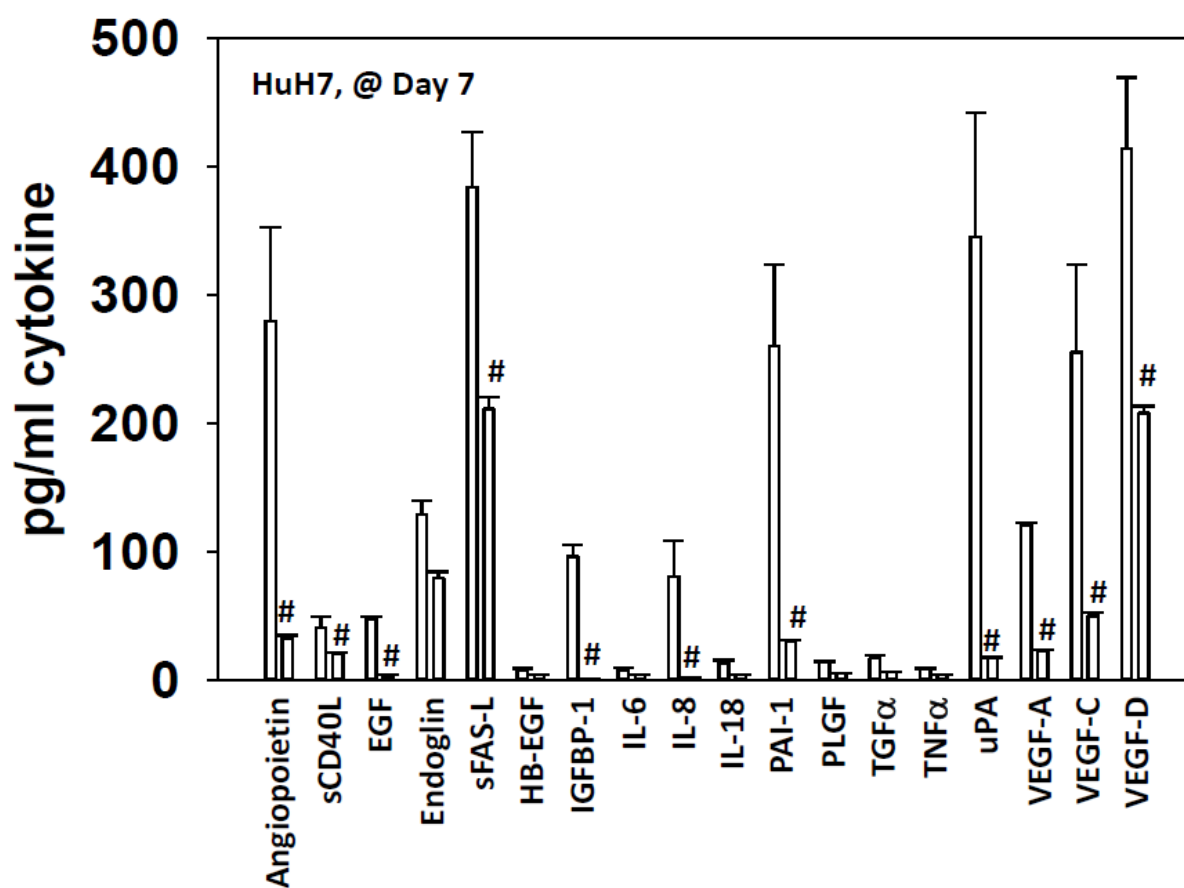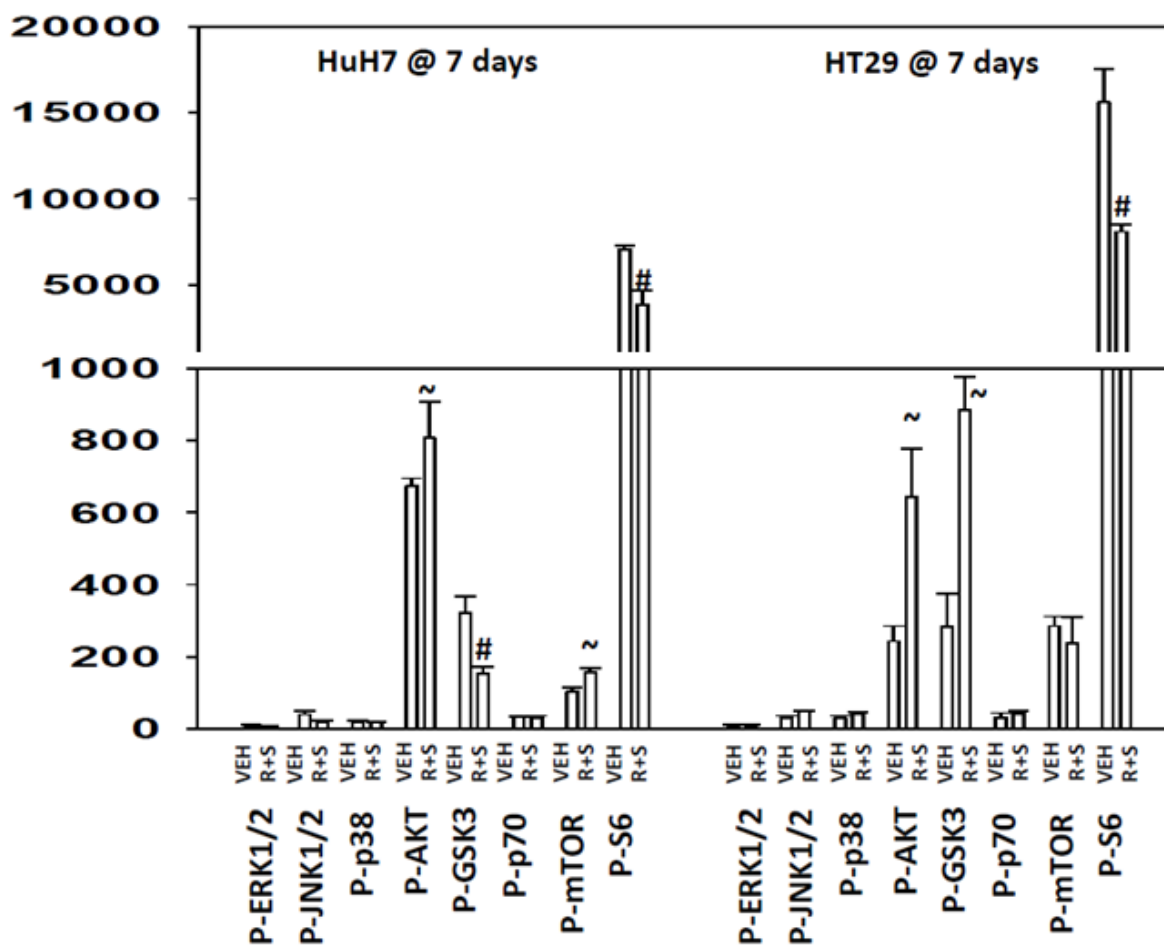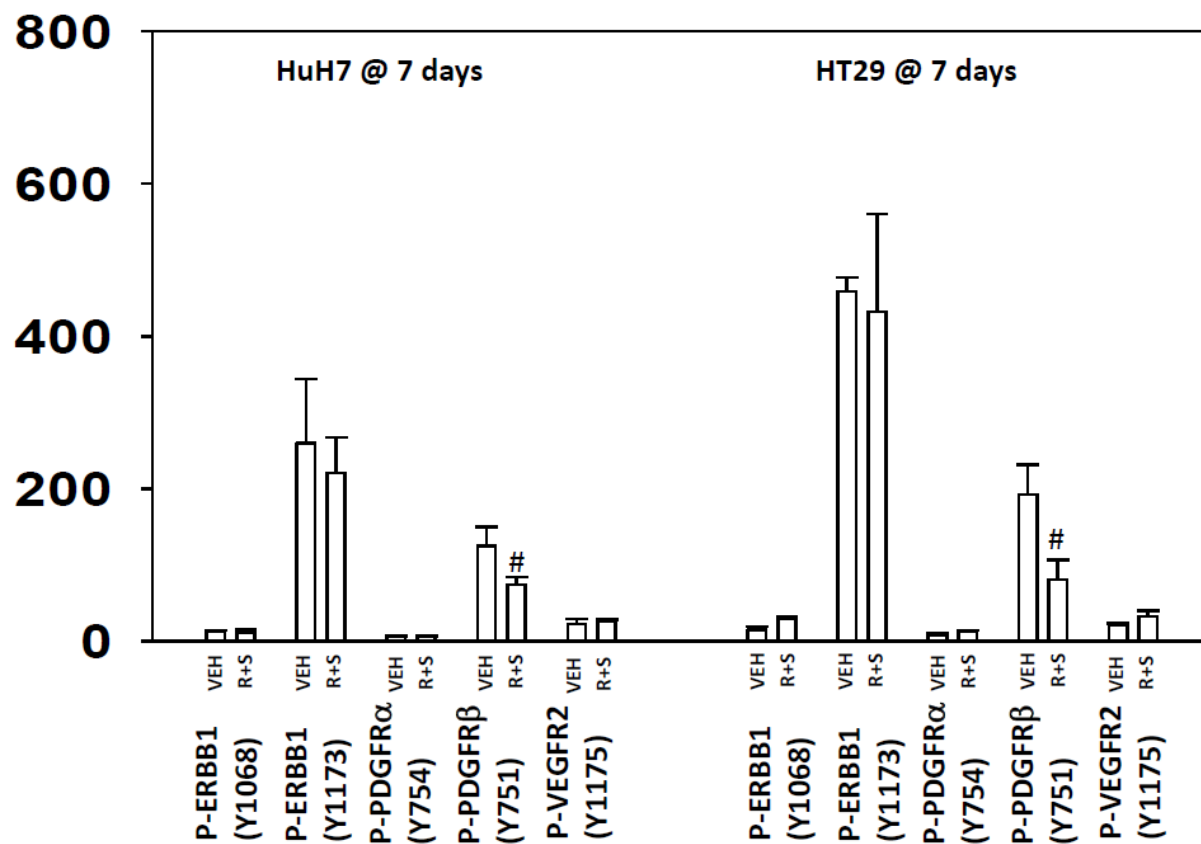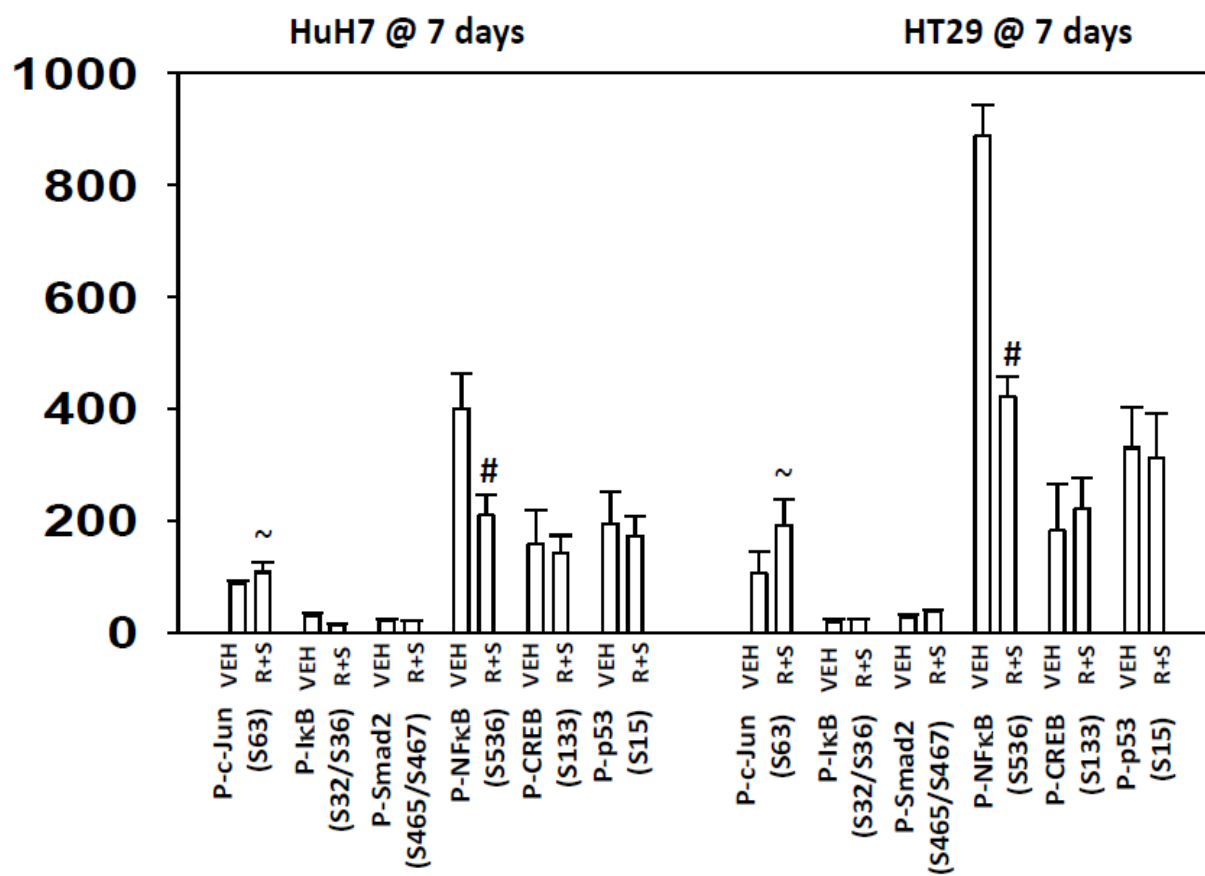
Discussion

Our data demonstrated that PDE5 inhibitor sildenafil and sorafenib/regorafenib interact to kill a genetically diverse set of hepatic and colon cancer cells *in vitro* and *in vivo*. Prior studies from our laboratory demonstrated that PDE5 inhibitors enhanced the toxicities of multiple chemotherapies.[145,146] In these studies PDE5 inhibitors, in a NOS-dependent fashion, were shown to enhance chemotherapy effect through activation of CD95 receptors, the generation of ROS, and mitochondrial dysfunction. In addition, in prior studies, we had demonstrated that PDGFRα/β play an important role in the biology of sorafenib and regorafenib in terms of its toxic combination with other therapeutics.[152] In agreement with our previous studies, knockdown of PDE5 recapitulated the combinatorial effect of a PDE5 inhibitor when combined with sorafenib whereas knockdown of PDGFRα/β recapitulated the combinatorial effect of sorafenib when combined with sildenafil. Thus, we further validated that the inhibition of PDE5 and PDGFRα/β does indeed play a major role in the induction of cell death by the drug combination. PDE5 inhibitors are known to enhance cGMP and NO levels; inhibition of NOS enzymes by L-NAME reduced the drug combination-mediated toxicity.

In our previous studies, we had described how sorafenib can interact with agents that generate ROS to facilitate activation of the death receptor CD95.[152] In these studies HUH7 cells, which lack endogenous CD95 expression, were particularly resistant to the tested sorafenib drug combinations. However, in this study, we have found that sorafenib and sildenafil interact to kill both CD95 null HUH7 cells and hepatoma cells that express CD95 (HEP3B and HEPG2), though the drug combination killing appears to be more efficient in HEP3B and HEPG2 cells. In order to further validate the role of death receptor CD95 signaling in drug combination-mediated cell death, we transfected HUH7 cells with a plasmid expressing wild type CD95, and managed

to immensely increase the combination-mediated lethality in these cells. Moreover, in cells expressing CD95, inhibition of both extrinsic and intrinsic apoptosis pathways suppressed the drug combination toxicity whereas in HUH7 cells cell death was due to the activation of intrinsic pathway. We also showed that activation of CD95 receptors was suppressed by inhibition of NOS enzymes. Studies by others have shown that nitrosylation of CD95 at its regulatory tyrosine residues inhibit CD95 signaling.[157] However, others have argued that NO signaling and activation of CD95 can cooperate to induce cell death.[158]

The drug combination also increased the numbers of autophagosomes and autolysosomes in a time dependent fashion that was inhibited by incubation of the cells with L-NAME and NAC. Inhibition of autophagy reduced cell death caused by the drug combination. NO signaling has been linked by others to the regulation of autophagy as in some primary non-transformed cells NO can inhibit autophagy by inhibiting JNK signaling.[159,160] However, in some transformed cells NO signaling can promote autophagy in an mTOR-dependent fashion, which seems to play a role in tumor cell death.[161,162] In this study, we demonstrated that the drug combination inactivated mTOR, and expression of an activated mTOR suppressed killing. Activation of the JNK pathway played a key role in the drug combination-mediated lethality. Therefore, NO signaling plays a role in de-repressing a brake on toxic autophagy (mediated by mTOR) as well as promoting activation of CD95-mediated apoptosis.

The drug combination rapidly increased the levels of ROS and RNS. Inhibition of NOS enzymes almost abolished cell killing caused by the drug combination whereas quenching of ROS by NAC was partially protective. In accordance with these findings, knockdown of iNOS and eNOS was also protective. One important mechanism by which NO is inactivated is by reaction with the superoxide anion (O_2^-).[163] Compared to non-transformed cells, tumor cells

generate considerably greater amounts of O_2^-.[164] As mentioned before, NOS activity depends on several cofactors, including NADPH and BH4. BH4 plays a critical role in NOS activity. Small ratio of BH4 relative to its oxidized form, BH2, causes NOS uncoupling, leading to production of ROS and RNS rather than NO, a phenomenon commonly observed in cancer cells.[87,89] Thus, whereas sildenafil is often associated with reduced oxidative stress in non-transformed cells, it promotes oxidative stress in tumor cells.[156] The reaction of NO with O_2^- forms the most potent oxidant peroxynitrite ($ONOO^-$).[165] Peroxynitrite causes oxidative damage and S-nitrosylation of proteins, lipids, and DNA.[166] Nitrosative stress by $ONOO^-$ has been implicated in DNA breakage, followed by PARP and ATM/ATR activation.[167] Further studies will be required to determine whether ATM/ATR signaling plays any role in the regulation of apoptosis/autophagy pathways and signal transduction pathways.

As previously stated, a major biological effect of sorafenib is the induction of ER stress/UPR, with reduced expression of proteins that have short half-lives such as Mcl-1 and Bcl-xL.[153,154] In agreement with these reports, the drug combination in this study also induced UPR as the levels of phospho-PERK and phospho-eIF2α rapidly increased within 6 hours after drug exposure. Of note, in addition to a reduction in Mcl-1 and GRP78 levels, the levels of multiple other chaperones such as GRP94, HSP90 and HSP70 as well as the ABC transporters ABCB1 and ABCG2 were significantly reduced *in vivo* as shown by immunohistochemistry data. Further investigations from our laboratory indicated that the combination of sildenafil and regorafenib/sorafenib reduced the levels of a wide range of surface receptors, including the receptors involved in viral and bacterial infections, which further highlighted the therapeutic value of chaperones, most notably GRP78, in treatment of multiple human diseases.[126,168] Inhibition of the UPR components such as PERK, ATF4 and CHOP significantly reduced the

drug combination lethality. Prior studies by our colleagues had reported that sorafenib treatment induced ER stress and activation of caspase 2 and 4, which directly induce apoptosis.[153] The role of ER-specific caspase activation was not explored in this study. However, our data argues that the ER stress is involved in the drug combination-induced cell death.

Based on our encouraging *in vitro* data, we moved our studies forward using several animal model systems in athymic mice. Short-term exposure to sildenafil and regorafenib killed tumor cells as judged by *ex vivo* colony formation assays. Long-term exposure to sildenafil and sorafenib suppressed HUH7 tumor growth over several weeks. This is of note as HUH7 cells, which lack CD95, would be predicted based on *in vitro* data to respond relatively poorly to the drug combination. Similarly, the growth of HT29 tumors treated with the combination of regorafenib and sildenafil was profoundly reduced both during and for many weeks following the cessation of treatment, which was reflected in a significant increase in animal survival. The drug combination anti-tumor activity *in vivo* is likely an amalgamation of a direct anti-tumor cell killing effect by the drug combination and increased tumor vasculature permeability caused by the actions of sildenafil on endothelial cells.[169] During our *in vitro* studies, we also noted an increase in ceramides and S1P in response to regorafenib treatment. S1P has previously been linked to the induction of colitis-associated cancer (CAC), and treatment with FTY720 has been shown to block CAC progression.[149,150] Our *in vitro* studies indicated that the addition of FTY720 to the drug combination significantly enhanced cell death in HT29 and HUH7 cells. Therefore, we determined whether FTY720 could replicate the same effect in the mouse models. To our surprise, FTY720-treated tumors resulted in an unexpected stronger re-growth of tumors after cessation of drug treatment than the tumors treated with regorafenib or the regorafenib and sildenafil combination. Images taken from the tumors indicated that the FTY720-treated tumors

had a more vascularized appearance. Multiplex analysis of cytokines in the blood of animals treated with FTY720 collected at day 7 revealed a significant increase in angiogenic factors, including VEGF-A, VEGF-D and angiopoietin. Additionally, treatment of tumors with regorafenib and FTY720 combination increased the expression of pro-growth/pro-angiogenic/pro-invasion cytokine endoglin, which enhances TGFβ signaling. Thus, we determined whether the toxicity of regorafenib and FTY720 combination was enhanced *in vitro* using TGFβ inhibitor LY2157299 (Galunisertib). Our data indicated that the inhibition of TGFβ receptor 1 signaling in a dose-dependent fashion significantly enhanced the toxicity of regorafenib and FTY720 combination.

Based on our multiplex analysis data from the collected tumors and blood from the animals at the time of sacrifice, we found that drug combination-treated tumors had stable high EGFR phosphorylation, expressed more FGF and had higher AKT activity. Consequently, we determined the impact of the inhibitors of EGFR (lapatinib), FGFR (BGJ398), and AKT (MK2206) on the toxicity of regorafenib and sildenafil combination. Inhibition of either AKT or EGFR enhanced the lethality of regorafenib and sildenafil combination. Thus, the activation of AKT and EGFR in response to the regorafenib and sildenafil combination seems to be the major compensatory survival pathways.

As the drugs used in this study are all FDA approved agents, our data argue for further determination as to whether sorafenib/regorafenib and sildenafil can interact in the same fashion in the clinic. Recently, a clinical trial in Massey Cancer Center (NCT02466802) evaluating the combination of regorafenib and sildenafil in all solid tumors has opened.
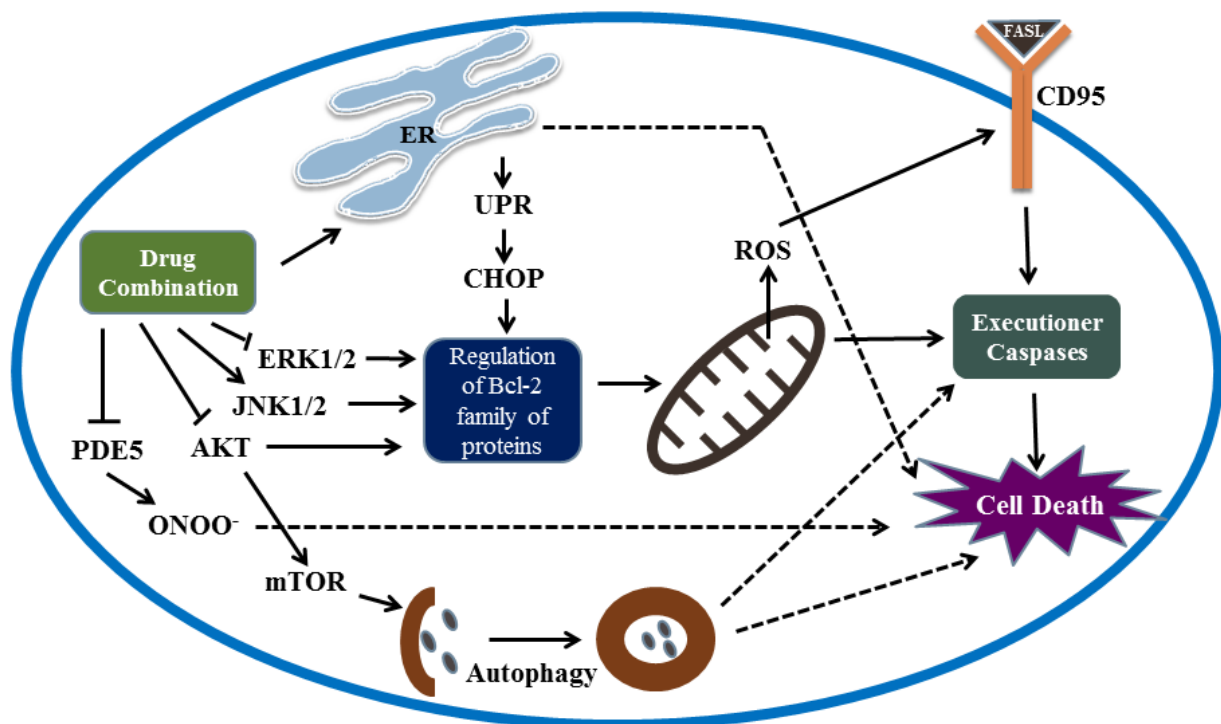
Figure 47. Proposed mechanism of the SOR/REGO+SIL combination-mediated cell death. The drug combination inhibited PDE5, thus increasing the levels of ROS and RNS in a NOS-dependent fashion. The generation of ROS was shown to activate death receptor CD95 signaling. The drug combination also inhibited ERK1/2 and AKT, and activated JNK1/2. Inhibition of AKT/mTOR pathway activated a toxic form of autophagy. In addition, the drug combination induced the UPR; resulting in an increase in transcription of CHOP. The induction of ER stress by the drug combination was shown to be involved in mediating cell death.(Guide: ⟶ represents explored pathways, --→ represents unexplored but feasible pathways)

Conclusion

Collectively, our data from this study demonstrated that sorafenib/regorafenib interacts with sildenafil to kill a genetically diverse set of hepatic and colon cancer cells *in vitro* and *in vivo* in a process that involves ER stress, autophagy, and intrinsic and extrinsic apoptotic pathways. The drug combination rapidly increased the levels of ROS and RNS in a NOS-dependent fashion. Incubation of cells with L-NAME, a NOS inhibitor, suppressed drug combination-induced CD95 activation. Long-term exposure to sildenafil and sorafenib suppressed HUH7 tumor growth over several weeks. Similarly, the growth of HT29 tumors treated with the combination of regorafenib and sildenafil was profoundly reduced both during and for many weeks following the cessation of treatment, which was reflected in a significant increase in animal survival. By applying multiplex technology, we were able to predict and validate various signaling biomarkers with AKT and EGFR being identified as major compensatory survival responses to the drug combination.

CHAPTER 4: Ruxolitinib and EGFR Inhibitors Interact to Kill Breast Cancer Cells in a Synergistic Fashion

Breast Cancer

Breast cancer is the leading cause of death in women worldwide. According to World Health organization (WHO), in 2012 breast cancer accounted for 23% of all cancer deaths across the globe.[170] The same year in the US, 200,000 new cases were diagnosed with about 40,000 of the patients losing their lives, making it the second deadliest disease among women after lung cancer.[171] Early detection due to screening, more effective adjuvant therapies, and lower rates of hormone replacement therapies have contributed to the declining mortality rates in the recent years.[171] Breast cancer is generally classified into three categories: hormone receptor (ER) positive, HER2 positive and triple negative breast cancer (TNBC).[171] Current treatments for breast cancer include: Surgery (breast-conserving or total mastectomy), radiation therapy, chemotherapy, hormone therapy, and targeted therapy.

Hormone receptor positive carcinomas account for nearly 70% of all breast cancers.[172] Adjuvant hormonal therapy with tamoxifen has been the standard therapy for postmenopausal women with ER positive breast cancer.[173] Recently, nonsteroidal aromatase inhibitors, such as letrozole and anastrozole have been shown to have superior effects over tamoxifen in reducing circulating estrogen levels. These compounds are currently approved by FDA for the fist- and second-line treatment of ER positive metastatic breast cancer.[173]

HER2 positive subtype accounts for 20-30% of all breast cancers. HER2 positive breast cancers are more aggressive, more likely to metastasize, and show increased resistance to hormonal therapy.[174] Adjuvant therapies that contained EGFR inhibitors, such as trastuzumab and lapatinib have significantly improved the clinical outcomes in HER2 positive patients.[174,46]

TNBCs constitute 15-20% of all the breast carcinomas, and are clinically defined as tumors that lack immunohistochemical expression of estrogen receptors (ER), progesterone receptors (PR) and HER2 overexpression.[175,176] This infamous subtype of breast cancer is known for its poor prognosis, aggressiveness, high rates of brain metastases and greater incidence of early recurrence with median survival rate of approximately 1 year.[175] Since TNBCs are generally resistant to chemotherapy with currently no alternative treatments available to those affected, it seems imperative to identify new molecular targets that these cells rely upon for proliferation, differentiation and growth.[171,176]

Ruxolitinib

Manufactured by Novartis, ruxolitinib (INCB018424, Jakafi) is a selective inhibitor of JAK1 and JAK2 with IC_{50} values of 3.3 and 2.8 nM, respectively. It was approved by the FDA in November 2011 for the treatment of intermediate or high-risk myelofibrosis, and phase I/II clinical trials have manifested its capability in the reduction of splenomegaly and alleviating the disease-associated symptoms.[177-179] Orally administered, ruxolitinib is absorbed rapidly and reaches C_{max} within 2 hours before undergoing metabolism by the hepatic CYP3A4 system with its mean half-life within the range of 3-4 hours.[177,179,180] The mean C_{max} value for a single dose of 25mg of the drug was measured to be approximately 1093 nM.[177,181] Throughout the clinical studies, ruxolitinib was well tolerated by the patients who received a safe dose of 15 mg bid, and the toxic effects have been limited to ecchymosis, anemia, dizziness and headache.[177,179] Ruxolitinib binds in the ATP binding pocket of its targets, inhibiting both wild-type JAK1 and JAK2 and mutant JAK2 V617F (a gain-of-function mutation commonly observed in myelofibrosis).[179] Clinical studies have also demonstrated that ruxolitinib, through inhibition of JAK1 and JAK2, suppressed phosphorylated-STAT3 and -STAT5 resulting in a reduction in

signal transduction and inflammatory cytokine levels, including IL-6, TNF α, and macrophage

inflammatory protein 1β.[178,179]
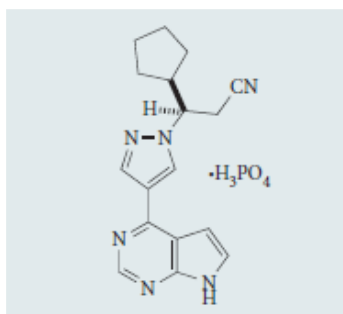
Figure 48. Chemical structure of ruxolitinib phosphate.[182]

Lapatinib

     Developed by GlaxoSmithKline, lapatinib (GW-572016, Tykerb) is a selective inhibitor

of EGFR/ERBB-1 and Her-2/ERBB-2 signaling, with IC_{50} values of 10.2 and 9.8 nanomolar,

respectively.[183-186] In January 2010, lapatinib was granted accelerated FDA approval to be used

in combination with letrozole for the treatment of postmenopausal women with hormone

receptor positive metastatic breast cancer that over-express ErbB-2 receptor (more information

available at http://www.cancer.gov/about-cancer/treatment/drugs/fda-lapatinib). Lapatinib

exhibits reversible, non-covalent inhibition of EGFR and ErbB-2 by binding in the ATP-binding

cleft located on the intracellular kinase domain of these receptors.[183] This leads to suppression of

signal transduction through downstream pathways, including Ras/MAPK, and PI3K/AKT

pathway, ultimately resulting in growth arrest or apoptosis of cancer cells.[184] Lapatinib reaches

its plasma C_{max} of nearly 4 μM 3-4 hours after the oral administration, and is metabolized mostly

by the hepatic CYP3A4 system. The elimination half-life of lapatinib is about 14 hours after

single dose administration.[185] Lapatinib caused minimal toxic effects in patients who received a

daily dose of 1500 mg with the adverse events being limited to diarrhea, skin rash, and fatigue.[186]
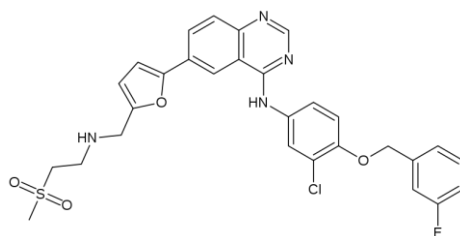
Figure 49. Chemical structure of lapatinib.[185]

Afatinib

Developed and manufactured by Boehringer Ingelheim, afatinib (BIBW2992, Gilotrif) is an oral inhibitor of ERBB family of tyrosine kinases.[187-189] It binds EGFR, ErbB2 and ErbB4 receptors with high selectivity with IC_{50} values of 0.5, 14 and 1nM, respectively.[187,188] Afatinib carries a Michael acceptor group, which allows for covalent binding to specific residues within the ATP binding pocket of its targets, resulting in irreversible inhibition of receptor autophosphorylation.[188] It also blocks transphosphorylation of ErbB3.[187] In the United States, afatinib is approved for the treatment of patients with metastatic NSCLC whose tumors contain EGFR exon 19 deletions or exon 21 (L858R) substitution mutations.[187] Afatinib is absorbed relatively fast, with steady state being reached within 8 days.[187,188] The mean half-life of afatinib is 30-48 hours.[188] It goes through minor hepatic metabolism, and is mainly eliminated via feces (85%), and urine (4%).[187] Afatinib caused minimal toxicity in patients who received a recommended daily dose of 40 mg, with side effects being limited to rash and diarrhea.[187,188]
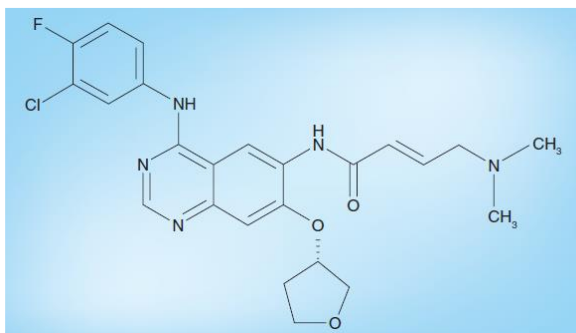
Figure 50. Chemical structure of Afatinib.[188]

The drug Combination Rationale

EGFR amplification and overexpression is commonly observed in many breast cancers, including 30-52% TNBC carcinomas.[190,191] It has been well documented that the tumors with alterations in EGFR receptor are more aggressive in nature and lead to more dismal clinical outcome.[82] Therefore, EGFR-targeted therapy in all types of breast carcinoma, including TNBC, emerged as a promising approach with many agents such as cetuximab, trastuzumab and lapatinib employed in numerous clinical trials.[46,82,174] However, there is growing evidence that inhibition of ErbB receptors as a monotherapy is not adequate for blocking the malignancy, and the combination of targeted inhibitors will most likely present a more feasible approach.[82]

Prior studies have suggested a prominent role for cytokine receptor signaling through JAK/STAT pathway in breast carcinogenesis, and prolactin, erythropoietin, and other cytokines such as IL-6 and IL-11 have been linked to an increase in breast cancer incidence.[192-195] In addition, STAT3 and STAT5 activation have been shown to contribute significantly to the induction of mammary carcinogenesis.[196,197] Between the two, STAT3 acts as a point of convergence for many well-known oncogenic pathways, and its role in promoting tumorigenesis and drug resistance has been supported by numerous studies.[198,199] However, no inhibitor of STAT3 has been approved by FDA yet.[198] Furthermore, EGFR and STAT signaling crosstalk through different mechanisms.[200] For instance, EGFR signaling can activate STAT3 in a process mediated by Src family of kinases, and STAT3 has been demonstrated to upregulate ErbB2 transcription in metastatic HER2 positive breast cancer.[83,201] These findings led us to hypothesize that the concurrent inhibition of JAK/STAT and EGFR pathways would cause detrimental effects in breast cancer cells. Since there are no FDA-approved STAT inhibitors available at the

moment, and knowing that STAT3 and STAT5 are both heavily involved in breast cancer, we repurposed ruxolitinib, a JAK1/2 inhibitor, as a novel therapeutic in treatment of breast cancer.

Hypothesis

Concurrent inhibition of JAK/STAT and EGFR signaling pathways induces cell death in breast cancer cells, and profoundly reduces mammary tumor growth.

Cell Line	Major Characteristics
SUM149PT	Triple Negative, Mutant p53
HCC38	Triple Negative, Mutant p53
BT549	Triple Negative, Mutant PTEN and p53
BT474	HER2 Overexpression, Mutant PI3K and p53
MCF7	ER positive, Mutant PI3K, Wild Type p53

Table 2. Breast cancer cell lines used in this study.

Results

Ruxolitinib and lapatinib synergize to kill breast cancer cells

Initial studies determined whether the ERBB1/2/4 inhibitor lapatinib (referred to as LAP in the figures) interacted with the JAK1/2 inhibitor ruxolitinib (referred to as RUX in the figures) to kill breast cancer cells. Our data indicated that lapatinib and ruxolitinib strongly interacted to kill a variety of breast cancer cells, including cells from all three subtypes; triple negative (SUM149PT, HCC38 and BT549), HER2 positive (BT474), and ER positive (MCF7) (Fig 51).

The synergistic interaction between ruxolitinib and lapatinib was determined by colony formation assay. Median dose effect isobologram analysis to determine synergism of drug interaction was carried out according to the methods of Chou and Talalay using the CalcuSyn program.[151] The data suggested that ruxolitinib and lapatinib interacted in a synergistic fashion to kill SUM149PT cells, with combination index (CI) values significantly below 1.0 (Figure 52).

Next, using molecular tools, we defined which ERBB family members in different cell types were responsible for the interaction of ERBB receptor inhibitors and ruxolitinib. SUM149PT cells were isolated from an inflammatory breast cancer patient whose tumor was defined as "triple negative" but which nevertheless in our hands expressed detectable basal levels of ERBB1, ERBB2, ERBB3 and ERBB4 by immuno-fluorescence of cells fixed in situ. In SUM149PT cells combined inhibition of ERBB1 and ERBB2 or ERBB1, ERBB2 and ERBB4 strongly enhanced ruxolitinib toxicity (Figure 53).

Ruxolitinib is claimed to be a specific inhibitor of the Janus kinases JAK1 and JAK2, but does not block JAK3 or TYK2. Thus we next determined whether knockdown of JAK1 and JAK2 could account for the effects of ruxolitinib. Knockdown of both JAK1 and JAK2 enhanced the lethality of lapatinib (Figure 54).

51A
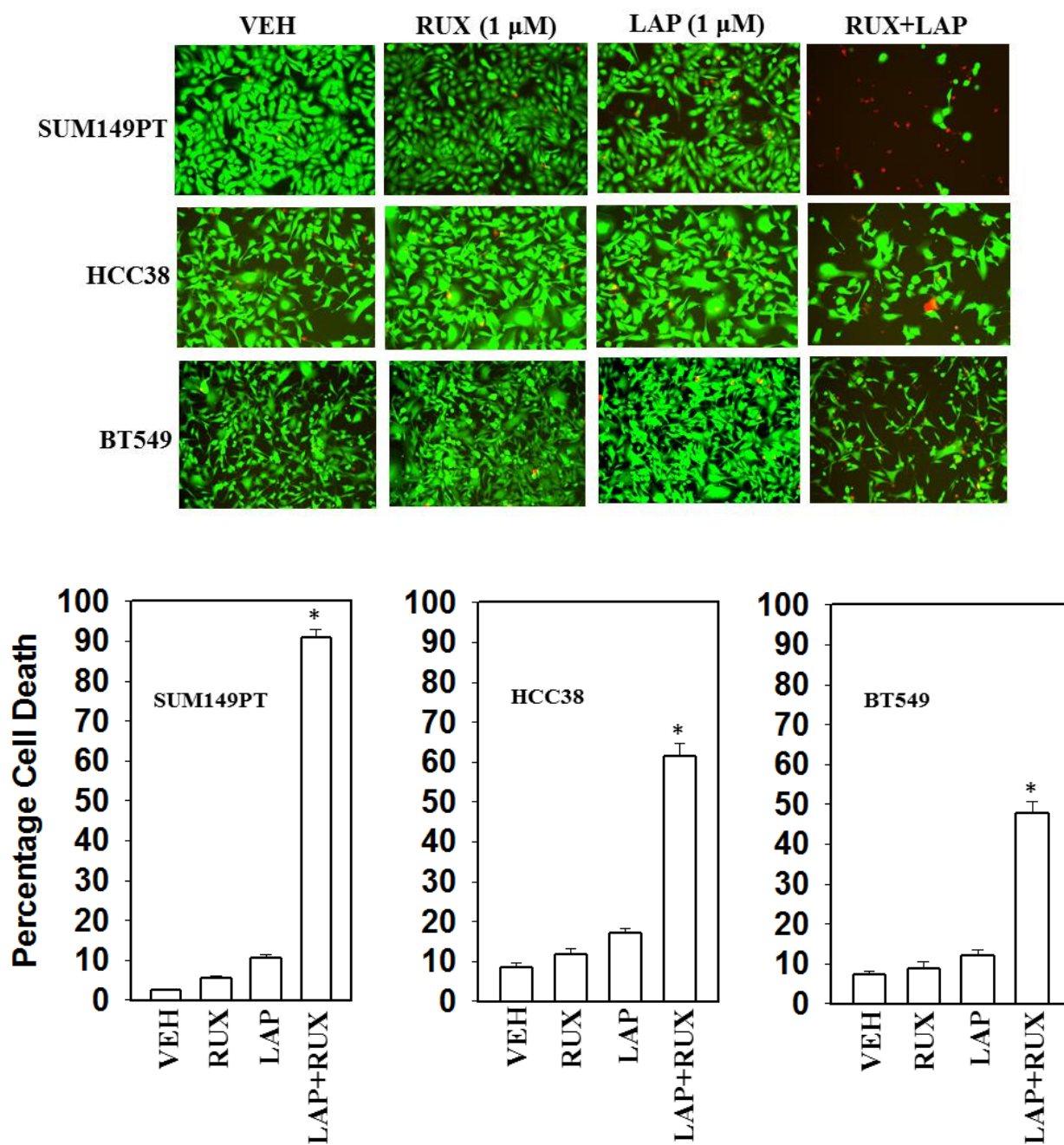
51B
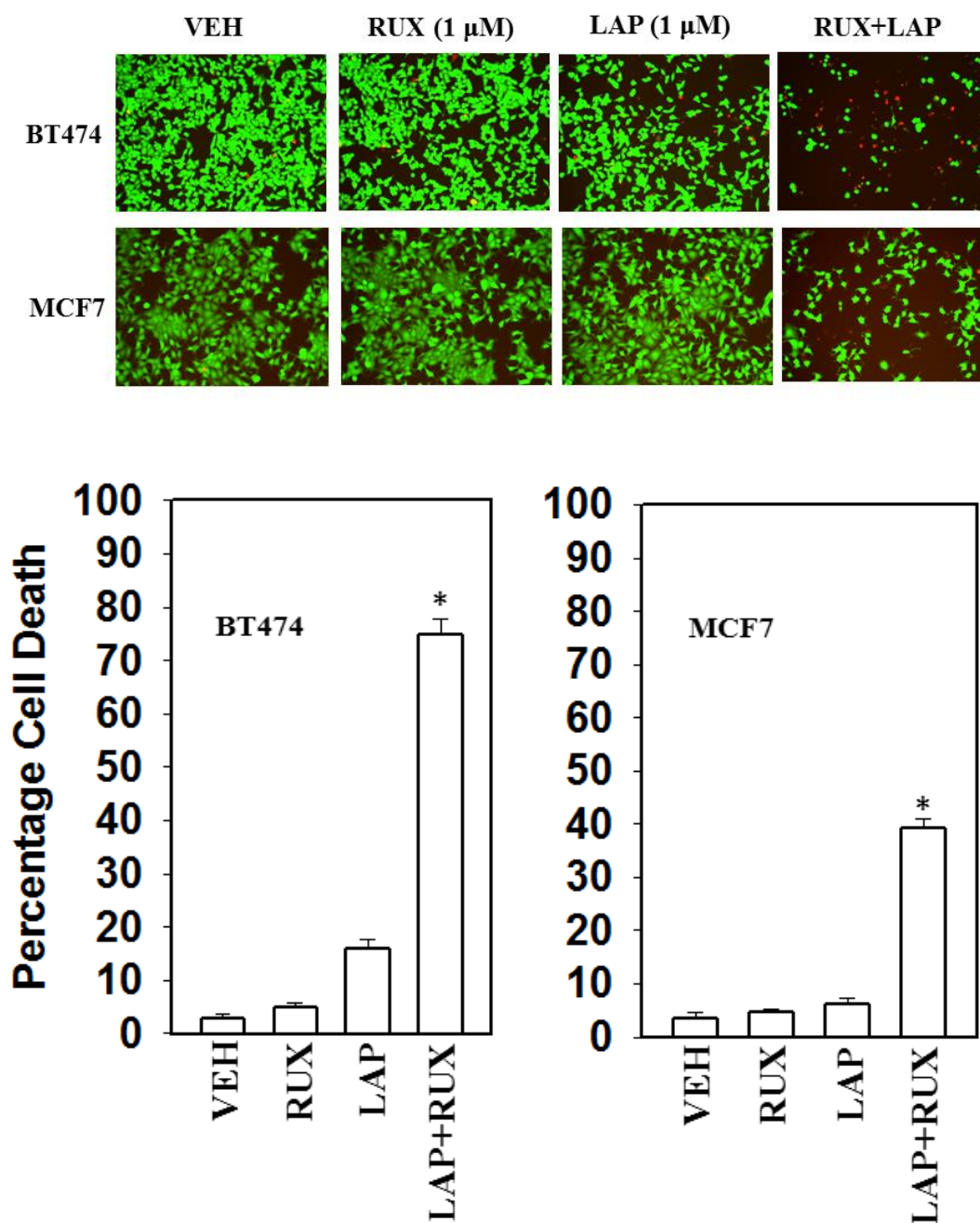
Figure 51. Ruxolitinib and lapatinib interact to kill breast cancer cells. Indicated cells were treated with vehicle (DMSO), ruxolitinib-phosphate (1.0 μM), lapatinib tosylate (1.0 μM) or the drugs in combination. Cell viability was assessed 24 hours after drug exposure using a Hermes Wiscan instrument (n = 3, ± SEM). *$P < 0.05$ greater than corresponding value in VEH cells.
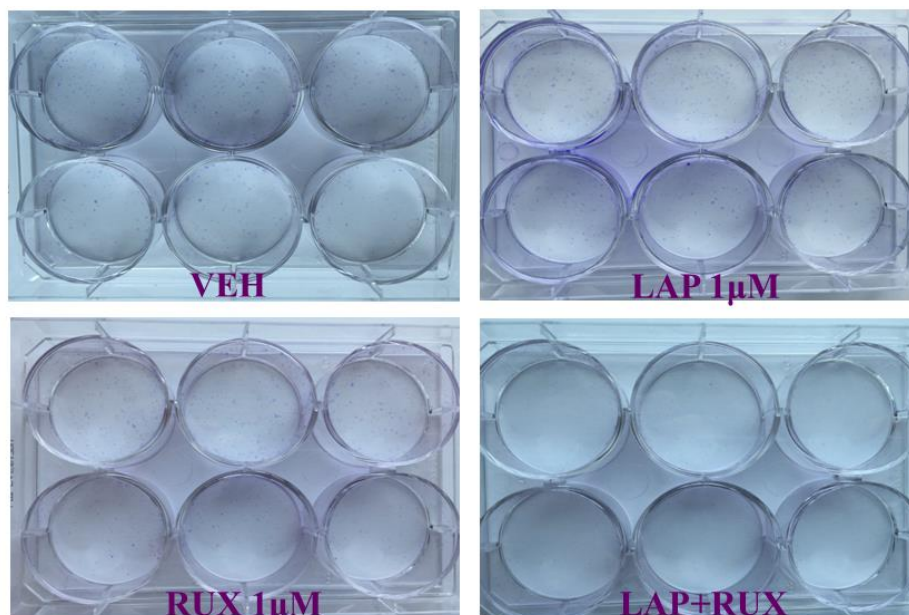
Drug Conc.	lapatinib ruxolitinib(CI)
R 0.25 + L 0.25	0.220219
R 0.50 + L 0.50	0.382543
R 0.75 + L 0.75	0.500607
R 1.00 + L 1.00	0.559090
R 1.25 + L 1.25	0.433378
R 1.50 + L 1.50	0.299603
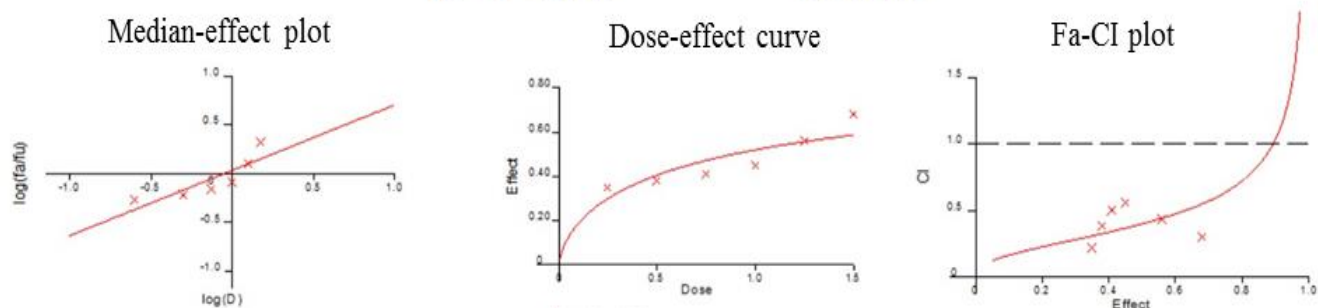
Figure 52. CI values provide proof of synergy between ruxolitinib and lapatinib. SUM149PT cells were plated (250-1500 cells/well) in sextuplicate, and were treated with vehicle (DMSO), ruxolitinib (0.25-1.50 µM), lapatinib (0.25-1.50 µM), or with both drugs combined. 24 hours after drug exposure, the medium was changed and cells were cultured in fresh medium for 10-14 days. Cells were then fixed and stained with crystal violet, and colonies were counted. Colony formation data were entered into the CalcuSyn program and CI values were determined. Based on this method, a combination index value of < 1.00 indicates synergistic effect, a value of 1.00 indicates additivity, and a value of greater > 1.00 equates antagonism of action between the drugs (n = 2; 12 individual wells per data point ± SEM).
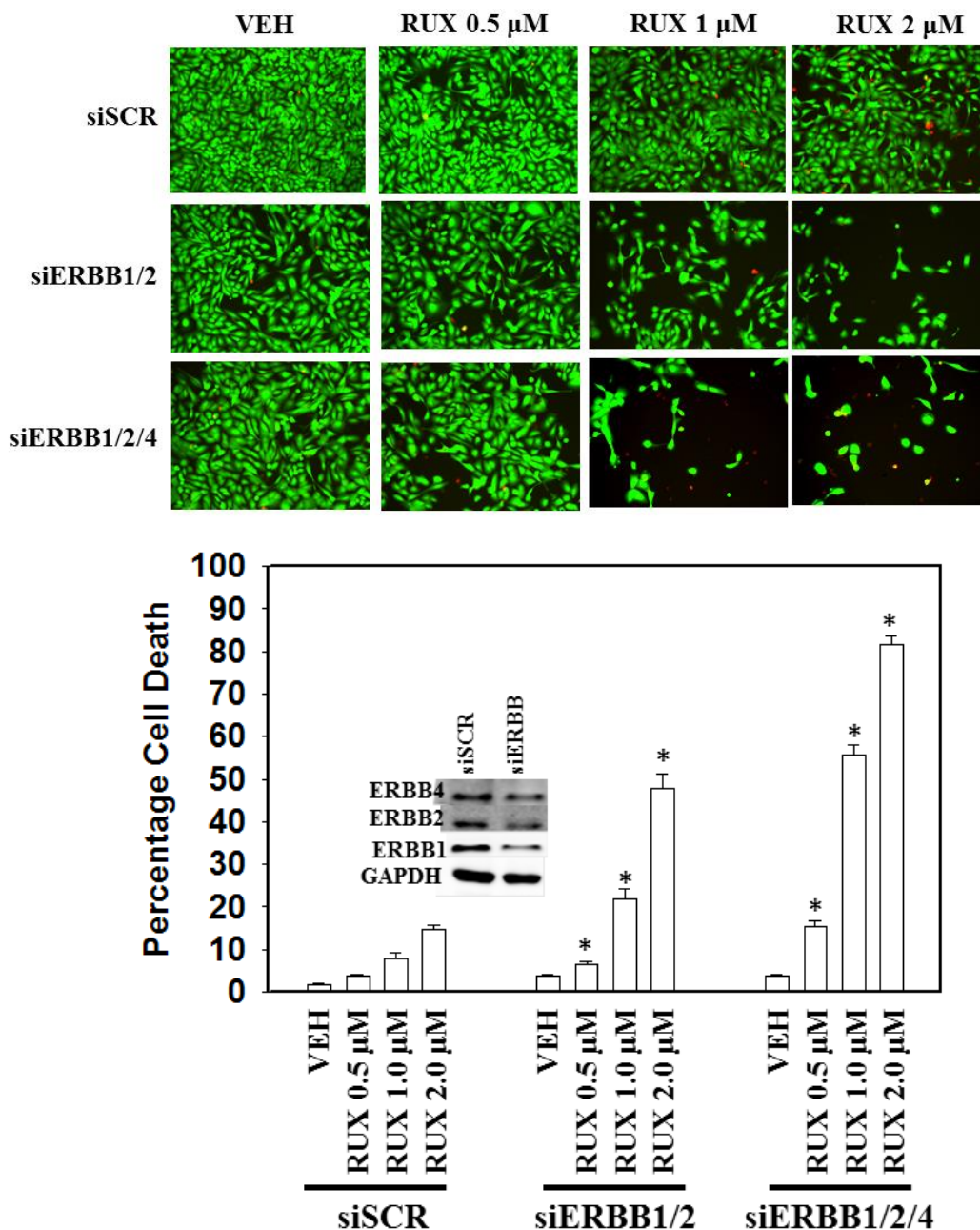
Figure 53. Inhibition of ERBB receptors enhances ruxolitinib toxicity. SUM149PT cells were transfected with a scrambled siRNA (siSCR) or with siRNA molecules to knock down the expression of ERBB1, ERBB2 and ERBB4 in combinations, as indicated in the figure. 24 hours after transfection cells were treated with vehicle control or ruxolitinib (0.5, 1, or 2 µM), as indicated. Cell viability was assessed 24 hours after drug exposure using a Hermes Wiscan instrument (n = 3, ± SEM). *$P< 0.05$ greater than corresponding value in siSCR cells.
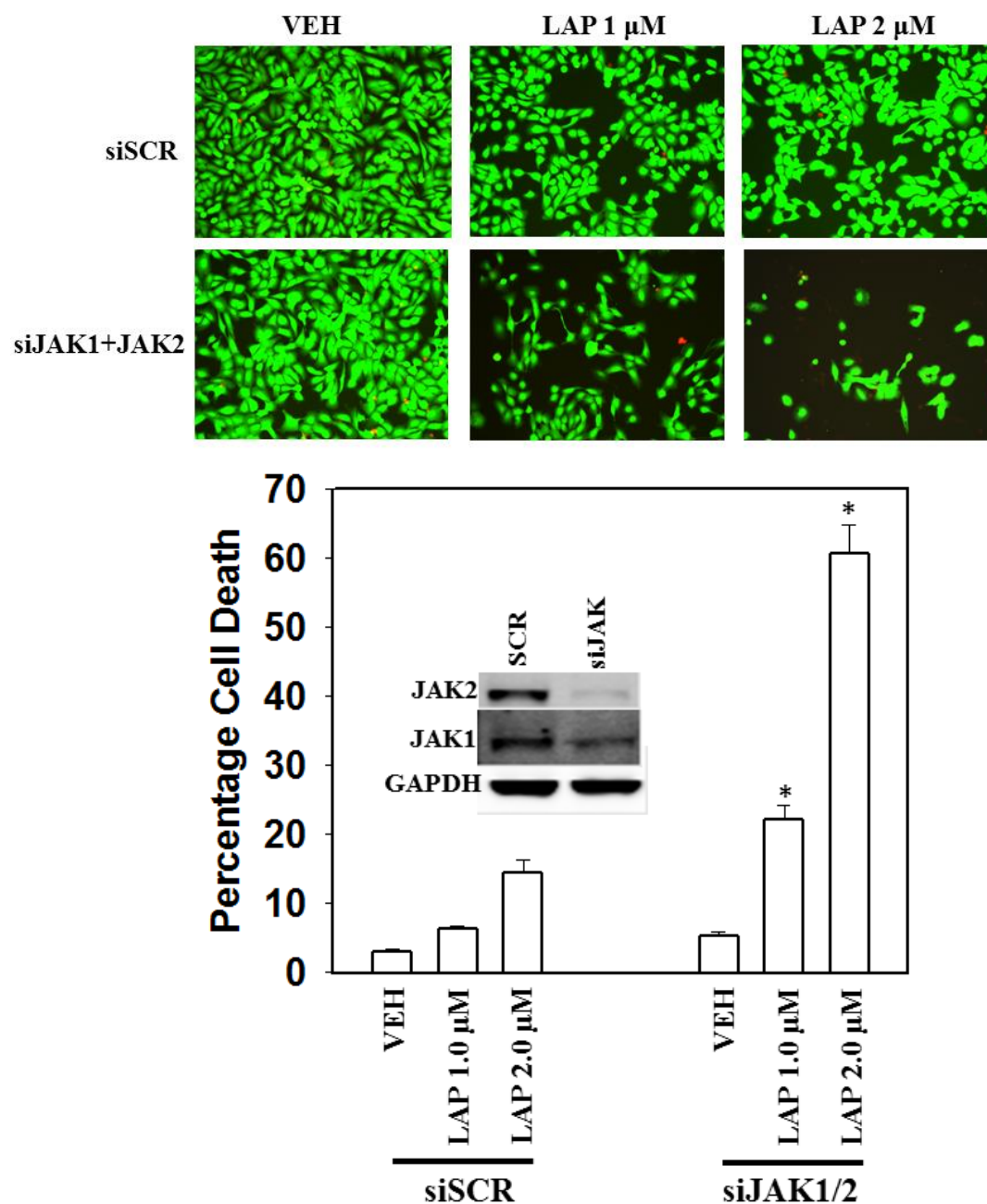
Figure 54. Inhibition of JAK1 and JAK2 enhances lapatinib toxicity. SUM149PT cells were transfected with a scrambled siRNA (siSCR) or with siRNA molecules to knock down the expression of JAK1 and JAK2 in combination. 24 hours after transfection cells were treated with vehicle control or lapatinib (1 or 2 μM), as indicated. Cell viability was assessed 24 hours after drug exposure using a Hermes Wiscan instrument (n = 3, ± SEM). *$P < 0.05$ greater than corresponding value in siSCR cells.

Ruxolitinib and lapatinib combination alter multiple survival signaling pathways

Ruxolitinib and lapatinib modulate the functions and activities of many intracellular signal transduction pathways, and we next explored the impact our ruxolitinib based drug combination had on cell signaling processes. In SUM149PT cells lapatinib and ruxolitinib inhibited the phosphorylation of EGFR, STAT3 and STAT5, as would be expected based on their declared kinase specificities (Figures 55). Drug combination treatment of SUM149PT cells reduced activity within the ERK1/2, p65 NFκB and AKT signaling pathways. The reduced activities within those well described "protective" signal transduction pathways correlated with reduced MCL-1 and Bcl-xL expression within 6 hours. The drug combination also increased the phosphorylation of JNK. To further examine changes in cell signaling after drug exposure we then made use of multiplex antibody array assays in a Bio-Rad MAGPIX machine (Figure 56A and B). The combination of ruxolitinib and lapatinib decreased the expression of multiple protective and pro-inflammatory cytokines, including CXCL1, IL-1β and IL-8, and as observed using immunoblotting, inactivated ERK1/2, AKT and NFκB signaling. In addition, the drug combination also reduced the phosphorylation of BAD, CREB, p70S6K and PDGFRα.

Based on the survival pathways that were inhibited by the drug combination, we further assessed if the inhibition of these pathways were involved in the induction of cell death. In SUM149PT triple negative breast cancer cells, expression of an activated form of STAT3, an activated form of AKT, an activated form of MEK1/2, an activated form of mTOR, or pre-treating cells with JNK inhibitory peptide suppressed the lethality of the drug combination (Figure 57).
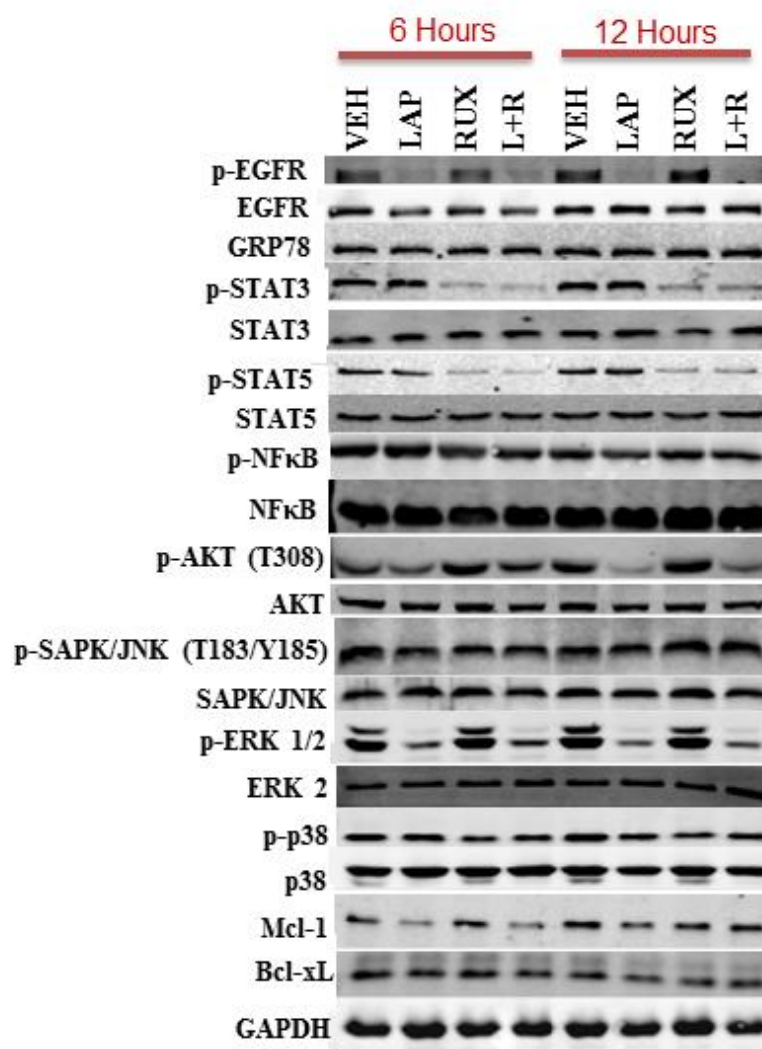
Figure 55. The LAP+RUX combination alters major signal transduction pathways. SUM149PT cells were treated with vehicle (DMSO), ruxolitinib (1.0 µM), lapatinib (1.0 µM), or the drug combination for 6 and 12 hours. Cells were lysed and expression of indicated proteins was determined by immunoblotting.

A
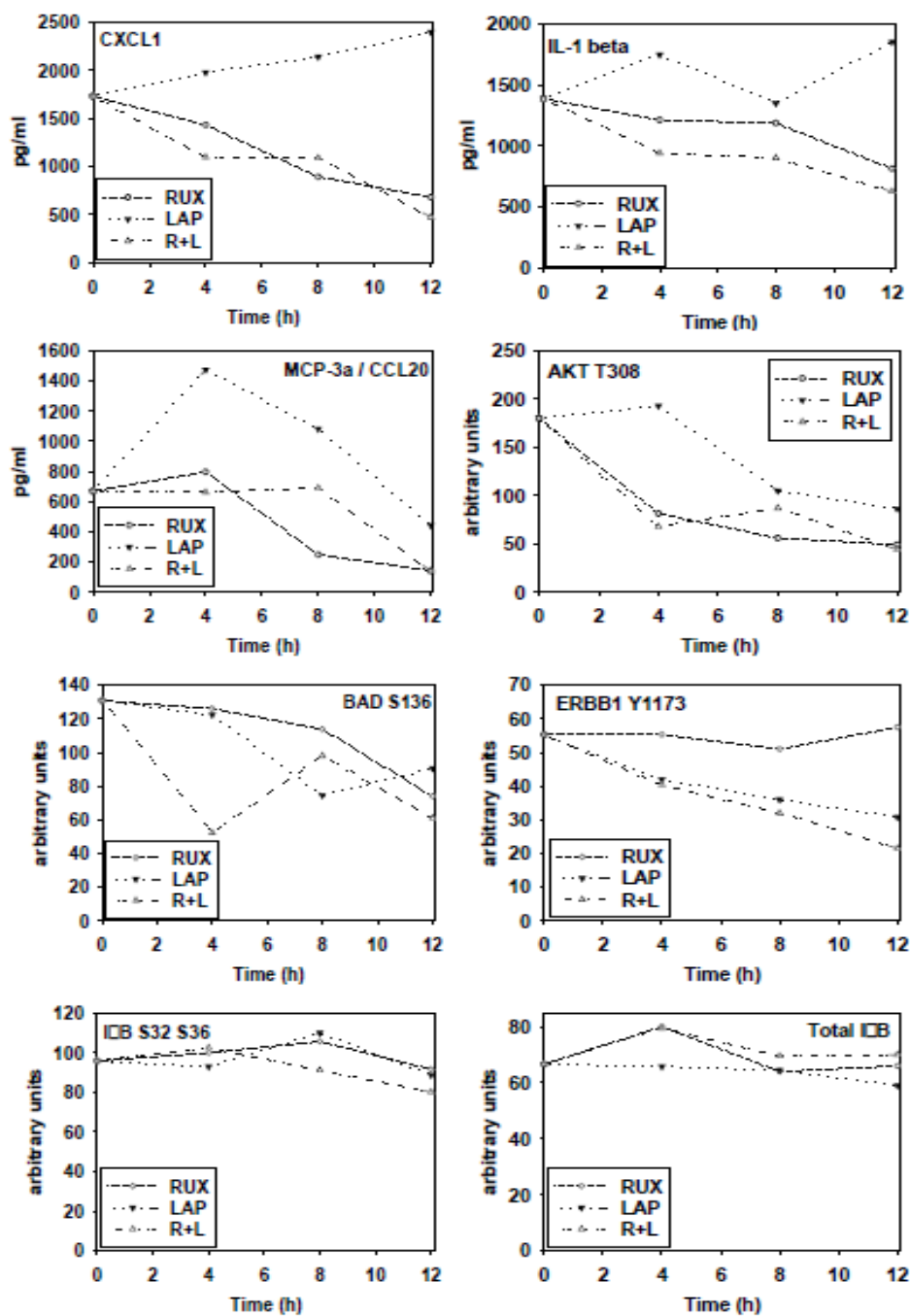
Figure 56. Multiplex analysis of SUM149PT cells treated with ruxolitinib, lapatinib or the drug combination. (A) and (B) SUM149 cells were treated with vehicle (DMSO), ruxolitinib (1.0 µM), lapatinib (1.0 µM) or the drugs in combination for 4h, for 8h and for 12h. At each time point cells were lysed and clarified by centrifugation. Clarified tumor cell lysates were then subjected to multiplex assays as described in the methods to detect the plasma levels of the indicated cytokines and phosphorylation status of signal transduction proteins using a BIO-RAD MAGPIX multiplex instrument (n = 3 ± SEM).

56B
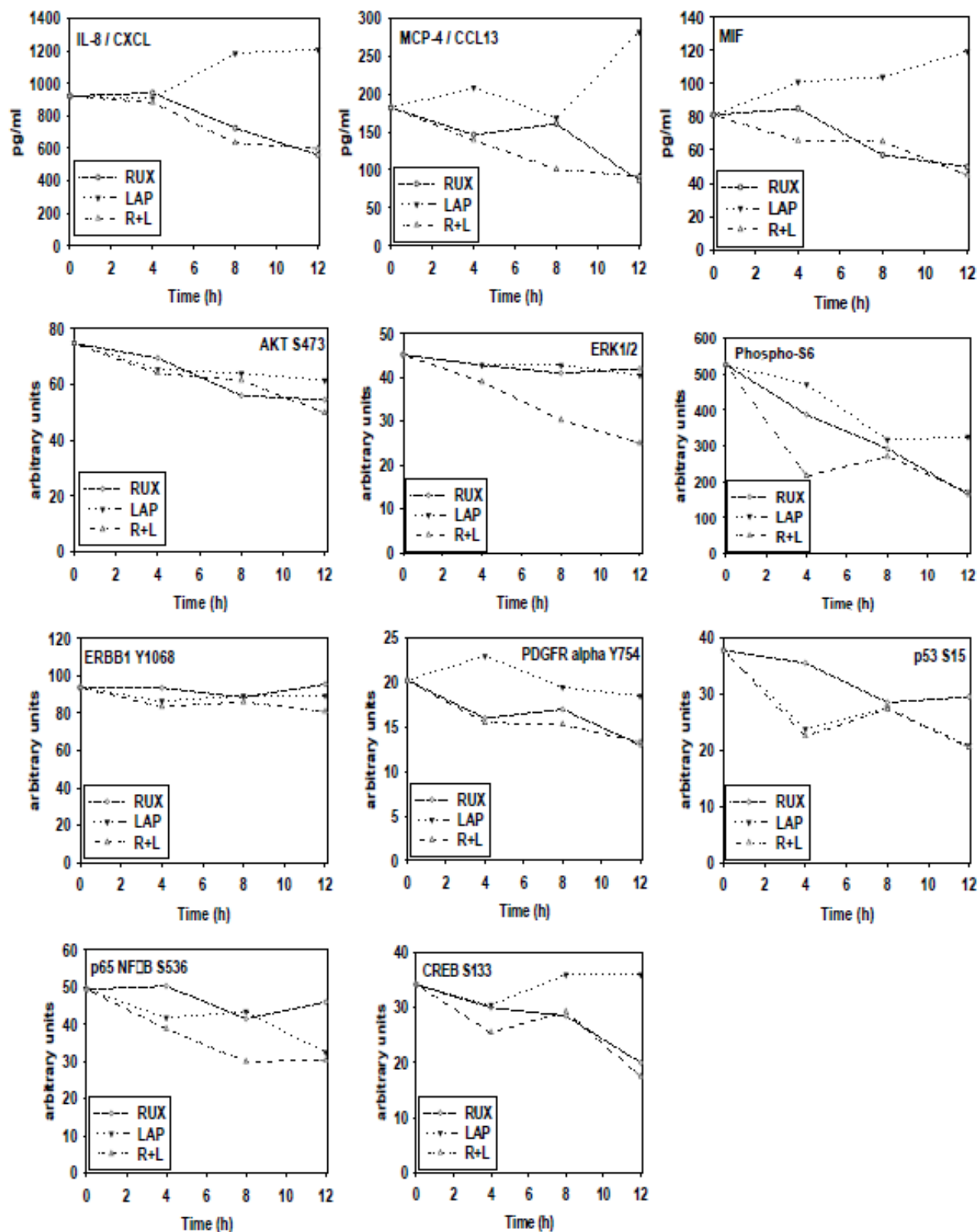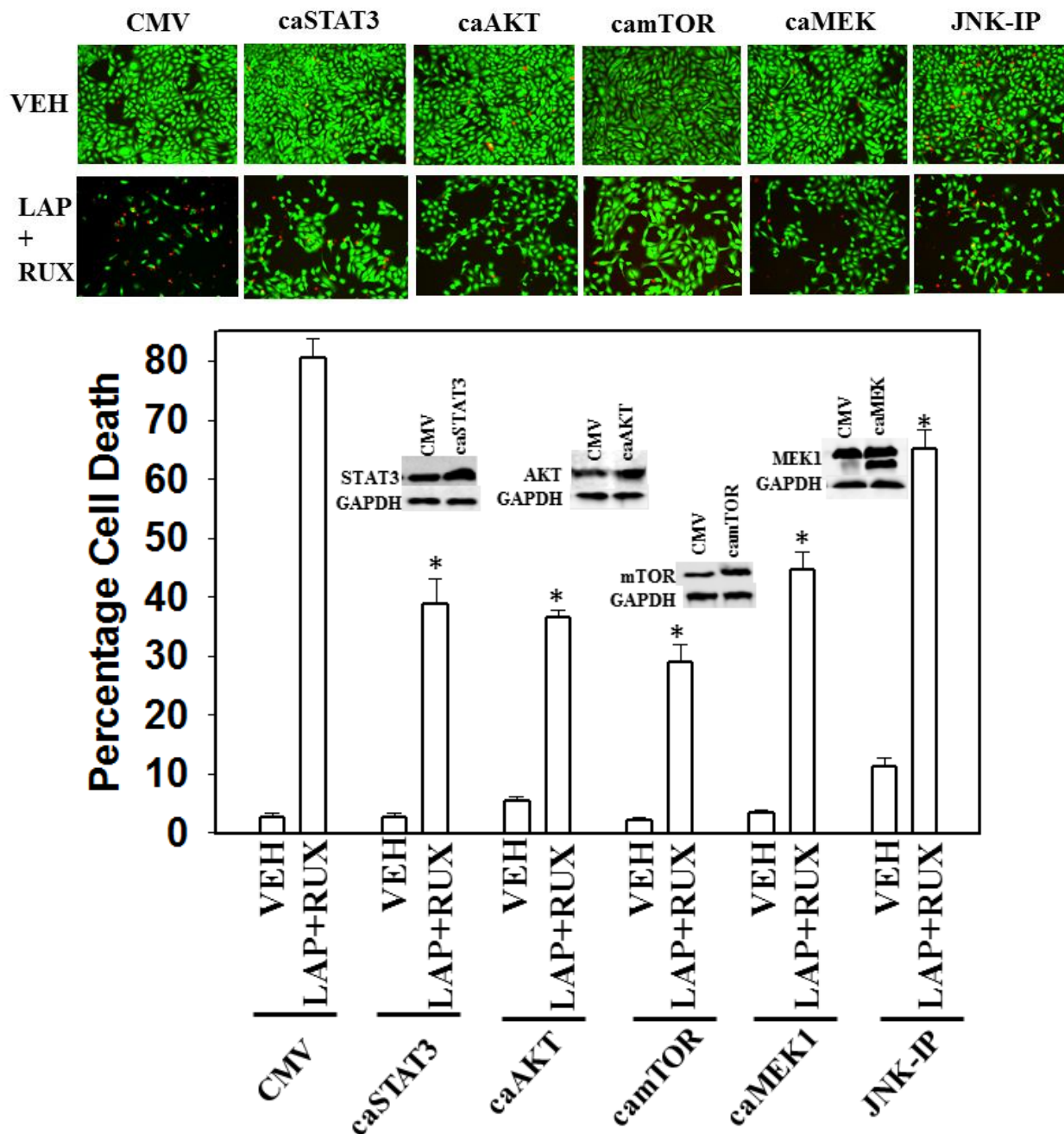
Figure 57. Inhibition of JNK1/2 or activation of STAT3, AKT, mTOR, and MEK1suppresses the LAP+RUX combination lethality. SUM149PT cells were transfected with plasmids to express either empty vector (CMV), activated STAT3 (caSTAT3), activated MEK1 (caMEK1), activated AKT (caAKT), or activated mTOR (ca mTOR). 24 hours after transfection, cells were treated with vehicle (DMSO) or ruxolitinib (1.0 μM) + lapatinib (1.0 μM) combination. Cell viability was assessed 24 hours after drug exposure using a Hermes Wiscan instrument (n = 3, ± SEM). *P< 0.05 lower than corresponding value in CMV cells. For JNK1/2 inhibition, plated cells were treated with the JNK inhibitory peptide (JNK-IP) for 30 minutes before the drugs were added accordingly. The viability was determined in a similar way using a Hermes Wiscan instrument.

Ruxolitinib and lapatinib combination induces cell death via apoptosis, autophagy and necroptosis

We next investigated the molecular mechanisms by which the combination of ruxolitinib and lapatinib was killing tumor cells. Initial studies using pharmacologic tools demonstrated that killing induced by the drug combination was suppressed by inhibition of RIP-1 (necroptosis; necrostatin-1), PI3K (autophagy; 3-methyl adenine (3-MA)), and caspases (apoptosis; Z-VAD) (Figure 58). Thus, we next determined whether the activation of intrinsic and extrinsic apoptotic pathways was triggered in the drug combination-treated cells. Inhibition of caspase 8 (death receptor signaling) by overexpression of c-FLIP-s did not significantly reduce the lethality of the drug combination treatment. Inhibition of caspase signaling downstream of mitochondria by expression of dominant negative caspase 9 partially suppressed the drug combination toxicity. Overexpression of Bcl-xL or knockdown of either BAX or BAK strongly reduced drug combination killing (Figures 59 and 60). Although knock down of PUMA or NOXA was protective, the effect of either knockdown on maintaining cell viability was less than that of inhibiting both BAX and BAK function together. Additionally, knockdown of BID and AIF reduced the drug combination-mediated lethality (Figure 61).

AIF is a mitochondrial protein that is released into the cytoplasm upon a lethal stimulus, and it then re-locates to the nucleus where it acts to promote a non-caspase dependent fragmentation of the DNA.[202] In unstimulated SUM149PT cells AIF co-localized with the mitochondrial protein AAA^+ ATPase protein ATAD3A but not with the nuclear protein eIF3A. Six hours after treatment with the combination of ruxolitinib and lapatinib, the co-localization of AIF with ATAD3A appeared to remain similar; however the association of AIF with eIF3A in the nucleus had increased (Figure 62).
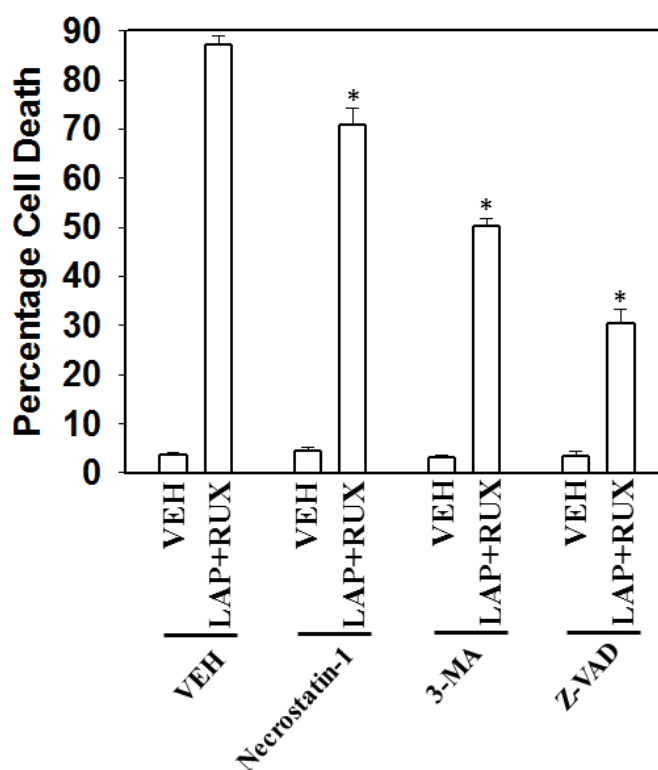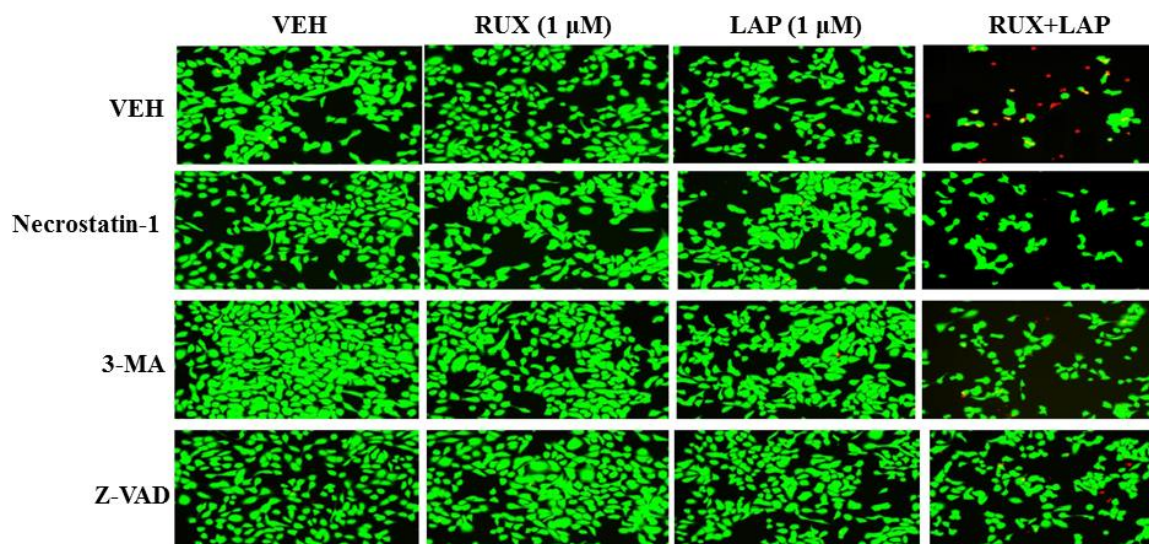
Figure 58. The LAP+RUX combination induces cell death via apoptosis, autophagy and necroptosis. Plated SUM149PT cells were pre-treated with necrostatin-1, 3-MA, or Z-VAD for 45 minutes and were then exposed to the drugs individually or in combination as indicated. Cell viability was assessed 24 hours after drug exposure using a Hermes Wiscan instrument (n = 3, ± SEM). *$P < 0.05$ lower than corresponding value in VEH cells.
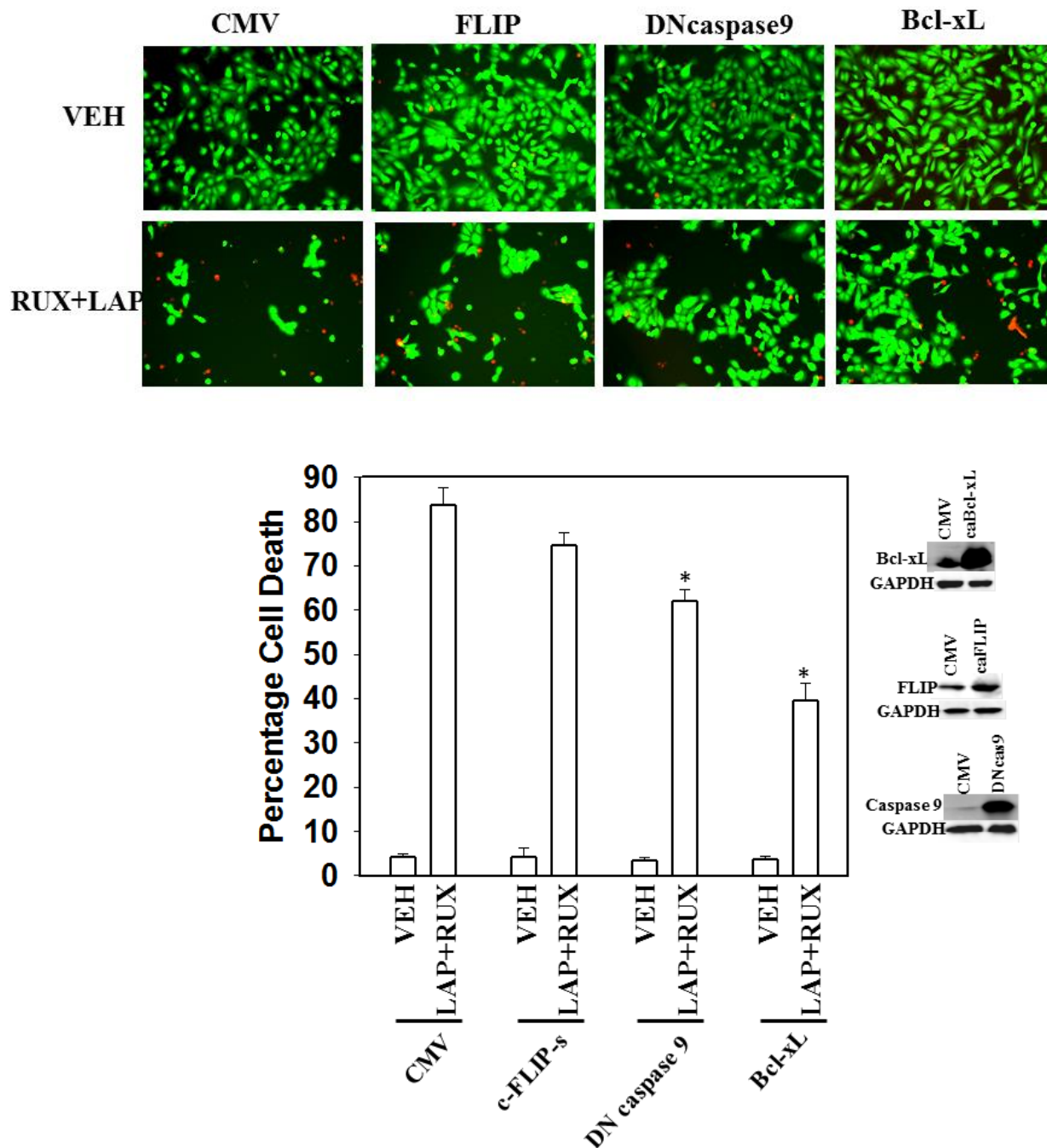
Figure 59. The LAP+RUX combination activates intrinsic apoptotic pathway. SUM149PT cells were infected with recombinant adenoviruses to express empty vector (CMV), dominant negative caspase 9 (DN casp 9), Bcl-xL, or c-FLIP-s. 24 hours after infection cells were treated with vehicle (DMSO), or the combination of ruxolitinib (1.0 μM) and lapatinib (1.0 μM). Cell viability was assessed 24 hours after drug exposure using a Hermes Wiscan instrument (n = 3, ± SEM). *$P< 0.05$ lower than corresponding value in CMV cells.
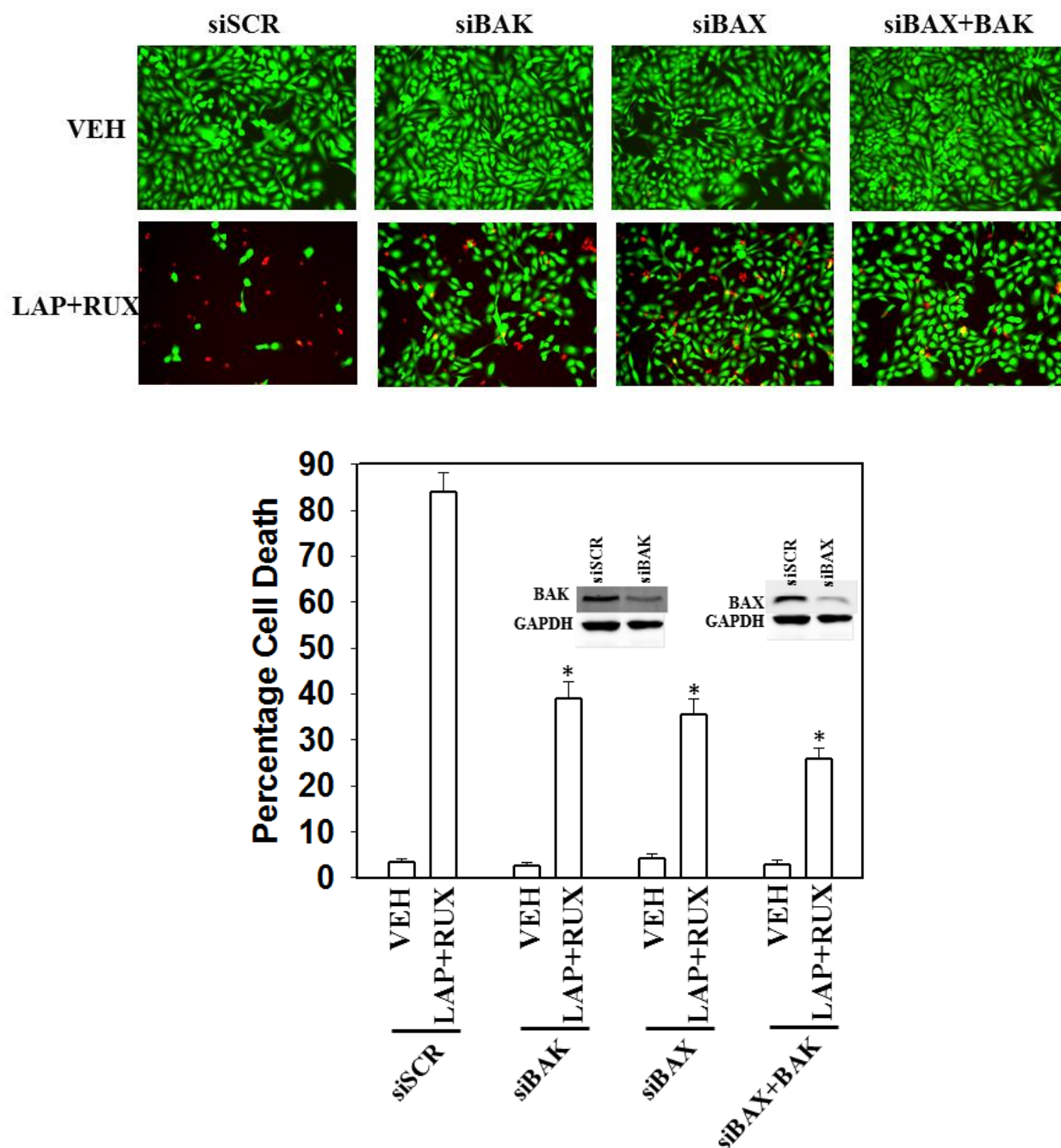
Figure 60. Knockdown of BAX and BAK significantly suppresses the LAP+RUX combination lethality. SUM149PT cells were transfected with a control scrambled siRNA (siSCR) or two different siRNAs to knockdown expression of BAX and BAK. 24 hours after transfection cells were treated with vehicle (DMSO), or the combination of ruxolitinib (1.0 μM) and lapatinib (1.0 μM). Cell viability was assessed 24 hours after drug exposure using a Hermes Wiscan instrument (n = 3, ± SEM). *$P < 0.05$ lower than corresponding value in siSCR cells.
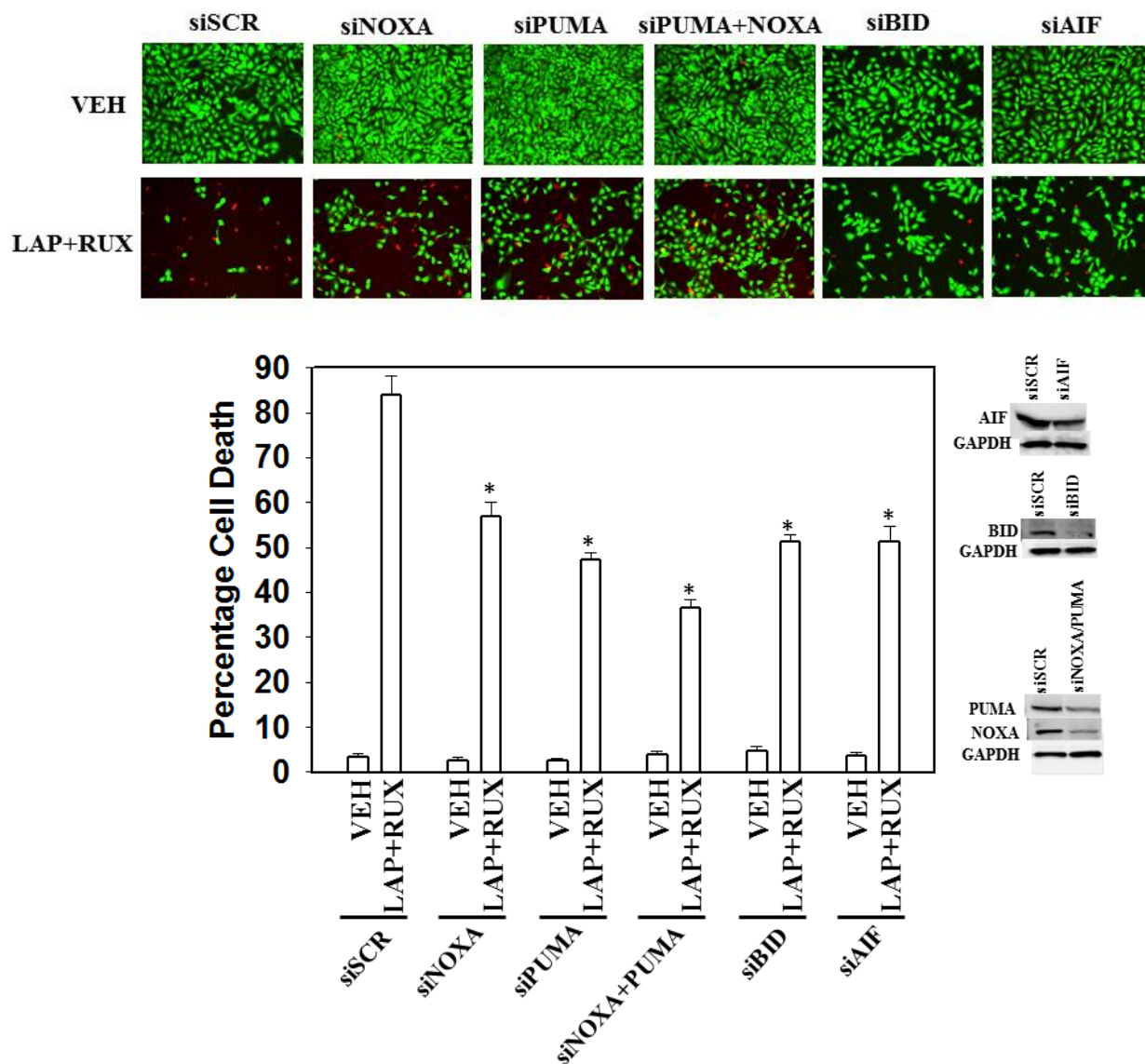
Figure 61. Knockdown of PUMA, NOXA, BID and AIF reduces the LAP+RUX combination lethality. SUM149PT cells were transfected with a control scrambled siRNA (siSCR) or different siRNAs to knockdown expression of NOXA, PUMA, BID and AIF. 24 hours after transfection cells were treated with vehicle (DMSO), or the combination of ruxolitinib (1.0 μM) and lapatinib (1.0 μM). Cell viability was assessed 24 hours after drug exposure using a Hermes Wiscan instrument (n = 3, ± SEM). *$P< 0.05$ lower than corresponding value in siSCR cells.
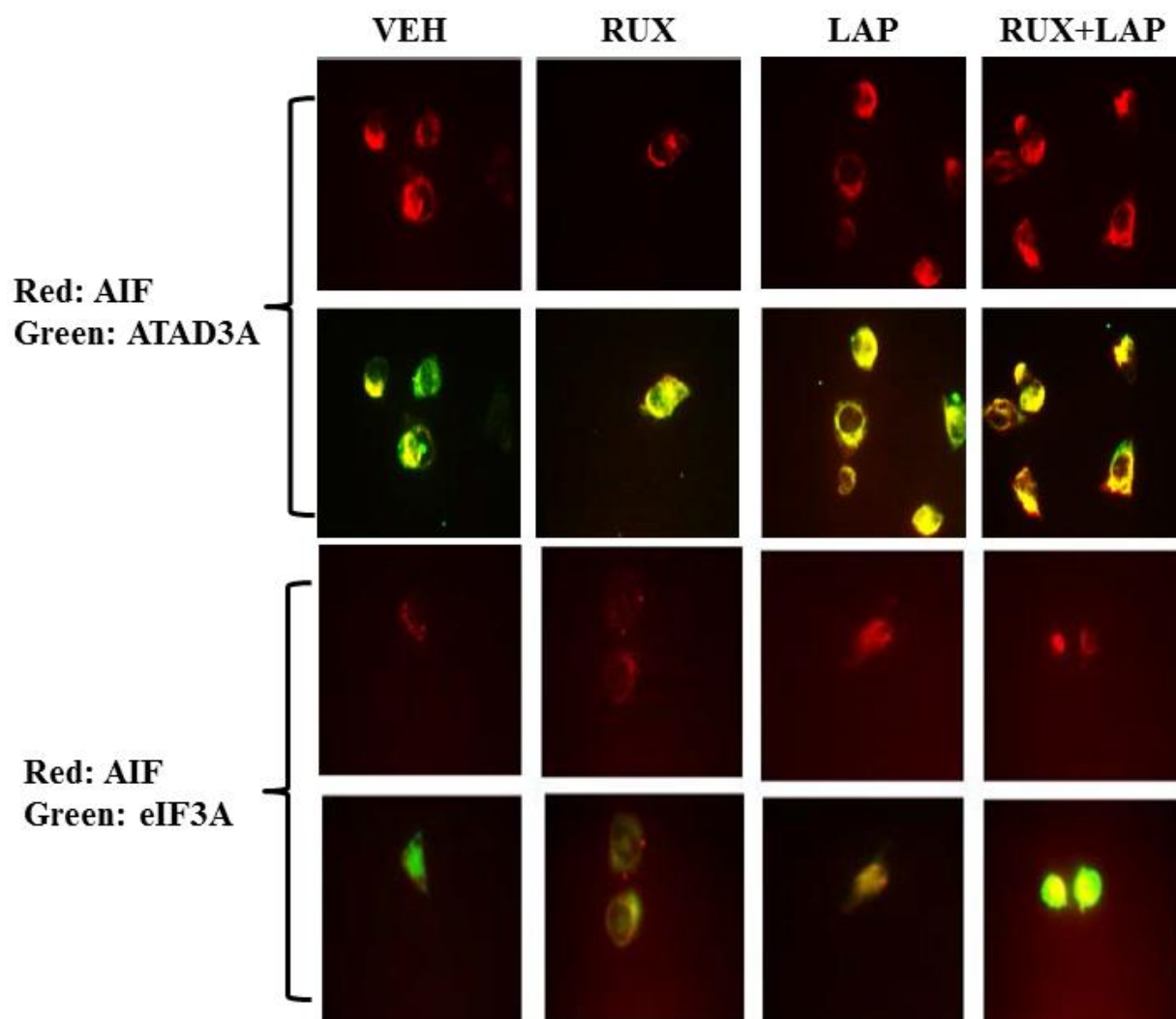
Figure 62. AIF translocates to the nucleus 6 hours after drug exposure. SUM149PT cells were treated with vehicle (DMSO), or the combination of ruxolitinib (1.0 μM) and lapatinib (1.0 μM) as indicated for 6 hours after which cells were fixed in place and permeabilized using 0.5% Triton X100. Immuno-fluorescence was performed at 60X magnification to detect the co-localization levels of the indicated proteins, and for the total expression level of AIF.

Based on the preliminary data from 3-MA-treated cells, and also knowing that overexpression of mTOR was strongly protective, we next investigated the induction of autophagy in SUM149PT cells in response to the drug combination. . Treatment of cells with the combination of ruxolitinib and lapatinib increased the numbers of autophagosomes in cells in a greater than additive fashion and in a time-dependent fashion (Figure 63). In agreement with our preliminary data using 3-MA, knock down of Beclin1 or of ATG5 suppressed, but did not completely abolish, tumor cell killing by the drug combination (Figure 64).

Of note, the treatment of cells with the drug combination caused LC3-GFP intense staining vesicles to co-localize with the mitochondria, an indicator of mitophagy (Figure 65). Treatment of cells with the combination of ruxolitinib and lapatinib also caused LC3-GFP staining vesicles to co-localize with acidic lysosomes (Figure 66).

We next determined whether the induction of autophagosome formation was an essential process for activation of BAX and BAK above the level of mitochondrial dysfunction or whether it was a consequence downstream of an early form of mitochondrial dysfunction. Treatment of SUM149 cells with the combination of ruxolitinib and lapatinib activated the toxic BH3 domain proteins BAX and BAK (Figure 67). Activation of BAX was almost abolished by knockdown of Beclin1 or of BID expression, whereas activation of BAK was only modestly impacted by BID knockdown (Figure 67).
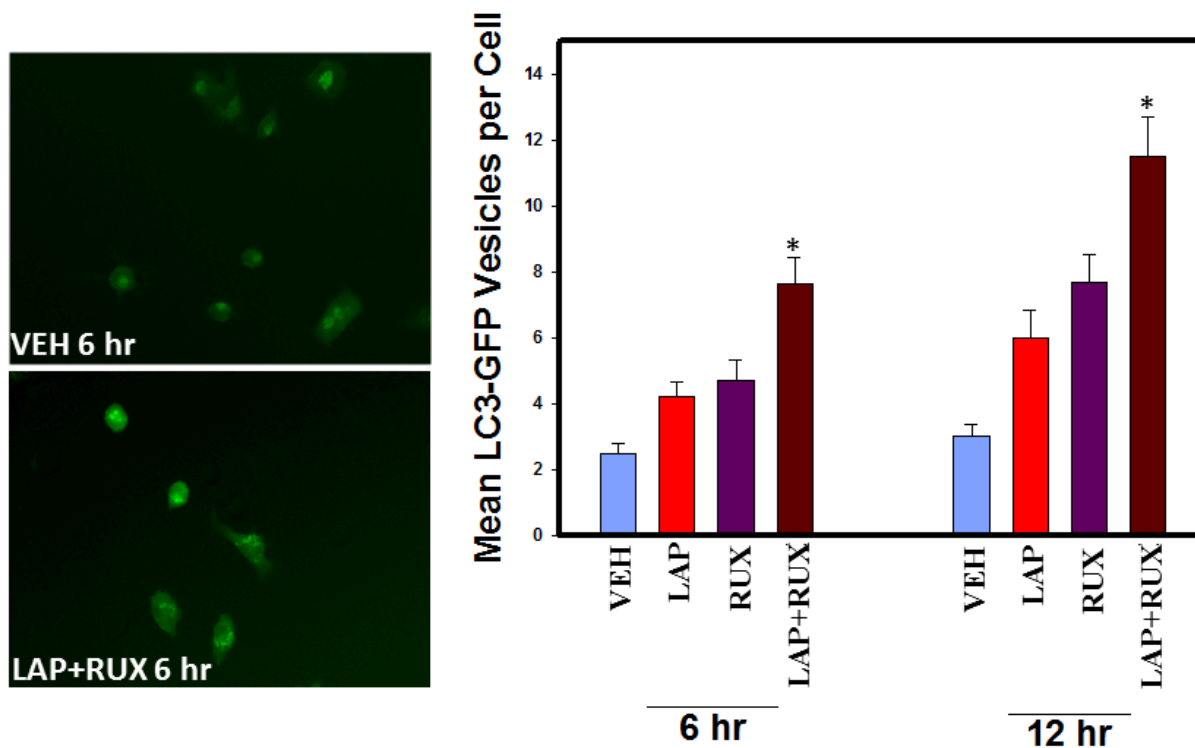
Figure 63. The LAP+RUX combination increases autophagosome formation. SUM149 cells were transfected with a plasmid to express LC3-GFP. Twenty four hours after transfection cells were treated with vehicle (DMSO), lapatinib (1.0 μM), ruxolitinib (1.0 μM), or in combination as indicated for 6 or 12 hours. At each time point cells were visualized using a fluorescent microscope at X40 magnification and the mean number of intense punctate GFP positive vesicles per cell determined in > 40 cells from random fields ± SEM (*$p < 0.05$ greater than lapatinib alone or ruxolitinib alone treatments).
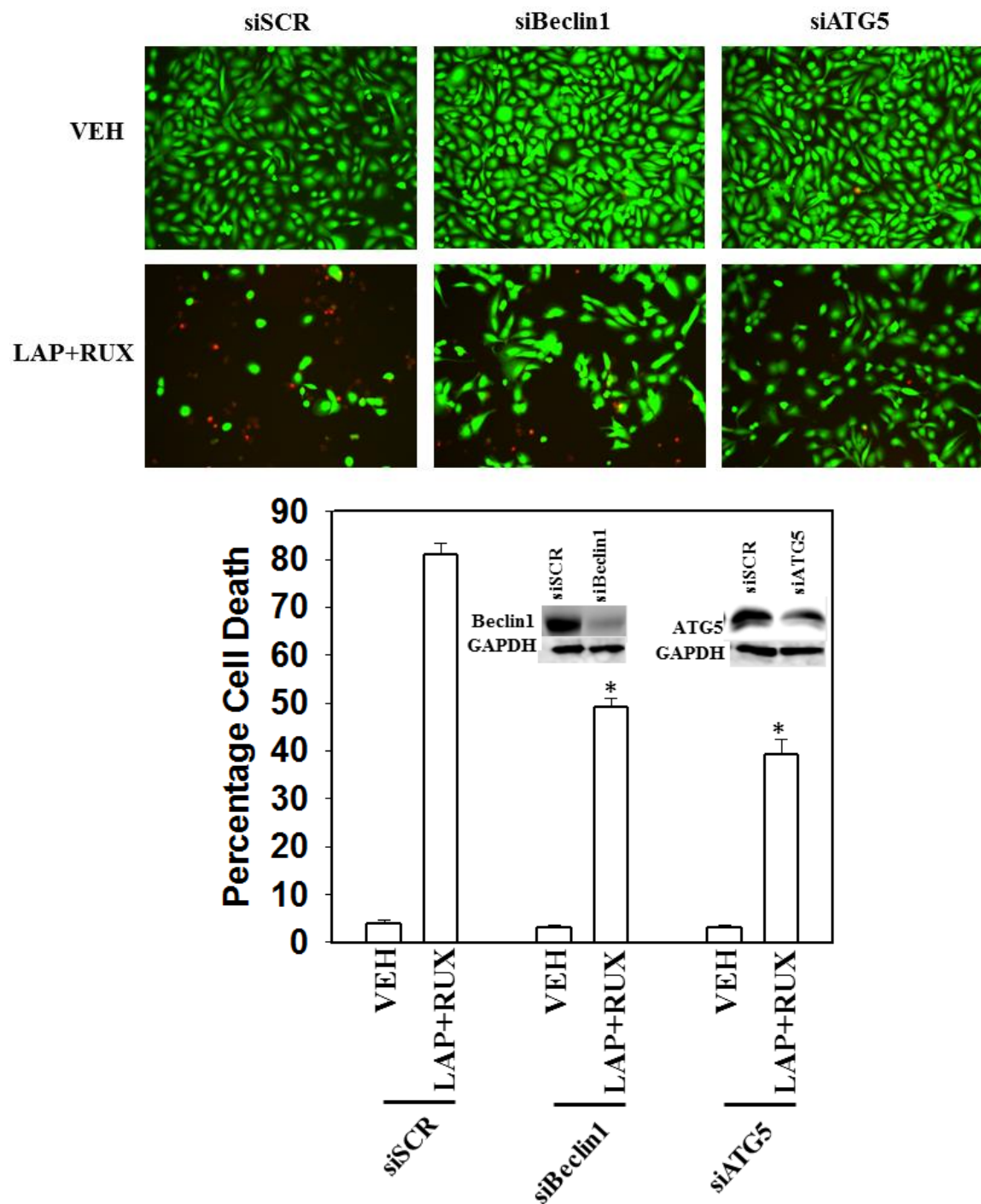
Figure 64. Knockdown of Beclin1 and ATG5 reduces the lethality of the LAP+RUX combination. SUM149PT cells were transfected with a control scrambled siRNA (siSCR) or two different siRNAs to knockdown expression of Beclin1 and ATG5. 24 hours after transfection cells were treated with vehicle (DMSO), or the combination of ruxolitinib (1.0 µM) and lapatinib (1.0 µM). Cell viability was assessed 24 hours after drug exposure using a Hermes Wiscan instrument (n = 3, ± SEM). *P< 0.05 lower than corresponding value in siSCR cells.
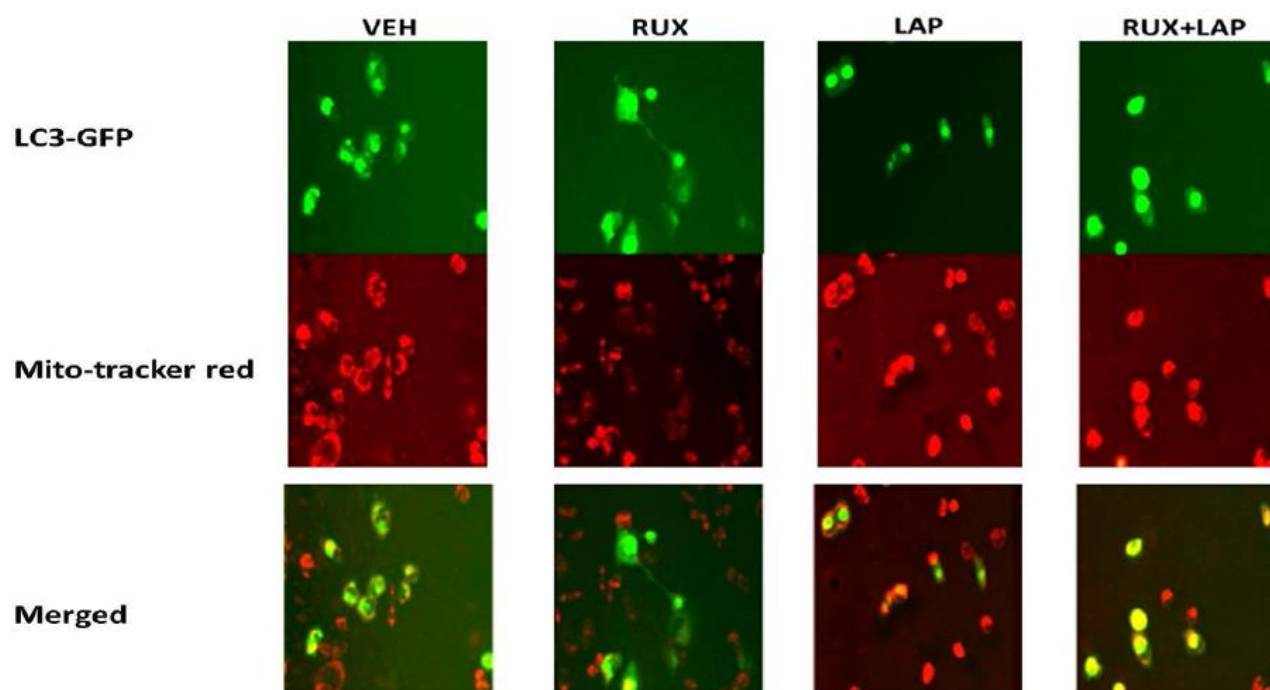
Figure 65. The LAP+RUX combination induces mitophagy. SUM149PT cells were transfected with a plasmid to express LC3-GFP. 24 hours after transfection cells were treated with vehicle (DMSO), lapatinib (1 μM), ruxolitinib (1 μM) or in combination as indicated for 6 hours. Cells were then treated with MitoTracker Red CMXRos (25 nM) for 30 min. Cells were visualized using a fluorescent microscope at 40X magnification in the red and green fluorescent channels. The red and green images were merged in Adobe Photoshop CS6; areas of yellow staining indicate the co-localization of GFP and MitoTracker Red staining.
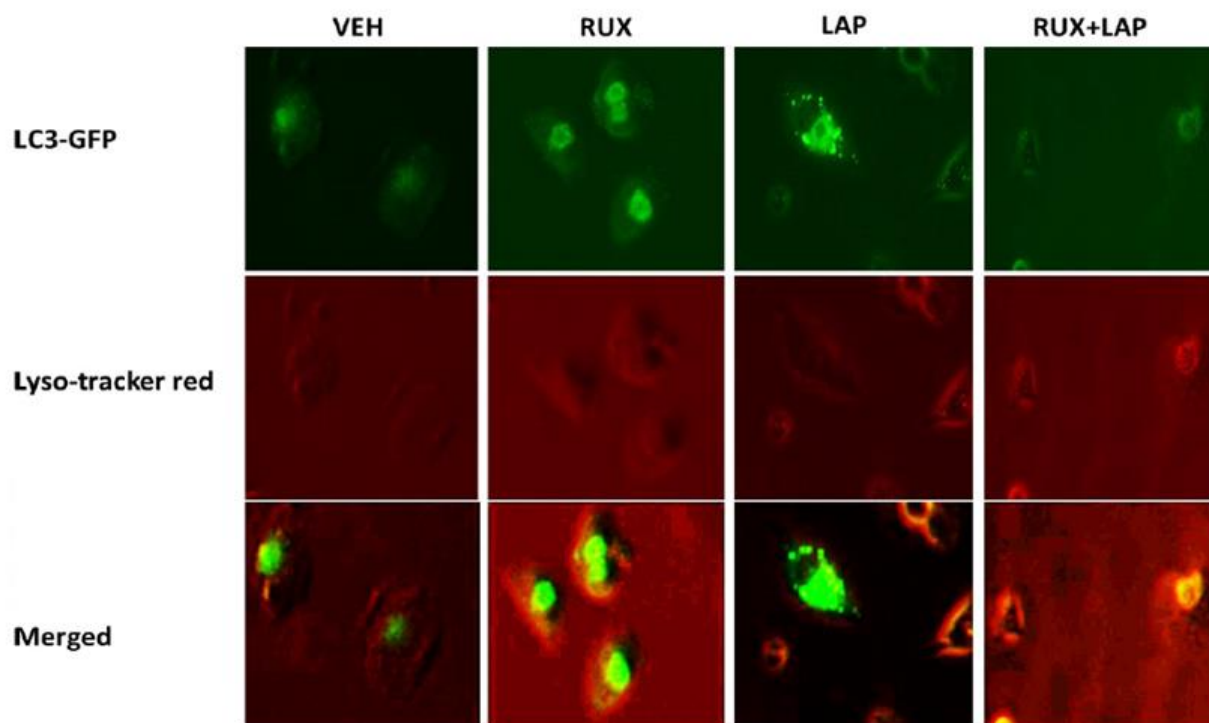
Figure 66. The LAP+RUX combination induces co-localization of autophagosomes to lysosomes. SUM149PT cells were transfected with a plasmid to express LC3-GFP. 24 hours after transfection cells were treated with vehicle (DMSO), lapatinib (1 µM), ruxolitinib (1 µM) or in combination as indicated for 6 hours. Cells were then treated with LysoTracker Red DND-99 (25 nM) for 30 min. Cells were visualized using a fluorescent microscope at 40X magnification in the red and green fluorescent channels. The red and green images were merged in Adobe Photoshop CS6; areas of yellow staining indicate the co-localization of GFP and LysoTracker Red staining.
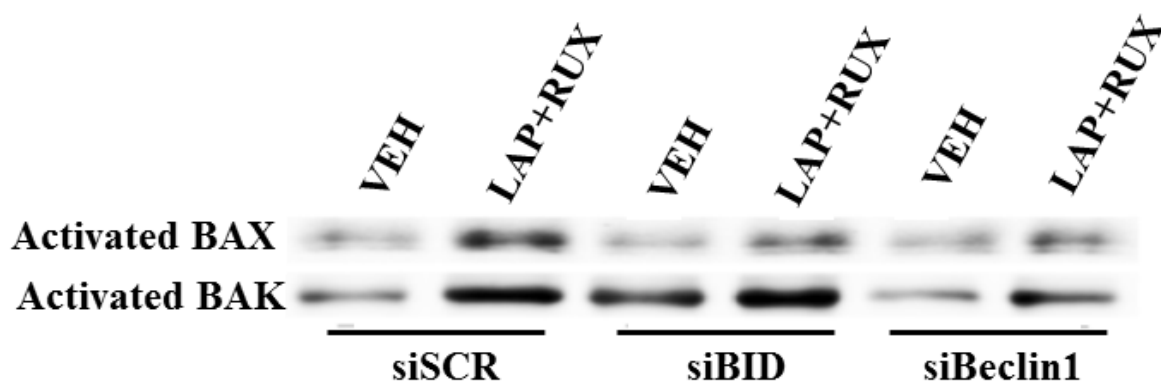
Figure 67. Knockdown of Beclin1 abolishes activation of BAX and BAK. SUM149PT cells were transfected with a scrambled nonsense siRNA molecule (siSCR), or siRNA molecules to knockdown the expression of BID or of Beclin1. 24 hours after transfection cells were treated for 6 hours with vehicle (DMSO) or with ruxolitinib (1 μM) and lapatinib (1 μM) combination for 6 hours. Cells were isolated and broken down using CHAPS based lysis buffer with vigorous trituration, followed by lysate clarification via centrifugation (5 min x 14,000 g). Equal protein mass portions of lysates were immunoprecipitated using antibodies that recognize epitopes in BAX and in BAK only open to detection when these toxic BH3 domain proteins are active. The total expression of BAX and of BAK under each condition was assessed by immunoblotting.

Discussion

This study was conducted to determine whether the concurrent inhibition of JAK/STAT and ERBB signaling could synergize to kill breast cancer cells. As stated before, EGFR amplification and overexpression is commonly observed in many breast cancers, including 30-52% TNBC carcinomas.[190,191] In addition, prior studies have suggested a prominent role for cytokine receptor signaling through JAK/STAT pathway in breast carcinogenesis, and prolactin, erythropoietin, and other cytokines such as IL-6 and IL-11 have been linked to an increase in breast cancer incidence.[192-195] Furthermore, EGFR and JAK/STAT signaling pathways have been shown to crosstalk through different mechanisms.[200] These reports led us to hypothesize that concurrent inhibition of these two pathways could be a potent novel therapeutic approach in treatment of breast cancer. Since there are no FDA-approved STAT inhibitors available at the moment, and knowing that STAT3 and STAT5 are both heavily involved in breast carcinogenesis, we repurposed ruxolitinib, a JAK1/2 inhibitor, as a novel therapeutic in treatment of breast cancer.

Our initial data indicated that lapatinib and ruxolitinib strongly interacted to kill a variety of breast cancer cells, including cells from all three subtypes; triple negative (SUM149PT, HCC38 and BT549), HER2 positive (BT474), and ER positive (MCF7). Colony formation assays and CI values were very well indicative of the synergistic interaction between the two drugs. Moreover, using molecular tools, we demonstrated that the inhibition of ERBB receptors and JAK1 and JAK2 is the major reason behind the strong interaction between these two kinase inhibitors. Knockdown of ERBB1/2/4 in SUM149PT cells recapitulated the toxic interaction with ruxolitinib. Similarly, combined knockdown of JAK1 and JAK2 could recapitulate the toxic effects of ruxolitinib when combined with ERBB1/2/4 inhibitors.

Lapatinib and ruxolitinib, as expected based on their declared kinase specificities, inhibited the phosphorylation of EGFR, STAT3 and STAT5. Additionally, the combination of the two drugs reduced activities within those well described survival signal transduction pathways, such as ERK1/2, p65 NFκB and AKT, which correlated with reduced MCL-1 and Bcl-xL expression within 6 hours. Further unbiased multiplex analyses indicated that the combination of ruxolitinib and lapatinib decreased the expression of multiple protective and pro-inflammatory cytokines, including CXCL1, IL-1β and IL-8, as well as the phosphorylation of BAD, CREB, p70S6K and PDGFRα. Decreased phosphorylation of CREB, BAD and p70S6K correlated with the decreased P-ERK1/2 and P-AKT as demonstrated by both immunoblotting and multiplex assay. However, a decrease in PDGFRα phosphorylation, which was also observed in cells treated with ruxolitinib alone, was somewhat unexpected, but could provide further evidence as why these two kinase inhibitors interacted in such synergistic fashion. In agreement with our data form multiplex assays and immunoblotting, overexpression of MEK1, STAT3, AKT and Bcl-xL significantly protected the cells, further providing proof for involvement of these inhibited signal transduction proteins in the induction of cell death. Studies to define the downstream effectors of AKT, STAT3 and ERK1/2 signaling that regulate the threshold for cell killing in the presence of ruxolitinib and lapatinib are outside the scope of the present manuscript.

As p70S6K phosphorylation, an mTOR substrate, was reduced, and the expression of an activated form of mTOR as well as pre-treating the cells with 3-MA strongly protected the cells, we next investigated the role of autophagy in cell death. In accordance with 3-MA data, the inhibition of Beclin1 and ATG5 significantly protected the cells. The drug combination increased the number of the LC3-GFP vesicles in a greater than additive fashion, and the LC3-

GFP vesicles were shown to co-localize to the acidic lysosomes in the combination-treated group. We also discovered that the drug combination induced mitophagy, as the LC3-GFP stained autophagosomes were shown to co-localize to the mitochondria.

Since pan-caspase inhibitor Z-VAD strongly suppressed the drug combination-mediated lethality, we next determined if the extrinsic and intrinsic apoptotic pathways were activated by the combination of ruxolitinib and lapatinib. The expression of dominant negative caspase 9 modestly protected the cells whereas the overexpression of c-FLIP-s did not protect the cells at all. This was specifically interesting since the knockdown of BID, a substrate of caspase 8, was strongly protective. The toxic BH3 domain protein BID is activated by proteolytic cleavage; a cleavage most commonly thought to be catalyzed by caspases 8 and 10 downstream of death receptors but also less commonly by cathepsin and calpain proteases released due to lysosomal dysfunction/autophagy flux.[203] More studies will be required to determine if the cleavage of BID occurs through cathepsin and calpain proteases. We also demonstrated that the mitochondrial permeabilization occurred through activation of BAX and BAK, which subsequently led to the release of AIF and its translocation to the nucleus.

Furthermore, our data indicated that activation of BAX and BAK was dependent on activation of autophagy and that the induction of autophagosome formation was an essential process for activation of BAX and BAK above the level of mitochondrial dysfunction.

As ruxolitinib and lapatinib interacted in a synergistic fashion to kill a variety of breast cancer types, we are planning to further expand our studies in the future by evaluating the efficacy of the drug combination *in vivo*. We are also concurrently evaluating a potential replacement of lapatinib with the more potent new generation ERBB inhibitor afatinib, which irreversibly inactivates ERBB1/2/4 and also blocks transphosphorylation of ErbB3.
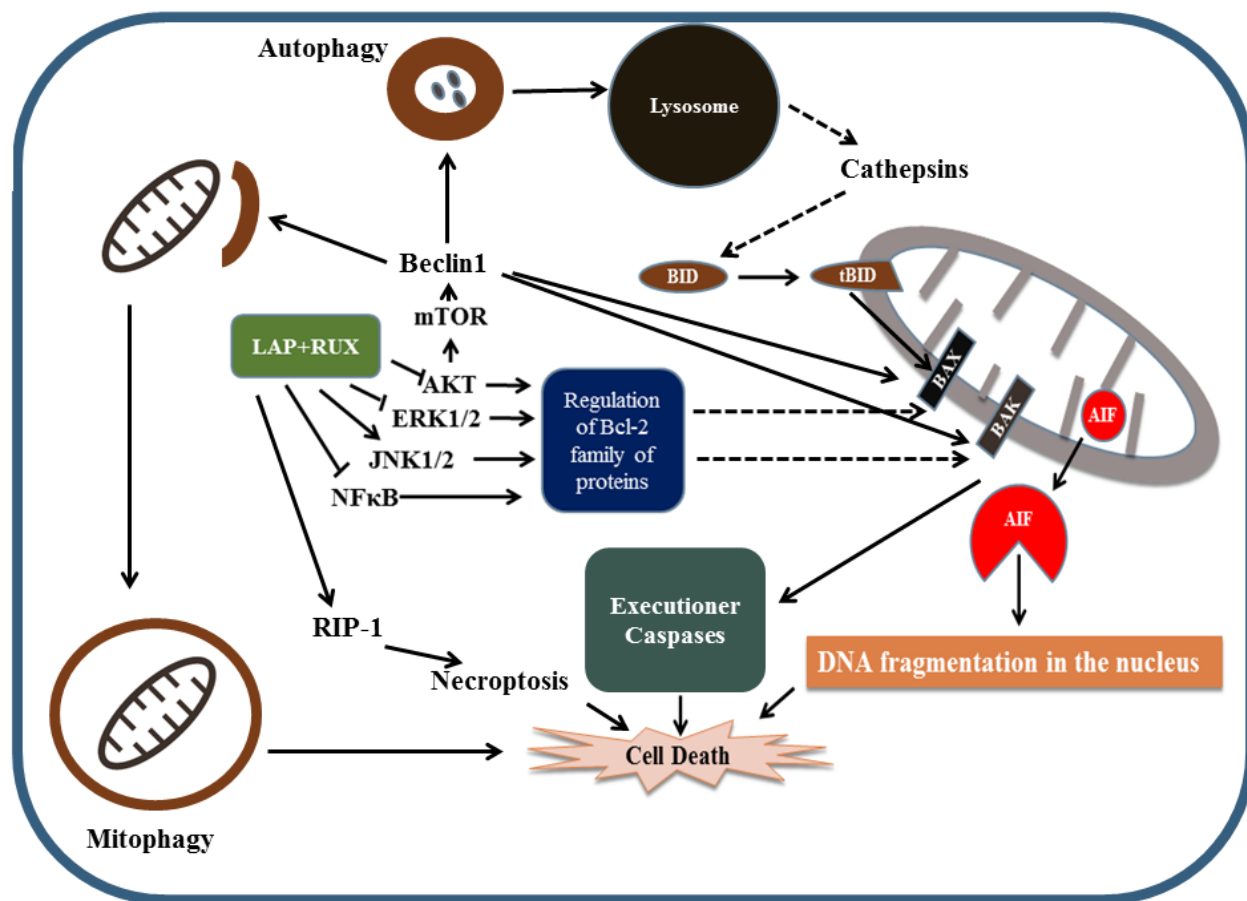
Figure 68. Proposed mechanism of cell death induced by the combination of RUX and LAP. The combination of ruxolitinib and lapatinib reduced the phosphorylation of AKT, ERK1/2 and p65 NFκB, which correlated with reduced MCL-1 and Bcl-xL expression. It also induced cell death through activation of JNK. The drug combination induced cytotoxic mitophagy, which acted upstream of the mitochondrial dysfunction, as Beclin1 mediated activation of BAX and BAK. Cleavage of BID also occurred in response to the treatment with the drug combination. As caspase 8 inhibition was not protective, we suspect that the cleavage of BID could have been mediated by cathepsins and calpains. In addition, mitochondrial dysfunction led to the release of AIF and its translocation to the nucleus. (Guide: ⟶ represents explored pathways, --➤ represents unexplored but feasible pathways)

Conclusion

In conclusion, the combination of ruxolitinib and lapatinib interacted to kill a variety of different breast cancer cells, including triple negative, HER2 positive and ER positive, in a synergistic fashion. Using pharmacologic and molecular tools, we demonstrated that the killing induced by the drug combination was mediated via necroptosis, apoptosis, and autophagy. We also demonstrated that the inhibition of ERBB receptors and JAK1 and JAK2 is the major reason behind the strong interaction between these two kinase inhibitors. Moreover, our data demonstrated that the induction of autophagosome formation and mitophagy acted upstream of the mitochondrial dysfunction, as knockdown of Beclin1 abolished BAX and BAK activation. In addition, we showed that whereas the inhibition of caspase 8 was not protective, the knockdown of BID significantly protected the cells. Therefore, this proteolytic cleavage of BID could be mediated by the cathepsin and calpain proteases although more studies will be required to fully elucidate the mechanism of BID activation. Our data also argued that the translocation of AIF from mitochondria to the nucleus played a significant role in inducing cell death.

CHAPTER 5: Concluding Remarks

The ultimate goal of the studies in this manuscript was to propose novel potent combinatorial targeted therapies for the treatment of cancers of liver, colon and breast using FDA-approved drugs. The aforementioned cancers are amongst the top five most prevalent and most fatal worldwide. Currently, surgical resection, radiotherapy and adjuvant chemotherapy, in some cases combined with certain approved targeted agents, constitute the front line therapies for HCC and CRC. Likewise, breast cancer, based on its characteristics, is usually treated with the combination of surgery, radiotherapy, chemotherapy, hormonal and targeted therapy.

The recent advancements in cancer genomics and identification of commonly mutated oncogenes coupled with poor chemotherapy response rates have shifted cancer therapy towards a more targeted approach based on better understanding of cancer biology.[11] Evidently, unlike chemotherapy, the major benefit of this type of tailored therapy is that it only interferes with distinct molecular targets that the cancer cells physiologically depend on, thereby providing high specificity, a broader therapeutic index, and less nonspecific toxicities.[12] However, a major setback to single-agent targeted therapy is the activation of parallel survival pathways. This oncogenic bypass mechanism results in the cell activating an alternative survival pathway in the event of blockade of a specific pathway; thus, leading to drug resistance.[22,23] Recent clinical trials have provided convincing evidence that the use of targeted therapeutics in combination provides a more rational strategy to increase the efficacy of the treatments.[11]

Mutations in *ras* gene have been frequently observed in liver and colorectal cancers, which led to approval of sorafenib and regorafenib for the treatment of HCC and CRC, respectively. However, both drugs only produced modest effects with low response rates in the

clinic.[128,204] Therefore, our major aim in this study was to potentiate the effect of sorafenib (SOR) and regorafenib (REGO) in these cancers by identifying/blocking another molecular target that hepatoma and colon cancer cells rely upon to survive. Recent studies have reported the elevated levels of PDE5 expression in many cancers including colon adenocarcinoma and commonly used colon cancer cell lines HT29 and HCT116 cells.[147,205] Activation of cGMP/PKG pathway reduces cellular growth and induces apoptosis through induction of β-catenin, which subsequently inhibits the function of multiple downstream survival proteins such as cyclin D1 and survivin.[205] Thus, elevated levels of PDE5, the enzyme that hydrolyzes cGMP, has been suggested to be involved in cancer progression.[205] We alongside our colleagues at VCU had previously reported the enhancing effect of PDE5 inhibitors in chemotherapy cell killing.[145-147] In these studies PDE5 inhibitors, in a NOS-dependent fashion, were shown to enhance chemotherapy effect through activation of CD95 receptors, the generation of ROS, and mitochondrial dysfunction.[145-147] As mentioned earlier in chapter 1, the cofactor BH4 plays a critical role in NOS activity. Small ratio of BH4 relative to its oxidized form, BH2, causes NOS uncoupling, leading to production of ROS and RNS rather than NO.[87,89] New studies have indicated that BH4:BH2 ratio is significantly lower in tumor cells than in normal tissue.[206] Thus, whereas sildenafil (SIL) is often associated with reduced oxidative stress in non-transformed cells, it promotes oxidative stress in tumor cells.[156] In agreement with these reports, we observed a significant increase in ROS and RNS levels as early as 2 hours after drug exposure. Our results suggested that the NOS activity and the ROS generation played a significant role in triggering a cytotoxic form of autophagy, and mediating cell death through activation of CD95 death receptor pathway. The crucial role of CD95 death receptor activation in [SOR/REGO+SIL]-mediated cell death was very well elucidated via expression of wild type CD95 in CD95 null- HUH7 cells.

Additionally, prior studies had indicated that the pro-apoptotic effect of cGMP/PKG pathway was also mediated through JNK.[205] Accordingly, our data showed an increase in phospho-JNK1/2 level in cells treated with REGO+SIL combination, and the pre-treatment of cells with JNK inhibitory peptide almost abolished the drug combination toxicity. Moreover, our *in vivo* tumor analysis revealed a significant increase in phospho-c-Jun level, which further approves the pro-apoptotic role of JNK. Furthermore, the drug combination inhibited the AKT/mTOR pathway, which was shown to play a major role in induction of cell death as the expression of an activated form of mTOR significantly reduced the [SOR/REGO+SIL]-mediated lethality. Reduction in phospho-AKT and phospho-mTOR levels could be the direct outcome of PDGFR inhibition, which our laboratory has repeatedly shown to be a major target for SOR and REGO.

SOR and REGO also induced ER stress. These drugs rapidly down-regulated GRP78, which resulted in a prolonged intense ER stress response leading to mitochondrial dysfunction. In addition to GRP78, recent studies from our laboratory indicated that these multi-kinase inhibitors interrupted the function of multiple other chaperones including HSP70, HSP90 and HSP27. Inhibition of multiple chaperones by SOR and REGO in cancer cells, which generally express more proteins than non-transformed cells and are heavily dependent on protein folding machinery, adds up another layer to the broad anti-tumor effects of these drugs.[207]

Collectively, the lethal effect of SOR/REGO+SIL combination *in vitro* is primarily mediated by the inhibition of multiple chaperones (induction of severe ER stress), the blockade of PDGFR signaling (decreased AKT/mTOR signaling), The NOS-dependent generation of ROS/RNS, pro-apoptotic function of JNK, and activation of CD95 death receptor signaling pathway. This explains why this drug combination responded well in multiple genetically diverse tumor cell types regardless of Ras mutation status.

The toxic effect of this drug combination translated well into our mouse models carrying pre-formed tumors as the combination of SOR+SIL and REGO+SIL profoundly reduced the growth of HUH7 and HT29 tumors *in vivo*, respectively. In addition, the *ex vivo* colony formation data revealed a significant reduction in plating efficiency of the cells treated with the combination of REGO+SIL as compared to REGO alone, which further approves the enhancing effect of PDE5 inhibition on REGO toxicity. Plus, the REGO+SIL combination-treated mice had significantly lower levels of VEGF and angiopoietin in their blood serum compared with the control group. The blockade of angiogenesis could be another way by which the drug combination exerted its anti-tumor effect in the mouse models. Collectively, the drug combination anti-tumor activity *in vivo* is likely an amalgamation of a direct anti-tumor cell killing effect by the drug combination (as previously discussed), antiangiogenic capability of SOR and REGO, inhibition of ABCB1/ABCG2 efflux pumps, and increased tumor vasculature permeability caused by the actions of sildenafil on endothelial cells.

In order to further tailor this drug combination, we investigated the potential addition of a third drug by searching for biomarkers for activated survival pathways. Prior studies from our group had shown that SOR could increase the levels of ceramides in hepatoma cells.[152] In this study, REGO was noticed to have a similar effect on ceramides. REGO also increased the level of S1P, a sphingolipid metabolite that regulates growth, survival, migration and angiogenesis.[127] Initial *in vitro* studies indicated that the multiple sclerosis drug FTY720, an HDAC inhibitor and S1P antagonist, enhanced the toxicity of REGO and REGO+SIL combination. However, to our surprise, HT29 tumors in mice treated with FTY720 re-grew at a much faster rate after cessation of drug treatment than either REGO alone or treatment with REGO+SIL, an effect seemingly to be mediated by an increase in angiogenesis and tumor vascularization. Undoubtedly, FTY720

possesses distinct anti-tumor activity as FTY720 treatment has been previously shown to block colitis-associated cancer progression.[149,150] However, our *in vivo* data demands further investigation into its mechanism of action as FTY720 treatment led to a significant increase in angiogenic/invasion regulatory cytokines.

In addition to S1P up-regulation, we also noticed a significant increase in phospho-AKT as well as stable high EGFR phosphorylation in response to the drug combination in both HUH7 and HT29 tumors collected 7 days after the start of treatment. Inhibition of either AKT or EGFR enhanced the lethality of REGO+SIL combination *in vitro*. Thus, activation of AKT and EGFR seemed to be amongst the major compensatory survival pathways counteracting the toxicity of SOR/REGO+SIL. It certainly requires further *in vivo* experiments to fully validate the effects of AKT and EGFR inhibition on SOR/REGO+SIL combination toxicity.

Our *in vitro* and animal studies are now an open clinical trial (NCT02466802) where patients with all solid tumors are receiving increasing doses of REGO+SIL once daily. We're hoping to be able to receive tumor and blood samples from the patients in order to analyze the tumor cell response and changes in the regulatory cytokines.

The second study in this manuscript was a proposal of a potent combinatorial targeted therapy for the treatment of all types of breast cancer, including the chemotherapy resistant, highly metastatic triple negative subtype. The study was designed based on the growing evidence supporting the role of STAT3 and STAT5 in breast cancer, and the heavy crosstalk between JAK/STAT and ERBB signaling pathways.[196-201] The effect of ERBB inhibitors as single agents, in combination with chemotherapy, hormonal therapy, or other targeted agents have been extensively studied in the past with some clinical trials yielding significant improvement over conventional therapy.[52,53,82,185] However, since there are no FDA-approved STAT inhibitors

currently available on the market, concurrent inhibition of STAT and ERBB signaling have not been examined before. In order to test this hypothesis, we utilized ruxolitinib (RUX), a JAK1/2 inhibitor, to suppress STAT3/5 activation. Thus, this study was undertaken to determine whether the myelofibrosis medication RUX could be re-purposed as a solid tumor cancer therapeutic, and synergize with ERBB inhibitor lapatinib (LAP) to kill breast cancer cells.

Our *in vitro* results indicated that RUX and LAP strongly interacted to kill a variety of genetically diverse breast cancer cells, including cells from all three subtypes; triple negative, HER2 positive, and ER positive. Colony formation assays and CI values were very well indicative of the synergistic interaction between the two drugs. Moreover, using molecular tools, we demonstrated that the inhibition of ERBB receptors and JAK1 and JAK2 is the major reason behind the strong interaction between these two kinase inhibitors, which further supported our hypothesis.

With regard to the mechanism of action of this drug combination, our studies strongly argued that the rapid inactivation of the PI3K/AKT/mTOR pathway led to a significant increase in autophagosome formation; autophagosomes that co-localized with mitochondria (mitophagy) and with lysosomes (autolysosomes). PI3K/AKT inhibition was also associated with decreased phosphorylation of pro-apoptotic protein BAD (S136), which allows BAD to heterodimerize with Bcl-xL and Bcl-2, and trigger apoptosis.[208] Furthermore, we noticed that activation of the executioner toxic BH3 domain proteins BAX and BAK required increased Beclin1 expression (autophagosome formation) and also the activation/cleavage of BID. In addition, we found that the autophagy-BAX/BAK/BID-dependent AIF release from the mitochondria and its translocation to the nucleus is one key mechanism by which the RUX+LAP combination was

killing tumor cells. We have our *in vivo* studies underway to determine if the combination of RUX and ERBB inhibitors become a potent therapy in the mouse models.

Our laboratory has constantly worked to identify new drug combinations that can be translated into potent therapies in the clinic. Recently, in a completed phase I trial (NCT01450384) proposed by our laboratory combining the anti-folate pemetrexed and SOR, 20 out of 33 patients had prolonged stable disease or tumor regression, with one complete response and multiple partial responses.[209] Further pre-clinical studies from our laboratory indicated that ERBB signaling functioned as a major compensatory survival pathway activated in response to SOR and pemetrexed, and that the addition of the pan ERBB inhibitor afatinib significantly enhanced the lethality of this drug combination.[209] We hope that the addition of afatinib to the combination of pemetrexed and SOR would be explored in a new phase I trial as it would provide us with invaluable information on the feasibility of tailoring targeted therapy.

Having had success in the clinical trials in the past, our studies presented in this manuscript strongly argue that the combination of REGO+SIL and RUX+LAP can possess significant therapeutic value in the clinic.

Literature Cited

1. Luo, J., Solimini, N. L., & Elledge, S. J. (2009). Principles of cancer therapy: Oncogene and non-oncogene addiction. *Cell, 136*(5), 823-837.

2. Hanahan, D., & Weinberg, R. A. (2011). Hallmarks of cancer: The next generation. *Cell, 144*(5), 646-674.

3. Weinstein, I. B. (2002). Cancer. addiction to oncogenes--the achilles heal of cancer. *Science (New York, N.Y.), 297*(5578), 63-64.

4. Wu, S., Powers, S., Zhu, W., & Hannun, Y. A. (2016). Substantial contribution of extrinsic risk factors to cancer development. *Nature, 529*(7584), 43-47.

5. Sudhakar, A. (2009). History of cancer, ancient and modern treatment methods. *Journal of Cancer Science & Therapy, 1*(2), 1-4.

6. Siegel, R., Naishadham, D., & Jemal, A. (2012). Cancer statistics, 2012. *CA: A Cancer Journal for Clinicians, 62*(1), 10-29.

7. Hajdu, S. I. (2011). A note from history: Landmarks in history of cancer, part 1. *Cancer, 117*(5), 1097-1102.

8. DeVita, V. T.,Jr, & Chu, E. (2008). A history of cancer chemotherapy. *Cancer Research, 68*(21), 8643-8653.

9. Tannock, I. F. (1998). Conventional cancer therapy: Promise broken or promise delayed? *The Lancet, 351*, SII9-SII16.

10. Hait, W. N., & Hambley, T. W. (2009). Targeted cancer therapeutics. *Cancer Research, 69*(4), 1263-7; discussion 1267.

11. Al-Lazikani, B., Banerji, U., & Workman, P. (2012). Combinatorial drug therapy for cancer in the post-genomic era. *Nature Biotechnology, 30*(7), 679-692.

12. Arora, A., & Scholar, E. M. (2005). Role of tyrosine kinase inhibitors in cancer therapy. *The Journal of Pharmacology and Experimental Therapeutics, 315*(3), 971-979.

13. Vasir, J. K., & Labhasetwar, V. (2005). Targeted drug delivery in cancer therapy. *Technology in Cancer Research & Treatment, 4*(4), 363-374.

14. Sawyers, C. (2004). Targeted cancer therapy. *Nature, 432*(7015), 294-297.

15. Krämer, I., & Lipp, H. (2007). Bevacizumab, a humanized anti-angiogenic monoclonal antibody for the treatment of colorectal cancer. *Journal of Clinical Pharmacy and Therapeutics, 32*(1), 1-14.

16. Smith, B. D., Levis, M., Beran, M., Giles, F., Kantarjian, H., Berg, K., . . . Small, D. (2004). Single-agent CEP-701, a novel FLT3 inhibitor, shows biologic and clinical activity in patients with relapsed or refractory acute myeloid leukemia. *Blood, 103*(10), 3669-3676.

17. Fischer, T., Stone, R. M., Deangelo, D. J., Galinsky, I., Estey, E., Lanza, C., . . . Giles, F. J. (2010). Phase IIB trial of oral midostaurin (PKC412), the FMS-like tyrosine kinase 3 receptor (FLT3) and multi-targeted kinase inhibitor, in patients with acute myeloid leukemia and high-risk myelodysplastic syndrome with either wild-type or mutated FLT3. *Journal of Clinical Oncology : Official Journal of the American Society of Clinical Oncology, 28*(28), 4339-4345.

18. Sawyers, C. L. (2002). Finding the next gleevec: FLT3 targeted kinase inhibitor therapy for acute myeloid leukemia. *Cancer Cell, 1*(5), 413-415.

19. Boehm, T., Folkman, J., Browder, T., & O'Reilly, M. S. (1997). Antiangiogenic therapy of experimental cancer does not induce acquired drug resistance. *Nature, 390*(6658), 404-407.

20. Escudier, B., Eisen, T., Stadler, W. M., Szczylik, C., Oudard, S., Staehler, M., . . . Bukowski, R. M. (2009). Sorafenib for treatment of renal cell carcinoma: Final efficacy and safety results of the phase III treatment approaches in renal cancer global evaluation trial. *Journal of Clinical Oncology : Official Journal of the American Society of Clinical Oncology, 27*(20), 3312-3318.

21. Ferrara, N., & Kerbel, R. S. (2005). Angiogenesis as a therapeutic target. *Nature, 438*(7070), 967-974.

22. Garraway, L. A., & Janne, P. A. (2012). Circumventing cancer drug resistance in the era of personalized medicine. *Cancer Discovery, 2*(3), 214-226.

23. Holohan, C., Van Schaeybroeck, S., Longley, D. B., & Johnston, P. G. (2013). Cancer drug resistance: An evolving paradigm. *Nature Reviews Cancer, 13*(10), 714-726.

24. Fletcher, J. I., Haber, M., Henderson, M. J., & Norris, M. D. (2010). ABC transporters in cancer: More than just drug efflux pumps. *Nature Reviews Cancer, 10*(2), 147-156.

25. Chang, G. (2003). Multidrug resistance ABC transporters. *FEBS Letters, 555*(1), 102-105.

26. Szakács, G., Paterson, J. K., Ludwig, J. A., Booth-Genthe, C., & Gottesman, M. M. (2006). Targeting multidrug resistance in cancer. *Nature Reviews Drug Discovery, 5*(3), 219-234.

27. Szakács, G., Annereau, J., Lababidi, S., Shankavaram, U., Arciello, A., Bussey, K. J., . . . Reimers, M. (2004). Predicting drug sensitivity and resistance: Profiling ABC transporter genes in cancer cells. *Cancer Cell, 6*(2), 129-137.

28. Durrant, D. E., Das, A., Dyer, S., Tavallai, S., Dent, P., & Kukreja, R. C. (2015). Targeted inhibition of phosphoinositide 3-Kinase/Mammalian target of rapamycin sensitizes pancreatic cancer cells to doxorubicin without exacerbating cardiac toxicity. *Molecular Pharmacology, 88*(3), 512-523.

29. Schwartz, G. K., & Casper, E. S. (1995). A phase II trial of doxorubicin HCL liposome injection in patients with advanced pancreatic adenocarcinoma. *Investigational New Drugs, 13*(1), 77-82.

30. Lhomme, C., Joly, F., Walker, J. L., Lissoni, A. A., Nicoletto, M. O., Manikhas, G. M., . . . Dugan, M. H. (2008). Phase III study of valspodar (PSC 833) combined with paclitaxel and carboplatin compared with paclitaxel and carboplatin alone in patients with stage IV or suboptimally debulked stage III epithelial ovarian cancer or primary peritoneal cancer. *Journal of Clinical Oncology : Official Journal of the American Society of Clinical Oncology, 26*(16), 2674-2682.

31. Meijer, C., Mulder, N. H., Hospers, G. A., Uges, D. R., & de Vries, E. G. (1990). The role of glutathione in resistance to cisplatin in a human small cell lung cancer cell line. *British Journal of Cancer, 62*(1), 72-77.

32. Carmo, A., Carvalheiro, H., Crespo, I., Nunes, I., & Lopes, M. (2011). Effect of temozolomide on the U-118 glioma cell line. *Oncology Letters, 2*(6), 1165-1170.

33. Hegi, M. E., Diserens, A., Gorlia, T., Hamou, M., de Tribolet, N., Weller, M., . . . Mariani, L. (2005). MGMT gene silencing and benefit from temozolomide in glioblastoma. *New England Journal of Medicine, 352*(10), 997-1003.

34. Johnson, B. E., & Janne, P. A. (2005). Epidermal growth factor receptor mutations in patients with non-small cell lung cancer. *Cancer Research, 65*(17), 7525-7529.

35. Rajan, A., Carter, C. A., Kelly, R. J., Gutierrez, M., Kummar, S., Szabo, E., . . . Giaccone, G. (2012). A phase I combination study of olaparib with cisplatin and gemcitabine in adults with solid tumors. *Clinical Cancer Research : An Official Journal of the American Association for Cancer Research, 18*(8), 2344-2351.

36. Fong, P. C., Boss, D. S., Yap, T. A., Tutt, A., Wu, P., Mergui-Roelvink, M., . . . O'Connor, M. J. (2009). Inhibition of poly (ADP-ribose) polymerase in tumors from BRCA mutation carriers. *New England Journal of Medicine, 361*(2), 123-134.

37. Miyashita, T., & Reed, J. C. (1992). Bcl-2 gene transfer increases relative resistance of S49.1 and WEHI7.2 lymphoid cells to cell death and DNA fragmentation induced by glucocorticoids and multiple chemotherapeutic drugs. *Cancer Research, 52*(19), 5407-5411.

38. Pandya Martin, A., Mitchell, C., Rahmani, M., Nephew, K. P., Grant, S., & Dent, P. (2009). Inhibition of MCL-1 enhances lapatinib toxicity and overcomes lapatinib resistance via BAK-dependent autophagy. *Cancer Biology & Therapy, 8*(21), 2084-2096.

39. Van Schaeybroeck, S., Karaiskou-McCaul, A., Kelly, D., Longley, D., Galligan, L., Van Cutsem, E., & Johnston, P. (2005). Epidermal growth factor receptor activity determines response of colorectal cancer cells to gefitinib alone and in combination with chemotherapy.

Clinical Cancer Research : An Official Journal of the American Association for Cancer Research, 11(20), 7480-7489.

40. Sumitomo, M., Asano, T., Asakuma, J., Asano, T., Horiguchi, A., & Hayakawa, M. (2004). ZD1839 modulates paclitaxel response in renal cancer by blocking paclitaxel-induced activation of the epidermal growth factor receptor-extracellular signal-regulated kinase pathway. *Clinical Cancer Research : An Official Journal of the American Association for Cancer Research, 10*(2), 794-801.

41. Lenz, H. J., Van Cutsem, E., Khambata-Ford, S., Mayer, R. J., Gold, P., Stella, P., . . . Rowinsky, E. K. (2006). Multicenter phase II and translational study of cetuximab in metastatic colorectal carcinoma refractory to irinotecan, oxaliplatin, and fluoropyrimidines. *Journal of Clinical Oncology : Official Journal of the American Society of Clinical Oncology, 24*(30), 4914-4921.

42. Wheeler, D. L., Huang, S., Kruser, T. J., Nechrebecki, M. M., Armstrong, E. A., Benavente, S., . . . Harari, P. M. (2008). Mechanisms of acquired resistance to cetuximab: Role of HER (ErbB) family members. *Oncogene, 27*(28), 3944-3956.

43. Sergina, N. V., Rausch, M., Wang, D., Blair, J., Hann, B., Shokat, K. M., & Moasser, M. M. (2007). Escape from HER-family tyrosine kinase inhibitor therapy by the kinase-inactive HER3. *Nature, 445*(7126), 437-441.

44. Engelman, J. A., Zejnullahu, K., Mitsudomi, T., Song, Y., Hyland, C., Park, J. O., . . . Janne, P. A. (2007). MET amplification leads to gefitinib resistance in lung cancer by activating ERBB3 signaling. *Science (New York, N.Y.), 316*(5827), 1039-1043.

45. Zhou, W., Ercan, D., Chen, L., Yun, C., Li, D., Capelletti, M., . . . Padera, R. (2009). Novel mutant-selective EGFR kinase inhibitors against EGFR T790M. *Nature, 462*(7276), 1070-1074.

46. Cameron, D., Casey, M., Press, M., Lindquist, D., Pienkowski, T., Romieu, C. G., . . . Crown, J. (2008). A phase III randomized comparison of lapatinib plus capecitabine versus capecitabine alone in women with advanced breast cancer that has progressed on trastuzumab: Updated efficacy and biomarker analyses. *Breast Cancer Research and Treatment, 112*(3), 533-543.

47. Garrett, M. D., & Collins, I. (2011). Anticancer therapy with checkpoint inhibitors: What, where and when? *Trends in Pharmacological Sciences, 32*(5), 308-316.

48. Thiessen, B., Stewart, C., Tsao, M., Kamel-Reid, S., Schaiquevich, P., Mason, W., . . . McIntosh, L. (2010). A phase I/II trial of GW572016 (lapatinib) in recurrent glioblastoma multiforme: Clinical outcomes, pharmacokinetics and molecular correlation. *Cancer Chemotherapy and Pharmacology, 65*(2), 353-361.

49. Akhavan, D., Pourzia, A. L., Nourian, A. A., Williams, K. J., Nathanson, D., Babic, I., . . . Mischel, P. S. (2013). De-repression of PDGFRbeta transcription promotes acquired resistance to EGFR tyrosine kinase inhibitors in glioblastoma patients. *Cancer Discovery, 3*(5), 534-547.

50. Hamed, H. A., Tavallai, S., Grant, S., Poklepovic, A., & Dent, P. (2015). Sorafenib/Regorafenib and lapatinib interact to kill CNS tumor cells. *Journal of Cellular Physiology, 230*(1), 131-139.

51. Osborne, C. K., Shou, J., Massarweh, S., & Schiff, R. (2005). Crosstalk between estrogen receptor and growth factor receptor pathways as a cause for endocrine therapy resistance in breast cancer. *Clinical Cancer Research, 11*(2), 865s-870s.

52. Chu, I., Blackwell, K., Chen, S., & Slingerland, J. (2005). The dual ErbB1/ErbB2 inhibitor, lapatinib (GW572016), cooperates with tamoxifen to inhibit both cell proliferation- and estrogen-dependent gene expression in antiestrogen-resistant breast cancer. *Cancer Research, 65*(1), 18-25.

53. Johnston, S., Pippen, J.,Jr, Pivot, X., Lichinitser, M., Sadeghi, S., Dieras, V., . . . Pegram, M. (2009). Lapatinib combined with letrozole versus letrozole and placebo as first-line therapy for postmenopausal hormone receptor-positive metastatic breast cancer. *Journal of Clinical Oncology : Official Journal of the American Society of Clinical Oncology, 27*(33), 5538-5546.

54. Dhillon, A., Hagan, S., Rath, O., & Kolch, W. (2007). MAP kinase signalling pathways in cancer. *Oncogene, 26*(22), 3279-3290.

55. Roberts, P., & Der, C. (2007). Targeting the raf-MEK-ERK mitogen-activated protein kinase cascade for the treatment of cancer. *Oncogene, 26*(22), 3291-3310.

56. Johnson, G. L., & Lapadat, R. (2002). Mitogen-activated protein kinase pathways mediated by ERK, JNK, and p38 protein kinases. *Science (New York, N.Y.), 298*(5600), 1911-1912.

57. Mor, A., & Philips, M. R. (2006). Compartmentalized ras/mapk signaling. *Annu.Rev.Immunol., 24*, 771-800.

58. Zarubin, T., & Jiahuai, H. (2005). Activation and signaling of the p38 MAP kinase pathway. *Cell Research, 15*(1), 11-18.

59. Chen, G., Hitomi, M., Han, J., & Stacey, D. W. (2000). The p38 pathway provides negative feedback for ras proliferative signaling. *The Journal of Biological Chemistry, 275*(50), 38973-38980.

60. Wagner, E. F., & Nebreda, Á. R. (2009). Signal integration by JNK and p38 MAPK pathways in cancer development. *Nature Reviews Cancer, 9*(8), 537-549.

61. Bubici, C., & Papa, S. (2014). JNK signalling in cancer: In need of new, smarter therapeutic targets. *British Journal of Pharmacology, 171*(1), 24-37.

62. Jing, L., & Anning, L. (2005). Role of JNK activation in apoptosis: A double-edged sword. *Cell Research, 15*(1), 36-42.

63. Kolch, W., Kotwaliwale, A., Vass, K., & Janosch, P. (2002). The role of raf kinases in malignant transformation. *Expert Reviews in Molecular Medicine, 4*(08), 1-18.

64. Wan, P. T., Garnett, M. J., Roe, S. M., Lee, S., Niculescu-Duvaz, D., Good, V. M., . . . Springer, C. J. (2004). Mechanism of activation of the RAF-ERK signaling pathway by oncogenic mutations of B-RAF. *Cell, 116*(6), 855-867.

65. Bonni, A., Brunet, A., West, A. E., Datta, S. R., Takasu, M. A., & Greenberg, M. E. (1999). Cell survival promoted by the ras-MAPK signaling pathway by transcription-dependent and -independent mechanisms. *Science (New York, N.Y.), 286*(5443), 1358-1362.

66. Ley, R., Balmanno, K., Hadfield, K., Weston, C., & Cook, S. J. (2003). Activation of the ERK1/2 signaling pathway promotes phosphorylation and proteasome-dependent degradation of the BH3-only protein, bim. *The Journal of Biological Chemistry, 278*(21), 18811-18816.

67. Vivanco, I., & Sawyers, C. L. (2002). The phosphatidylinositol 3-kinase–AKT pathway in human cancer. *Nature Reviews Cancer, 2*(7), 489-501.

68. Manning, B. D., & Cantley, L. C. (2007). AKT/PKB signaling: Navigating downstream. *Cell, 129*(7), 1261-1274.

69. Cully, M., You, H., Levine, A. J., & Mak, T. W. (2006). Beyond PTEN mutations: The PI3K pathway as an integrator of multiple inputs during tumorigenesis. *Nature Reviews Cancer, 6*(3), 184-192.

70. Kim, J., Kundu, M., Viollet, B., & Guan, K. (2011). AMPK and mTOR regulate autophagy through direct phosphorylation of Ulk1. *Nature Cell Biology, 13*(2), 132-141.

71. Salmena, L., Carracedo, A., & Pandolfi, P. P. (2008). Tenets of PTEN tumor suppression. *Cell, 133*(3), 403-414.

72. Luo, J., Manning, B. D., & Cantley, L. C. (2003). Targeting the PI3K-akt pathway in human cancer: Rationale and promise. *Cancer Cell, 4*(4), 257-262.

73. Quintas-Cardama, A., & Verstovsek, S. (2013). Molecular pathways: Jak/STAT pathway: Mutations, inhibitors, and resistance. *Clinical Cancer Research : An Official Journal of the American Association for Cancer Research, 19*(8), 1933-1940.

74. Quintas-Cardama, A., Vaddi, K., Liu, P., Manshouri, T., Li, J., Scherle, P. A., . . . Verstovsek, S. (2010). Preclinical characterization of the selective JAK1/2 inhibitor INCB018424: Therapeutic implications for the treatment of myeloproliferative neoplasms. *Blood, 115*(15), 3109-3117.

75. Buettner, R., Mora, L. B., & Jove, R. (2002). Activated STAT signaling in human tumors provides novel molecular targets for therapeutic intervention. *Clinical Cancer Research : An Official Journal of the American Association for Cancer Research, 8*(4), 945-954.

76. Constantinescu, S. N., Girardot, M., & Pecquet, C. (2008). Mining for JAK–STAT mutations in cancer. *Trends in Biochemical Sciences, 33*(3), 122-131.

77. O'Shea, J. J., Gadina, M., & Schreiber, R. D. (2002). Cytokine signaling in 2002: New surprises in the Jak/Stat pathway. *Cell, 109*(2), S121-S131.

78. Li, W. X. (2008). Canonical and non-canonical JAK–STAT signaling. *Trends in Cell Biology, 18*(11), 545-551.

79. Valentino, L., & Pierre, J. (2006). JAK/STAT signal transduction: Regulators and implication in hematological malignancies. *Biochemical Pharmacology, 71*(6), 713-721.

80. Yoshikawa, H., Matsubara, K., Qian, G., Jackson, P., Groopman, J. D., Manning, J. E., . . . Herman, J. G. (2001). SOCS-1, a negative regulator of the JAK/STAT pathway, is silenced by methylation in human hepatocellular carcinoma and shows growth-suppression activity. *Nature Genetics, 28*(1), 29-35.

81. Roskoski, R. (2014). The ErbB/HER family of protein-tyrosine kinases and cancer. *Pharmacological Research, 79*, 34-74.

82. Hynes, N. E., & Lane, H. A. (2005). ERBB receptors and cancer: The complexity of targeted inhibitors. *Nature Reviews Cancer, 5*(5), 341-354.

83. Olayioye, M. A., Beuvink, I., Horsch, K., Daly, J. M., & Hynes, N. E. (1999). ErbB receptor-induced activation of stat transcription factors is mediated by src tyrosine kinases. *The Journal of Biological Chemistry, 274*(24), 17209-17218.

84. Britten, C. D. (2004). Targeting ErbB receptor signaling: A pan-ErbB approach to cancer. *Molecular Cancer Therapeutics, 3*(10), 1335-1342.

85. Morgillo, F., Bareschino, M. A., Bianco, R., Tortora, G., & Ciardiello, F. (2007). Primary and acquired resistance to anti-EGFR targeted drugs in cancer therapy. *Differentiation, 75*(9), 788-799.

86. Mrugala, M. M., & Chamberlain, M. C. (2008). Mechanisms of disease: Temozolomide and glioblastoma—look to the future. *Nature Clinical Practice Oncology, 5*(8), 476-486.

87. Lundberg, J. O., Gladwin, M. T., & Weitzberg, E. (2015). Strategies to increase nitric oxide signalling in cardiovascular disease. *Nature Reviews Drug Discovery, 14*(9), 623-641.

88. Francis, S. H., Busch, J. L., Corbin, J. D., & Sibley, D. (2010). cGMP-dependent protein kinases and cGMP phosphodiesterases in nitric oxide and cGMP action. *Pharmacological Reviews, 62*(3), 525-563.

89. Cardnell, R. J., Rabender, C. S., Ross, G. R., Guo, C., Howlett, E. L., Alam, A., . . . Mikkelsen, R. B. (2013). Sepiapterin ameliorates chemically induced murine colitis and azoxymethane-induced colon cancer. *The Journal of Pharmacology and Experimental Therapeutics, 347*(1), 117-125.

90. Dimmeler, S., Fleming, I., Fisslthaler, B., Hermann, C., Busse, R., & Zeiher, A. M. (1999). Activation of nitric oxide synthase in endothelial cells by akt-dependent phosphorylation. *Nature, 399*(6736), 601-605.

91. Elmore, S. (2007). Apoptosis: A review of programmed cell death. *Toxicologic Pathology, 35*(4), 495-516.

92. Schmitz, I., Kirchhoff, S., & Krammer, P. H. (2000). Regulation of death receptor-mediated apoptosis pathways. *The International Journal of Biochemistry & Cell Biology, 32*(11), 1123-1136.

93. Sharma, K., Wang, R., Zhang, L., Yin, D., Luo, X., Solomon, J., . . . Scott, D. (2000). Death the fas way: Regulation and pathophysiology of CD95 and its ligand. *Pharmacology & Therapeutics, 88*(3), 333-347.

94. Youle, R. J., & Strasser, A. (2008). The BCL-2 protein family: Opposing activities that mediate cell death. *Nature Reviews Molecular Cell Biology, 9*(1), 47-59.

95. Adams, J., & Cory, S. (2007). The bcl-2 apoptotic switch in cancer development and therapy. *Oncogene, 26*(9), 1324-1337.

96. Yu, J., Zhang, L., Hwang, P. M., Kinzler, K. W., & Vogelstein, B. (2001). PUMA induces the rapid apoptosis of colorectal cancer cells. *Molecular Cell, 7*(3), 673-682.

97. Oda, E., Ohki, R., Murasawa, H., Nemoto, J., Shibue, T., Yamashita, T., . . . Tanaka, N. (2000). Noxa, a BH3-only member of the bcl-2 family and candidate mediator of p53-induced apoptosis. *Science (New York, N.Y.), 288*(5468), 1053-1058.

98. Li, H., Zhu, H., Xu, C., & Yuan, J. (1998). Cleavage of BID by caspase 8 mediates the mitochondrial damage in the fas pathway of apoptosis. *Cell, 94*(4), 491-501.

99. Brown, J. M., & Attardi, L. D. (2005). The role of apoptosis in cancer development and treatment response. *Nature Reviews Cancer, 5*(3), 231-237.

100. Amundson, S. A., Myers, T. G., Scudiero, D., Kitada, S., Reed, J. C., & Fornace, A. J.,Jr. (2000). An informatics approach identifying markers of chemosensitivity in human cancer cell lines. *Cancer Research, 60*(21), 6101-6110.

101. Tagawa, H., Karnan, S., Suzuki, R., Matsuo, K., Zhang, X., Ota, A., . . . Seto, M. (2005). Genome-wide array-based CGH for mantle cell lymphoma: Identification of homozygous deletions of the proapoptotic gene BIM. *Oncogene, 24*(8), 1348-1358.

102. Mestre-Escorihuela, C., Rubio-Moscardo, F., Richter, J. A., Siebert, R., Climent, J., Fresquet, V., . . . Martinez-Climent, J. A. (2007). Homozygous deletions localize novel tumor suppressor genes in B-cell lymphomas. *Blood, 109*(1), 271-280.

103. Kuribara, R., Honda, H., Matsui, H., Shinjyo, T., Inukai, T., Sugita, K., . . . Inaba, T. (2004). Roles of bim in apoptosis of normal and bcr-abl-expressing hematopoietic progenitors. *Molecular and Cellular Biology, 24*(14), 6172-6183.

104. Tan, T., Degenhardt, K., Nelson, D. A., Beaudoin, B., Nieves-Neira, W., Bouillet, P., . . . White, E. (2005). Key roles of BIM-driven apoptosis in epithelial tumors and rational chemotherapy. *Cancer Cell, 7*(3), 227-238.

105. Weinstein, J. N., Myers, T. G., O'Connor, P. M., Friend, S. H., Fornace, A. J.,Jr, Kohn, K. W., . . . Paull, K. D. (1997). An information-intensive approach to the molecular pharmacology of cancer. *Science (New York, N.Y.), 275*(5298), 343-349.

106. Marino, G., & Lopez-Otin, C. (2004). Autophagy: Molecular mechanisms, physiological functions and relevance in human pathology. *Cellular and Molecular Life Sciences CMLS, 61*(12), 1439-1454.

107. Amaravadi, R. K., & Thompson, C. B. (2007). The roles of therapy-induced autophagy and necrosis in cancer treatment. *Clinical Cancer Research : An Official Journal of the American Association for Cancer Research, 13*(24), 7271-7279.

108. Takahashi, Y., Meyerkord, C. L., Hori, T., Runkle, K., Fox, T. E., Kester, M., . . . Wang, H. (2011). Bif-1 regulates Atg9 trafficking by mediating the fission of golgi membranes during autophagy. *Autophagy, 7*(1), 61-73.

109. Itakura, E., & Mizushima, N. (2009). Atg14 and UVRAG: Mutually exclusive subunits of mammalian beclin 1-PI3K complexes. *Autophagy, 5*(4), 534-536.

110. Russell, R. C., Tian, Y., Yuan, H., Park, H. W., Chang, Y., Kim, J., . . . Guan, K. (2013). ULK1 induces autophagy by phosphorylating beclin-1 and activating VPS34 lipid kinase. *Nature Cell Biology, 15*(7), 741-750.

111. Mizushima, N., Ohsumi, Y., & Yoshimori, T. (2002). Autophagosome formation in mammalian cells. *Cell Structure and Function, 27*(6), 421-429.

112. Ding, W., & Yin, X. (2008). Sorting, recognition and activation of the misfolded protein degradation pathways through macroautophagy and the proteasome. *Autophagy, 4*(2), 141-150.

113. Apel, A., Zentgraf, H., Büchler, M. W., & Herr, I. (2009). Autophagy—A double-edged sword in oncology. *International Journal of Cancer, 125*(5), 991-995.

114. Kondo, Y., Kanzawa, T., Sawaya, R., & Kondo, S. (2005). The role of autophagy in cancer development and response to therapy. *Nature Reviews Cancer, 5*(9), 726-734.

115. Mathew, R., Kongara, S., Beaudoin, B., Karp, C. M., Bray, K., Degenhardt, K., . . . White, E. (2007). Autophagy suppresses tumor progression by limiting chromosomal instability. *Genes & Development, 21*(11), 1367-1381.

116. Aita, V. M., Liang, X. H., Murty, V., Pincus, D. L., Yu, W., Cayanis, E., . . . Levine, B. (1999). Cloning and genomic organization of beclin 1, a candidate tumor suppressor gene on chromosome 17q21. *Genomics, 59*(1), 59-65.

117. Kang, R., Zeh, H., Lotze, M., & Tang, D. (2011). The beclin 1 network regulates autophagy and apoptosis. *Cell Death & Differentiation, 18*(4), 571-580.

118. Schröder, M. (2008). Endoplasmic reticulum stress responses. *Cellular and Molecular Life Sciences, 65*(6), 862-894.

119. Wek, R. C., & Cavener, D. R. (2007). Translational control and the unfolded protein response. *Antioxidants & Redox Signaling, 9*(12), 2357-2372.

120. Verfaillie, T., Garg, A. D., & Agostinis, P. (2013). Targeting ER stress induced apoptosis and inflammation in cancer. *Cancer Letters, 332*(2), 249-264.

121. Puthalakath, H., O'Reilly, L. A., Gunn, P., Lee, L., Kelly, P. N., Huntington, N. D., . . . Motoyama, N. (2007). ER stress triggers apoptosis by activating BH3-only protein bim. *Cell, 129*(7), 1337-1349.

122. Hitomi, J., Katayama, T., Eguchi, Y., Kudo, T., Taniguchi, M., Koyama, Y., . . . Tohyama, M. (2004). Involvement of caspase-4 in endoplasmic reticulum stress-induced apoptosis and abeta-induced cell death. *The Journal of Cell Biology, 165*(3), 347-356.

123. Lee, A. S. (2007). GRP78 induction in cancer: Therapeutic and prognostic implications. *Cancer Research, 67*(8), 3496-3499.

124. Moenner, M., Pluquet, O., Bouchecareilh, M., & Chevet, E. (2007). Integrated endoplasmic reticulum stress responses in cancer. *Cancer Research, 67*(22), 10631-10634.

125. Lee, A. S. (2001). The glucose-regulated proteins: Stress induction and clinical applications. *Trends in Biochemical Sciences, 26*(8), 504-510.

126. Booth, L., Roberts, J. L., Cash, D. R., Tavallai, S., Jean, S., Fidanza, A., . . . Cornelissen, C. N. (2015). GRP78/BiP/HSPA5/Dna K is a universal therapeutic target for human disease. *Journal of Cellular Physiology, 230*(7), 1661-1676.

127. Hait, N. C., Allegood, J., Maceyka, M., Strub, G. M., Harikumar, K. B., Singh, S. K., . . . Spiegel, S. (2009). Regulation of histone acetylation in the nucleus by sphingosine-1-phosphate. *Science (New York, N.Y.), 325*(5945), 1254-1257.

128. Almhanna, K., Kim, R., & Kalmadi, S. (2007). Treatment approaches for hepatocellular carcinoma. *Clinical Medicine: Oncology, 1*, 11-19.

129. El-Serag, H. B. (2004). Hepatocellular carcinoma: Recent trends in the united states. *Gastroenterology, 127*(5), S27-S34.

130. Abou-Alfa, G. K., Schwartz, L., Ricci, S., Amadori, D., Santoro, A., Figer, A., . . . Saltz, L. B. (2006). Phase II study of sorafenib in patients with advanced hepatocellular carcinoma. *Journal of Clinical Oncology : Official Journal of the American Society of Clinical Oncology, 24*(26), 4293-4300.

131. Keating, G. M., & Santoro, A. (2009). Sorafenib. *Drugs, 69*(2), 223-240.

132. Wilhelm, S., Carter, C., Lynch, M., Lowinger, T., Dumas, J., Smith, R. A., . . . Kelley, S. (2006). Discovery and development of sorafenib: A multikinase inhibitor for treating cancer. *Nature Reviews Drug Discovery, 5*(10), 835-844.

133. Kane, R. C., Farrell, A. T., Saber, H., Tang, S., Williams, G., Jee, J. M., . . . Pazdur, R. (2006). Sorafenib for the treatment of advanced renal cell carcinoma. *Clinical Cancer Research : An Official Journal of the American Association for Cancer Research, 12*(24), 7271-7278.

134. Wilhelm, S. M., Adnane, L., Newell, P., Villanueva, A., Llovet, J. M., & Lynch, M. (2008). Preclinical overview of sorafenib, a multikinase inhibitor that targets both raf and VEGF and PDGF receptor tyrosine kinase signaling. *Molecular Cancer Therapeutics, 7*(10), 3129-3140.

135. Strumberg, D., Scheulen, M., Schultheis, B., Richly, H., Frost, A., Büchert, M., . . . Boix, O. (2012). Regorafenib (BAY 73-4506) in advanced colorectal cancer: A phase I study. *British Journal of Cancer, 106*(11), 1722-1727.

136. Gill, S., Thomas, R., & Goldberg, R. (2003). Colorectal cancer chemotherapy. *Alimentary Pharmacology & Therapeutics, 18*(7), 683-692.

137. Benson, A. B.,3rd, Schrag, D., Somerfield, M. R., Cohen, A. M., Figueredo, A. T., Flynn, P. J., . . . Haller, D. G. (2004). American society of clinical oncology recommendations on adjuvant chemotherapy for stage II colon cancer. *Journal of Clinical Oncology : Official Journal of the American Society of Clinical Oncology, 22*(16), 3408-3419.

138. Shirley, M., & Keating, G. M. (2015). Regorafenib: A review of its use in patients with advanced gastrointestinal stromal tumours. *Drugs, , 1-9.*

139. Strumberg, D., & Schultheis, B. (2012). Regorafenib for cancer. *Expert Opinion on Investigational Drugs, 21*(6), 879-889.

140. Abou-Elkacem, L., Arns, S., Brix, G., Gremse, F., Zopf, D., Kiessling, F., & Lederle, W. (2013). Regorafenib inhibits growth, angiogenesis, and metastasis in a highly aggressive, orthotopic colon cancer model. *Molecular Cancer Therapeutics, 12*(7), 1322-1331.

141. Goldenberg, M. M. (1998). Safety and efficacy of sildenafil citrate in the treatment of male erectile dysfunction. *Clinical Therapeutics, 20*(6), 1033-1048.

142. Ghofrani, H. A., Osterloh, I. H., & Grimminger, F. (2006). Sildenafil: From angina to erectile dysfunction to pulmonary hypertension and beyond. *Nature Reviews Drug Discovery, 5*(8), 689-702.

143. Scott, L. J. (2011). Fingolimod. *CNS Drugs, 25*(8), 673-698.

144. Brinkmann, V., Billich, A., Baumruker, T., Heining, P., Schmouder, R., Francis, G., . . . Burtin, P. (2010). Fingolimod (FTY720): Discovery and development of an oral drug to treat multiple sclerosis. *Nature Reviews Drug Discovery, 9*(11), 883-897.

145. Booth, L., Roberts, J. L., Cruickshanks, N., Conley, A., Durrant, D. E., Das, A., . . . Dent, P. (2014). Phosphodiesterase 5 inhibitors enhance chemotherapy killing in gastrointestinal/genitourinary cancer cells. *Molecular Pharmacology, 85*(3), 408-419.

146. Roberts, J. L., Booth, L., Conley, A., Cruickshanks, N., Malkin, M., Kukreja, R. C., . . . Dent, P. (2014). PDE5 inhibitors enhance the lethality of standard of care chemotherapy in pediatric CNS tumor cells. *Cancer Biology & Therapy, 15*(6), 758-767.

147. Das, A., Durrant, D., Mitchell, C., Dent, P., Batra, S. K., & Kukreja, R. C. (2015). Sildenafil (viagra) sensitizes prostate cancer cells to doxorubicin-mediated apoptosis through CD95. *Oncotarget,* doi:10.18632/oncotarget.6749

148. Shi, Z., Tiwari, A. K., Shukla, S., Robey, R. W., Singh, S., Kim, I. W., . . . Chen, Z. S. (2011). Sildenafil reverses ABCB1- and ABCG2-mediated chemotherapeutic drug resistance. *Cancer Research, 71*(8), 3029-3041.

149. Pyne, N. J., & Pyne, S. (2013). Sphingosine 1-phosphate is a missing link between chronic inflammation and colon cancer. *Cancer Cell, 23*(1), 5-7.

150. Liang, J., Nagahashi, M., Kim, E. Y., Harikumar, K. B., Yamada, A., Huang, W., . . . Avni, D. (2013). Sphingosine-1-phosphate links persistent STAT3 activation, chronic intestinal inflammation, and development of colitis-associated cancer. *Cancer Cell, 23*(1), 107-120.

151. Chou, T. C. (2010). Drug combination studies and their synergy quantification using the chou-talalay method. *Cancer Research, 70*(2), 440-446.

152. Park, M. A., Mitchell, C., Zhang, G., Yacoub, A., Allegood, J., Haussinger, D., . . . Dent, P. (2010). Vorinostat and sorafenib increase CD95 activation in gastrointestinal tumor cells through

a ca(2+)-de novo ceramide-PP2A-reactive oxygen species-dependent signaling pathway. *Cancer Research, 70*(15), 6313-6324.

153. Rahmani, M., Davis, E. M., Crabtree, T. R., Habibi, J. R., Nguyen, T. K., Dent, P., & Grant, S. (2007). The kinase inhibitor sorafenib induces cell death through a process involving induction of endoplasmic reticulum stress. *Molecular and Cellular Biology, 27*(15), 5499-5513.

154. Rahmani, M., Davis, E. M., Bauer, C., Dent, P., & Grant, S. (2005). Apoptosis induced by the kinase inhibitor BAY 43-9006 in human leukemia cells involves down-regulation of mcl-1 through inhibition of translation. *The Journal of Biological Chemistry, 280*(42), 35217-35227.

155. Musicki, B., Bivalacqua, T. J., Champion, H. C., & Burnett, A. L. (2014). Sildenafil promotes eNOS activation and inhibits NADPH oxidase in the transgenic sickle cell mouse penis. *The Journal of Sexual Medicine, 11*(2), 424-430.

156. Das, A., Durrant, D., Mitchell, C., Mayton, E., Hoke, N. N., Salloum, F. N., . . . Kukreja, R. C. (2010). Sildenafil increases chemotherapeutic efficacy of doxorubicin in prostate cancer and ameliorates cardiac dysfunction. *Proceedings of the National Academy of Sciences of the United States of America, 107*(42), 18202-18207.

157. Reinehr, R., Gorg, B., Hongen, A., & Haussinger, D. (2004). CD95-tyrosine nitration inhibits hyperosmotic and CD95 ligand-induced CD95 activation in rat hepatocytes. *The Journal of Biological Chemistry, 279*(11), 10364-10373.

158. González, R., Ferrín, G., Aguilar-Melero, P., Ranchal, I., Linares, C. I., Bello, R. I., . . . Álamo, J. M. (2013). Targeting hepatoma using nitric oxide donor strategies. *Antioxidants & Redox Signaling, 18*(5), 491-506.

159. Benavides, G. A., Liang, Q., Dodson, M., Darley-Usmar, V., & Zhang, J. (2013). Inhibition of autophagy and glycolysis by nitric oxide during hypoxia–reoxygenation impairs cellular bioenergetics and promotes cell death in primary neurons. *Free Radical Biology and Medicine, 65*, 1215-1228.

160. Shen, C., Yan, J., Erkocak, O. F., Zheng, X. F., & Chen, X. D. (2014). Nitric oxide inhibits autophagy via suppression of JNK in meniscal cells. *Rheumatology (Oxford, England), 53*(6), 1022-1033.

161. Yu, Y., Fan, S. M., Yuan, S. J., Tashiro, S., Onodera, S., & Ikejima, T. (2012). Nitric oxide (• NO) generation but not ROS plays a major role in silibinin-induced autophagic and apoptotic death in human epidermoid carcinoma A431 cells. *Free Radical Research, 46*(11), 1346-1360.

162. Tripathi, D. N., Chowdhury, R., Trudel, L. J., Tee, A. R., Slack, R. S., Walker, C. L., & Wogan, G. N. (2013). Reactive nitrogen species regulate autophagy through ATM-AMPK-TSC2-mediated suppression of mTORC1. *Proceedings of the National Academy of Sciences of the United States of America, 110*(32), E2950-7.

163. Valez, V., Cassina, A., Batinic-Haberle, I., Kalyanaraman, B., Ferrer-Sueta, G., & Radi, R. (2013). Peroxynitrite formation in nitric oxide-exposed submitochondrial particles: Detection, oxidative damage and catalytic removal by Mn–porphyrins. *Archives of Biochemistry and Biophysics, 529*(1), 45-54.

164. Haklar, G., Sayin-Özveri, E., Yüksel, M., Aktan, A. Ö., & Yalçin, A. S. (2001). Different kinds of reactive oxygen and nitrogen species were detected in colon and breast tumors. *Cancer Letters, 165*(2), 219-224.

165. Hirst, D. G., & Robson, T. (2007). Nitrosative stress in cancer therapy. *Front Biosci, 12*, 3406-3418.

166. Felley-Bosco, E. (1998). Role of nitric oxide in genotoxicity: Implication for carcinogenesis. *Cancer and Metastasis Reviews, 17*(1), 25-37.

167. Negi, G., Kumar, A., & Sharma, S. S. (2010). Concurrent targeting of nitrosative stress–PARP pathway corrects functional, behavioral and biochemical deficits in experimental diabetic neuropathy. *Biochemical and Biophysical Research Communications, 391*(1), 102-106.

168. Roberts, J. L., Tavallai, M., Nourbakhsh, A., Fidanza, A., Cruz-Luna, T., Smith, E., . . . Doern, C. D. (2015). GRP78/Dna K is a target for Nexavar/Stivarga/Votrient in the treatment of human malignancies, viral infections and bacterial diseases. *Journal of Cellular Physiology,*

169. Black, K. L., Yin, D., Ong, J. M., Hu, J., Konda, B. M., Wang, X., . . . Espinoza, A. (2008). PDE5 inhibitors enhance tumor permeability and efficacy of chemotherapy in a rat brain tumor model. *Brain Research, 1230*, 290-302.

170. Donepudi, M. S., Kondapalli, K., Amos, S. J., & Venkanteshan, P. (2014). Breast cancer statistics and markers. *Journal of Cancer Research and Therapeutics, 10*(3), 506-511.

171. Chavez, K. J., Garimella, S. V., & Lipkowitz, S. (2010). Triple negative breast cancer cell lines: One tool in the search for better treatment of triple negative breast cancer. *Breast Disease, 32*(1-2), 35-48.

172. Watson, C. J., & Hughes, K. (2014). Breast cancer: The menacing face of janus kinase. *Cell Death and Differentiation, 21*(2), 185-186.

173. Winer, E. P., Hudis, C., Burstein, H. J., Wolff, A. C., Pritchard, K. I., Ingle, J. N., . . . Somerfield, M. R. (2005). American society of clinical oncology technology assessment on the use of aromatase inhibitors as adjuvant therapy for postmenopausal women with hormone receptor-positive breast cancer: Status report 2004. *Journal of Clinical Oncology : Official Journal of the American Society of Clinical Oncology, 23*(3), 619-629.

174. Engel, R. H., & Kaklamani, V. G. (2007). HER2-positive breast cancer. *Drugs, 67*(9), 1329-1341.

175. O'Shaughnessy, J., Schwartzberg, L., Danso, M. A., Miller, K. D., Rugo, H. S., Neubauer, M., . . . Winer, E. P. (2014). Phase III study of iniparib plus gemcitabine and carboplatin versus gemcitabine and carboplatin in patients with metastatic triple-negative breast cancer. *Journal of Clinical Oncology : Official Journal of the American Society of Clinical Oncology, 32*(34), 3840-3847.

176. Isakoff, S. J. (2010). Triple-negative breast cancer: Role of specific chemotherapy agents. *Cancer Journal (Sudbury, Mass.), 16*(1), 53-61.

177. Naqvi, K., Verstovsek, S., Kantarjian, H., & Ravandi, F. (2011). A potential role of ruxolitinib in leukemia. *Expert Opinion on Investigational Drugs, 20*(8), 1159-1166.

178. Verstovsek, S., Kantarjian, H., Mesa, R. A., Pardanani, A. D., Cortes-Franco, J., Thomas, D. A., . . . Erickson-Viitanen, S. (2010). Safety and efficacy of INCB018424, a JAK1 and JAK2 inhibitor, in myelofibrosis. *New England Journal of Medicine, 363*(12), 1117-1127.

179. Verstovsek, S. (2013). Ruxolitinib: An oral janus kinase 1 and janus kinase 2 inhibitor in the management of myelofibrosis. *Postgraduate Medicine, 125*(1), 128-135.

180. Galli, S., McLornan, D., & Harrison, C. (2014). Safety evaluation of ruxolitinib for treating myelofibrosis. *Expert Opinion on Drug Safety, 13*(7), 967-976.

181. Shilling, A. D., Nedza, F. M., Emm, T., Diamond, S., McKeever, E., Punwani, N., . . . Yeleswaram, S. (2010). Metabolism, excretion, and pharmacokinetics of [14C]INCB018424, a selective janus tyrosine kinase 1/2 inhibitor, in humans. *Drug Metabolism and Disposition: The Biological Fate of Chemicals, 38*(11), 2023-2031.

182. Mesa, R. A., Yasothan, U., & Kirkpatrick, P. (2012). Ruxolitinib. *Nature Reviews Drug Discovery, 11*(2), 103-104.

183. Wood, E. R., Truesdale, A. T., McDonald, O. B., Yuan, D., Hassell, A., Dickerson, S. H., . . . Shewchuk, L. (2004). A unique structure for epidermal growth factor receptor bound to GW572016 (lapatinib): Relationships among protein conformation, inhibitor off-rate, and receptor activity in tumor cells. *Cancer Research, 64*(18), 6652-6659.

184. Burris, H. A.,3rd, Hurwitz, H. I., Dees, E. C., Dowlati, A., Blackwell, K. L., O'Neil, B., . . . Spector, N. L. (2005). Phase I safety, pharmacokinetics, and clinical activity study of lapatinib (GW572016), a reversible dual inhibitor of epidermal growth factor receptor tyrosine kinases, in heavily pretreated patients with metastatic carcinomas. *Journal of Clinical Oncology : Official Journal of the American Society of Clinical Oncology, 23*(23), 5305-5313.

185. Opdam, F. L., Guchelaar, H. J., Beijnen, J. H., & Schellens, J. H. (2012). Lapatinib for advanced or metastatic breast cancer. *The Oncologist, 17*(4), 536-542.

186. Chu, Q. S., Cianfrocca, M. E., Goldstein, L. J., Gale, M., Murray, N., Loftiss, J., . . . Rowinsky, E. K. (2008). A phase I and pharmacokinetic study of lapatinib in combination with

letrozole in patients with advanced cancer. *Clinical Cancer Research : An Official Journal of the American Association for Cancer Research, 14*(14), 4484-4490.

187. Keating, G. M. (2014). Afatinib: A review of its use in the treatment of advanced non-small cell lung cancer. *Drugs, 74*(2), 207-221.

188. Hirsh, V. (2011). Afatinib (BIBW 2992) development in non-small-cell lung cancer. *Future Oncology, 7*(7), 817-825.

189. Lin, N. U., Winer, E. P., Wheatley, D., Carey, L. A., Houston, S., Mendelson, D., . . . Garcia, A. A. (2012). A phase II study of afatinib (BIBW 2992), an irreversible ErbB family blocker, in patients with HER2-positive metastatic breast cancer progressing after trastuzumab. *Breast Cancer Research and Treatment, 133*(3), 1057-1065.

190. Wykosky, J., Fenton, T., Furnari, F., & Cavenee, W. K. (2011). Therapeutic targeting of epidermal growth factor receptor in human cancer: Successes and limitations. *Chinese Journal of Cancer, 30*(1), 5-12.

191. Secq, V., Villeret, J., Fina, F., Carmassi, M., Carcopino, X., Garcia, S., . . . Charpin, C. (2014). Triple negative breast carcinoma EGFR amplification is not associated with EGFR, kras or ALK mutations. *British Journal of Cancer, 110*(4), 1045-1052.

192. Clevenger, C. V., Gadd, S. L., & Zheng, J. (2009). New mechanisms for PRLr action in breast cancer. *Trends in Endocrinology & Metabolism, 20*(5), 223-229.

193. Zhou, B., Damrauer, J. S., Bailey, S. T., Hadzic, T., Jeong, Y., Clark, K., . . . Kim, W. Y. (2014). Erythropoietin promotes breast tumorigenesis through tumor-initiating cell self-renewal. *The Journal of Clinical Investigation, 124*(2), 553-563.

194. Rodriguez-Barrueco, R., Yu, J., Saucedo-Cuevas, L. P., Olivan, M., Llobet-Navas, D., Putcha, P., . . . Castillo-Martin, M. (2015). Inhibition of the autocrine IL-6-JAK2-STAT3-calprotectin axis as targeted therapy for HR-/HER2 breast cancers. *Genes Dev, *, 1631-1648.

195. Johnstone, C. N., Chand, A., Putoczki, T. L., & Ernst, M. (2015). Emerging roles for IL-11 signaling in cancer development and progression: Focus on breast cancer. *Cytokine & Growth Factor Reviews, 26*(5), 489-498.

196. Clevenger, C. V. (2004). Roles and regulation of stat family transcription factors in human breast cancer. *The American Journal of Pathology, 165*(5), 1449-1460.

197. Walker, S. R., Nelson, E. A., Zou, L., Chaudhury, M., Signoretti, S., Richardson, A., & Frank, D. A. (2009). Reciprocal effects of STAT5 and STAT3 in breast cancer. *Molecular Cancer Research : MCR, 7*(6), 966-976.

198. Zhao, C., Li, H., Lin, H., Yang, S., Lin, J., & Liang, G. (2016). Feedback activation of STAT3 as a cancer drug-resistance mechanism. *Trends in Pharmacological Sciences, 37*(1), 47-61.

199. Yu, H., Kortylewski, M., & Pardoll, D. (2007). Crosstalk between cancer and immune cells: Role of STAT3 in the tumour microenvironment. *Nature Reviews Immunology, 7*(1), 41-51.

200. Quesnelle, K. M., Boehm, A. L., & Grandis, J. R. (2007). STAT-mediated EGFR signaling in cancer. *Journal of Cellular Biochemistry, 102*(2), 311-319.

201. Venturutti, L., Romero, L., Urtreger, A., Chervo, M., Russo, R. C., Mercogliano, M., . . . Izzo, F. (2015). Stat3 regulates ErbB-2 expression and co-opts ErbB-2 nuclear function to induce miR-21 expression, PDCD4 downregulation and breast cancer metastasis. *Oncogene*

202. Daugas, E., Nochy, D., Ravagnan, L., Loeffler, M., Susin, S. A., Zamzami, N., & Kroemer, G. (2000). Apoptosis-inducing factor (AIF): A ubiquitous mitochondrial oxidoreductase involved in apoptosis. *FEBS Letters, 476*(3), 118-123.

203. Česen, M. H., Pegan, K., Špes, A., & Turk, B. (2012). Lysosomal pathways to cell death and their therapeutic applications. *Experimental Cell Research, 318*(11), 1245-1251.

204. Bos, J. L., Fearon, E. R., Hamilton, S. R., Verlaan–de Vries, M., van Boom, J. H., van der Eb, Alex J, & Vogelstein, B. (1987). Prevalence of ras gene mutations in human colorectal cancers. *Nature, 327*(6120), 293-297.

205. Das, A., Durrant, D., Salloum, F. N., Xi, L., & Kukreja, R. C. (2015). PDE5 inhibitors as therapeutics for heart disease, diabetes and cancer. *Pharmacology & Therapeutics, 147*, 12-21.

206. Rabender, C. S., Alam, A., Sundaresan, G., Cardnell, R. J., Yakovlev, V. A., Mukhopadhyay, N. D., . . . Mikkelsen, R. B. (2015). The role of nitric oxide synthase uncoupling in tumor progression. *Molecular Cancer Research : MCR, 13*(6), 1034-1043

207. Booth, L., Shuch, B., Albers, T., Roberts, J. L., Tavallai, M., Proniuk, S., . . . Dent, P. (2016). Multi-kinase inhibitors can associate with heat shock proteins through their NH2-termini by which they suppress chaperone function. *Oncotarget.*

208. Fang, X., Yu, S., Eder, A., Mao, M., Bast, R. C., Boyd, D., & Mills, G. B. (1999). Regulation of BAD phosphorylation at serine 112 by the ras-mitogen-activated protein kinase pathway. *Oncogene, 18*(48)

209. Booth, L., Roberts, J. L., Tavallai, M., Chuckalovcak, J., Stringer, D. K., Koromilas, A. E., … Dent, P. (2016). [Pemetrexed + Sorafenib] lethality is increased by inhibition of ERBB1/2/3-PI3K-NFκB compensatory survival signaling. *Oncotarget.*

VITA

Mehrad Tavallai

August 23, 1985, Tehran, Iran

Education

Doctor of Philosophy in Biochemistry (April 2016)
Virginia Commonwealth University, School of Medicine

Dissertation: Introducing novel combinatorial targeted therapies in multiple types of cancer.
Advisor: Dr. Paul Dent

Master of Science in Biochemistry (December 2013)
Virginia Commonwealth University, School of Medicine

Thesis: Lapatinib and sorafenib kill GBM tumor cells in a greater than additive manner.
Advisor: Dr. Paul Dent

Bachelor of Science in Biology (January 2011)
George Mason University, College of Science

Associate of Science in Zoology (December 2007)
University of Tehran, Faculty of Science

Publications

1. Tavallai, M., Booth, L., Roberts, JL., McGuire, WP., Poklepovic, A., Dent, P. (2016) Ruxolitinib synergizes with DMF to kill via BIM+BAD induced mitochondrial dysfunction and via reduced SOD2/TRX expression and ROS. *Oncotarget*.

2. Booth, L., Roberts, JL., Tavallai, M., Webb, T., Leon, D., Chen, J., McGuire, WP., Poklepovic, A., Dent, P. (2016) The afatinib resistance of in vivo generated H1975 lung cancer cell clones is mediated by SRC/ERBB3/c-KIT/c-MET compensatory survival signaling. *Oncotarget*.

3. Booth, L., Shuch, B., Albers, T., Roberts, J L., Tavallai, M., Proniuk, S., Zukiwski, A., Wang, D., Chen, CS., Bottaro, D., Ecroyd, H., Lebedyeva, IO., Dent, P. (2016) Multi-kinase inhibitors can associate with heat shock proteins through their NH2-termini by which they suppress chaperone function. *Oncotarget.*

4. Durrant, DE., Das, A., Dyer, S., Tavallai, M., Dent, P., Kukreja, RC. (2015) Targeted inhibition of phosphoinositide 3-kinase/mammalian target of rapamycin sensitizes pancreatic cancer cells to doxorubicin without exacerbating cardiac toxicity. *Molecular Pharmacology* 3,

512-23.

5. Roberts, JL., Tavallai, M., Nourbakhsh, A., Fidanza, A., Cruz-Luna, T., Smith, E., Siembida, P., Plamondon, P., Cycon, KA., Doern, CD., Booth, L., Dent, P. (2015) GRP78/Dna K is a target for Nexavar/ Stivarga/ Votrient in the treatment of human malignancies, viral infections and bacterial diseases. *Journal of Cellular Physiology* 10, 2552-78.

6. Cruickshanks, N., Roberts, JL., Bareford, MD., Tavallai, M., Poklepovic, A., Booth, L., Dent, P. (2015) Differential regulation of autophagy and cell viability by ceramide species. *Cancer Biology and Therapy* 5, 733-42.

7. Booth, L., Roberts, JL., Tavallai, M., Nourbakhsh, A., Chuckalovcak, J., Carter, J., Poklepovic, A., Dent, P. (2015) OSU-03012 and Viagra treatment inhibits the activity of multiple chaperone proteins and disrupts the blood brain barrier: implications for anti-cancer therapies. *Journal of Cellular Physiology* 8, 1982-98.

8. Tavallai, M., Hamed, HA., Roberts, JL., Cruickshanks, N., Chuckalovcak, J., Poklepovic, A., Booth, L., Dent, P. (2015) Nexavar/Stivarga and Viagra interact to kill tumor cells. *Journal of Cellular Physiology* 9, 2281-98.

9. Booth, L., Roberts, JL., Cash, DR., Tavallai, M., Jean, S., Fidanza, A., Cruz-Luna, T., Siembiba, P., Cycon, KA., Cornelissen, CN., Dent, P.(2014) GRP78/ BiP/ HSPA5/ Dna K is a universal therapeutic target for human disease. *Journal of Cellular Physiology* 7, 1661-76.

10. Booth, L., Cruickshanks, N., Tavallai, M., Roberts, JL., Peery, M., Poklepovic, A., Dent, P. (2014) Regulation of dimethyl-fumarate toxicity by proteasome inhibitors. *Cancer Biology and Therapy* 12, 1646-57.

11. Booth, L., Roberts, J., Cruickshanks, N., Tavallai, M., Webb, T., Samuel, P., Conley, A., Binion, B., Young, H., Poklepovic, A., Speigel, S., Dent, P. (2014) PDE5 inhibitors enhance celecoxib killing in multiple tumor types. *Journal of Cellular Physiology 5*, 1115-27.

12. Hamed, H., Tavallai, M., Grant, S., Poklepovic, A., Dent, P. (2014) Sorafenib/regorafenib and lapatinib interact to kill CNS tumor cells. *Journal of Cellular Physiology* 1, 131-9.

13. Tavallai, M., Hamed, H., Grant, S., Poklepovic, A., Dent, P. (2014) Pazopanib and HDAC inhibitors interact to kill sarcoma cells. *Cancer Biology and Therapy* 5, 578-85.

14. Booth, L., Tavallai, M., Hamed, H., Cruickshanks, Dent, P. (2014) The role of cell signalling in the crosstalk between autophagy and apoptosis. *Cell Signal.* **3**, 549-55.

15. Cruickshanks, N., Hamed, H., Booth, L., Tavallai, M., Syed, J., Sajithlal, G., Grant, S., Poklepovic, A., Dent, P. (2013) Histone deacetylase inhibitors restore toxic BH3 domain protein expression in anoikis-resistant mammary and brain cancer stem cells, thereby enhancing the response to anti-ERBB1/ERBB2 therapy. *Cancer Biology and Therapy* **10**, 982-96.

16. Sajithlal, G., Hamed, H., Cruickshanks, N., Booth, l., <u>Tavallai, M</u>., Syed, J., Grant, S., Poklepovic, A., Dent, P. (2013) Sorafenib/Regorafenib and phosphatidyl inositol 3 kinase/thymoma viral proto-oncogene inhibition interact to kill tumor cells. *Molecular Pharmacology* **4**, 562-71.

Presentations

1. "Sorafenib/Regorafenib and Sildenafil interact to kill tumor cells"
<u>Tavallai, M</u>., Hamed, HA., Roberts, JL., Cruickshanks, N., Chuckalovcak, J., Poklepovic, A., Booth, L., Dent, P.
Poster
Daniel T. Watts Research Symposium, VCU, October 2015

2. "Sorafenib/Regorafenib and Sildenafil interact to kill tumor cells"
<u>Tavallai, M</u>., Hamed, HA., Roberts, JL., Cruickshanks, N., Chuckalovcak, J., Poklepovic, A., Booth, L., Dent, P.
Poster
AACR Annual Meeting, April 2015

3. "Sorafenib/Regorafenib and Sildenafil interact to kill HCC and CRC cells"
Oral presentation
Biochemistry Department Journal Club, VCU, February 2015

4. "Pazopanib and HDAC inhibitors interact to kill sarcoma cells"
<u>Tavallai, M</u>., Hamed, H., Grant, S., Poklepovic, A., Dent, P.
Poster
Daniel T. Watts Research Symposium, VCU, October 2014

5. "Lapatinib and sorafenib interact to kill GBM tumor cells"
Oral presentation
Biochemistry Department Journal Club, VCU, May 2014

Laboratory Skills

- Fluorescent and confocal microscopy
- Cell/tissue culture techniques: transfection, infection and drug treatment
- Tumor cell isolation (PDX models)
- Western blotting
- Immunohistochemistry
- PCR/ qPCR
- Immunoprecipitation
- Animal handling techniques (tumor implantation, oral gavage, intracranial/ intratracheal/ tail vein injections and blood/organ collection)

Professional Affiliations

- American Association for the Advancement of Science (AAAS)

- American Association for Cancer Research (AACR)

- American Society for Biochemistry and Molecular Biology (ASBMB)